

**Resilience of UAE high-rise buildings to climate change:
Impacts of projected climate changes on annual energy
demands**

مرونة المباني الشاهقة في الإمارات العربية المتحدة في مواجهة تغير المناخ: تأثير
التغيرات المناخية المتوقعة على الطلب السنوي للطاقة.

by

DUAA M.A KH. SALLAM

**Dissertation submitted in fulfilment
of the requirements for the degree of
MSc BUILDING SERVICES ENGINEERING**

at

The British University in Dubai

July 2020

DECLARATION

I warrant that the content of this research is the direct result of my own work and that any use made in it of published or unpublished copyright material falls within the limits permitted by international copyright conventions.

I understand that a copy of my research will be deposited in the University Library for permanent retention.

I hereby agree that the material mentioned above for which I am author and copyright holder may be copied and distributed by The British University in Dubai for the purposes of research, private study or education and that The British University in Dubai may recover from purchasers the costs incurred in such copying and distribution, where appropriate.

I understand that The British University in Dubai may make a digital copy available in the institutional repository.

I understand that I may apply to the University to retain the right to withhold or to restrict access to my thesis for a period which shall not normally exceed four calendar years from the congregation at which the degree is conferred, the length of the period to be specified in the application, together with the precise reasons for making that application.

Signature of the student

COPYRIGHT AND INFORMATION TO USERS

The author whose copyright is declared on the title page of the work has granted to the British University in Dubai the right to lend his/her research work to users of its library and to make partial or single copies for educational and research use.

The author has also granted permission to the University to keep or make a digital copy for similar use and for the purpose of preservation of the work digitally.

Multiple copying of this work for scholarly purposes may be granted by either the author, the Registrar or the Dean only.

Copying for financial gain shall only be allowed with the author's express permission.

Any use of this work in whole or in part shall respect the moral rights of the author to be acknowledged and to reflect in good faith and without detriment the meaning of the content, and the original authorship.

Abstract

The impact of climate change and global warming on buildings energy consumption has been an arguable topic in many studies all around the world. However, there are limited studies on the effect of climate change on UAE buildings and its impact on energy demand. As global warming is hitting all areas in the entire world, designing and retrofitting buildings based on future weather conditions is essential to avoid early deterioration of buildings especially in countries with high air temperatures like UAE.

This motivates the research on finding to most energy efficient solutions that would reduce energy consumption of UAE high-rise buildings in present and future weather conditions. To achieve this goal, future weather datasets in hourly time step for UAE were collected from three statistical tools representing stabilization and high emission scenarios. Those datasets were analyzed and compared with present weather files. This study has revealed that the derived future weather files daily dry-bulb temperatures are increasing throughout the years, while the daily relative humidity ratio and global horizontal solar radiation values are marginally decreasing from the present values.

Then, energy efficient solutions were selected to test their effect on total system and cooling energy of high-rise buildings in UAE. Those solutions include increasing the insulation of external walls, improving the glazing thermal properties, and adding heat recovery units to the HVAC system. In this study, a high-rise building with 60% WWR which represents a typical UAE high-rise building was used as a base case to test the selected solutions on it.

This study has shown that the energy consumption of UAE high-rise building will keep increasing in future and it can reach up to 50% more from the present consumption in period

2090 in high emission scenario. Using glazing with enhanced thermal properties would reduce more energy than applying sensible and latent heat recovery units. However, after 50 years the sensible and latent recovery units would reduce more energy than the enhanced glazing.

Applying the three best options in this study was able to reduce total system and cooling energy by 20% to 21% in present and future periods.

نبذة مختصرة عن البحث

يعتبر تأثير تغير المناخ والاحترار العالمي على استهلاك الطاقة في المباني موضوعاً قابلاً للجدال في العديد من الدراسات في جميع أنحاء العالم. ولكن هناك دراسات قليلة حول تأثير تغير المناخ على استهلاك طاقة المباني في دولة الإمارات العربية المتحدة. وبما أن الاحترار العالمي يشمل جميع مناطق العالم، فإن تصميم المباني وإعادة تجهيزها لمقاومة الظروف الجوية المستقبلية أمر ضروري لتجنب التدهور المبكر للمباني خاصة في البلدان الحارة مثل دولة الإمارات العربية المتحدة.

وهذا يحفز البحث على أفضل الحلول الموفرة للطاقة التي من شأنها أن تقلل من الاستهلاك في المباني الشاهقة في دولة الإمارات العربية المتحدة في الظروف الجوية الحالية والمستقبلية. ولتحقيق هذا الهدف، تم جمع مجموعة بيانات مسجلة لحالة الطقس في كل ساعة على عدة فترات مستقبلية لدولة الإمارات العربية المتحدة. جمعت هذه الملفات من ثلاث أدوات إحصائية تمثل سيناريوهات التثبيت والانبعثات المرتفعة. وقد تم تحليل مجموعة البيانات هذه ومقارنتها بملفات الطقس الحالية. اكتشفت هذه الدراسة أن هنالك تزايد في درجات الحرارة الجافة اليومية في ملفات الطقس المستقبلية على مر السنين، في حين أن نسبة الرطوبة النسبية اليومية و الإشعاع الشمسي الأفقي اليومي يتناقصون بشكل ضئيل من القيم الحالية.

وبعد ذلك، تم اختيار حلول ذات كفاءة عالية في توفير الطاقة لاختبار تأثيرها على استهلاك الطاقة الكلية والطاقة التبريدية للمباني الشاهقة في دولة الإمارات العربية المتحدة. وتشمل هذه الحلول زيادة عزل الجدران الخارجية، وتحسين الخصائص الحرارية لزجاج النوافذ، وإضافة وحدات استرجاع الحرارة المستنفذة إلى نظام التكييف. في هذه الدراسة، تم تصميم مبنى شاهق، نسبة النافذة للجدار فيه هي 60%، كنموذج للمباني الشاهقة في دولة الإمارات العربية المتحدة و سوف يستخدم لاختبار الحلول المختارة الموفرة للطاقة عليه.

قد أظهرت هذه الدراسة أن زيادة استهلاك الطاقة في المباني الشاهقة سوف يستمر في المستقبل، ويمكن أن تصل هذه الزيادة إلى 50% من الاستهلاك الحالي في فترة 2090 في حال استمرار سيناريو الانبعثات العالية. وقد توصلت أيضاً إلى ان استخدام زجاج نوافذ ذو خصائص حرارية جيدة يقلل الاستهلاك للطاقة أكثر من تطبيق وحدات استرجاع الحرارة المستنفذة إلى نظام التكييف في الوقت الحالي. ولكن، بعد 50 عاماً سوف توفر وحدات استرجاع الحرارة المستنفذة إلى نظام التكييف من طاقة المبنى أكثر من زجاج النوافذ المحسن. و قد تم خفض استهلاك الطاقة الكلية والطاقة التبريدية بنسبة 20% إلى 21% في الوقت الحالي والمستقبلي عند تطبيق أفضل ثلاثة خيارات في هذه الدراسة.

Acknowledgement

I would like to thank my family for their continuous support, especially my parents, husband, and my sons. I could never have reached this academic accomplishment without you all.

Also, I would like to thank my supervisor, Dr. Kirk Shanks, for his tremendous support and encouragement during my dissertation, and all my BUiD professors for making this journey enjoyable and knowledgeable.

Table of Contents

List of Figures	v
List of Tables	xiii
List of Abbreviations	v
Chapter 1: Introduction	1
1.1- Built Environment effecting climate change	2
1.2- An overview of Dubai city	5
1.3- Energy demand in Dubai	6
1.4- Research problem statement:	8
1.5- Aims and objectives:.....	8
1.5.1- Objectives	9
1.6- Dissertation Organization	10
Chapter 2: Literature Review	12
2.1- Climate Change and Predicted Future Weather Datasets.....	13
2.2- GCMs downscaling approaches	18
2.2.1- Downscaling using dynamical approach	19
2.2.2- Downscaling using statistical approach.....	20
2.3- Study cases on impact of climate change on building energy consumption	23
2.4- Technologies and solutions to reduce energy demand in buildings	29

2.4.1- Increasing insulation layers and changing glazing properties	29
2.4.2- Case studies	30
2.4.3- Double skin façade (DSF)	34
2.4.3.1- Buildings with DSF in Dubai	37
2.4.4- Applying Heat recovery wheel (HRW) to HVAC system	41
Chapter 3: Methodology	45
3.1- Base Case Model	47
3.2- Future weather datasets	53
3.2.1- CCWorldWeatherGen tool	54
3.2.2- WeatherShift™ tool.....	61
3.2.3- Meteonorm tool	75
3.3- Energy saving solutions/technologies	80
3.3.1- Increasing thermal insulation of the building	80
3.3.2- Applying different glazing types for the base case model.....	82
3.3.3- Adding heat exchanger and enthalpy recovery wheel (HRW) to the HVAC system.....	84
3.4 Summary of energy efficiency technologies tested	87
Chapter 4: Results and Discussion	89
4.1- Base case model HVAC system auto-sizing and simulation.....	92
4.1.1- HVAC system auto-sizing	92
4.1.2- Base case model simulation with present and future weather files	96

4.2- Increasing the thermal insulation of external walls	100
4.2.1- The effect of adding 150 mm of mineral fiber slab insulation for external wall.....	
.....	101
4.2.2: The effect of adding 200 mm of (EPS) insulation material for external wall	
.....	104
4.3- Improving the glazing properties of the external windows.	107
4.3.1- Applying Krypton filled double glazing with lower SHGC and higher U-value	
.....	108
4.3.2- Applying Krypton filled double glazing with lower SHGC and lower U-value ...	111
4.3.3- Applying Krypton filled triple glazing with lower SHGC and lower U-value	115
4.4- Adding a heat recovery unit to the building HVAC system.....	119
4.4.1- Adding cross-flow air-to-air heat exchanger to the HVAC system with 70% sensible efficiency.....	120
4.4.2- Adding cross-flow air-to-air heat exchanger to the HVAC system with 75% sensible efficiency.....	123
4.4.3- Adding cross-flow air-to-air heat exchanger to the HVAC system with 80% sensible efficiency.....	127
4.4.4- Adding an enthalpy HRW to the HVAC system with 70% sensible efficiency and 68% latent efficiency	130
4.4.5- Adding an enthalpy HRW to the HVAC system with 75% sensible efficiency and 73% latent efficiency	134

4.4.6- Adding an enthalpy HRW to the HVAC system with 80% sensible efficiency and 78% latent efficiency	138
4.5- Comparison of this study with previous studies/researches	141
4.6- Summary of the simulation results	144
4.7- Applying options A2, B3, and C6	146
Chapter 5: Conclusion and Recommendations.....	151
5.1- Conclusion	152
5.2- Research limitations and recommendations	154
References	156
Appendices.....	164
Appendix A.....	165
Appendix B	171

List of Figures

Figure 1: Percentage of time that occupants spent in urbanized area (Kořir 2019)	2
Figure 2: Annual CO ₂ emission by sector (Global Alliance for Buildings and Construction 2018)	3
Figure 3: The center of Dubai city, “Sheikh Zayed Road” (Johnson 2020).....	6
Figure 4: Number and percentages of electricity consumers in Dubai (Dubai Electricity & Water Authority (DEWA) Annual Statistics 2018).....	7
Figure 5: Description of natural and enhanced greenhouse effect process (Greenhouse effect n.d.)	14
Figure 6: Emitted compounds and their radiative forcing and level of confidence (IPCC: Summary for Policymakers 2013).	17
Figure 7: Percentages of the types and approaches of future climate data that used in simulation tools to asses building performance in 111 articles (Moazami et al., 2019).....	21
Figure 8: Average temperature in 2020 in Dubai, UAE (Meteonorm 7, 2019).....	22
Figure 9: Average temperature in 2050 in Dubai, UAE (Meteonorm 7, 2019).....	22
Figure 10: Flowchart of the methods used to generate predicted future weather datasets for building simulation software (Moazami et al. 2019).....	23
Figure 11: Amount of annual required cooling energy needed for campus for the 3 future periods based on 4 emission scenarios (Zhai & Helman 2019).....	25
Figure 12: Percentage increase in total energy consumption of the campus (Zhai & Helman 2019).	25
Figure 13: Types of the 16 buildings used in the project (Moazami et al., 2019).....	27

Figure 14: annual cooling loads reduction percentage for simulated types of window glass (Tibi & Mokhtar 2014).	31
Figure 15: Conduction gains of the base case model for present and future years (Shanks, 2018).	33
Figure 16: Schematic diagram of natural and hybrid double skin façade (Straube & Straaten 2001).	35
Figure 17: DSF of Renaissance hotel (Haggag 2007).	38
Figure 18: Cross section of the selected building part for the study (Radhi, Sharples & Fikiry 2013).	39
Figure 19: Annual cooling savings % based on the three selected materials and perforation ratio (Johnny & Shanks 2018).	41
Figure 20: Typical heat recovery wheel (HWR) unit (Understanding Energy Recovery Wheels - Uponor Blog 2020)	42
Figure 21: Base case 3-D model (IES Virtual Environment 2019).	48
Figure 22: Layout of a typical floor in the model (IES Virtual Environment 2019).	48
Figure 23: schematic description of heat balance method on an opaque surface (ASHRAE fundamental 2017).	51
Figure 24: Schematic diagram of through-the-wall conduction process (ASHRAE fundamental 2017).	52
Figure 25: Comparison between average daily dry-bulb temperature in C° of the three CCWorldWeatherGen tool future weather files and IWEC present file (Dataviewer n.d.).	57
Figure 26: Average daily relative humidity ratio (RH%) of the three CCWorldWeatherGen tool future weather files compared with IWEC present file (Dataviewer n.d.).	58

Figure 27: Average daily global horizontal solar radiation in Wh/m² of the three CCWorldWeatherGen tool future weather files compared with IWEC present file (Dataviewer n.d.). 60

Figure 28: Comparison between the average daily dry-bulb temperature in C° between IWEC present weather file and WeatherShift™ tool future files with 50% percentile (Dataviewer n.d.). 65

Figure 29: Comparison between the average daily dry-bulb temperature in C° between IWEC present weather file and WeatherShift™ tool future files with 90% percentile (Dataviewer n.d.). 66

Figure 30: Comparison between the average daily dry-bulb temperature in C° between IWEC present weather file and WeatherShift™ tool future files with 95% percentile (Dataviewer n.d.). 67

Figure 31: Comparison between the average daily RH% between IWEC present weather file and WeatherShift™ tool future files with 50% percentile (Dataviewer n.d.). 68

Figure 32: Comparison between the average daily RH% between IWEC present weather file and WeatherShift™ tool future files with 90% percentile (Dataviewer n.d.). 69

Figure 33: Comparison between the average daily RH% between IWEC present weather file and WeatherShift™ tool future files with 95% percentile (Dataviewer n.d.). 70

Figure 34: Comparison between the average daily global horizontal solar radiation in Wh/m² of IWEC present weather file and WeatherShift™ tool future files with 50% percentile (Dataviewer n.d.). 72

Figure 35: Comparison between the average daily global horizontal solar radiation in Wh/m ² of IWEC present weather file and WeatherShift™ tool future files with 90% percentile (Dataviewer n.d.).	73
Figure 36: Comparison between the average daily global horizontal solar radiation in Wh/m ² of IWEC present weather file and WeatherShift™ tool future files with 95% percentile (Dataviewer n.d.).	74
Figure 37: Comparison between the average daily dry-bulb temperature in C° between Meteororm tool present and future predicted weather files (Dataviewer n.d.).	76
Figure 38: Comparison between the RH% between Meteororm tool present and future predicted weather files (Dataviewer n.d.).	78
Figure 39: Comparison between the average daily global horizontal solar radiation between Meteororm tool present and future predicted weather files (Dataviewer n.d.).	79
Figure 40: Structure of double and triple glazing windows (Pros & Cons of Double-Glazing Vs Triple-Glazing Windows 2020).	83
Figure 41: Cross flow air-to-air heat exchanger (ASHRAE 2008).	86
Figure 42: Enthalpy heat recovery wheel (ASHRAE 2008).	86
Figure 44: 3-D Sun cast view of the base case model in January, April, and July at 12p.m and 2p.m (IES Virtual Environment 2019).	96
Figure 45: Total system energy of the base case model simulated with present and future weather files.	98
Figure 46: Total cooling energy of the base case model simulated with present and future weather files.	98

Figure 47: Percentage increase of the total system energy consumption of the base case in the future selected periods.	100
Figure 48: Total system energy of the base case model with option A1 simulated with present and future weather files.....	102
Figure 49: Total cooling energy of the base case model with option A1 simulated with present and future weather files.....	102
Figure 50: Percentage increase from present consumption in the total system energy of the base case with option A1 in the future selected periods.	104
Figure 51: Total system energy of the base case model with option A2 simulated with present and future weather files.....	105
Figure 52: Total cooling energy of the base case model with option A2 simulated with present and future weather files.....	105
Figure 53: Percentage increase from present consumption in the total system energy of the base case with option A2 in the future selected periods.	107
Figure 54: Total system energy of the base case model with option B1 simulated with present and future weather files.....	108
Figure 55: Total cooling energy of the base case model with option B1 simulated with present and future weather files.....	109
Figure 56: Percentage increase from present consumption in the total system energy of the base case with option B1 in the future selected periods.	110
Figure 57: Total system energy of the base case model with option B2 simulated with present and future weather files.....	112

Figure 58: Total cooling energy of the base case model with option B2 simulated with present and future weather files.....	112
Figure 59: Percentage increase from present consumption in total system energy of the base case with option B2 in the future selected periods.	113
Figure 60: Total system energy of the base case model with option B3 simulated with present and future weather files.....	116
Figure 61: Total cooling energy of the base case model with option B3 simulated with present and future weather files.....	116
Figure 62: Percentage increase from present consumption in total system energy of the base case with option B3 in the future selected periods.	117
Figure 63: Total system energy of the base case model with option C1 simulated with present and future weather files.....	120
Figure 64: Total cooling energy of the base case model with option C1 simulated with present and future weather files.....	121
Figure 65: Percentage increase from present consumption of the total system energy of the base case with option C1 in the future selected periods.	122
Figure 66: Total system energy of the base case model with option C2 simulated with present and future weather files.....	124
Figure 67: Total cooling energy of the base case model with option C2 simulated with present and future weather files.....	124
Figure 68: Percentage increase from present consumption of the total system energy of the base case with option C2 in the future selected periods.	125

Figure 69: Total system energy of the base case model with option C3 simulated with present and future weather files.....	127
Figure 70: Total cooling energy of the base case model with option C2 simulated with present and future weather files.....	128
Figure 71: Percentage increase from present consumption of the total system energy of the base case with option C3 in the future selected periods.	129
Figure 72: Total system energy of the base case model with option C4 simulated with present and future weather files.....	131
Figure 73: Total system energy of the base case model with option C4 simulated with present and future weather files.....	131
Figure 74: Percentage increase from present consumption of the total system energy of the base case with option C4 in the future selected periods.	133
Figure 75: Total system energy of the base case model with option C5 simulated with present and future weather files.....	135
Figure 76: Total cooling energy of the base case model with option C5 simulated with present and future weather files.....	135
Figure 77: Percentage increase from present consumption of the total system energy of the base case with option C5 in the future selected periods.	136
Figure 78: Total system energy of the base case model with option C2 simulated with present and future weather files.....	138
Figure 79: Total cooling energy of the base case model with option C2 simulated with present and future weather files.....	139

Figure 80: Percentage increase from present consumption of the total system energy of the base case with option C6 in the future selected periods.	140
Figure 81: Total system energy of the base case model with options A2, B3, and C6 simulated with present and future weather files.	147
Figure 82: Total cooling energy of the base case model with options A2, B3, and C6 simulated with present and future weather files.	148
Figure 83: Percentage increase from present consumption of the total system energy of the base case with option C6 in the future selected periods.	149
Figure A- 1: Base case external wall construction materials including option A1 (IES Virtual Environment 2019).	166
Figure A- 2: Base case external wall construction materials including option A2 (IES Virtual Environment 2019).	167
Figure A- 3: Base case external window construction materials including option B1 (IES Virtual Environment 2019).	168
Figure A- 4: Base case external window construction materials including option B2 (IES Virtual Environment 2019).	169
Figure A- 5: Base case external window construction materials including option B3 (IES Virtual Environment 2019).	170

List of Tables

Table (1): UAE Rank for GHG emissions and planned future % reduction per capita (Climatecollege.unimelb.edu.au 2020).....	15
Table (2): RCPs Total radiative forcing, type of scenarios, predicted changes in global mean temperature and CO ₂ concentration for year 2100 based on AR5 report of the IPCC (IPCC: Summary for Policymakers 2013).	18
Table (3): Types and functions of morphing transformation algorithms (Moazami et al. 2019).	21
Table (4): Years used by the generating tool for each adopted future term (Moazami et al. 2019).	27
Table (5): Amount of peak cooling load for each type of buildings used in the project and the neighborhood, the cooling peak load in summer is compared using multiple weather files of TDY and EWY and the percentage of change is represented (Moazami et al. 2019).	28
Table (6): Type and thermal characteristics of the studies window glazing (Tibi and Mokhtar 2014)	31
Table (7): Comparison between DSFs and other glass insulation technologies (Straube & Straaten 2001).	36
Table (8): Ton refrigeration of the system with and without HRW (AL HUSSAINI & Khan 2017).	43
Table (9): Base case construction and building fabric specifications.....	48
Table (10): Internal heat gain of base case model.	49
Table (11): Base case model thermal properties (Al Safat, Dubai Green Building Evaluation System 2016).	50

Table (12): Highest and lowest average daily dry bulb temperature in C° of IWEC present file and CCWorldWeatherGen tool future files for periods 2020, 2050, and 2080 based on figure 25.	56
Table (13): Highest and lowest RH% of IWEC present file and CCWorldWeatherGen tool future files for periods 2020, 2050, and 2080 based on figure 26.....	59
Table (14): Highest and lowest global horizontal radiation in Wh/m ² of IWEC present file and CCWorldWeatherGen tool future files for periods 2020, 2050, and 2080 based on figure 27. ...	61
Table (15): WeatherShift™ tool percentiles description (Climatology - Paducah, KY - February Temperature Percentiles n.d.).	62
Table (16): Highest and lowest average daily temperatures of the future WeatherShift™ files for periods 2035, 2065, and 2095 in 50 th , 90 th , and 95 th percentiles based on figures 28, 29, and 30.	64
Table (17): Highest and lowest average daily RH% of the future WeatherShift™ files for periods 2035, 2065, and 2095 in 50 th , 90 th , and 95 th percentiles based on figures 31, 32, and 33.	71
Table (18): Highest and lowest average daily global horizontal solar radiation in Wh/m ² of the future WeatherShift™ files for periods 2035, 2065, and 2095 in 50 th , 90 th , and 95 th percentiles based on figures 33, 34, and 35.....	75
Table (19): Highest and lowest average daily RH% of present and future Meteonorm tool weather files based on figure 38.	77
Table (20): Highest and lowest average daily global horizontal solar radiation in Wh/m ² of the present and future Meteonorm tool files based on figure 39.	80
Table (21): Insulation materials types and thermal properties.....	81
Table (22): Four window types with different glazing layers, air fill, and thermal properties.....	84
Table (23): Tested energy efficiency technology options.....	88

Table (24): HVAC components details for Zone 1, Zone 2, and Zone 3 (IES Virtual Environment 2019).	93
Table (25): Fan coil unit design air-flow and cooling coil capacity for each room/space in the building, see layout in figure 20, chp.3 (IES Virtual Environment 2019).....	94
Table (26): Percentage reduction in total system energy and total cooling energy from the base case model for present and future periods by applying option (A1).....	103
Table (27): Percentage reduction in total system energy and total cooling energy from the base case model for present and future periods by applying option (A2).....	106
Table (28): Percentage reduction in total system energy and total cooling energy from the base case model for present and future periods by applying option (B1).....	110
Table (29): Percentage reduction in total system energy and total cooling energy from the base case model for present and future periods by applying option (B2).....	114
Table (30): Percentage reduction in total system energy and total cooling energy from the base case model for present and future periods by applying option (B3).....	118
Table (31): Percentage reduction in total system energy and total cooling energy from the base case model for present and future periods by applying option (C1).....	122
Table (32): Percentage reduction in total system energy and total cooling energy from the base case model for present and future periods by applying option (C2).....	126
Table (33): Percentage reduction in total system energy and total cooling energy from the base case model for present and future periods by applying option (C3).....	129
Table (34): Percentage reduction in total system energy and total cooling energy from the base case model for present and future periods by applying option (C4).....	134

Table (35): Percentage reduction in total system energy and total cooling energy from the base case model for present and future periods by applying option (C5).....	137
Table (36): Percentage reduction in total system energy and total cooling energy from the base case model for present and future periods by applying option (C6).....	140
Table (37): Summary of annual total system energy for the base case and all proposed options in kwh/m ² .yr.....	144
Table (38): Summary of annual total cooling energy for the base case and all proposed options in kwh/m ² .yr.....	144
Table (39): Summary of percentage reduction from base case in total system energy for all proposed options.	145
Table (40): Summary of percentage reduction from base case in total cooling energy for all proposed options.	146
Table (41): Percentage reduction in total system energy and total cooling energy from the base case model for present and future periods by applying options A2, B3, and C6.....	149
Table (B- 1): Peak cooling load of rooms 1, 2, 3, and 4 of the 12 th floor (IES Virtual Environment 2019).	172

List of Abbreviations

WORD	DEFINITION
A2	Very heterogeneous world scenario from IPCC Third Assessment Report
AR4	IPCC Fourth Assessment Report
AR5	IPCC Fifth Assessment Report
ASHRAE	American Society of Heating, Refrigeration, and Air-Conditioning Engineers
BES	Building energy simulation
CCWorldWeatherGen.	Climate change world weather generating
CDF	Cumulative distribution function
CFD	Computational fluid dynamic
CFM	Cubic feet/minute
CH ₄	Methane
CIBSE	Chartered Institution of Building Services Engineers
CMPI5	Coupled Model Intercomparison Project Phase 5
CO ₂	Carbon dioxide
COP	Coefficient of performance
CRFS	Climate interactive façade system
DDC	Data distribution center
DEWA	Dubai Electricity and Water Authority
DSF	Double skin façade
DSM	Demand side management
EAD	Environmental Agency of Abu Dhabi
EPS	Expanded polystyrene foam
EPW	EnergyPlus Weather

EWY	Extreme weather year
FAHU	Fresh-air handling unit
FCU	Fan coil unit
GCM	Global Climate Model or General Circulation Model
GHG	Green house gases
GWh	Gigawatt hours
HadCM3	Hadley Centre Coupled Model 3
HAP	Hourly analysis program
HRW	Heat recovery wheel
HVAC	Heating, ventilation and air conditioning
IAQ	Indoor air quality
IES VE	Integrated Environmental Solutions – Virtual Environment
IPCC	Intergovernmental Panel on Climate Change
ISH	Integrated Surface Hourly
IWEC	International weather for energy calculations
kwh	Kilowatt-hour
LCC	Life cycle cost
MWH	Megawatt-hour
N ₂ O	Nitrous oxide
NCAR	National Center of Atmospheric Research
PCM	Phase change material
ppb	Parts per billion

ppm	Parts per million
RCA4	Rosby Centre Regional Atmospheric Climate Model
RCM	Regional Climate Model
RCP	Representative Concentration Pathway
RF	Radiative forcing
RH%	Relative humidity ratio
SC	Shading coefficient
SHGC	Solar heat gain coefficient
TDY	Typical downscaled year
TMY	Typical meteorological year
UNFCCC	United Nations Framework Convention on Climate Change
U-value	Thermal transmittance
WRF	Weather Research and Forecasted Model
WS	WeatherShift™
WWR	Window to wall ratio

Chapter 1: Introduction

1.1- Built Environment effecting climate change

The built environment is an indispensable element of modern life. Over the past century there has been a dramatic increase in using buildings because humans in developed countries spend between 80% ~ 90% of their time there. As shown in figure 1, a person living in an urbanized area would spend around 86.9% of his/her life in an indoor environment including residence, workplace, bar/restaurant, and other indoor locations (Košir 2019). Moreover, as buildings are an inevitable element of daily life, they are also one of the main sources of greenhouse gas (GHG) emissions due to the large amount of energy they consume. For that reason, finding the most appropriate building services technologies/solutions to reduce energy consumption of buildings is essential both for present climate conditions and for any predicted climate changes in the future.

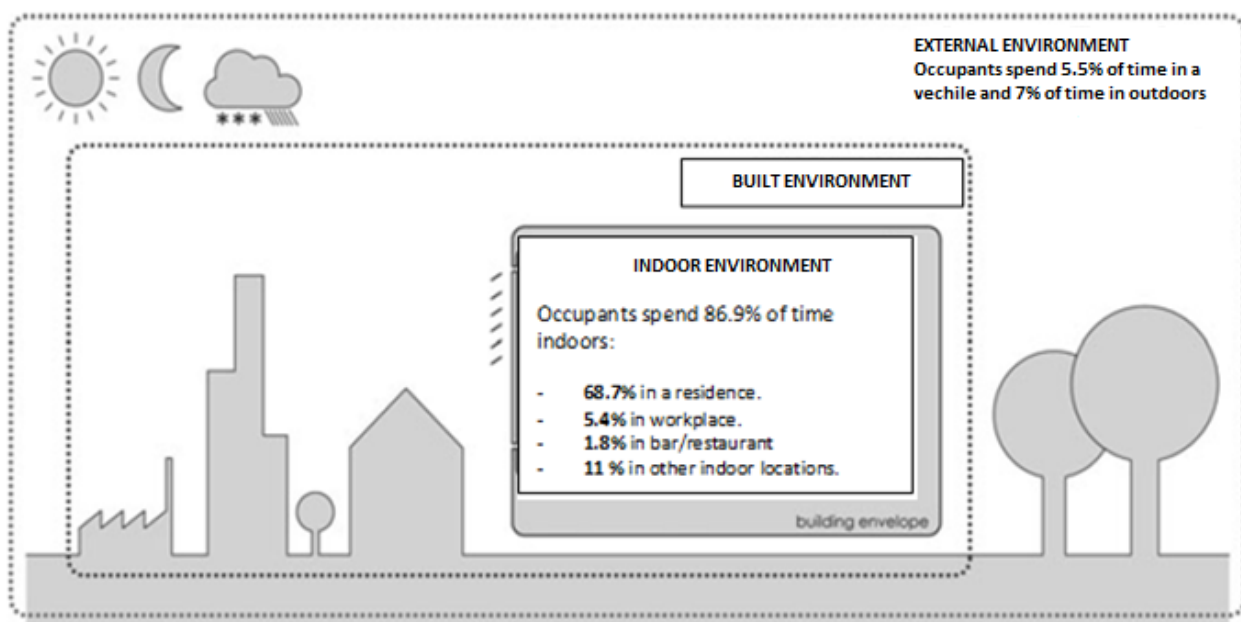


Figure 1: Percentage of time that occupants spent in urbanized area (Košir 2019)

Currently, designers and engineers are moving toward more sustainable built environments taking into consideration human health, energy consumption, and climate change. Assuming two thirds of existing buildings will still be in use by 2050, the overall contribution of human activities caused by buildings, i.e. due to their materials, construction and operation, will remain around 39% of annual global CO₂ emissions, see figure 2 below (Global Alliance for Buildings and Construction 2018).

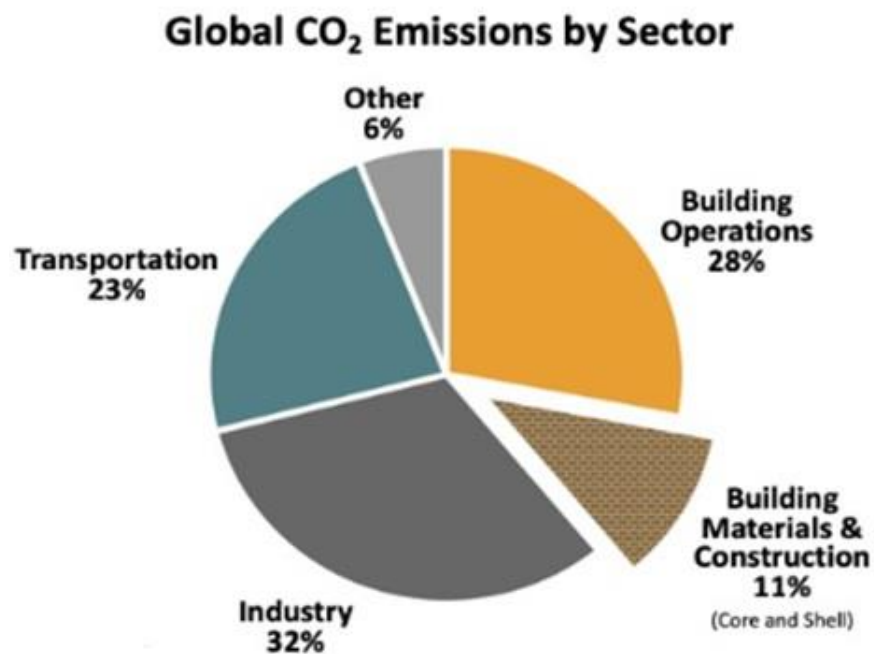


Figure 2: Annual CO₂ emission by sector (Global Alliance for Buildings and Construction 2018)

In the meantime, there is a lack of retrofitting and efficient renovation solutions for existing buildings whilst only 0.5%-1% of them get renovated annually and this is causing a significant increase in energy consumption and GHG emissions from these buildings (Architecture2030.org 2019). Therefore, energy efficient techniques should be used not only for new buildings but also in retrofitting existing buildings to reduce the energy consumption and emissions caused by building stocks.

As we know, climate change is considered as one of the main concerns that are affecting our planet. This change is due to rising global temperatures caused by GHG emissions where the global warming has affected species and ecosystems negatively. Although international and governmental agencies have implemented mitigation plans, global warming is expected to continue rising. This change in climate conditions increases future environmental risks such as more frequency of severe weather events including heat waves, sea level rise, floods, and hurricanes. Therefore, it is important to find ways to adapt to this climate change, and building sectors should take future climate change predictions into consideration to limit the negative impact on building energy demand (Cox et al. 2015).

Optimizing building energy demand will contribute to reducing CO₂ emissions and increasing occupant comfort. Heating and cooling demand in buildings are the most critical energy uses that will be directly affected by global warming in the future. Nowadays, there is a worldwide interest in investigating how climate change will affect weather in the future. However, in many countries and regions forecasted future weather data sets are still unavailable (Cox et al. 2015).

As we know, changes in climate are inevitable, for that reason the Intergovernmental Panel on Climate Change (IPCC) has explored predicted climate changes under four scenarios of GHG emissions and other climate drivers. Those scenarios are divided into one mitigation scenario, two stabilization scenarios, and one with high GHG emissions. The four scenarios revealed that global temperature will continue to rise but the percentage of temperature increase is highly dependent on GHG emissions. The Coupled Model Intercomparison Project Phase 5 (CMIP5) and other earth system models are usually used to predict future weather conditions and emissions up to year 2100 (IPCC: Summary for Policymakers 2013).

The main way of testing how the energy performance of new and existing buildings can be improved is by using simulation programs to evaluate how they would perform dynamically under various weather parameters. These weather parameters include dry bulb temperature, wet bulb temperature, relative humidity, solar irradiation, precipitation, and some of them might include wind speed and wind direction (Guan 2009).

All building simulation programs utilize weather datasets which are derived from historic weather measurements and are therefore likely to become unrepresentative of future years. Designing and testing buildings and services design options based on future weather data can be used to evaluate the energy impacts of future climate changes and will play a major role in identifying design options to reduce energy demands and CO₂ emissions (Farah et al. 2019).

1.2- An overview of Dubai city

One location where there is a lack of forecasted future dynamical downscaled weather datasets under climate changes is Dubai. Dubai city, the most popular city in UAE, is located at a latitude of 25.26° North and 55.31° East and its northern sub-region is covered with desert belt (Latlong.net 2020). The climate of Dubai city is hot arid, with an average temperature ranging from 19.5° in winter to 36.5° in summer. Though, often there are some cold days in winter from December to February and the winter sometimes extends into March. The rainfall of the city is low, around 100 millimeters/year, and the amount of solar radiation is high ranging from 8-11 hours per day (Climatestotravel.com 2020).

In the past few decades, Dubai has experienced rapid transformation of its built environment which requires more development analysis for the city. The profile of the city is facing four main challenges including high population growth, being an international trading center, its urban

expansion, and its economic growth (Haggag 2007). These challenges are readily seen in the center of the city around “*Sheikh Zayed Road*”, where we can note high-rise buildings, a metro station, and a highway with six driving lanes on each side of the road (Johnson 2020), see figure 3 below.



Figure 3: The center of Dubai city, “*Sheikh Zayed Road*” (Johnson 2020).

1.3- Energy demand in Dubai

Dubai Electricity and Water Authority (DEWA) is implementing a demand side management (DSM) strategy which has 9 programs and is aiming to achieve 30% reduction of energy and water consumption by 2030 (Innogy.ae 2020). These DSM initiatives include retrofitting, energy efficient solution/ technologies, conservation measurement, and lighting replacement (Dubai Electricity & Water Authority (DEWA) | Annual Statistics 2018). Although energy conservation

plans are created and implemented in Dubai, the demand of energy is still increasing and this is due to the high population growth of the country. According to DEWA annual statistical report 2018, and as shown in figure 4, the number of customers has increased by 48,156 (around 5.7%) from 2017 to 2018.

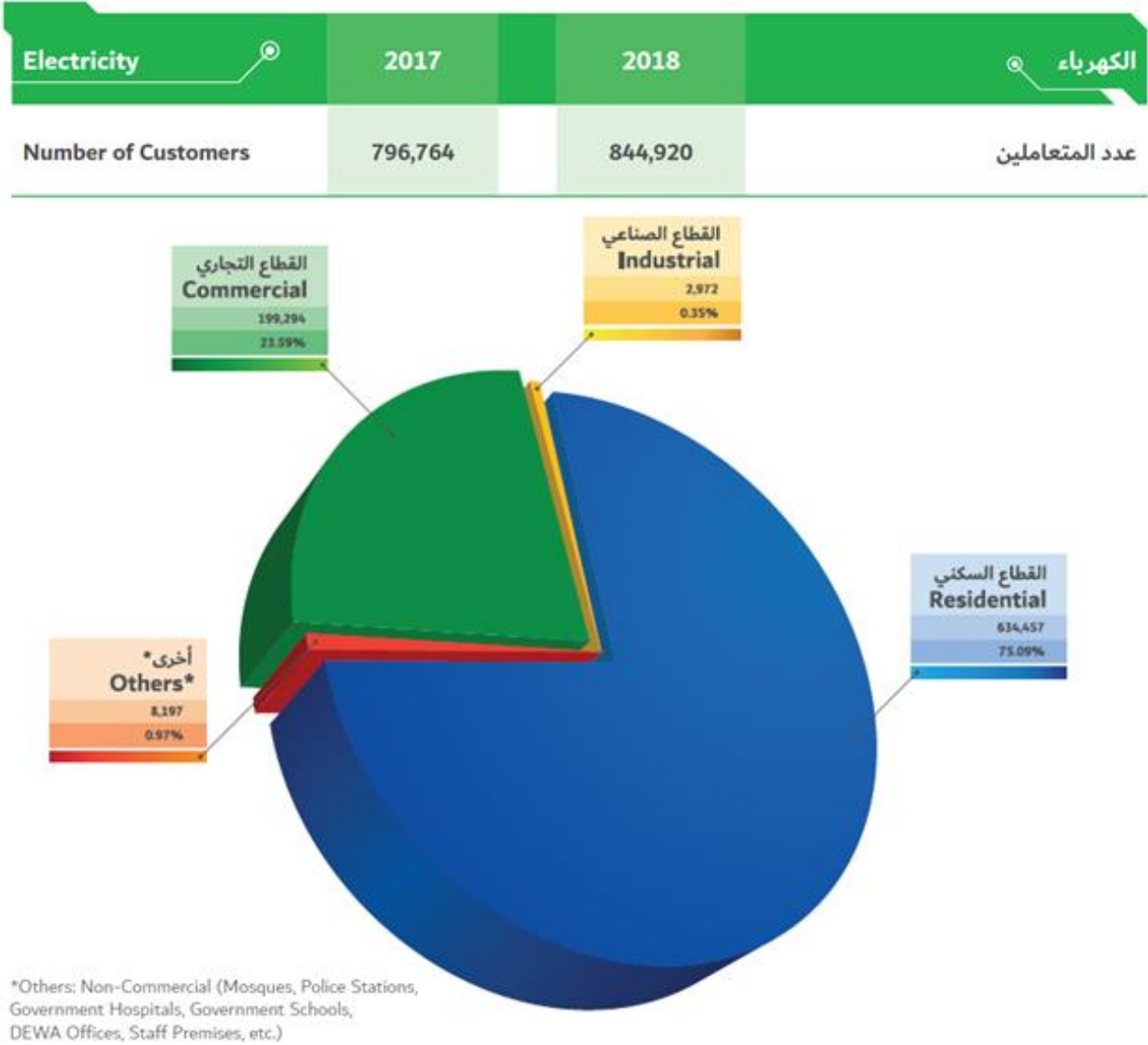


Figure 4: Number and percentages of electricity consumers in Dubai (Dubai Electricity & Water Authority (DEWA) | Annual Statistics 2018).

Moreover, the report shows that the annual system energy requirement increased by 798GWh from 2017 to reach 45,960 GWh in 2018 with the buildings sector consuming around 85.28% of the annual electricity in 2018 which is the highest percentage compared to power and desalination stations, and industrial sector where they consumed 8.28% and 6.44% respectively (Dubai Electricity & Water Authority (DEWA) | Annual Statistics 2018). Therefore, applying energy saving technologies and retrofit solutions for buildings is important to achieve the sustainable goals of Dubai city and to reduce GHG emissions caused by buildings.

1.4- Research problem statement:

All dynamic building simulation tools are based on present weather conditions. Thus, as climate is changing, those buildings will deteriorate and the cooling/heating demand will increase. Our problem in UAE and Gulf region is that most of the buildings are designed and simulated based on present weather data and it doesn't take into account the future climate change, which in fact will lead to significant increase in annual energy consumption in building sector and will reduce the resilience of buildings to weather change in future. The solution of this problem is to use future weather datasets in building simulation tools to examine solutions and techniques that will improve buildings performance and resilience to reduce energy bills and minimize any increase due to changes in future weather conditions. Solutions and techniques will include improving insulation properties, glazing characteristics, and enhancing building services systems for new and existing buildings.

1.5- Aims and objectives:

- This research aims to find the optimal energy saving solutions for high-rise buildings in the UAE that address the local predicted future climate changes using dynamic thermal

modelling tools. Forecasted annual hourly weather data files with different periods throughout the 21st century and emission scenarios will be used to investigate how well energy efficiency solutions improve the energy related resilience of a typical UAE high-rise building to climate change. The study aims to produce findings that support engineers, designers, and facility managers to design and retrofit high-rise buildings according to the present and future weather conditions. The outputs will also provide electricity suppliers with indications of how building electricity demands in the UAE will likely change in the future.

1.5.1- Objectives

- Characterize the building cooling energy related features of projected future changes in the UAE climate through the 21st century accounting for industry accepted IPCC emission scenarios and data sources.
- Evaluate the impact of projected climate change on building energy demands of a typical high-rise building in UAE.
- Identify suitable energy efficiency solutions for reduction of annual cooling demand in a typical high-rise building.
- Evaluate how the energy savings from energy efficiency solutions vary as the climate changes in the future using projected future weather data and dynamic thermal simulation.

1.6- Dissertation Organization

The overall structure of the study takes the form of five chapters, including this introductory chapter, the content of each chapter is described below:

- The first chapter of this dissertation is the introduction, this chapter explains the need of taking climate change into consideration regarding designing and retrofitting buildings in UAE. Moreover, it gives an overview of Dubai city and its annual energy consumption. To demonstrate the research necessity, research problem statement, aims and objectives are included in this chapter.
- The next chapter is the literature review, this chapter provides previous studies on relevant topics to the research such as climate change, future energy consumption by buildings taking into consideration global warming, and energy efficient technologies and their effect on present and future energy consumption.
- The third chapter is concerned with the methodology used for this study. It includes the base case model specifications and how it complies with Dubai city regulations and standards. Then, it provides a description and analyses of the selected present and future weather files, the methods used to make them, the models used to derive them, and which period and emission scenario they represent. The last part of this chapter includes the selected energy efficient solutions/technologies and their specifications.
- The fourth chapter is results and simulation, this chapter include the results of HVAC auto-sizing of the base case model and the amount of cooling and total energy required to operate the building. Furthermore, it explains how applying the selected solutions/technologies will reduce the energy in present and future periods, and it gives

an insight about the percentage increase of energy consumption by high-rise buildings in UAE in stabilization and high emission scenarios.

- The last chapter is the conclusion and recommendation for future studies, also it include the research limitation and some suggestions to further research in future.

To resist the climate change challenges and its effect on high-rise buildings energy consumption in a country with hot arid climate like UAE was the main goal in this research. To achieve this, different solutions/technologies were applied to the base case model including different insulation layers, glazing with different characteristics, and adding heat recovery units to the HVAC system. Subsequently, several simulations with the selected weather files were conducted to study how applying those technologies would affect the present and future energy consumption and to test how they would improve the building resilience toward climate change.

Chapter 2: Literature Review

2.1- Climate Change and Predicted Future Weather Datasets

Implications of climate change on the building sector and the expected rise in future extreme weather events due to global warming are driving designers and engineers to consider ways of improving building energy performance more often in their designs and use of retrofit solutions.

The external envelope of a building is highly affected by climate change, it is expected that an increase of temperatures will lead to increased cooling loads whilst decreasing heating loads.

This expectation that global warming will highly affect the energy demands of buildings is of particular concern in countries that requires high levels of cooling throughout the year.

One of the main natural processes that is driving climate change is the greenhouse effect.

Greenhouse effect is caused by the greenhouse gasses (GHG) where they accumulate in the atmosphere and trap the sun light. This process is responsible to increase the earth temperature by 33°C more than it could be to allow the life to exist on earth. However, due to the increase of GHG emissions that is caused by agriculture and industrial revolutions and fossil fuel burning,

more GHG are released into the atmosphere. As a result, additional heat is trapped in the atmosphere causing the temperatures in earth to increase (Greenhouse effect n.d.). Figure 5

below illustrated the greenhouse gas effect in 6 steps. Steps 1 to 4 are the natural greenhouse effect that gives earth the needed warm to sustain life on it, while steps 5 and 6 describes how the release of GHG from human activities is trapping extra heat in earth causing an enhanced greenhouse effect.

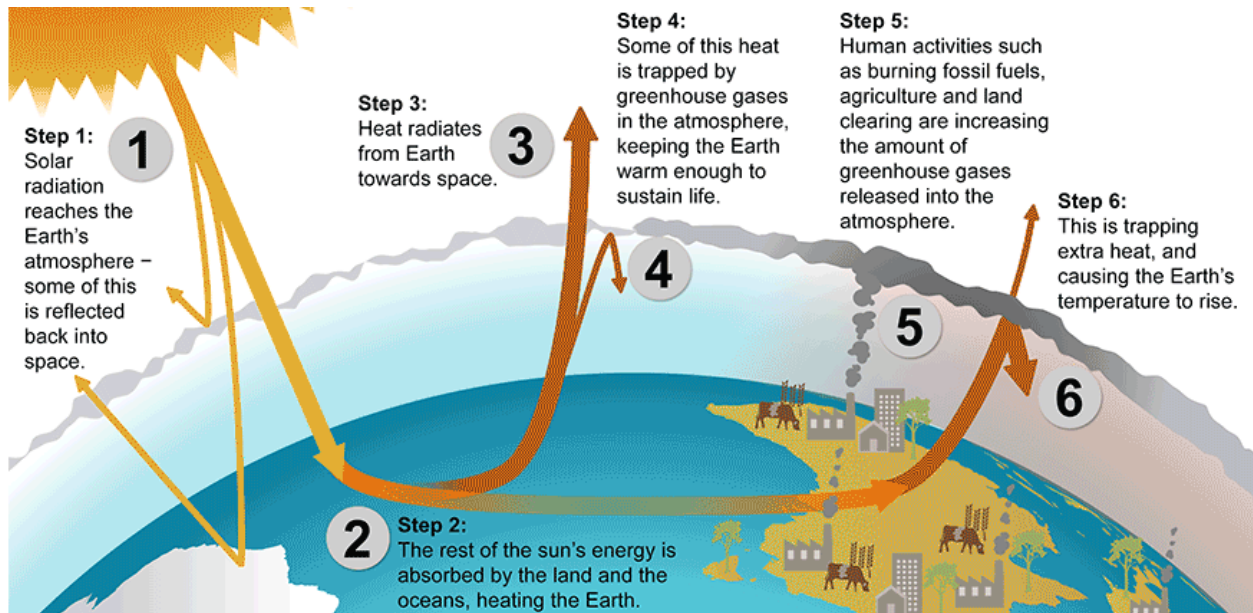


Figure 5: Description of natural and enhanced greenhouse effect process (Greenhouse effect n.d.).

The hot arid climate of the United Arab Emirates (UAE) indicates that buildings in the UAE are expected to consume more energy for cooling in coming years. Therefore, creating future weather datasets that cover the lifetime of buildings and can be used in building simulation tools will enable designers and engineers to find the most appropriate building services and building envelope technologies that increase a buildings energy robustness and overall reduce energy consumption, with its associated GHG emissions into the future.

Building simulation software such as the Integrated Environmental Solutions – Virtual Environment (IES VE) are widely used to evaluate the effect of climate on building performance and energy consumption. They use different weather parameters such as dry bulb temperature, wet bulb temperature, wind speed and its direction, cloud cover, solar radiation; altitude and azimuth etc. These parameters are provided on an hourly basis for a typical meteorological year (TMY) that is usually sourced from a meteorological office representative of the climate at the specific geographical location of a building project.

To evaluate how building energy performance can be expected to be affected by climate change, weather datasets for future years, covering all the weather parameters noted above (hourly & daily) for a specific location are needed. These datasets are not usually available as standard with most building simulation software but they can be generated using different methods and tools. Historical climate data can be converted to future weather data sets by downscaling the Global Climate Models or General Circulation Models (GCMs) either by the dynamical downscaling or statistical downscaling. Then, the generated files need to be converted into readable format by the simulation tool (Moazami et al. 2019).

Awareness of future climate change is rising and there is much work by environmental agencies on investigating climate change risks by studying effects and developing mitigation plans. Many countries signed the Paris Agreement with the United Nations Framework Convention on Climate Change (UNFCCC) including the UAE. With the UAE being ranked 34th in the world for GHG emissions, it contributed to the global climate change mitigation effort on 22nd October 2015 by planning to reduce per-capita emissions by 9% between 2010 to 2030, see Table (1) below (Climatecollege.unimelb.edu.au 2020).

Table (1): UAE Rank for GHG emissions and planned future % reduction per capita (Climatecollege.unimelb.edu.au 2020)				
Country	Rank or worldwide emission in year 2011	Percentage of per Capita Reduction (2010 – 2030)	2010 emissions per capita <u>(tCO₂eq/cap)</u>	2030 emissions per capita <u>(tCO₂eq/cap)</u>
UAE	34	-9%	27.9	25.6

The Intergovernmental Panel on Climate Change (IPCC) created different emissions scenarios based on socio-economic characteristics to represent expected changes in global GHG emissions and in turn these have been used in climate models to predict how the climate will change in the future. It is mentioned in the latest IPCC's fifth assessment report (AR5) that was created in 2014 that GHG atmospheric concentrations in year 2011 for CO₂, CH₄, and N₂O were measured to be 391 ppm, 1803 ppb, and 324 ppb respectively. These concentrations represent percentage increases from pre-industrial times of 40% for CO₂, 150% for CH₄, and 20% for N₂O (IPCC: Summary for Policymakers 2013). As mentioned before, the increase of GHG's in the atmosphere is enhancing the greenhouse effect and thereby climate changes. Therefore, reducing emissions of these GHG's from operating buildings is a key area of climate change mitigation.

One scientific measure of the effect human related GHG emissions on the climate is the anthropogenic radiative forcing (RF) effect. This measure represents the extent to which the concentration of a GHG has on earth energy fluxes. The AR5 report noted that the total anthropogenic RF change measured for year 2011 compared to year 1750 showed an increase by 2.29 W.m⁻² (see figure 6 below). As shown in figure 6, CO₂ is the GHG which causes the largest RF (1.68 W.m⁻¹ at a very high level of confidence) followed by CH₄ with (0.97 W.m⁻¹ at high confidence) which is affected by CO₂ as well. This reveals that CO₂ emission plays a major role in climate change. Positive RF accounts for temperature increase and it is the main cause of global warming while negative RF accounts for temperature decrease (IPCC: Summary for Policymakers 2013).

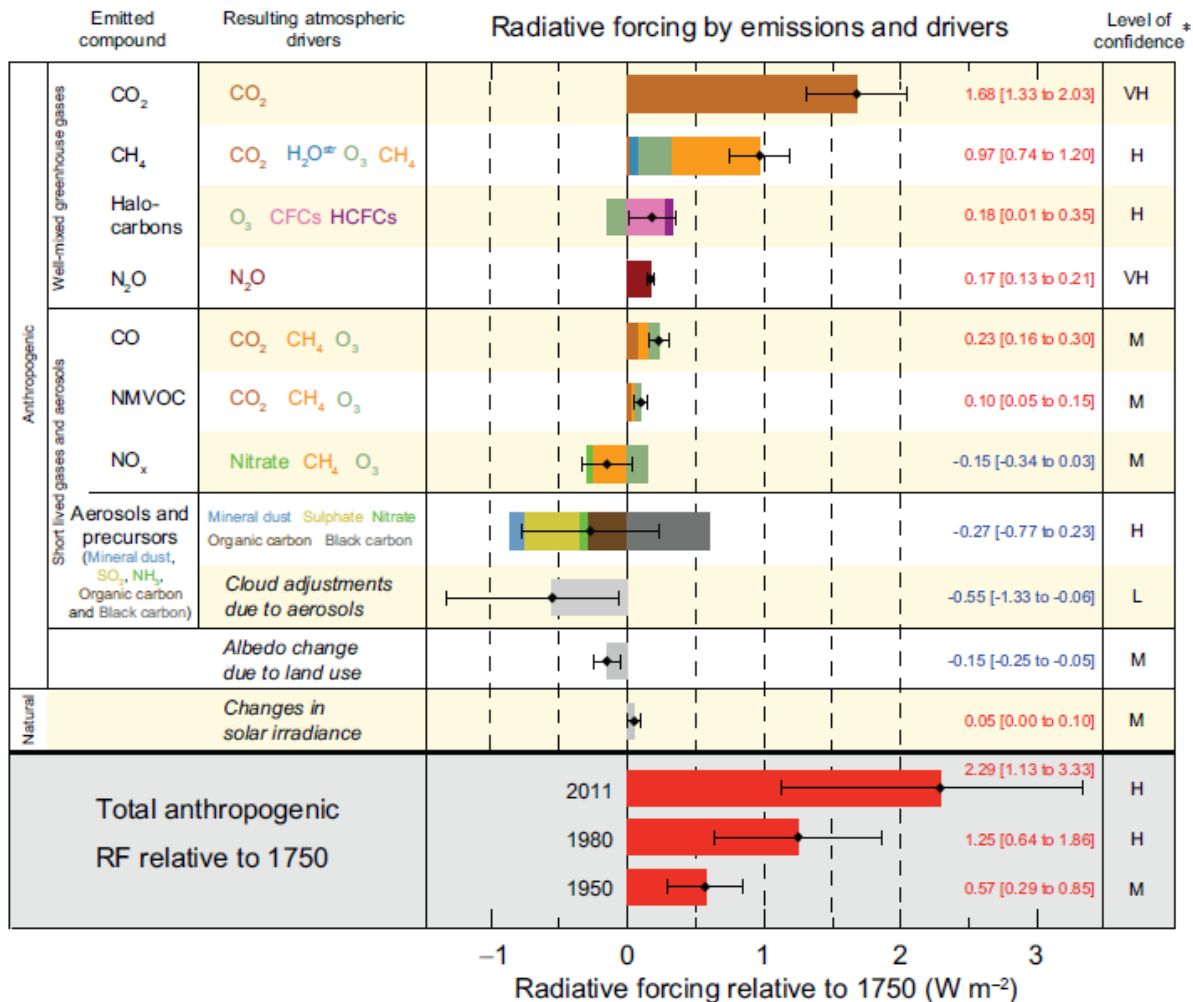


Figure 6: Emitted compounds and their radiative forcing and level of confidence (IPCC: Summary for Policymakers 2013).

*In the right side of the figure is the source level of confidence: VH - is very high level of confidence, H - is high level of confidence, M - is medium level of confidence, and L - is low level of confidence

As mentioned before in section 1.1, the IPCC created a range of different emission scenarios. Those scenarios are called “Representative Concentration Pathways” (RCPs), see Table (2) below.

Table (2): RCPs Total radiative forcing, type of scenarios, predicted changes in global mean temperature and CO₂ concentration for year 2100 based on AR5 report of the IPCC (IPCC: Summary for Policymakers 2013).

Representative Concentration Pathways (RCPs)	Total radiative forcing in 2100 (W.m ⁻²)	Type of scenario	Increase of Global Mean Temperature (Celsius)	CO ₂ concentrations
RCP 2.6	2.6	Mitigation scenario	0.3° - 1.7°	421 ppm
RCP 4.5	4.5	Stabilization scenario	1.1° - 2.6°	538 ppm
RCP 6.0	6.0	Stabilization scenario	1.4° - 3.1°	670 ppm
RCP 8.5	8.5	Very high GHG emissions	2.6° - 4.8°	936 ppm

RCP's are used to generate future predicted climate conditions using Global Climate Models or General Circulation Models (GCMs). These models are based on a monthly temporal resolution and have a coarse geographical spatial grid of between 100~300 km². Results from GCMs can be downscaled to an appropriate resolution to be used in building simulation software by using either a dynamical downscaling or statistical downscaling techniques. Then, hourly weather files can be generated and converted into a readable format to be used in a building simulation tool (Moazami et al. 2019).

2.2- GCMs downscaling approaches

GCMs can be downscaled using a dynamical approach to produce Regional Climate Models (RCMs) or by using statistical approach which downscale the GCM either by morphing or stochastic methods, see figure 10 below. RCMs are refined projections of GCMs with a higher

resolution of topographic data (Moazami et al. 2019) taking into account more detailed information about each grid and can include future extreme weather conditions into account.

2.2.1- Downscaling using dynamical approach

A dataset was prepared by the Environmental Agency of Abu Dhabi (EAD) in collaboration with the National Center of Atmospheric Research (NCAR) to generate present and future dynamical downscaled weather data files. They used GCMs with 3-dimensional data sets and 6-hours' time step. The future predicted files include future changes in average temperature, daily, annual, and average rainfall, wind speed, diurnal cycle, mean precipitation, wet day index (total number of days with rainfall > 1mm over 20 years period), specific humidity, heat wave duration index, wind change, and sea level pressure (Glavan 2015).

RCMs were prepared using GCMs from the 4th and 5th reports of the IPCC (AR4 & AR5) indicating the climate changes of the UAE and Arabian Peninsula. The NCAR used the Weather Research and Forecasted Model (WRF) to dynamically downscale the GCM into 36 km grid resolution for the eastern hemisphere, 12 km grid resolution for the Arabian Peninsula and 4 km grid resolution for the UAE. Deriving the RCM from GCM requires large storage and computational power to do the spatial and temporal downscaling, and the quality of the results is dependent on the accuracy of the GCM used. This NCAR model included two different scenarios (RCP 4.5 & RCP 8.5) for the 3 mentioned grid spacing resolutions. For the UAE, 10-year bias-corrected conditions were simulated using the NCAR Community Earth System Model Version 4 (CCSM4) for the historical period (1990 to 2000) along with the future period (2065 to 2075). In the simulated future period, the project has listed 2° ~ 3° C increase of average temperature for UAE for the RCP 8.5 scenario, and it's expected to have 50-100% increase of rainfall in Dubai, Sharjah and Abu Dhabi city. The daily mean precipitation is expected to increase from 0.38mm

in 1980 to 0.43mm in 2100. Humidity is expected to increase by 10% across the UAE and the change in humidity is greater in summer periods (Glavan 2015).

2.2.2- Downscaling using statistical approach

The alternative approach to generating RCMs to produce more location specific models of future climates is to apply statistical downscaling to climate results produced by GCMs. In this statistical based approach historical weather data is used to formulate the spatial downscaling then the temporal downscaling is done by using either morphing or stochastic methods that maps variations from historical data to predicted future weather data. Due to the complexity of dynamical downscaling, designers, engineers, and building simulation software users prefer to use the statistical approach. However, RCMs produced by dynamical downscaling can provide high resolution hourly weather data in any location worldwide. Therefore, the use of dynamical downscaling is expected to increase in the future (Moazami et al. 2019).

Figure 7 below illustrates a comparison from a study done by Moazami et al. (2019), which compared between 111 articles that used future climate data in simulation tools to assess building performance. It was found that 34% of data included typical and extreme future climate conditions while 66% used only typical future climate conditions. The statistical downscaling recorded about 52% of the total articles, while dynamical downscaling, hybrid downscaling, and recorded data achieved 13%, 25%, and 10% respectively. Therefore, it is noted that statistical downscaling is the most popular approach that is used by building simulation tool users.

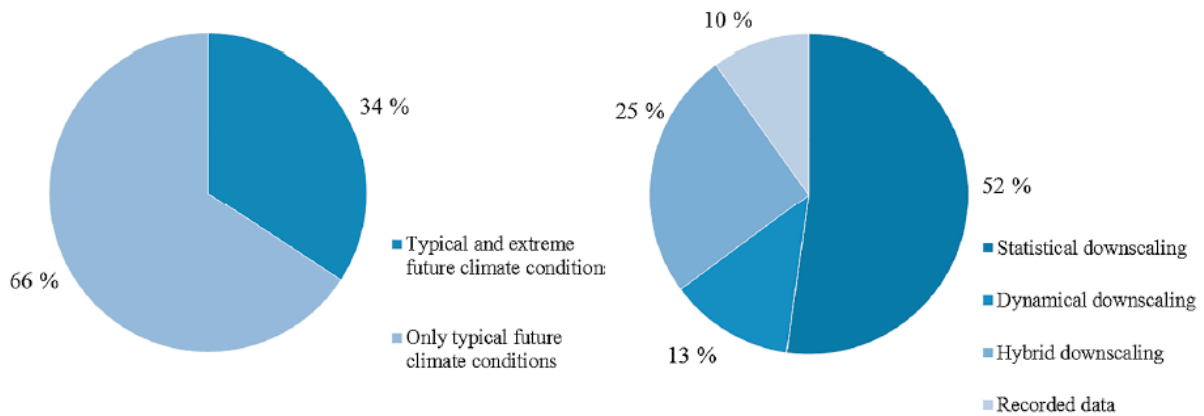


Figure 7: Percentages of the types and approaches of future climate data that used in simulation tools to assess building performance in 111 articles (Moazami et al. 2019).

Morphing is a downscaling method that uses algorithms to transform hourly weather variables based on monthly conditions and differences of GCMs or RCMs for a specific location. Those algorithms are shifting, stretching, and the combination of shifting and stretching, methods and their function are described in table (3) below. Selection of the appropriate algorithm method is dependent on the weather variable. For example, shifting is used to calculate the atmospheric pressure, while stretching is used to calculate wind speed, and the combination of shifting and stretching is used to calculate air temperature. WeatherShiftTM and CCWorldWeatherGen are two main tools that use morphing method to create future weather files for simulation tools.

Algorithm method	Shifting	Stretching	Combination of shifting and stretching
Equation	$x m = x_0 + x_m$	$x m = m \cdot x_0$	$x m = x_0 + x_m + \alpha_m (x_0 - x_{0,m})$
Description	Shifting method is performed by adding the absolute monthly mean change (x_m) with weather variables	Stretching method is performed by multiplying and scaling	Shifting and stretching are combined in one

	hourly values (x_0) for a specific month (m). (x_m) is derived from RCMs and GCMs	the weather variables hourly values (x_0) with the absolute monthly mean change (x_m)	linear equation to find the weather variable.
--	--	---	---

Downscaling by stochastic method creates future weather datasets by analyzing previous climate data (Moazami et al. 2019). Only few independent weather parameters are used as an input to derive the other parameters. Meteonorm is a software that uses this method to generate future weather files by interpolating weather variables to create weather datasets for any location in the world. The output datasets are available in many formats depending on the simulation tool used and they include many variables such as daily global radiation, daily temperature, solar radiation, average temperature, precipitation, and sunshine duration (Meteonorm 7 2019). Figures 8 and 9 below illustrates the differences between future average temperatures in Dubai city between 2020 and 2050 using the stochastic method. It is noted that minimum and maximum temperatures vary by $1^{\circ}\sim 2^{\circ}$ C from 2020 to 2050. Therefore, the city is expected to have cooler winters and hotter summers in future.



Figure 8: Average temperature in 2020 in Dubai, UAE (Meteonorm 7 2019).

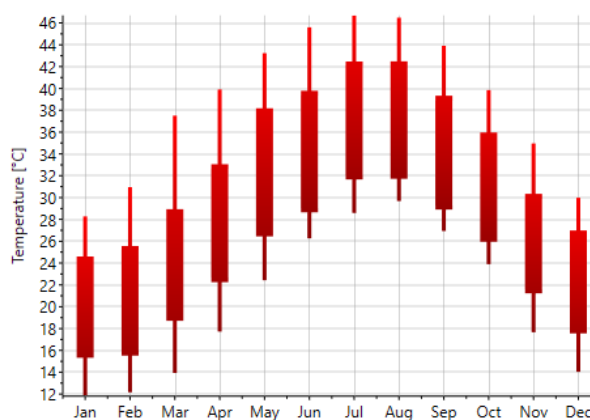


Figure 9: Average temperature in 2050 in Dubai, UAE (Meteonorm 7 2019).

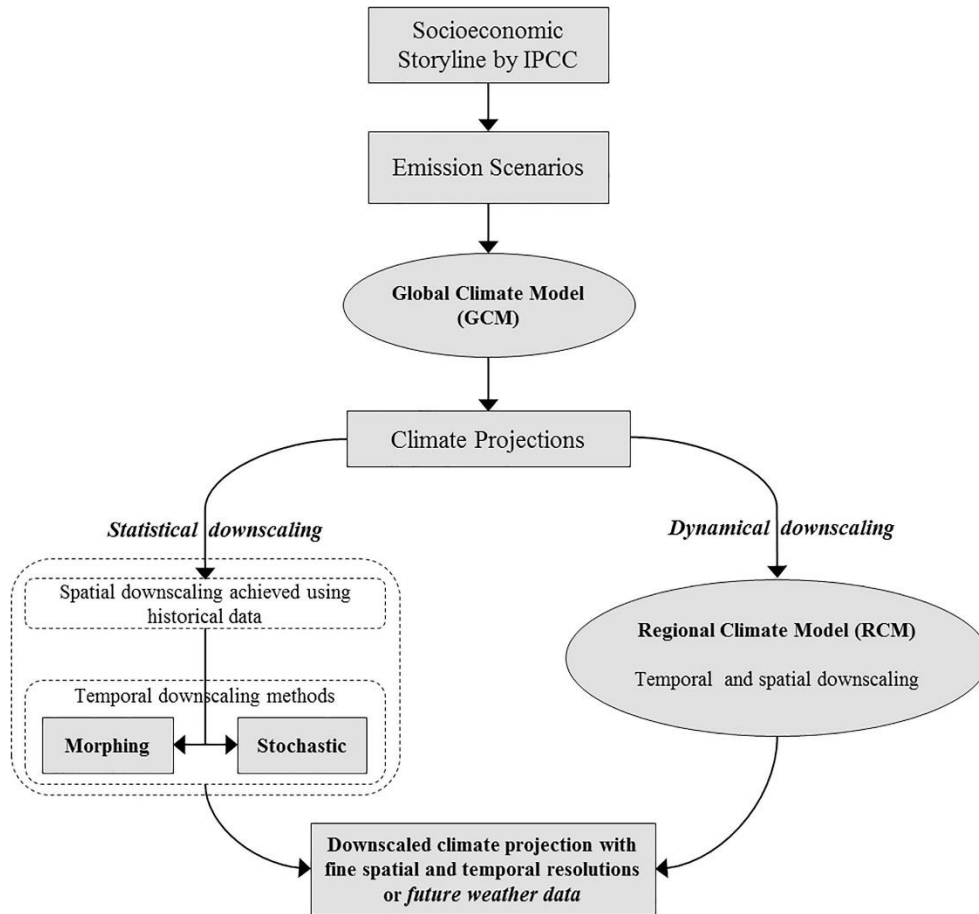


Figure 10: Flowchart of the methods used to generate predicted future weather datasets for building simulation software (Moazami et al. 2019).

Figure 10 above summarize how the predicted future weather datasets are generated and downscaled by different methods. It starts by selecting the internationally accepted emission scenario provided by IPCC, then the emission scenario is applied to the GCMs to get the climate projections. After that, a downscaling method is used to create required future weather dataset.

2.3- Study cases on impact of climate change on building energy consumption

A study by Zhai and Helman (2019) analyzed the impact of climate change on the campus of University of Michigan in the United States. This site was selected because it has several types of buildings, which make it easier to find energy consumption for large scale area rather than

selecting the whole city. As energy use intensity varies depending on the building type, they divided the university campus building stock into 5 building types based on size and use. The proposed design included labs, clinics, residential, services, and campus buildings. Five typical models were created using energy plus software to evaluate the change in annual energy consumption, heating and cooling energy, and peak hour energy demand in the future. Four climate models were selected based on their emissions which were classified as low, low-mid, mid-high, and high emissions. They were used to prepare 12 weather data files that represent 3 future periods with average hourly time step. The first, second, and third periods are created by averaging the years 2010-2039, 2040-2069, and 2070-2099 respectively. Then, those weather files were implemented to the 5 typical building models. The power plant that is feeding the campus produces around 150,000 MWh/year (Zhai & Helman 2019).

Figure 11 below illustrates the annual added cooling load for the 3 periods. The average of the 4 models recorded an annual increase of 11,800 MWh for period 1, 20,775 MWh for period 2, and 31,939 MWh for period 3. This makes an increase of 8%, 14%, and 21% from the total annual production of the current power plant. Moreover, the high emissions model resulted in an increase of 68,800 MWh in period 3 which is an increase of around 46% of the total annual production of the current power plant (Zhai & Helman 2019).

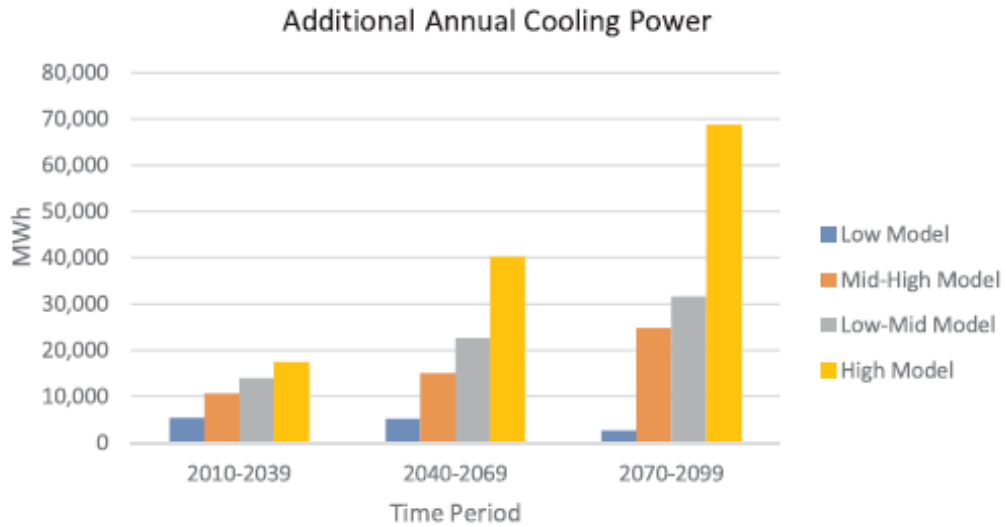


Figure 11: Amount of annual required cooling energy needed for campus for the 3 future periods based on 4 emission scenarios (Zhai & Helman 2019).

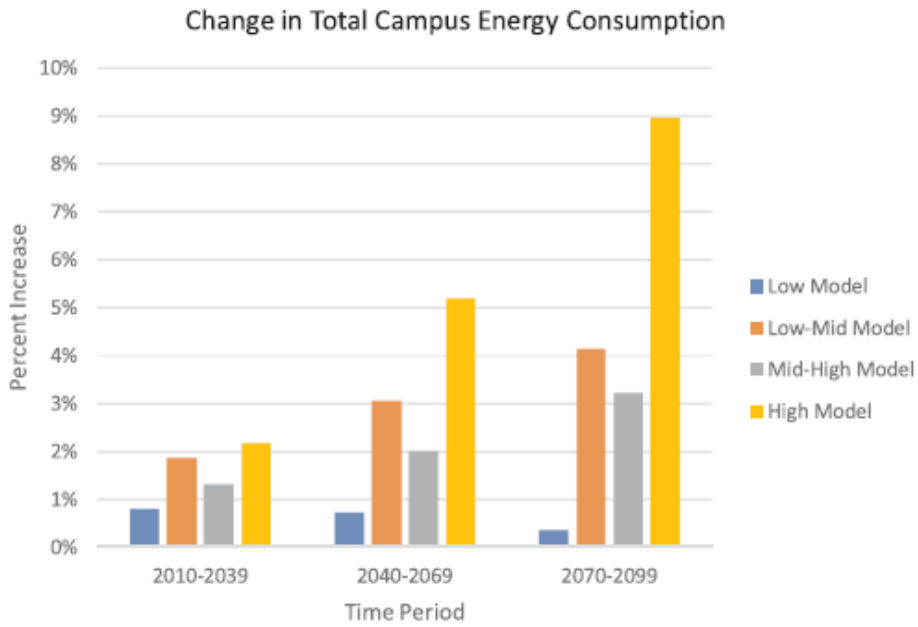


Figure 12: Percentage increase in total energy consumption of the campus (Zhai & Helman 2019).

As shown in figure 12 above, the total energy consumption is increasing in the 3 time periods and for the 4 models. The study has revealed that the energy consumption is predicted to change widely. Low model which represents 2.6 RCP scenario has recorded less than 1% increase of energy consumption in the 3 periods. On the other hand, the high model had the highest percentages among the four through periods 1 to 3 with 2%, 5%, and 9%, respectively (Zhai & Helman 2019).

Furthermore, the study showed that 27% increase in peak hours energy demand is expected in future. This creates an alarm to the campus utility providers to increase the production to achieve the expected future energy demands (Zhai & Helman 2019).

Another study by Moazami et al. (2019) compared different types of future predicted weather files based on their downscaling method and checked its effect on building energy consumption. The aim of this study was to allow designers and engineers to test their building energy robustness against future climate change. Dynamical and statistical downscaling were included in the study. Moreover, future weather data that depends on historical weather conditions were compared with data that depends on extreme weather conditions. Three weather generating statistical tools that were used in this study are Meteonorm tool, WeatherShift™ tool, and CCWorldWeatherGen tool. Moreover, one RCM weather data set dynamically downscaled from the Rossby Centre Regional Atmospheric Climate Model (RCA4) with hourly temporal resolution and 12.5 km² spatial resolution was generated as well (Moazami et al. 2019).

A total of 74 weather data files were created, two files represent typical metrological year, 9 files are statistically downscaled where 6 of them were generated by morphing method and the other 3 were generated by stochastic method, and 63 files were dynamically downscaled where 21 of them represent typical weather conditions and the other 42 include extreme weather conditions.

Weather files were classified for three time periods, near-term, medium-term, and long-term as shown in table (4) (Moazami et al. 2019).

Table (4): Years used by the generating tool for each adopted future term (Moazami et al. 2019).

Adopted Term	CCWorldWeatherGen	WeatherShift™	Meteonorm	RCA4
Near-term	2011-2040	2026-2045	2011-2030	2010-2039
Medium-term	2041-2070	2056-2075	2046-2065	2040-2069
Long-term	2071-2100	2081-2100	2080-2099	2070-2099

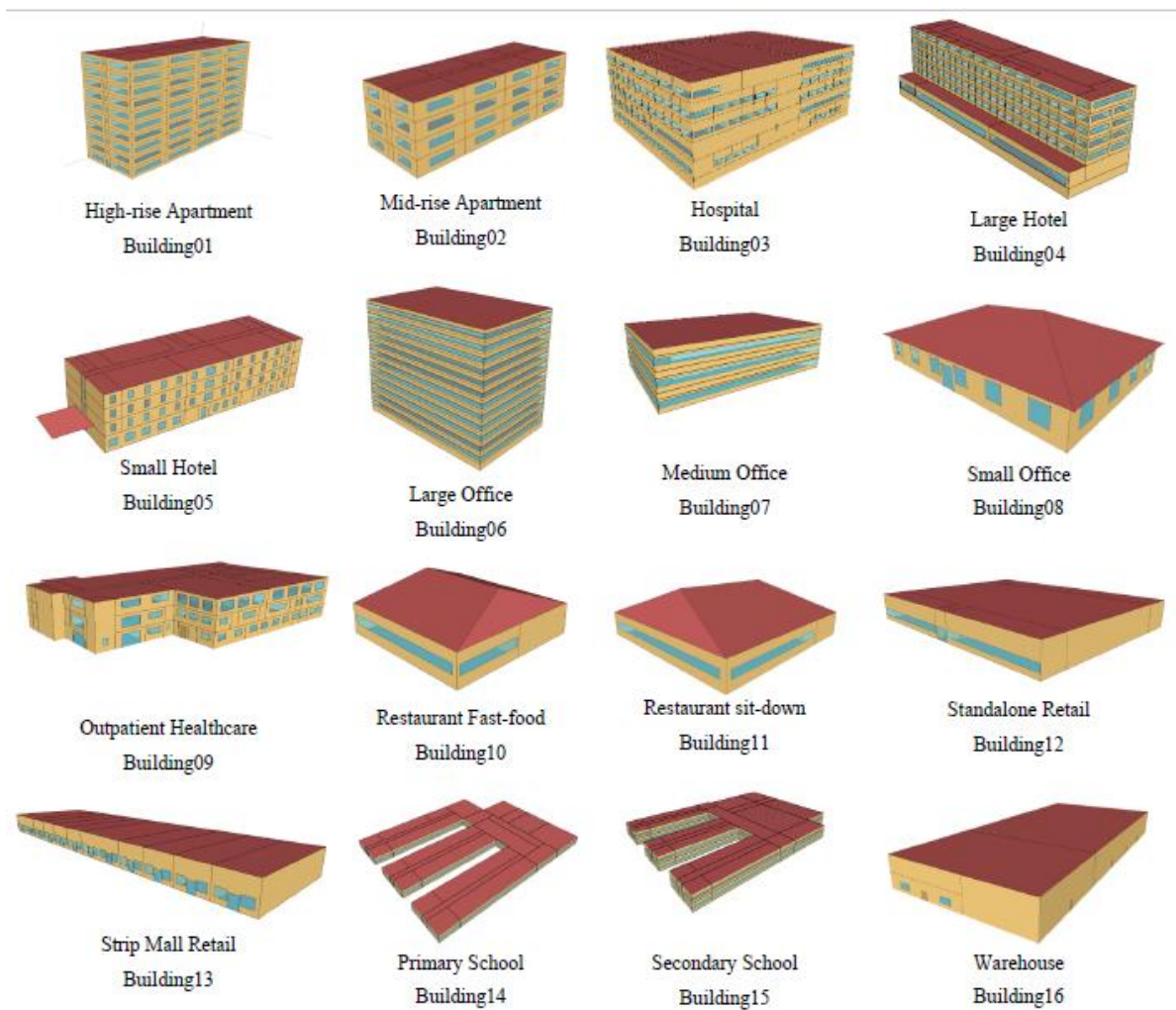


Figure 13: Types of the 16 buildings used in the project (Moazami et al. 2019).

City of Geneva, Switzerland was the location in this study and as shown in figure 13, the building stock was divided into 16 buildings based on type, size, U-value, and solar heat gain coefficient complying with ASHRAE 90.1 standard, each type was simulated using energy plus software. Also, a neighborhood was created by combining single buildings with ASHRAE standard referenced buildings and simulated as well.

Their results show that all predicted future weather files are useful to find the effect on climate change on energy demand of buildings. However, the 16 buildings simulated and compared for summer months where heat waves are expected using extreme weather year (EWY) data and typical downscaled year (TDY) data found that peak load cooling using EWY, a year that considered extreme weather conditions, recorded higher percentages 2% - 28.5% more than the TDY, see table (5) below. Therefore, including extreme weather conditions in predicted future weather datasets is critical to reduce the risks on building designs and increase their resilience to future climate change (Moazami et al. 2019).

Table (5): Amount of peak cooling load for each type of buildings used in the project and the neighborhood, the cooling peak load in summer is compared using multiple weather files of TDY and EWY and the percentage of change is represented (Moazami et al. 2019).

Building name	Dynamical-typical TDY _{Multiple}		Dynamical-extreme EWY _{Multiple}		Peak cooling load relative change EWY _{Multiple} to TDY _{Multiple} (%)
	Peak load for cooling (kW)	Date-Time	Peak load for cooling (kW)	Date-Time	
High-rise Apartment	59.97	19 Jul-17:00	62.27	24 Jul-19:00	3.8%
Mid-rise Apartment	18.76	19 Jul-15:00	21.22	27 Jul-15:00	13.1%
Hospital	235.01	20 Jun-15:00	239.67	24 Jul-15:00	2.0%
Large Hotel	147.61	28 Jul-19:00	172.21	19 Jul-16:00	16.7%
Small Hotel	34.71	19 Jul-16:00	38.06	27 Jul-16:00	9.6%
Large Office	430.21	20 Jun-17:00	453.95	24 Jul-15:00	5.5%
Medium Office	63.03	19 Jul-15:00	70.55	27 Jul-16:00	11.9%
Small Office	5.00	19 Jul-16:00	5.47	27 Jul-16:00	9.5%
Outpatient Healthcare	93.32	20 Jun-15:00	100.82	7 Jul-16:00	8.0%
Restaurant Fast-food	11.30	19 Jul-13:00	14.16	3 Jul-18:00	25.4%
Restaurant sit-down	17.96	19 Jul-12:00	23.08	3 Jul-18:00	28.5%
Standalone Retail	34.69	19 Jul-15:00	42.29	27 Jul-15:00	21.9%
Strip Mall Retail	30.57	19 Jul-15:00	38.64	27 Jul-15:00	26.4%
Primary School	97.27	20 Jun-15:00	109.06	13 Jun-15:00	12.1%
Secondary School	316.51	20 Jun-15:00	348.09	13 Jun-15:00	10.0%
Warehouse	5.54	19 Jul-16:00	6.78	27 Jul-17:00	22.5%
Neighborhood	3457.14	19 Jul-16:00	3753.82	27 Jul-16:00	8.6%

2.4- Technologies and solutions to reduce energy demand in buildings

There are many technologies and solutions that can be implemented to new and existing buildings that reduce the energy consumption and GHG emissions significantly. To increase the resilience of UAE buildings and resist climate change in future retrofit initiatives and energy saving solutions should be applied to new and existing buildings. Nowadays, sustainable designs, retrofit solutions, and following building rating standards are highly recommended by government entities in UAE. Moreover, tenants and owners prefer to live in green buildings due to the reduction in electricity bills and the thermal comfort they provide. Therefore, reducing energy demand will improve building performance and increase user satisfaction and long-term financial return (Tobias & Vavaroutsos 2012). Due to expected global warming, finding innovative technologies and appropriate systems to reduce cooling demand in UAE buildings is critical. Several technologies with potential to reduce impacts of future climate changes such as double skin façades (DSF), increasing or optimizing the insulation layers of a building, improving the glazing properties of the building, and adding heat recovery equipment to HVAC systems.

2.4.1- Increasing insulation layers and changing glazing properties

Building envelope type and properties play a major role in defining the amount of required cooling loads particularly in a hot arid country like UAE with high temperatures and levels of solar radiation. It is noticeable that many high-rise buildings in UAE have a large portion of glazing that can reach up to 80% of its exterior envelope area (Tibi & Mokhtar 2014). Therefore, selecting appropriate glazing properties and insulation layers to the building envelope can reduce cooling loads and optimize energy consumption significantly. Glazing properties include window to wall ratio (WWR), solar heat gain coefficient (SHGC) or shading coefficient (SC),

light transmittance, and thermal transmittance (U-value). According to Al Sa'fat, Dubai green building regulation, the thermal transmittance (U-value) is defined as the rate of heat transfer in unit time through one m^2 of a structure times temperature difference between each side of the structure, and it has a unit of W/m^2K . Increasing the structure elements insulation will reduce the U-value and vice versa (Al Safat, Dubai Green Building Evaluation System 2016). The shading coefficient is defined as the amount of solar radiation that pass through a glazing compared with the amount of heat that pass through single clear glass (Al Safat, Dubai Green Building Evaluation System 2016). However, most window standards nowadays are using the SHGC rather than the shading coefficient. ASHRAE 90.1 defines SHGC as is "*The ratio of the solar heat gain entering the space through the fenestration area to the incident solar radiation.*" (ASHRAE Standard 90.1 2004 cited in Moazami et al. 2019, p.703). Therefore, trying to reduce the U-value and SHGC will reduce the cooling loads of a building.

2.4.2- Case studies

A study was done by Tibi and Mokhtar (2014) on a typical high-rise residential building (30 m x 30 m) with 50% WWR using IES software. The aim of the study is to compare the cooling energy loads and price between typical single glazing and double glazing with different properties in UAE. As shown in table (6) below, one type of single glazing windows (6mm pane) and 8 types of double glazing windows (two 6mm panes with 12 mm air gap), low-e Film, different SHGC's, and U-values were applied to the building and simulated on IES software (Tibi & Mokhtar 2014).

Table (6): Type and thermal characteristics of the studies window glazing (Tibi and Mokhtar 2014)

Type No.	Composition	Thermal Characteristics	
		U-Value (W/m ² .°K)	SHGC
a	Single glazing (6mm pane)	6.81	0.25
b		2.00	0.29
c		1.90	0.26
d	Double glazing (6mm pane + 12mm air gap + 6mm pane) and low-e Film	1.70	0.21
e		1.50	0.20
f		1.30	0.18
g		1.10	0.14
H		0.14	0.14
I			

Figure 14 illustrates the percentage of annual cooling loads reduction for each glass type. It is noted that the annual cooling loads can be reduced by 5.6% to 9.7% by improving the building glazing properties. Also, we can conclude that type **I** glazing with 1.10 U-value and 0.14 SHGC has the highest amount of reduction (9.7%) amongst other types. While **c** and **d** glazing types has almost the same percentage and performance, same applies to **f** and **g**. Applying the other types results in bigger differences in annual cooling loads reduction. The study has revealed that impact of reducing U-value is small compared to SHGC reduction and this is due to the high annual average solar radiation hours (around 9.7 hrs/day) in UAE (Tibi & Mokhtar 2014).

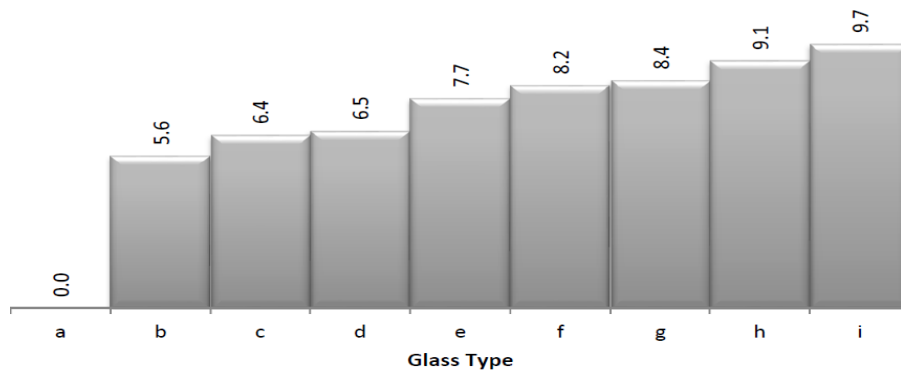


Figure 14: annual cooling loads reduction percentage for simulated types of window glass (Tibi & Mokhtar 2014).

Moreover, this study recommends using type **g** glazing with 1.3 U-value and 0.2 SHGC as it is the most appropriate solution for this type of building taking into consideration the window to wall ratio (WWR), orientation (north-south), life cycle cost (LCC), and climate conditions of UAE. Additionally, the energy saving properties of this type of glass are higher than the minimum requirements of UAE standards and regulations such as Estidama (Tibi & Mokhtar 2014).

Another study done by (Shanks 2018) discussed the effect of different retrofit solutions by simulating one floor of a commercial high-rise building in UAE to study the future climate change impact on energy consumption. The floor is air-conditioned and operates on 10 working hours, with typical heat gains, and has 38% WWR which is similar to many high-rise buildings in UAE. A base case model was created using IES software and simulated with EnergyPlus Weather (EPW) files for present and future years. This study indicates that the solar heat gain will be almost the same in future, while the external conduction gain and the infiltration gain will increase significantly.

As shown in figure 15, the conduction gain by external walls is increasing gradually throughout the years where it started at 3 MWh/yr in 2018 and reached about 6 MWh/yr in 2080. While the glazing conduction gain is increasing rapidly where it started at 4 MWh/yr in 2018 and reached slightly higher than 15 MWh/yr in 2080.

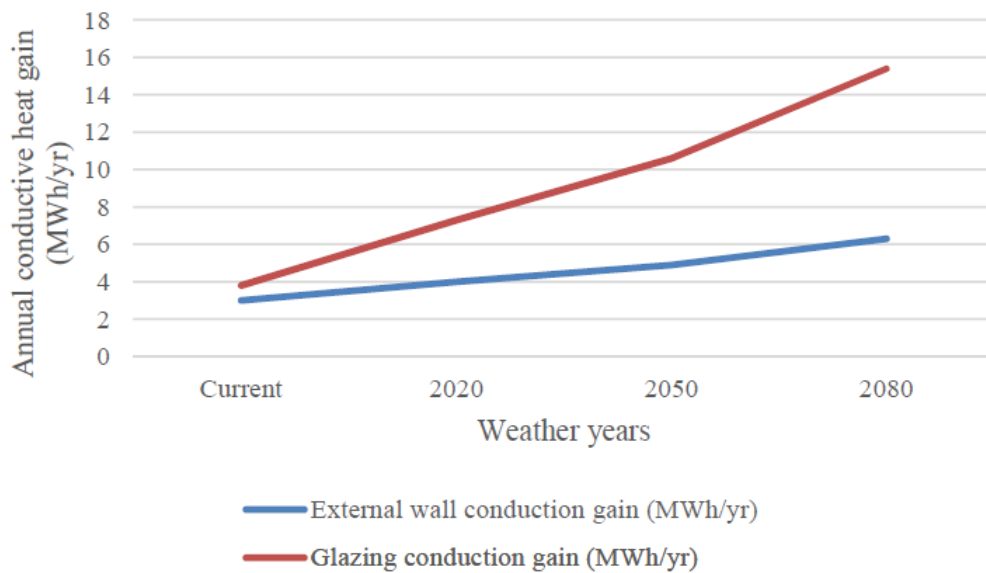


Figure 15: Conduction gains of the base case model for current and future years (Shanks, 2018).

Consequently, some retrofit solutions were applied to the base case model and simulated to study their effect of future annual cooling demand for years (2020, 2050, and 2080) such as improving the glazing, improving external walls, and adding fixed external shading to the building.

Improving the glazing of the base case building was done by retrofitting with double glazing krypton filled glass with low-e film coating, and by changing the U-value from 1.8 to 0.76 W/m²K and g-Value from 28% to 27%. This solution has reduced the future annual cooling demand by 1.5% to 3.1%. The second option was improving the external walls by adding an EPS extra layer (125mm thickness) behind the external panel which improved the U-value from 0.35 to 0.18 W/m²K. However, this solution reduced only 0.5% to 1% from the annual future cooling.

The third option was adding external shadings to the large glazing areas of the building, it achieved a reduction between 3.9% and 5.5% which seemed to be the highest percentage amongst the three options (Shanks 2018). This study also suggests that addressing the internal gains of a building is critical in improving the resilience of buildings to climate change. Also,

further HVAC technologies that provides cooling the incoming fresh air should be provided and simulated to achieve higher annual cooling loads reduction in future.

2.4.3- Double skin façade (DSF)

Double skin facades (DSF) are systems that consist of an additional glazed external envelope (skin) placed up to 1.0m from the external skin of conditioned indoor spaces of a building which creates a cavity that can incorporate ventilation controllers and solar protection devices. They come in a wide range of configurations and are used as an insulation layers to reduce heating loads in cold weather and cooling loads in hot weather which reduces the building energy consumption and GHG emissions. Also, DSF have other advantages such as being an acoustical insulation, decreasing day light transmission, and enhancing natural ventilation in buildings. The airflow between the two outer layers is generally driven by the natural buoyancy force where hot air rises due to pressure differences. However, in some systems, the HVAC air stream passes through the DSF glazing cavity before exhausting to the outside. In some designs, solar fans can be added to DSF rather than connecting with HVAC (Straube & Straaten 2001). The in-between cavity of the DSF comes in different sizes, it can range from 20 cm to few meters (ArchDaily 2020).

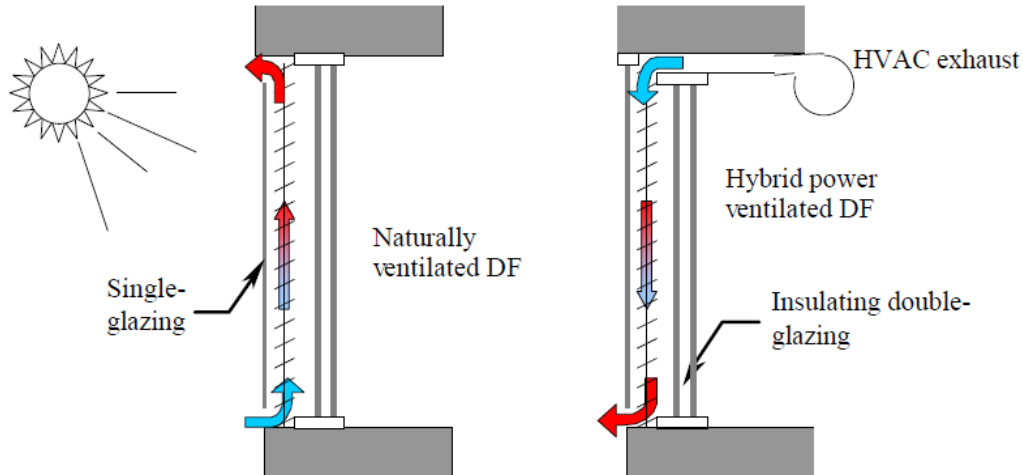


Figure 16: Schematic diagram of natural and hybrid double skin façade (Straube & Straaten 2001).

Figure 16 above illustrates a generic description of DSF glazing, it is noted that the airflow direction is dependent on the type of the ventilation. The DSF can be installed in many ways, it can cover all building stories, a portion of a building height as per design needs, or a single story in a building (Straube & Straaten 2001).

On the other hand, some additional effective techniques can be used to reduce buildings cooling loads such as adding a layer to opaque wall, using extra coatings on external walls to reflect solar radiation, and installing shading system to the building. DSF with transparent enclosure will not be effective to reduce cooling load due to its high solar gain absorption (Straube & Straaten 2001).

Generally, clear glass building facades will absorb high amount of sun light and this can save energy by using daylighting as an alternative to artificial lighting. Nevertheless, this will cause overheating and high levels of heat gains to a building (Straube and Straaten, 2001).

Shading elements are also useful for cooling loads reduction, however; to be effective they should be accompanied with exterior shading. Reflective glazing with high solar heat gain

coefficient (SHGC) is not recommended, as it will increase glare and heat gain to adjoining buildings (Straube & Straaten 2001). Also, using reflective coatings with low (SHGC) (below 20%) is better than using clear glazing because they will reduce the amount of sunlight transmittance especially in countries with high solar radiation like UAE.

Natural ventilation that accompanies double skin façade creates a buffer space between the building and outside which help in providing thermal comfort. However, protected and operable openings should be added to prevent dust, noise, insects, and rain. DSF natural ventilation can be accompanied with mechanical ventilation depending on weather conditions and design requirements (Straube & Straaten 2001).

Table (7): Comparison between DSFs and other glass insulation technologies (Straube & Straaten 2001).

	Solar Heat Gain Coefficient	Visual transmittance	U-value	Sound dB
Opaque wall	<0.02	0.00	<0.35	>45
Double glazing	0.28 – 0.40	0.55 – 0.68	1.1 – 1.4	33 - 35
Double glazing with exterior shades	0.05 – 0.10	0.55 – 0.68	1.1 – 1.4	33 - 35
Double glazing with reflective coating	0.07 – 0.20	0.15 – 0.40	1.4 – 1.5	33 – 35
Triple glazing with argon fill	0.25 – 0.35	0.52 – 0.62	0.8 – 1.1	38 – 45
DSF - vented outer with shades	0.10 – 0.30	0.65 – 0.75	1.0 – 1.5	35 – 40
DSF - exhaust vented with shades	0.07 – 0.15	0.70 – 0.75	<0.70	35 - 40

DSF was discussed and simulated in many previous studies, and they concluded that adding DSF to a building can reduce up to 30% of its energy consumption. However, according to table (7) that is provided by Straube and Straaten (2001), other insulation technologies can achieve the same or even better results of DSF will less cost. For example, table (7) illustrates that the SHGC of the DSF would achieve 0.07 to 0.3, while a typical double glazing with reflective coatings can attain a better SHGC value from the proposed DSF (Straube & Straaten 2001). In general,

applying DSF to buildings will reduce energy significantly, but it has to be simulated and evaluated properly to achieve an economically feasible design.

2.4.3.1- Buildings with DSF in Dubai

Despite the significant advantages of the DSF, it is rarely used in UAE and other GCC countries and most probably the reason is the additional cost that associates its construction. Therefore, developers and clients should have a clear knowledge of its environmental and economical long-term benefits (Haggag 2007). Specially with the expected future global warming, buildings tend to consume more energy for cooling on the long term, which will result in higher electricity bills, lower thermal comfort, and more GHG emissions.

Haggag (2007) study has investigated the thermal performance of DSF that was implemented to a hotel building in Dubai, UAE. He started his research by interviewing designers and engineers to get information for his study. Then he simulated single skin façade and DSF for Renaissance hotel in Dubai. A DSF was applied by using a box-window system as shown in figure 17 below. It was constructed by adding an exterior single glazing panel attached with aluminum frames. The building has interior double-glazing windows with controllable blinds to reduce the solar gains and glare. The cavity has a gap of 40 cm between the two facades. Also, horizontal shading made of laminated sheets was added to the cavity to protect the rooms from fire and sound, and to reduce solar gains (Haggag 2007).

This building was simulated and results have shown that the airflow between the inner and outer skin caused a temperature drop of the inner skin. Therefore, the heat gain was reduced in the internal spaces of the building which lead to lower cooling loads and energy consumption. Besides the cooling loads reduction, the study has proved that DSF has many benefits by

providing better ventilation, fire protection, and acoustical insulation specially for buildings that are located close to highways and airports (Haggag 2007).

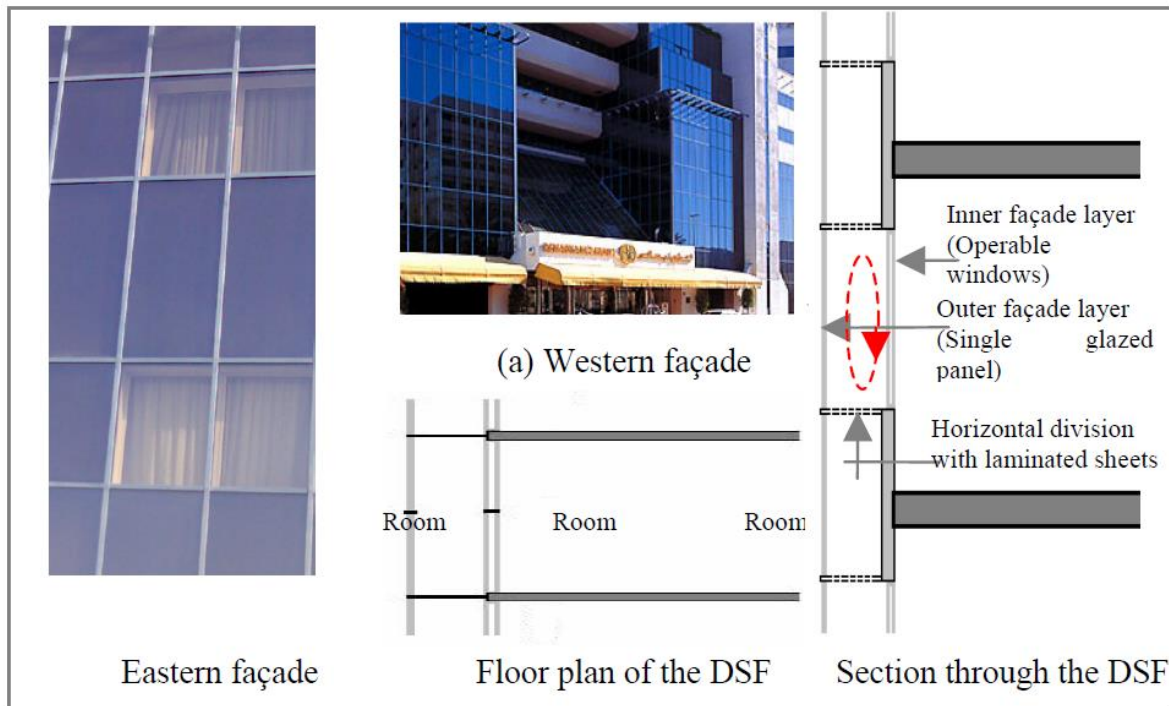


Figure 17: DSF of Renaissance hotel (Haggag 2007).

Also, results have concluded that DSF has many advantages that can offset its construction cost but it depends on the building function, façade design, and site characteristics. So, it is recommended to follow these steps at the initial phases of the DSF design. First, it is important to define the type of ventilation, façade function, location, heating and cooling loads, solar radiation, and acoustical control of the building. Then, the most suitable type of DSF can be selected based on the previous building characteristics. And the last step is to optimize the HVAC design based on the DSF and building design (Haggag 2007).

Another study was done by Radhi, Sharples, and Fikiry (2013) which evaluates the effect of DSF or what is called climate interactive façade system (CRFS) system on fully glazed building in

UAE. The new building of the Architecture Department of UAE University that is located in Al-Ain city was selected for this study. The study included both building energy simulation (BES) to calculate the cooling loads, heat gain, and amount of cooling energy reduction and computational fluid dynamic (CFD) simulation to evaluate the performance of system cavity with indoor and outdoor environment.

Figure 18 below illustrates a section of the building (east oriented), it is noted that the building consist of three floors and each floor has 3 studios (13 m x 13 m), one double glazing window with height of 2.9 m, width of 12 m and 1.1 m window sill for each floor. The exterior layer consists of single glazing DSF system with three opening (60 cm each) at zero level of each floor that act as an air inlet and one opening at the top of the building that acts as an air outlet. DFS dimensions are (10 mm) screen thickness with (12 m) height and (65 m) length and it has aluminum grills that splits the system cavity into three parts (Radhi, Sharples & Fikiry 2013).

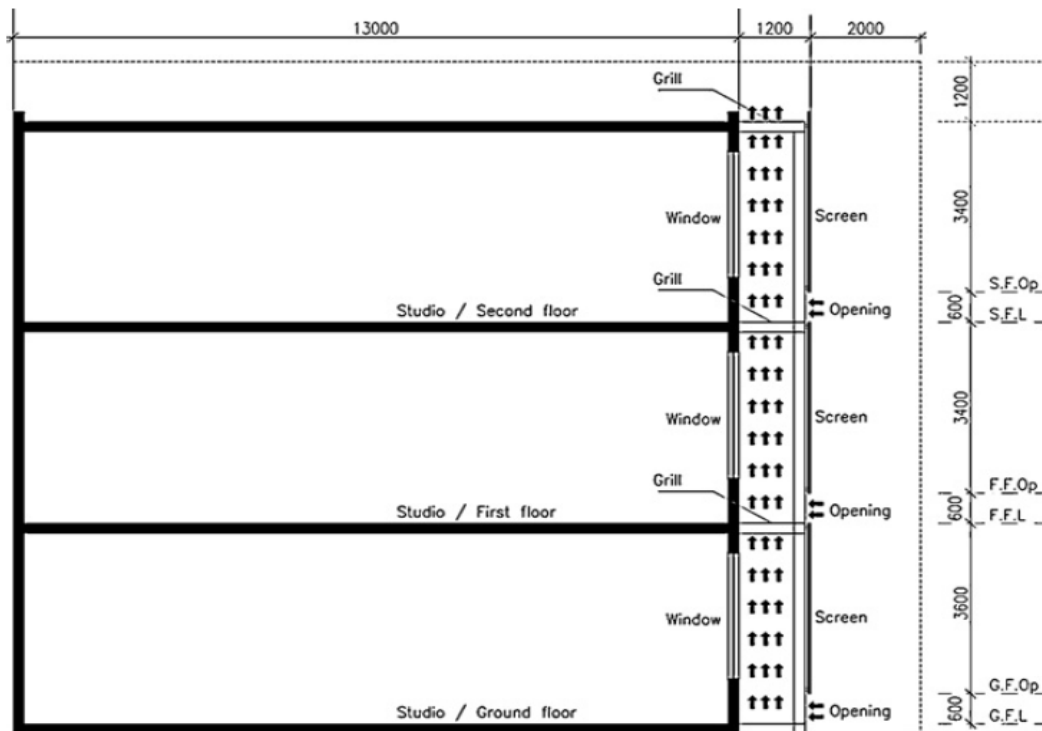


Figure 18: Cross section of the selected building part for the study (Radhi, Sharples & Fikiry 2013).

The study has concluded that DSF on fully glazed multi-story building can reduce around 17%-20% of building cooling loads depending on orientation, irradiance, and angle of incidence, whereas a higher angle of incidence (around 90°) allows the system to perform better. Also, percentage of cooling energy reduction is different throughout the building and this is based on floor level, glazing properties, and cavity depth. Applying this system to the south side gives a slight difference in heat transfer rates although this side has the highest amount of solar radiation. Therefore, it is recommended to apply this system on east and west sides as they have less solar gain. Higher floors tend to have higher heat transfer coefficients because air gets warmer as it rises. Optimization of system openings is required to avoid green-house effect in the system cavity and it is recommended to have the gap size between (0.7 to 1.2 m) that would control the heat transmission and solar gain. Moreover, study has concluded that reducing the system screen optical properties (SHGC) will cause a significant reduction in cooling loads, however; having a low U-value with low SHGC will cause the area between cavity to overheat (Radhi, Sharples and Fikiry 2013).

Another study done by Johnny and Shanks (2018) on a high-rise building in UAE has tested three different materials, transparent glass, opaque concrete, and impregnated concrete on the outer skin of the DSF. Besides, they evaluated how applying perforations in the outer skin of on the selected materials will affect the building cooling demand. The study has revealed that increasing the thermal mass of the outer skin will increase the energy reduction. Also, it found out that cooling energy savings by applying DSF with perforations for this type of buildings in UAE would reach 8%~23% by applying transparent glass, 15%~45% by applying opaque concrete, and 31%~50% by applying impregnated concrete (see figure 19 below).

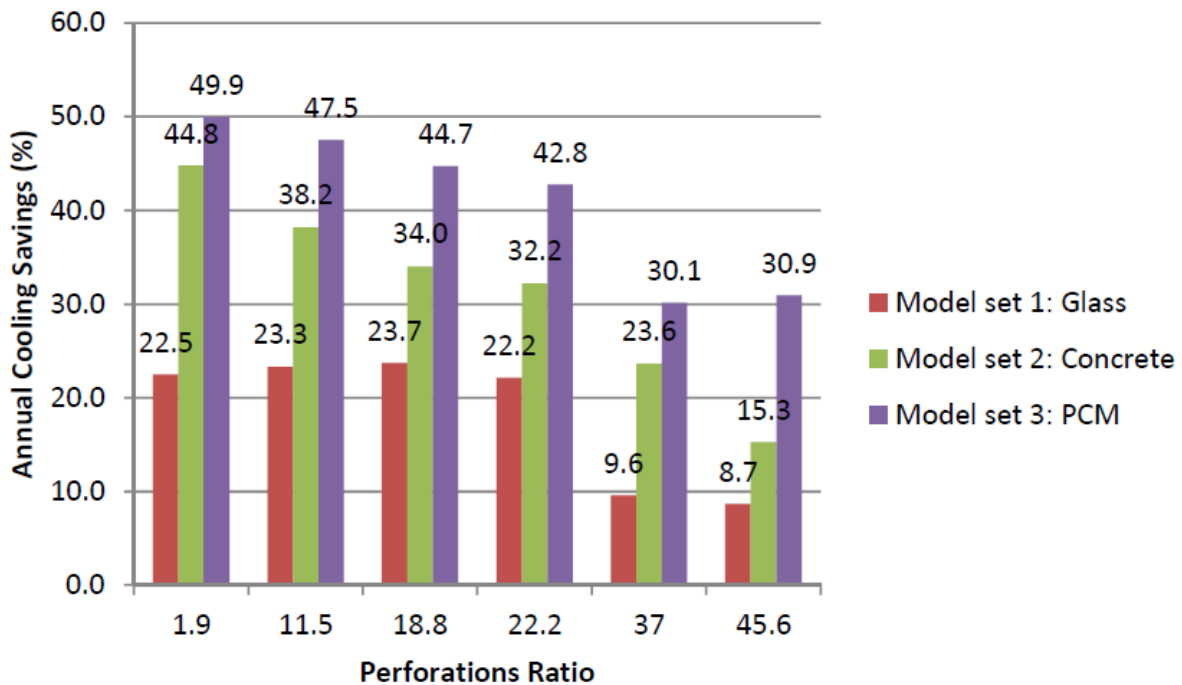


Figure 19: Annual cooling savings % based on the three selected materials and perforation ratio (Johny & Shanks 2018).

As shown in figure 19, annual cooling saving by applying perforation on DSF was different for each material. The glass material would achieve its highest saving percent (23.7%) with 18.8 perforation ratio, while both concrete and PCM performed better with the lowest perforation ratio (1.9). This study has concluded that applying DSF has a positive impact in reducing the annual cooling energy of high-rise buildings in UAE. Also, it has reported that having perforations in the outer skin of DSF is significant but the perforation ratio should be selected based on the material type (Johny & Shanks 2018).

2.4.4- Applying Heat recovery wheel (HRW) to HVAC system

In countries with hot arid climate like UAE, air-conditioning system is required in all building types as it has a high external gain from the outside air temperature and solar radiation.

Therefore, to reduce the annual energy consumption many energy recovery technologies and

devices can be installed to the HVAC system in buildings to reduce cooling loads and electricity bills. Heat recovery wheels are an example of those technologies. Those units are air to air rotating heat exchangers and considered as an energy efficient option. The two basic types of them are the sensible heat recovery wheel (transfers sensible energy) and enthalpy heat recovery wheel (transfers sensible and latent energy). This recovery unit is able to reduce the moisture content by 30%-50% and it doesn't affect the indoor air quality of the building (Heat Recovery Wheel (HW) 2020).

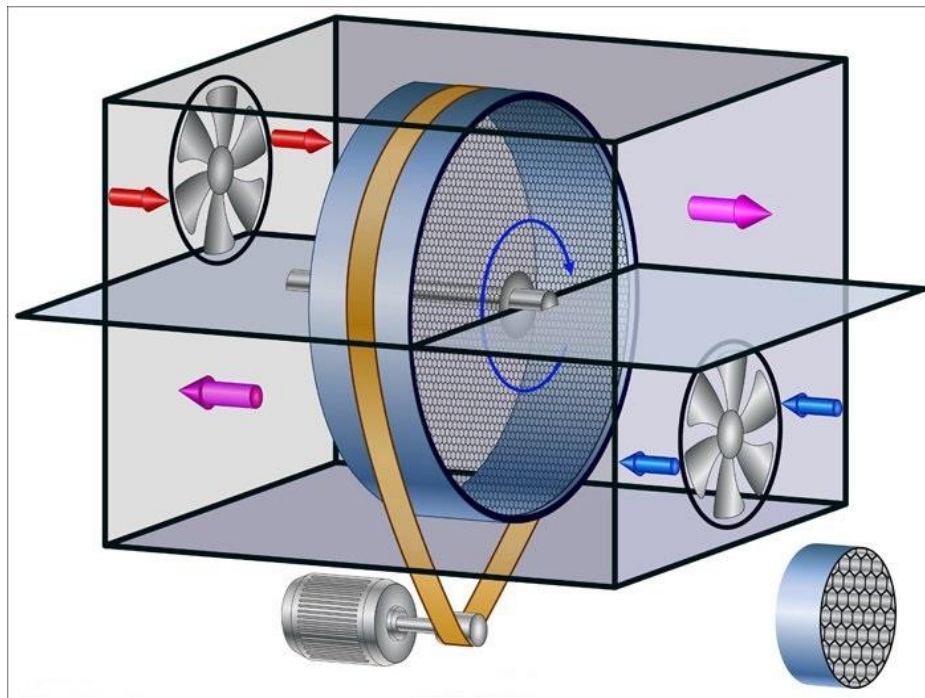


Figure 20: Typical heat recovery wheel (HWR) unit (Understanding Energy Recovery Wheels - Uponor Blog 2020)

As shown in figure 20, heat recovery wheel unit is a rotating cylinder that contains parallel flutes, and its diameter usually comes between 0.5 to 5m (AL HUSSAINI & Khan 2017). The supply airstream passes through the wheel before the cooling and heating coils and the exhaust airstream passes through the wheel before leaving the system. This will allow the wheel to

absorb/adsorb the heat and moisture. Therefore, in summer when the system is on cooling mode, the wheel will pre-cool and dehumidify the incoming fresh air before reaching the cooling coil.

While it will humidify and pre-heat the supplied air in winter (Energy Recovery Wheels 2020).

A study was performed by AL HUSSAINI and Khan (2017) has compared the energy efficiency of an HVAC system with and without HRW, the study was implemented on auditorium with an area of 5630 m² in Hyderabad, India. The Hourly analysis program (HAP) was used to calculate the cooling loads of the system without HRW. Then, the ECO-FRESH enthalpy wheel software was used to do the load calculation of the system with the HRW, the three inputs of the software are location, supply airflow in (cubic feet/minute) CFM, and return airflow in CFM (usually 80% of supply airflow). Moreover, some parameters were taken into consideration such as fan location, filtration requirements, and wheel speed control (AL HUSSAINI & Khan 2017).

Table (8): Ton refrigeration of the system with and without HRW (AL HUSSAINI & Khan 2017).

EQUIPMENT	HAP (TR)	ECO-FRESH (TR)	ENERGY RECOVERED(%)
AHU-1	54.9	29.91	45.5
AHU-2	48.6	26.78	44.89
AHU-3	45.5	23.64	48.0
AHU-4	45.5	21.93	51.8
AHU-5	24.5	15.09	38.4
AHU-6	32.7	18.51	43.39
TOTAL	251.7	135.86	46.02

As shown in table (8), the campus is served by 6 Air-handling units and the ton of refrigeration was reduced in all units, total reduction has reached 46% of energy by adding the HRW.

Therefore, this study has concluded that using an enthalpy HRW can save energy significantly (AL HUSSAINI & Khan 2017).

Another article was done by SULLIVAN (2010) has mentioned that the enthalpy wheel is able to reduce up to 80% of HVAC system energy. Consequently, this have many benefits such as reducing the carbon footprint, saving energy and money. Therefore, HRW should be considered for new building designs and as a retrofit solution. Moreover, 80% load reduction of cooling coil can be provided by HRW and it can downsize the heating and cooling system up to 40% which make it worth an investment (SULLIVAN 2010).

Chapter 3: Methodology

The aim of this project is to determine the most suitable technologies for new and existing buildings that would reduce the annual cooling energy consumption and improve building resilience to climate change in future. There are several energy efficiency technologies that can be applied to buildings nowadays. However, would they provide the same amount of energy savings in future? This study will answer this question by finding the percentage change of energy reduction of applying each solution/technology over the future years. Also, it will discover the most efficient technology that would respond properly with the expected global warming in future. Some solutions might be able to reduce cooling energy demand in buildings significantly now, but this is dependent on the present weather conditions. Hence, this will probably increase/decrease throughout the years depending on which weather parameters will be affected the most in future. For example, if the air temperature is expected to increase significantly in future years but solar radiation will slightly increase, this means that the technologies which reduce heat gain from air (ex: HVAC heat recovery unit) would improve the building resilience more than the technologies that reduce solar gain. Consequently, proposing different energy efficient solutions and simulating them with future weather files will solve this issue and will reveal the most efficient solutions for the long-term.

The first step was collecting future predicted weather files from different sources in a readable format by IES software. Then, a schematic high-rise building that represents a common UAE building type was modelled using IES software, and an HVAC system was assigned to it. This building, modelled to reflect the present building standards in Dubai, was used as the base case model for this study where a range of different energy efficiency technologies were applied to it and the resultant annual cooling demands analyzed. The energy efficiency technologies tested included increasing the insulation of opaque external walls; improving the performance of

glazing and increasing the performance of ventilation energy recovery. All solutions will be simulated with present and future weather datasets, more details about the selected technologies are explained in section 3.3 below.

The collected future weather datasets were applied to the model and the building simulated to calculate the cooling and the total building energy demands of the whole building in the present period and the future periods of 2020, 2030, 2050, 2065, 2080, and 2090. Those future periods represent different time slices which will be explained later on in section 3.2.

3.1- Base Case Model

The base case model was created using Integrated Environmental Solutions – Virtual Environment (IES-VE) software, version 2019. This software is a dynamic thermal modeling tool that allows designers and engineers to build 3-D models and study buildings performance using active and passive solutions. In this research, IES software is used to create a 3-D model as a schematic building with an HVAC system. The base case model has a rectangular form of 30 m x 40 m layout and it consists of (G+24) floors, with 3 m floor-to-floor height, and it is north oriented. For simplicity, each floor consists of 4 indoor conditioned spaces with a core area in the middle and it has 60% WWR (double glazing with 6mm pane + 12mm air filled + 6mm pane) on all sides which represents a typical UAE commercial high-rise speculative office building (see figures 21 and 22 below). The thermal characteristics of the base case building fabric and systems were specified as per the requirements of the current Dubai green building standards (Al Safat, Dubai Green Building Evaluation System 2016), see Table (9) below for details.

Table (9): Base case construction and building fabric specifications	
Building specifications	
Total Area	30,000 m ²
Floor area	1200 m ²
Total number of floors	G+24
Thermal characteristics	
U-value (external windows)	1.6 W/m ² K
WWR	60%
Solar heat gain coefficient SHGC (external windows)	0.3955
U-value (external walls)	0.3194 W/m ² K
U-value (Roof)	0.1800 W/m ² K
U-value (Ground/exposed floor)	0.2200 W/m ² K
U-value (internal partition)	1.7888 W/m ² K
U-value (internal ceiling/floor)	1.0866 W/m ² K

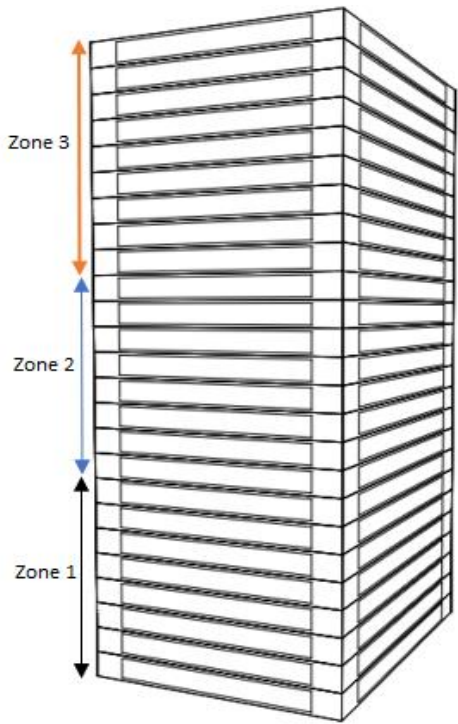


Figure 21: Base case 3-D model (IES Virtual Environment 2019).

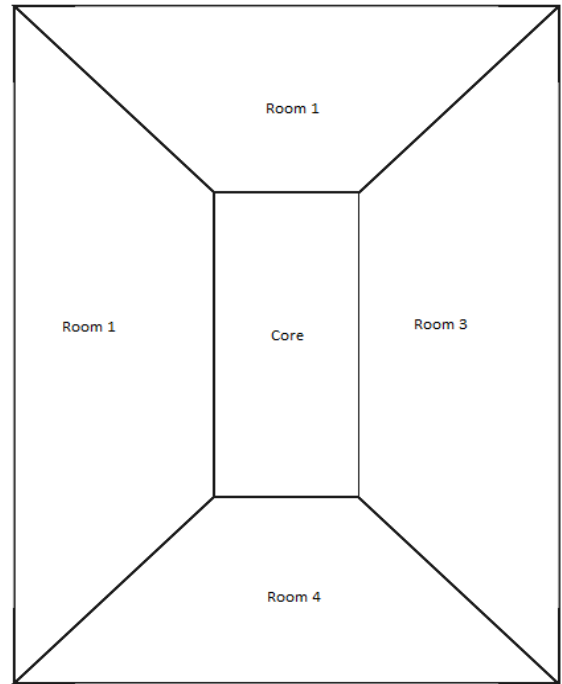


Figure 22: Layout of a typical floor in the model (IES Virtual Environment 2019).

As shown in table (10), three internal heat gain sources were assigned to the building including people, fluorescent lighting, and computers. The external heat gain source is the solar radiation which was taken into consideration as well. Moreover, an infiltration rate of (0.25 ach) was added as an air exchange source of the building, which is considered as a good air tightness rate (Ueno & Lstiburek 2015).

Internal Gain	Fluorescent lighting	10 W/m ²	as per Al Safat, Dubai Green Building Evaluation System (2016)
	People	Maximum sensible gain: 90 W/m Maximum latent gain: 60 W/m Occupant density: 10 m ² /person	(as per CIBSE guide A 2015, p. 272)
	Computers	15 W/m ²	(as per CIBSE guide A 2015, p. 272)

Initially, an HVAC system was selected and applied to the base case model, it consists of three full fresh-air handling units (FAHU's) that supplies conditioned fresh air to the fan coil units (FCU's), then the FCU supplies mixed conditioned air to each room. As shown in the floor layout, see figure 22 above, rooms 1 and 3 are typical in each floor with an area of 319 m², also rooms 2 and 4 are typical with an area of 209 m². The core area in the middle of the layout represent the building services location in each floor and it has a total area of 144 m². Design thermal characteristics were selected as shown in table (11) and it complies with AlSa'fat evaluation system.

Table (11): Base case model thermal properties (Al Safat, Dubai Green Building Evaluation System 2016).		
Design thermal characteristics		
Design maximum outdoor temperature	Dry bulb: 46° C	Wet bulb: 29° C
Dry bulb temperature	lower limit: 22.5° C	Upper limit: 25.5° C
Relative Humidity	Minimum: 30%	Maximum: 60%
CO₂ concentration	less than 800 ppm	

The second step was designing the model, selecting location and the thermal characteristics, adding internal gains, and infiltration rate. Then, an HVAC system was required to control the air temperature in the rooms. To do this, the building was divided into three zones, and each zone has one FAHU. The first zone includes floors from ground G to 7, the second zone includes floors from 8 to 15, and the third zone includes floors from 16 to 24 (see figure 21 above). Each room/space in the building has a separate FCU, all HVAC system components and sizing details are explained in depth in section 4.1.

Thereafter, the HVAC system was auto-sized by using ASHRAE (heat balance method) in IES software. This method calculates surfaces temperature taking into account all heat gains by convection, conduction, and radiation for all conditioned surfaces and then it updates the HVAC system level sizing based on the calculated loads (Tosh 2017).

According to ASHRAE fundamental (2017), the heat balance method is based on some core assumptions. Firstly, this method assumes that the air in the room is mixed well and have a uniform temperature. Also, the surfaces temperature and the irradiation short and long waves in the room are assumed to be uniform. Moreover, it assumes that the radiation of all surfaces is diffused and the heat conduction have one dimension inside the room.

Furthermore, the four processes that are used in the heat balance method are the outdoor-face heat balance, through-the-wall conduction, the indoor-face heat balance and the air heat balance (ASHRAE fundamental 2017). Figure 23 below illustrates the schematic procedure of the method on a single opaque surface and describes the connection between the processes. To apply the heat balance method, the upper grey part in the figure below is calculated for each surface in the zone, then the infiltration rate and the convection heat gain from internal sources are also considered to calculate the air heat balance for the HVAC air system.

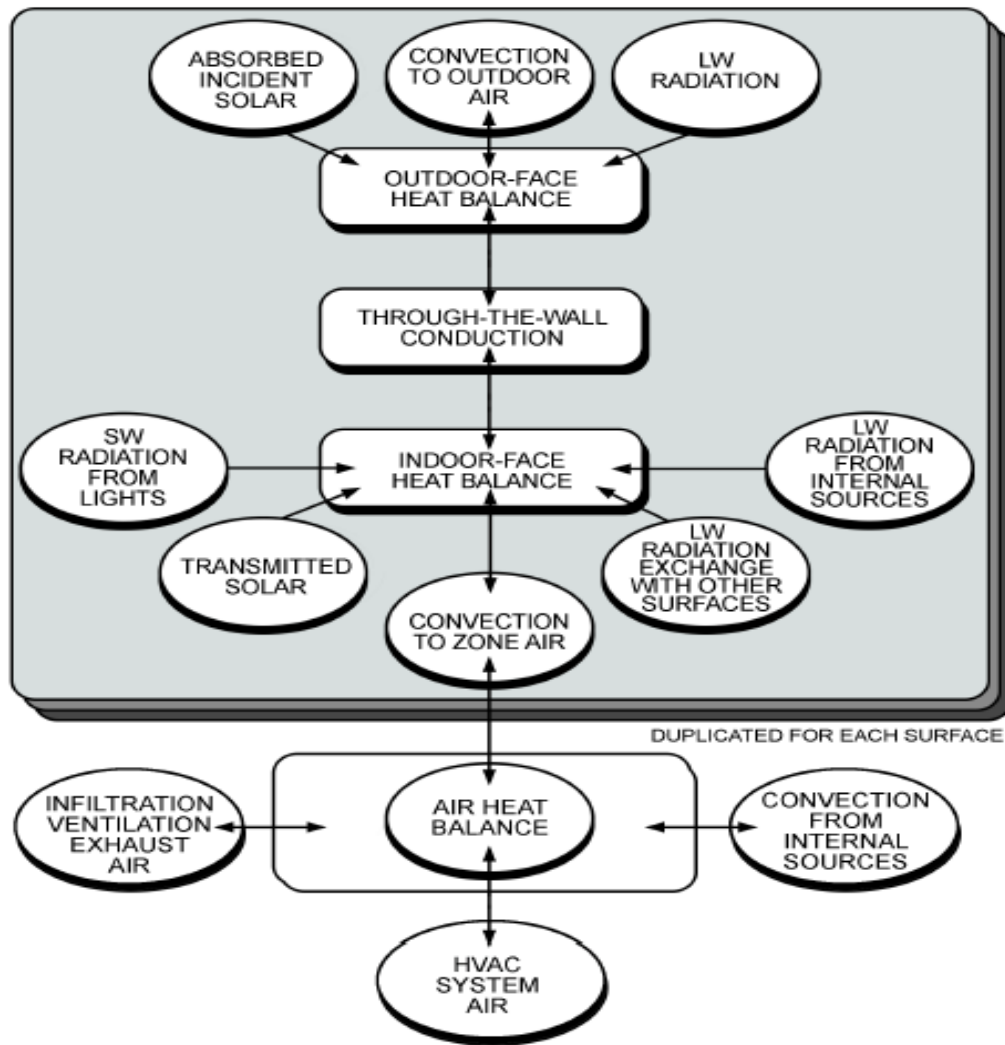


Figure 23: Schematic description of heat balance method on an opaque surface (ASHRAE fundamental 2017).

As per ASHRAE fundamental (2017) standard, the outdoor-air heat balance process can be calculated using the below equation:

$$q''_{sol} + q''_{LWR} + q''_{conv} - q''_{ko} = 0$$

Where:

q''_{sol} = absorbed direct and diffuse solar radiation flux (q/A), W/m^2

q''_{LWR} = net long-wave radiation flux exchange with air and surroundings, W/m^2

q''_{conv} = convective exchange flux with outdoor air, W/m^2

q''_{ko} = conductive flux (q/A) into wall, W/m^2

And the second process which is through-the-wall

conduction is illustrated in figure 24. Where it shows

the heat conductive fluxes from outside to inside and

the temperature of outdoor and indoor surfaces (T_{so}

and T_{si}). In this process, the two shown temperatures

are used as an input to the create the conductive flux

into the wall (q_{ko}) and the conductive flux through the

wall (q_{ki}) as an output.

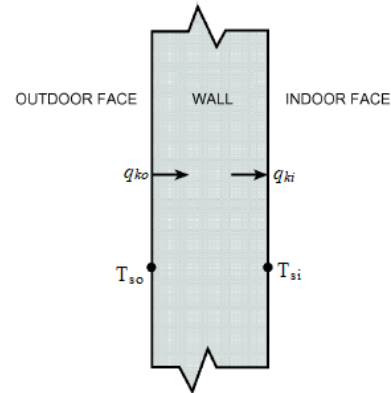


Figure 24: Schematic diagram of through-the-wall conduction process (ASHRAE fundamental 2017).

Besides, the third process is the indoor-face heat balance and it can be computed by using the

below equation:

$$q''_{LWX} + q''_{SW} + q''_{LWS} + q''_{ki} + q''_{sol} + q''_{conv} = 0$$

Where:

q''_{LWX} = net long-wave radiant flux exchange between zone surfaces, W/m^2

q''_{SW} = net short-wave radiation flux to surface from lights, W/m^2

q''_{LWS} = long-wave radiation flux from equipment in zone, W/m^2

q''_{ki} = conductive flux through wall, W/m^2

q''_{sol} = transmitted solar radiative flux absorbed at surface, W/m^2

q''_{conv} = convective heat flux to zone air, W/m^2

In addition to, the fourth process which is air heat balance can be calculated using the following equation:

$$q_{conv} + q_{CE} + q_{IV} + q_{sys} = 0$$

where

q_{conv} = convective heat transfer from surfaces, W

q_{CE} = convective parts of internal loads, W

q_{IV} = sensible load caused by infiltration and ventilation air, W

q_{sys} = heat transfer to/from HVAC system, W

Moreover, the IES auto sizing uses weather data from the International weather for energy calculations (IWEC) weather files for Abu Dhabi and Dubai city imported from ASHRAE design weather database v6.0 (IES Virtual Environment 2019). The IWEC weather files are derived from Integrated Surface Hourly (ISH) weather datasets that is available at National Climatic Data Center (Climate Data Download Center 2013). The auto-sizing in IES-VE software is based on Abu Dhabi/Dubai IWEC present file only because auto-sizing for future years feature is not available in IES software.

3.2- Future weather datasets

Three statistical downscaling weather generating tools are used in this research to study the resilience of UAE buildings to future climate change and its impact on cooling energy demand. Those tools are CCWorldWeatherGen, WeatherShift™, and Meteonorm, they have been developed on different climate scenarios and also cover projections for different future years. Dynamical downscaled weather datasets for UAE were requested from the Environment Agency in Abu Dhabi (EAD). However, due to the complexity of extracting those files and time restrictions, only statistical downscaled weather datasets were used in this study.

To keep the consistency and uniform comparisons between all simulations, all the selected files in this study will be used in EPW format. The weather parameters that are included in EPW files are dry bulb temperature, dew point temperature, relative humidity, atmospheric station pressure, direct normal radiation, horizontal infrared radiation, global horizontal radiation, direct normal radiation, global horizontal illuminance, direct normal illuminance, diffuse horizontal illuminance, zenith luminance, wind direction, wind speed, total sky cover, opaque sky cover, visibility, precipitable water, aerosol optical depth, snow depth, and precipitation depth (EnergyPlus Weather File (EPW) Data Dictionary 2011).

Weather files are available for present and future years up to year 2100. The expected lifetime of UAE building around is 30 years due to the harsh weather conditions and the quality of construction materials that are used. However, retrofit solutions, good maintenance, and high-quality materials can increase UAE buildings lifetime to 50 years (Abdullah 2001). Therefore, simulating the base case model with future years weather files up to 2070 is needed.

The three statistical main data sources of future weather files are analyzed in the three sections below. Future files of CCWorldWeatherGen tool and WeatherShiftTM tool are compared with IWEC present file, while Meteonorm future files are compared with a present file that is provided by Meteonorm tool. In general, future weather files from the three tools predict an increase in daily dry-bulb temperature, while the daily RH% and global horizontal radiation values vary between the files.

3.2.1- CCWorldWeatherGen tool

Climate change world weather generating CCWorldWeatherGen. tool was created in 2013 (Jentsch et al. 2013). A methodology was established to provide predicted future weather files

for different locations all around the world. It is a free online tool that is developed using Microsoft Excel, and it is used to create future weather files for building simulation programs in Energy Plus Weather (EPW) format and Typical Meteorological Year (TMY) format. This tool uses morphing approach to downscale weather data from the Hadley Centre Coupled Model 3 (HadCM3) summary experiment which is available in IPCC data distribution center (DDC) and is based on IPCC Third Assessment Report A2 emission scenario (Jentsch, et al. 2013; Moazami, et al. 2019). HadCM3-A2 data was created by simulating monthly values of three different time slices for future years (2020, 2050, and 2080) with the baseline climate of typical metrological year 2 (TMY 2) which is a 30 year average of meteorological records for the period 1961-1990 and is the weather data that is used throughout the industry to represent the present climate. For this study, three weather files were generated for the following three future periods:

- 2011-2040 represented as 2020 (*HadCM3-A2-2020*)
- 2041-2070 represented as 2050 (*HadCM3-A2-2050*)
- 2071-2100 represented as 2080 (*HadCM3-A2-2080*)

These files were generated for Abu Dhabi location, i.e. the closest available geographical location to Dubai in EPW format, to be used in IES software. For the Abu Dhabi location, coarse General Circulation Model (GCM) data was used. Also, generating EPW weather files from this tool is simple but it is available without HadCM3-A2 baseline weather data files, therefore; users should follow the tool guideline to download those baseline weather files and add them to the tool.

Figure 25 below represents the average daily dry-bulb temperatures of the selected future weather files for Abu Dhabi city from CCWorldWeatherGen tool and the IWEC present weather file. According to the International weather for energy calculations, IWEC present weather files

are derived from 12 to 25 years previous weather records (ASHRAE International Weather Files for Energy Calculations 2.0 (IWEC2) 2019). The highest recorded temperature of the present file is 38.8°C and lowest recorded temperature is 15.7°C.

Table (12) below illustrates the highest and lowest of average daily dry-bulb temperatures of EPW (HadCM3-A2) weather files, all highest temperatures were recorded in 29th of January and all lowest temperatures were recorded in 5th of August.

Table (12): Highest and lowest average daily dry bulb temperature in C° of IWEC present file and CCWorldWeatherGen tool future files for periods 2020, 2050, and 2080 based on figure 25.			
EPW weather file	HadC3-A2-2020	HadC3-A2-2050	HadC3-A2-2080
Highest dry-bulb temperature	40.2° C	41.9° C	43.7° C
Lowest dry-bulb temperature	16.8° C	18.2° C	19.8° C

Moreover, the below figure shows that the predicted temperature rise between period 2020 and 2050 is between 1°C~1.9°C, whereas the temperature rise between 2050 and 2080 weather files is between 1.2°~2.2°C. Those values are considered reasonable as they are based on high emission scenarios which will result in high temperature increase throughout the years.

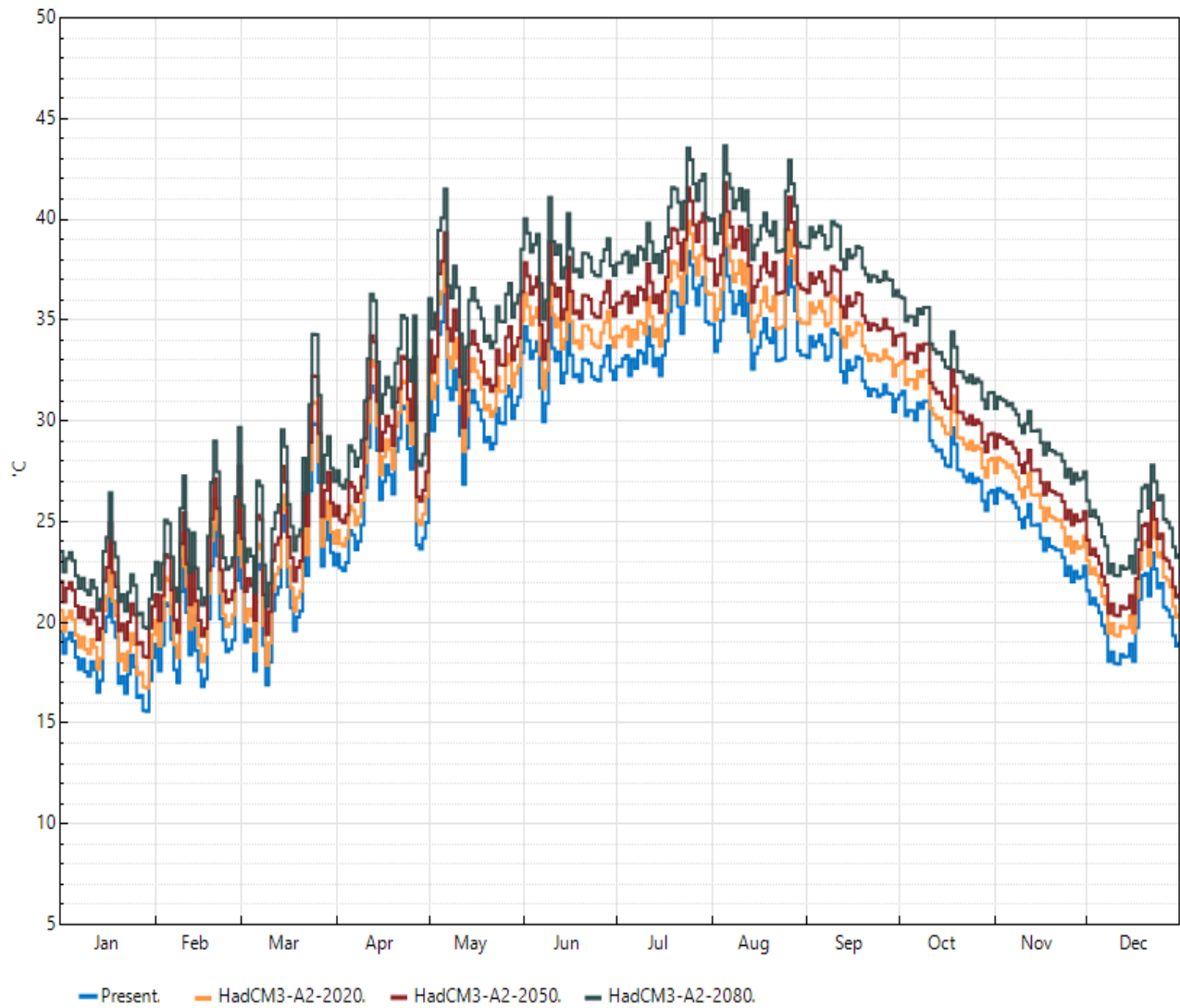


Figure 25: Comparison between average daily dry-bulb temperature in C° of the three CCWorldWeatherGen tool future weather files and IWEC present file (Dataviewer n.d.).

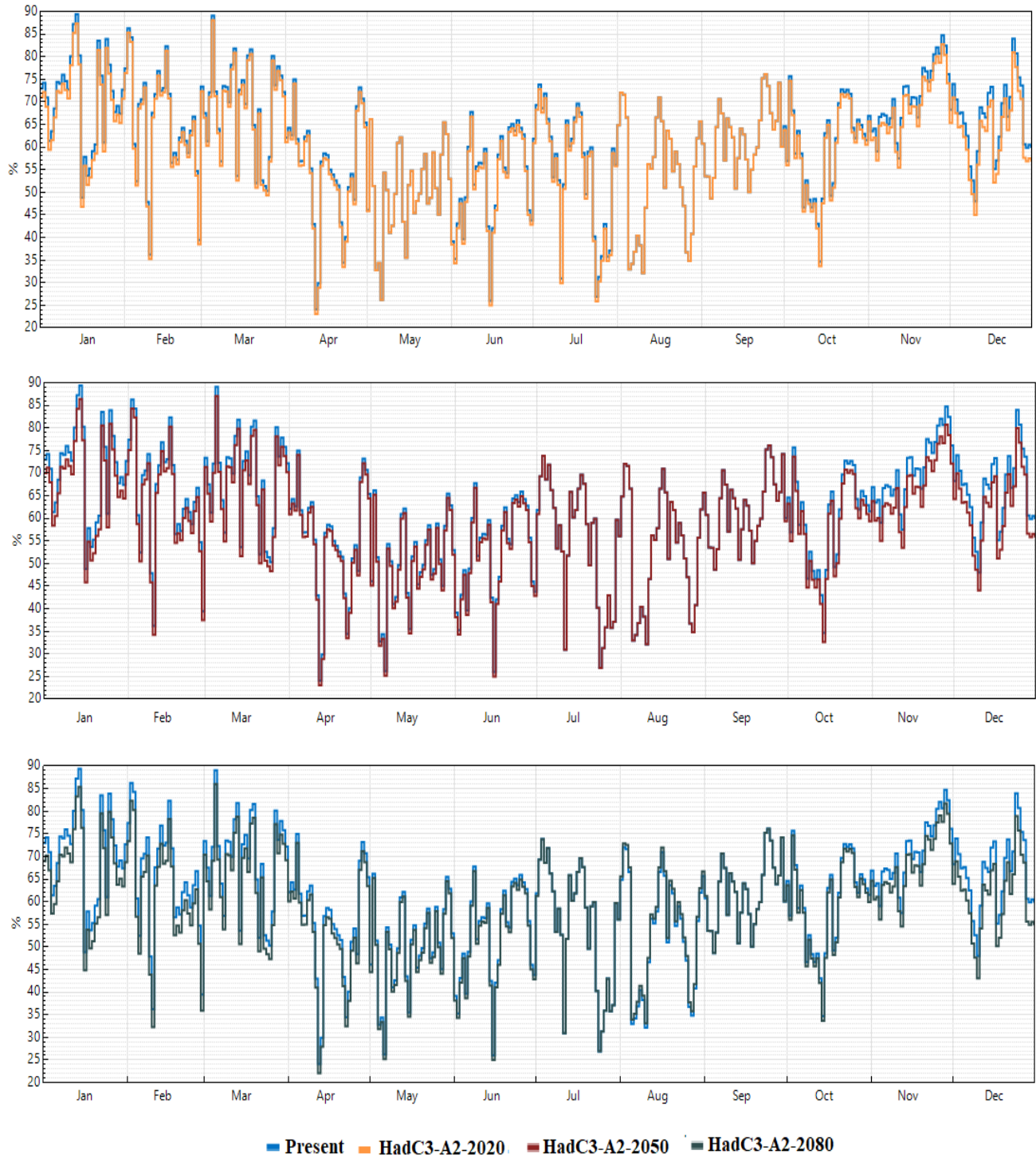


Figure 26: Average daily relative humidity ratio (RH%) of the three CCWorldWeatherGen tool future weather files compared with IWEC present file (Dataviewer n.d.).

Figure 26 above illustrates the relative humidity ratio (RH%) of the three future HadC3-A2 selected weather files. It is noticed in the first line graph which is comparing between the IWEC present file and HadC3-A2-2020 file that the RH% is the same in the months of August, Sempetmber, and May, while IWEC present values are higher than HadC3-A2-2020 values in the other months. The second line graph compares between the IWEC present and HadC3-A2-2050 weather files, the RH% is the same in the months of July, August, and semptember, whilst the present file recorded higher values in the other months of the year. The third line graph compares between IWEC present and HadC3-A2-2080 weather files, months with the same RH% are July and September, in August RH% of HadC3-A2-2080 is higher than the present weather file and in the other months of the year the present weather file recorded higher values than HadC3-A2-2080. The lowest and highest RH% ratios are presented in table (13) below.

Table (13): Highest and lowest RH% of IWEC present file and CCWorldWeatherGen tool future files for periods 2020, 2050, and 2080 based on figure 26.				
Weather file	IWEC present	HadC3-A2-2020	HadC3-A2-2050	HadC3-A2-2080
Highest RH%	89.6	88	87	86
Lowest RH%	24	23	23	22

It can be seen from the three-line graphs in figure 27 below that the global horizontal radiation values of the three selected future weather files are decreasing from the IWEC present file values from May until October. Also, the three-line graphs show that the values are almost the same for all weather files from January to April. In the first line graph, HadC3-A2-2020 values are slightly decreasing in October, then it starts to increase a little in November and December. The second line graph shows that the global horizontal radiation values of IWEC present and HadC3-

A2-2050 weather files are almost the same in November and December. In addition to, the third line graph shows that the global horizontal radiation values of HadC3-A2-2080 are slightly less than IWEC present weather file in October and November, and it is the same in December.

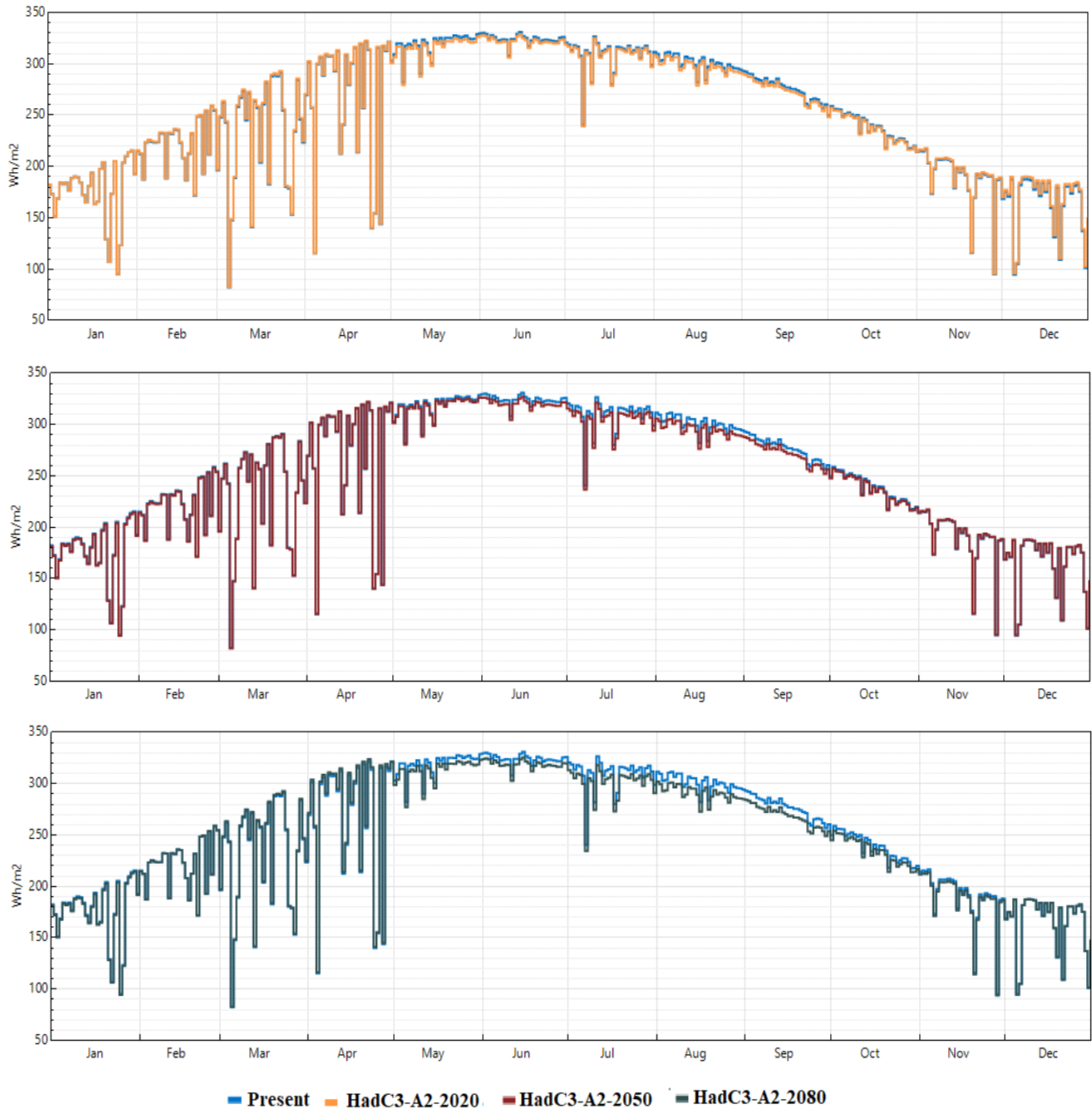


Figure 27: Average daily global horizontal solar radiation in Wh/m² of the three CCWorldWeatherGen tool future weather files compared with IWEC present file (Dataviewer n.d.).

Generally, the three-line graphs in figure 27 above indicate that the global horizontal solar radiation is slightly decreasing throughout the future years of HadC3-A2 weather files. The highest and lowest recorded values of global horizontal solar radiation are shown in table (14).

Table (14): Highest and lowest global horizontal radiation in Wh/m² of IWECC present file and CCWorldWeatherGen tool future files for periods 2020, 2050, and 2080 based on figure 27.				
Weather file	IWECC present	HadC3-A2-2020	HadC3-A2-2050	HadC3-A2-2080
Highest	331	328	327	326
Lowest	82	83	82	82

3.2.2- WeatherShift™ tool

This tool is developed by an architectural consulting firm called Arup and analytics consulting firm Argos and it uses statistical downscaling to create future weather datasets. It is based on two future emissions scenarios, i.e. Representative Concentration Pathways (RCPs) RCP 4.5 and RCP 8.5 from the IPCC Fifth Assessment Report (AR5). The morphing method is used based on the results of 14 General Circulation Models (GCMs) available from AR5. This tool uses the typical meteorological year 3 TMY3 climate as a baseline which represents 15-year averages of meteorological records from the period 1991 to 2005 along with the two mentioned future emission scenarios to create the three weather files for three time periods mentioned above. The first period is 2035 which represents the averages of weather parameters for years (2026 to 2045), the second period is 2065 which refers to years (2056-2075), and the third period is 2090 which refers to years (2081-2100) (Moazami, et al. 2019). The averages are derived from a linear interpolation of the cumulative distribution function (CDF) of weather parameter values

predicted by GCM's of each time step in the related time period. For this study, EPW present and future weather files with hourly time-step for Abu Dhabi location (closest location to Dubai) was provided by Arup and Argos for academic use.

Both CCWorldWeatherGen tool and WeatherShift™ tool use morphing method to create weather files. However, as mentioned before, each tool has different times slices and they are different in the way that they were developed, especially with the GCM projection evolution. Therefore, this research will use years 2020, 2060, and 2080 from CCWorldWeatherGen tool and years 2035, 2065, and 2090 from WeatherShift™ tool. The selected files from CCWorldWeatherGen tool are limited to HadCM3-A2 emission scenario with TMY2 morphing, whereas the selected WeatherShift™ tool files are derived from CDFs of 50th, 90th, and 95th percentiles by morphing TMY3 and using RCP 8.5 emission scenario.

Weather files for RCP 4.5 and RCP 8.5 emissions scenarios for the present and future years with 10th, 50th, 90th, and 95th percentiles were obtained. Each percentile represents different weather values based on the future expectation of warming; the four percentiles are described below in table (15):

Table (15): WeatherShift™ tool percentiles description (Climatology - Paducah, KY - February Temperature Percentiles n.d.).	
Percentile	Description
10 th percentile	The chance of weather values to fall below the given values threshold is 10%. Which means that the temperature is expected to be warmer 90% of the time than the specified temperatures. (usually used for heating systems)
50 th percentile	It is the median percentile, there is a 50% chance for the weather values to fall below or above the given values. (usually used for cooling and heating systems)

90 th percentile	The chance of weather values to fall above the given values threshold is 10%. Which means that the temperature is expected to be cooler 90% of the time than the specified temperatures. (usually used for cooling systems)
95 th percentile	The chance of weather values to fall above the given values threshold is 5%. Which means that the temperature is expected to be cooler 95% of the time than the specified temperatures. (usually used for cooling systems)

However, as recommended in IES weather files user guide, buildings with 25 years lifespan or less that have cooling systems (such as UAE buildings) are recommended to use RCP 8.5 as it will not highly differ from RCP 4.5 for this short period, also midpoint and upper tail global warming (50th and 90th percentiles) should be used in this case. While buildings with more than 25 years lifespan are recommended to use both RCP 8.5 and RCP 4.5 (Guidelines for specifying WeatherShift™ future weather files Argos Analytics, LLC 2017). Although the buildings that require cooling systems are recommended to use RCP 8.5 at 50th and 90th percentiles which will provide the highest emission scenario at midpoint and upper tail global warming. But the latest version of WeatherShift™ tool has developed a higher upper tail percentile (the 95th percentile). Therefore, ten files from this tool for Abu Dhabi city will be used in this study representing IWEC present, and future years 2035, 2065, 2090 for RCP 8.5 at 50th, 90th, and 95th percentiles. The IWEC present file is obtained from WeatherShift™ tool but it can be freely downloaded from energy plus website.

As shown in figures 28, 29, and 30 below, the average daily dry-bulb temperatures of the WeatherShift™ tool selected files are different, and they are significantly rising throughout the years. As mentioned before in section 3.2.1, the highest temperature recorded in IWEC present file is 38.8°C in 5th of August while the lowest temperature is 15.7°C in 29th of January.

The highest and lowest average daily dry-bulb temperatures of WeatherShift™ tool future selected weather files are represented in table (16) below. All lowest temperatures are recorded in 29th of January and all highest temperatures are recorded in 5th of August. Furthermore, the table below shows that the highest and lowest temperatures of the 90th and 95th percentile for the periods 2035 and 2065 are close. However, figures 29 and 30 illustrate that the 95th percentile temperature values are higher than those from the 90th percentile in other months by (0.1° C ~ 0.3° C) for period 2035, and by (0.1° C ~ 0.4° C) for period 2065. Furthermore, the 50th percentile temperatures are significantly less than the 90th and 95th percentiles in all periods.

Table (16): Highest and lowest average daily temperatures of the future WeatherShift™ files for periods 2035, 2065, and 2095 in 50th, 90th, and 95th percentiles based on figures 28, 29, and 30.

Percentile	2035		2065		2090	
	Highest temperature	Lowest temperature	Highest temperature	Lowest temperature	Highest temperature	Lowest temperature
50th	40.4° C	17.2° C	42.3° C	18.5° C	44.0° C	20.0° C
90th	41.2° C	17.8° C	42.8° C	19.8° C	46.0° C	21.4° C
95th	41.3° C	17.8° C	42.9° C	20.0° C	46.1° C	21.9° C

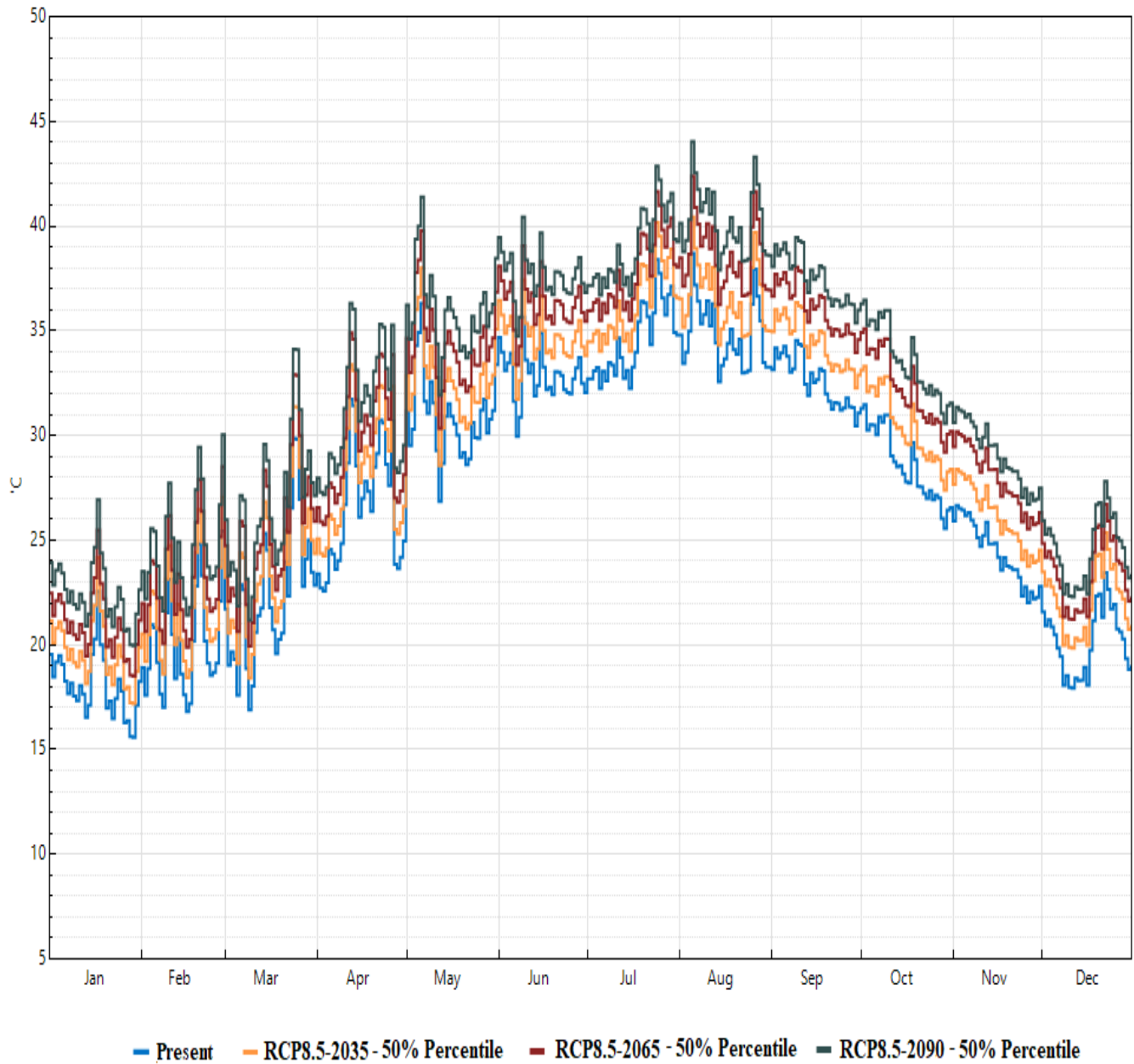


Figure 28: Comparison between the average daily dry-bulb temperature in C° between IWEC present weather file and WeatherShift™ tool future files with 50% percentile (Dataviewer n.d.).

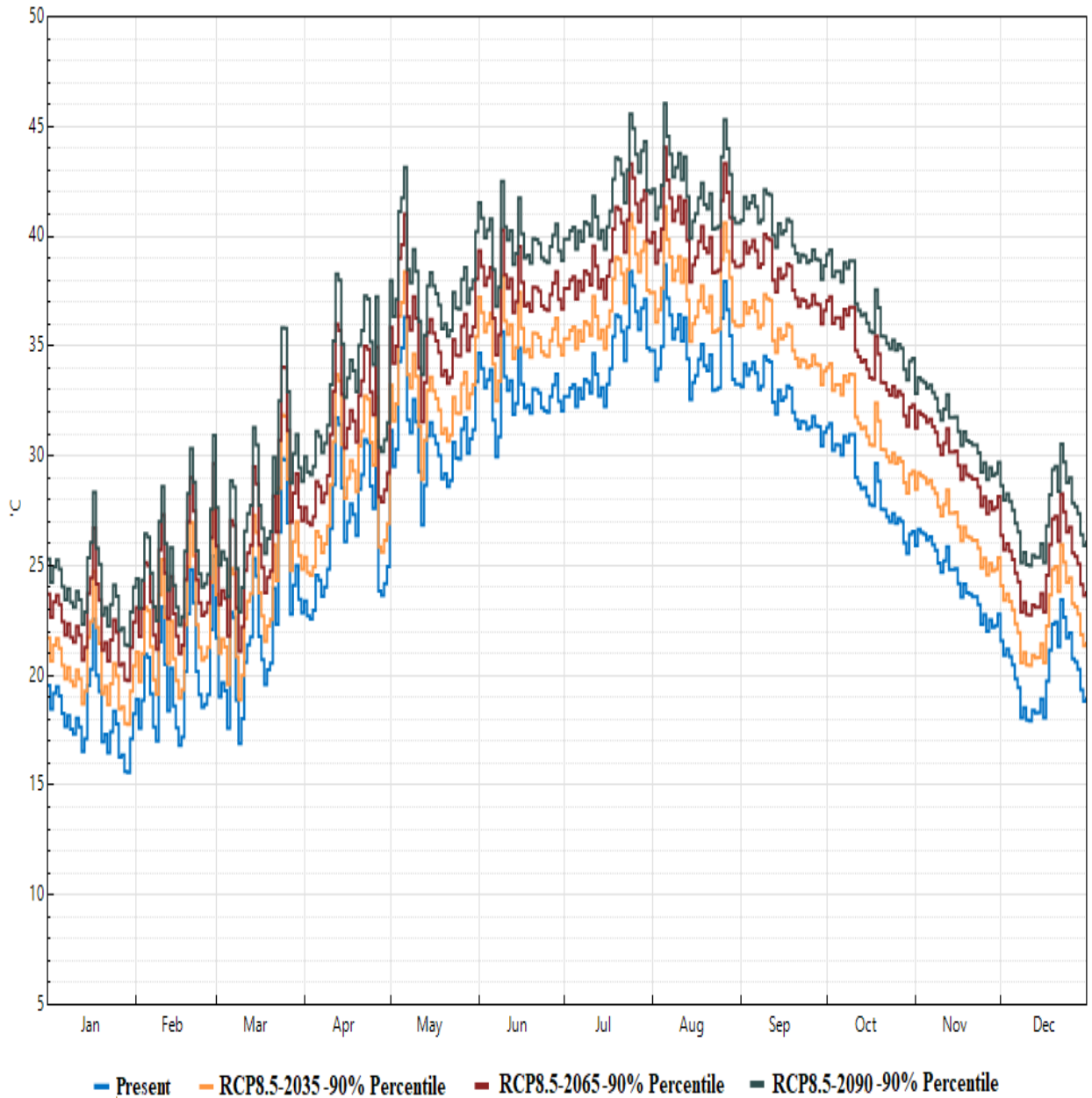


Figure 29: Comparison between the average daily dry-bulb temperature in C° between IWEC present weather file and WeatherShift™ tool future files with 90% percentile (Dataviewer n.d.).

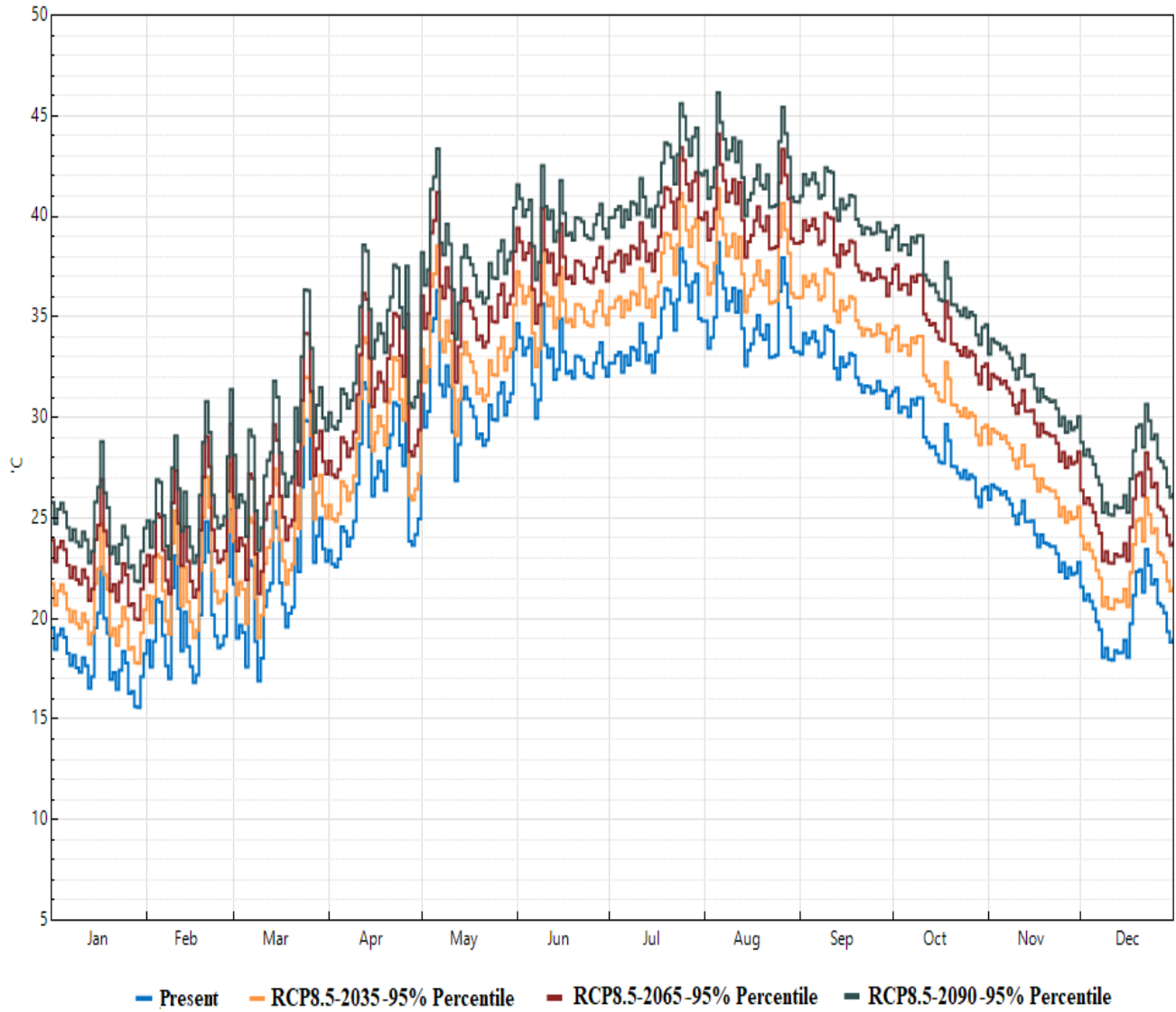


Figure 30: Comparison between the average daily dry-bulb temperature in C° between IWEC present weather file and WeatherShift™ tool future files with 95% percentile (Dataviewer n.d.).

The next three figures below represent the RH% of WeatherShift™ tool future files compared with the IWEC present file. In figure 31, it is noticed that the RH% of the all 50% percentile future files are either the same or slightly less than the IWEC present file.

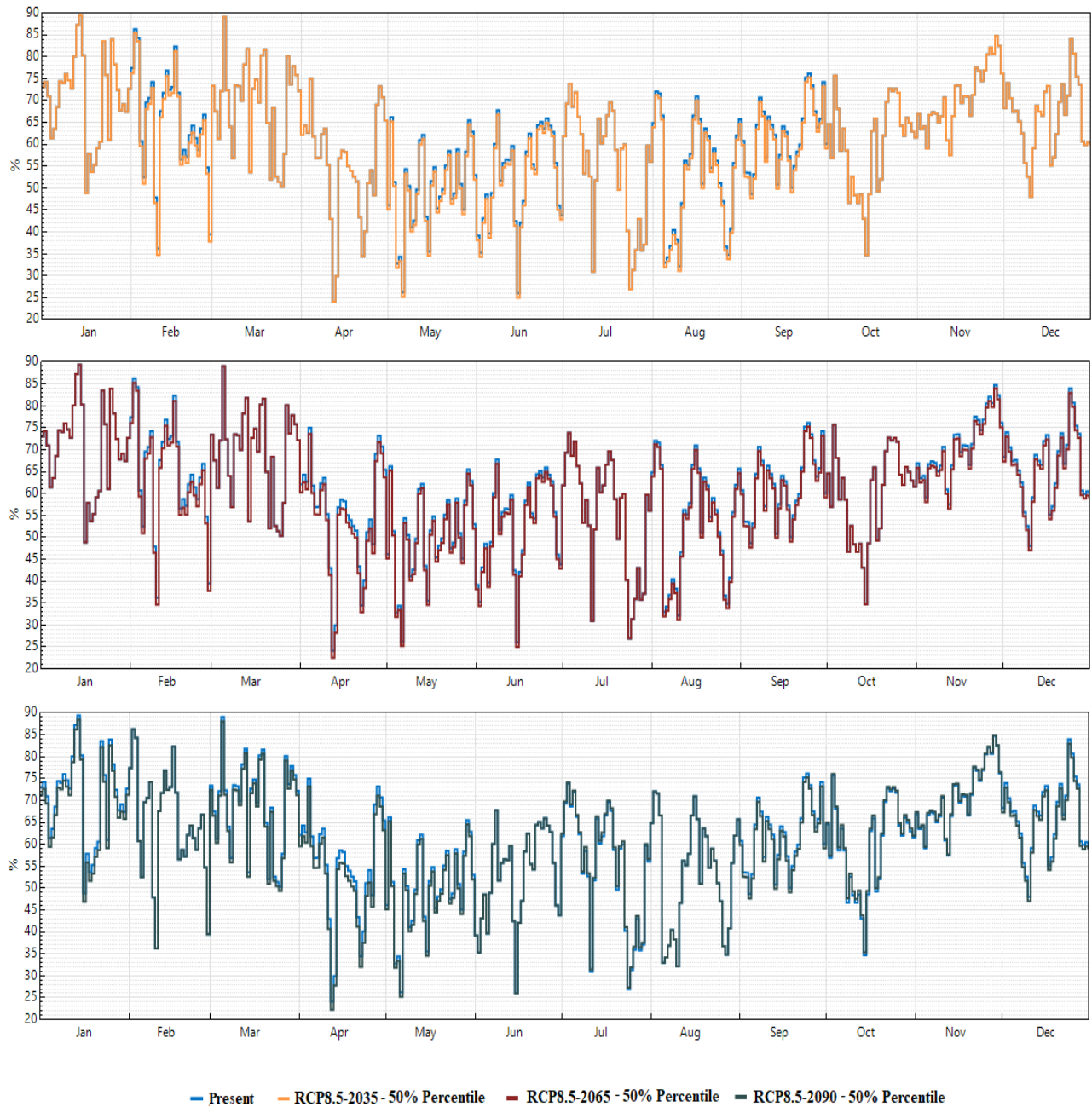


Figure 31: Comparison between the average daily RH% between IWEC present weather file and WeatherShift™ tool future files with 50% percentile (Dataviewer n.d.).

As can be seen from figure 32 below, the IWEC present weather file and period 2035 with 90% percentile have the same RH% in the months of September, June, and April, while in other months of the year the RH% of period 2035 with 90% percentile is less than IWEC present file.

The second line graph shows that the RH% of period 2065 with 90% percentile is less than the IWEC present weather file in all months of the year except July, August, and October. The third line graph shows the RH% of period 2090 with 90% percentile is higher than IWEC present file in October, November, June, and July whilst in other months of the year it is either the same or lower than IWEC present weather file.

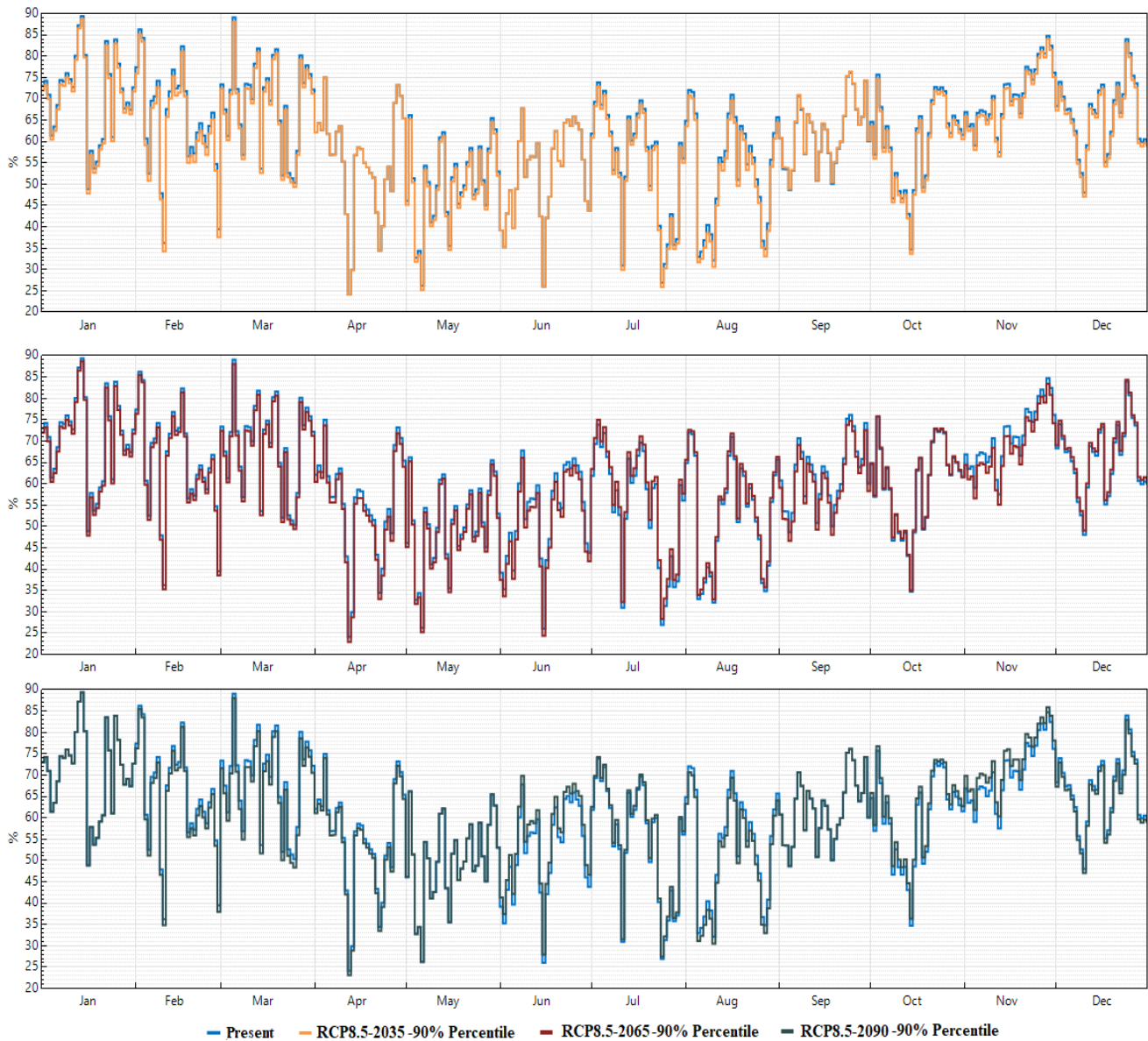


Figure 32: Comparison between the average daily RH% between IWEC present weather file and WeatherShift™ tool future files with 90% percentile (Dataviewer n.d.).

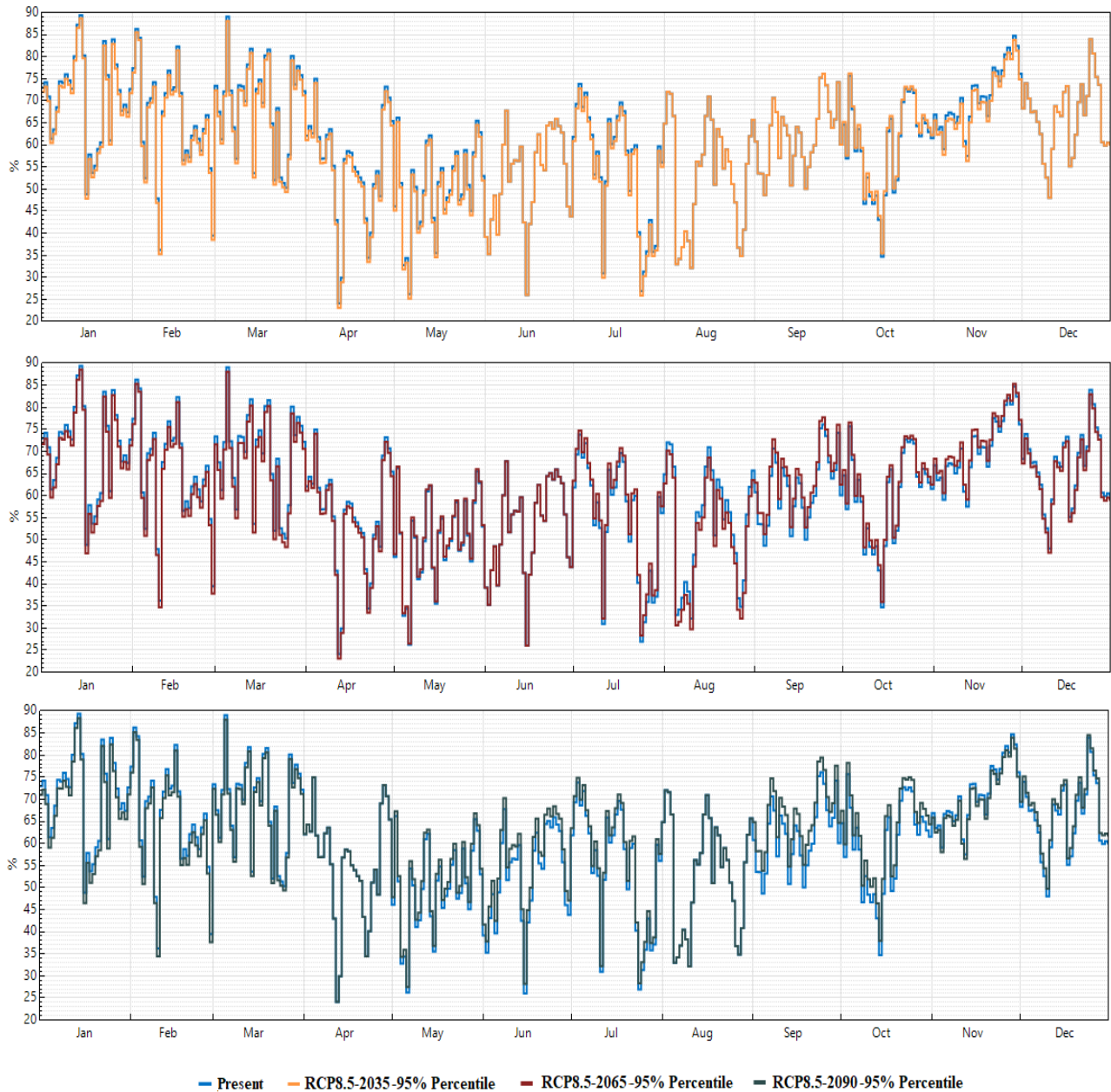


Figure 33: Comparison between the average daily RH% between IWEC present weather file and WeatherShift™ tool future files with 95% percentile (Dataviewer n.d.).

Figure 33 above shows that the RH% in for period 2035 with 95% percentile is either the same or slightly less than IWEC present weather file. In the second line graph, period 2065 with 95% percentile is higher than IWEC present weather files in July, September, October, and

November. While the third line graph shows that the RH% of period 2090 with 95% percentile is higher than IWEC present weather file in May, June, July, September, October, and December.

Table (17): Highest and lowest average daily RH% of the future WeatherShift™ files for periods 2035, 2065, and 2090 in 50th, 90th, and 95th percentiles based on figures 31, 32, and 33.						
Percentile	2035		2065		2090	
	Highest RH%	Lowest RH%	Highest RH%	Lowest RH%	Highest RH%	Lowest RH%
50th	89.3	24	89.3	22.5	88.4	22
90th	88.6	24	88.6	22.7	89.4	23
95th	88.6	23	88.5	23	88.4	23.9

The table above illustrates the highest and lowest RH% of the selected future WeatherShift™ files, all highest RH% values were recorded in 14th of January and all the lowest values were recorded in 12th of April. By comparing the nine selected files, the highest RH% between them was noted in period 2035 with 50% percentile and the lowest RH% was noted in period 2090 with 50% percentile.

Moreover, the three figures below represent the global horizontal solar radiation of the selected future WeatherShift™ files in 50%, 90%, and 95% percentiles. In figure 34, the three-line charts represent the future years of 50% percentile, the values of period 2035 are similar to IWEC present file in April and November while they are less than present file in the other months. The second line chart that represent period 2065 shows that the values of present file are almost the same in April, February, October, and November and they are less in the other months. Also, the third line chart shows that period 2090 will have the same results of present file in April and December while it recorded lower values in the other months.

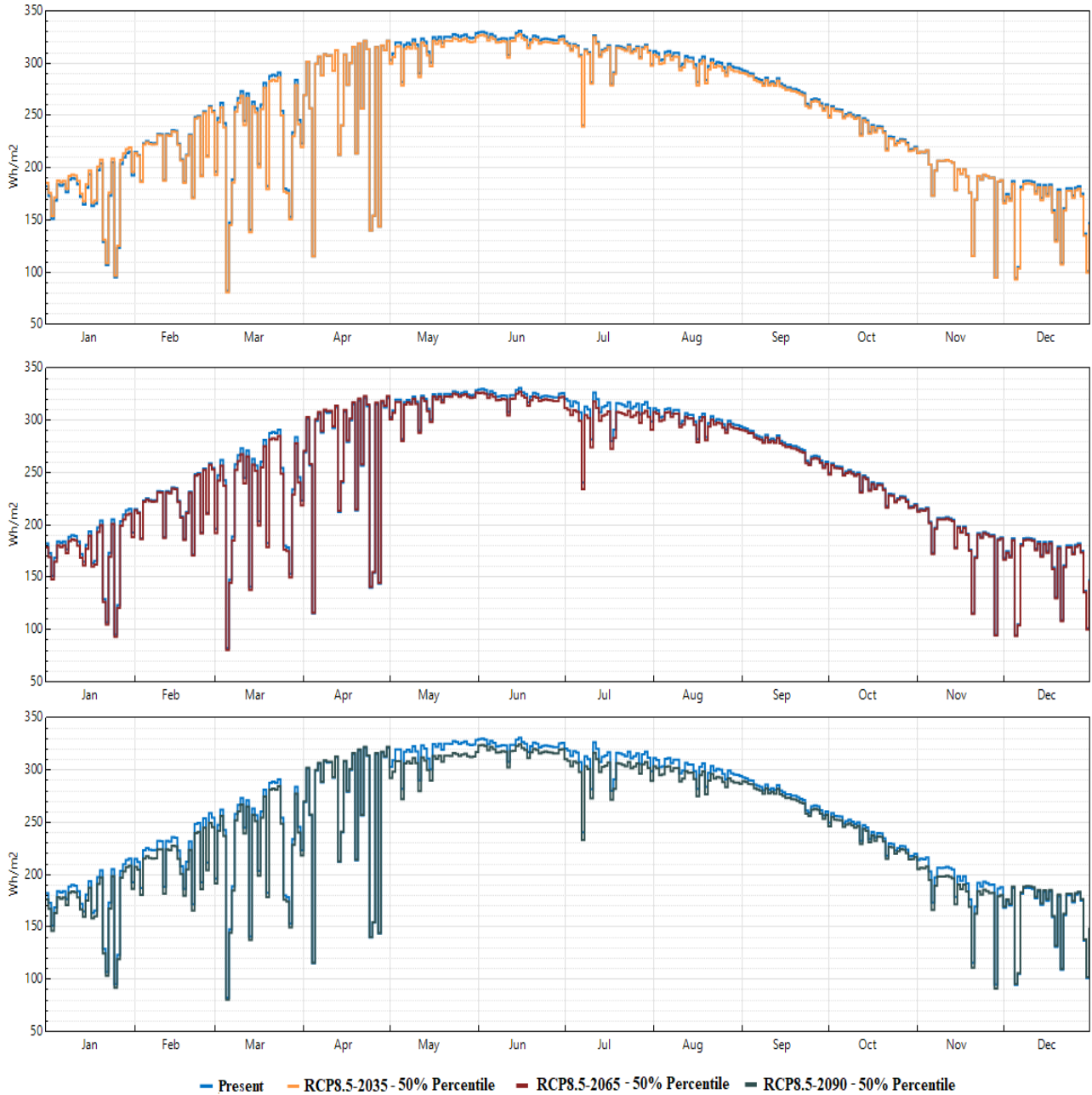


Figure 34: Comparison between the average daily global horizontal solar radiation in Wh/m^2 of IWEC present weather file and WeatherShift™ tool future files with 50% percentile (Dataviewer n.d.).

It can be seen from figure 35 below which compares between IWEC present file and WeatherShift™ tool future files with 90% percentile that the global horizontal solar radiation is decreasing throughout the years. In the first line graph, the values of present file and period 2035

file are almost the same in February and July, while in other months period 2035 values are less than IWEC present values. The next line chart that represent period 2065 shows that the values are similar to present file in February, May, and June but they are less in the other months. The last line chart in the figure represents period 2090 and shows that all values are less than the present file.

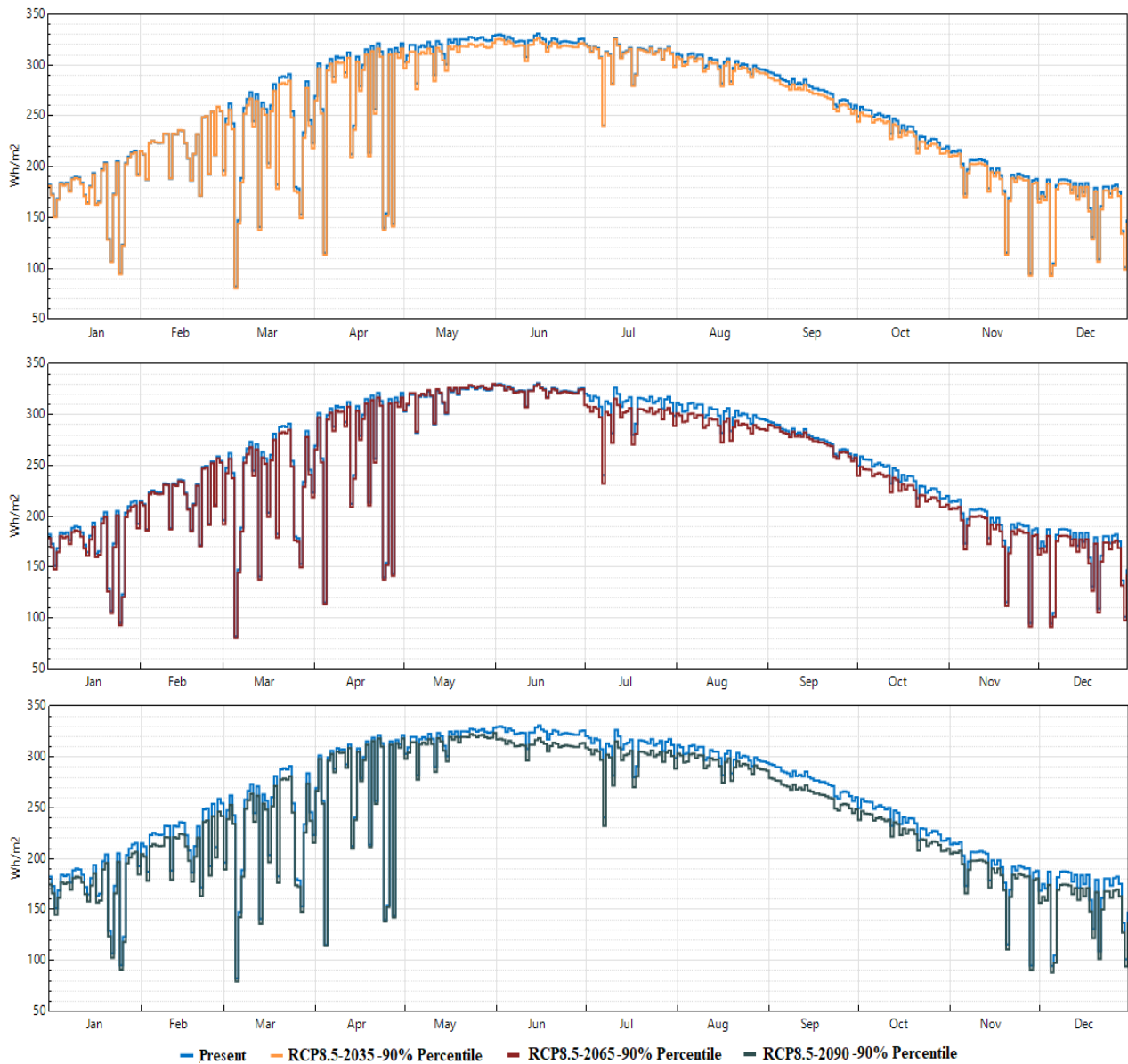


Figure 35: Comparison between the average daily global horizontal solar radiation in Wh/m² of IWEC present weather file and WeatherShift™ tool future files with 90% percentile (Dataviewer n.d.).

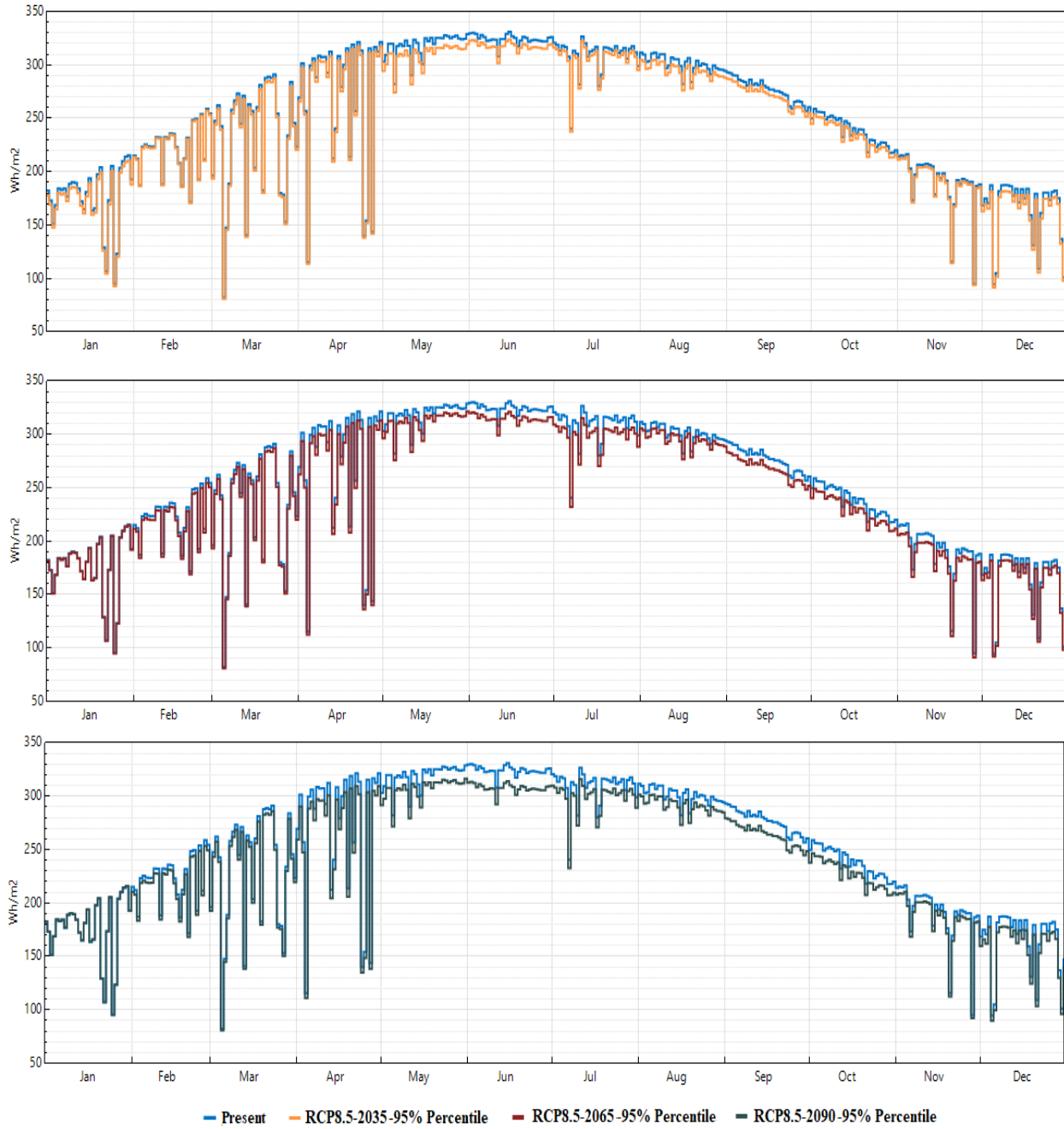


Figure 36: Comparison between the average daily global horizontal solar radiation in Wh/m² of IWECC present weather file and WeatherShift™ tool future files with 95% percentile (Dataviewer n.d.).

It is noted from figure 36 above that period 2090 reported lower values than the two other periods in the 95% percentile. Period 2035 shows that all values are less than IWEC present file, while in periods 2065 and 2090 all values are less than present file except the month of January.

Table (18): Highest and lowest average daily global horizontal solar radiation in Wh/m² of the future WeatherShift™ files for periods 2035, 2065, and 2090 in 50th, 90th, and 95th percentiles based on figures 33, 34, and 35.						
Percentile	2035		2065		2090	
	Highest global horizontal	Lowest global horizontal	Highest global horizontal	Lowest global horizontal	Highest global horizontal	Lowest global horizontal
50th	327	80	326	80	325	80
90th	326	80	330	80	324	79
95th	324	80	322	81	317	80

It is apparent from table (18) above that the highest recorded value of global horizontal radiation between the nine WeatherShift™ future selected files is 330 Wh/m² in period 2065 with 90% percentile, and the lowest value is 79 Wh/m² recorded in period 2090 with 90% percentile.

3.2.3- Meteonorm tool

This tool generates future weather files by integrating spatial interpolation, a stochastic method (defined in section 2.2.2), and climate data base. It can provide weather files for present and future years in any location in the world. Also, it allows the users to select historical, present, or future years, weather parameters, and files format based on their requirements. Future weather files in this tool are based on IPCC fourth assessment report (AR4) for three emission scenarios (A1B, A2, and B1) (Moazami, et al. 2019).

For this study, Meteonorm version 7.3 tool was used to provide weather files based on IPCC AR4-A1B emission scenario, which is equivalent to RCP 6.0 scenario (defined in table (2)),

section 2.1) (GlobalChange.gov 2014). Each file represents average weather parameters for a 10-years period, the first future period represents years 2020-2030 is referred as 2020 will be used along with two future periods of 2050-2060 referred as 2050, and 2080-2090 referred as 2080 for Dubai city. These files were generated from Meteonorm tool in EPW format in hourly time step.

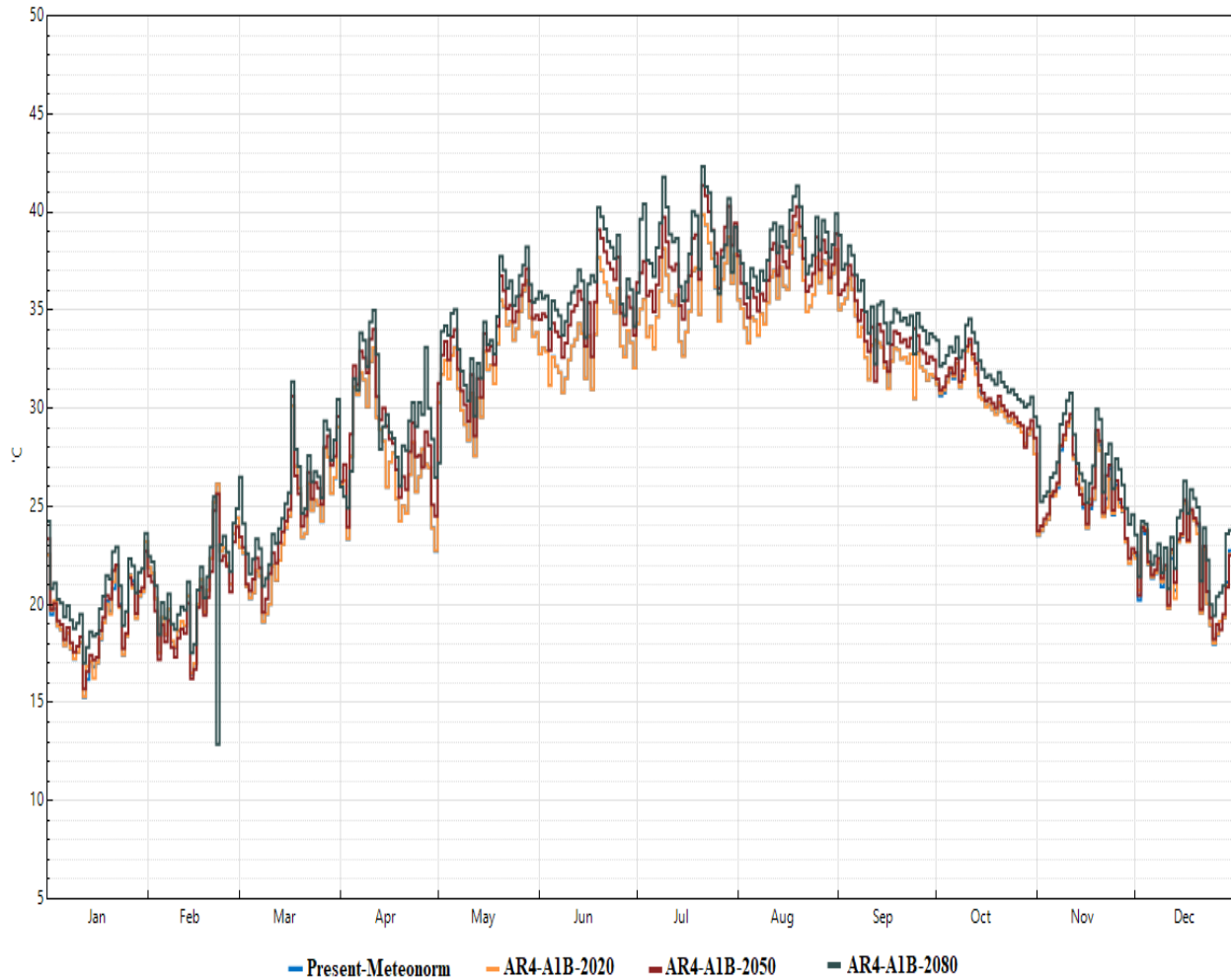


Figure 37: Comparison between the average daily dry-bulb temperature in C° between Meteonorm tool present and future predicted weather files (Dataviewer n.d.).

Figure 37 above illustrates the average daily dry-bulb temperature of the present and the three future weather files provided by Meteonorm tool. The present weather file of Meteonorm tool is an average of previous years, as mentioned before in section 2.2.2, stochastic method uses two

independent weather parameters to derive other weather parameters. For the present file, the temperature was derived from period 2000-2009 and the radiation was derived from period 1991-2010. It is noted from the figure that the temperature of period 2020 and present period are almost the same except a slightly increase in January and December. The highest temperature of period 2020 was recorded as 39.9° C in the 21st of July while the lowest temperature is 15.3° in 12th of January. While in period 2050, the highest temperature is 41.3° C in 21st of July and the lowest temperature is 15.7° C in 12th of January. The third period is 2080 has its lowest temperature is 12.9° C in 22nd of February which is considered to be an extreme weather condition, the second lowest temperature is 17° C in 12th of January, and the highest temperature is 42.3° C in 21st of July. Generally, it is clear from the figure above that the dry-bulb temperature values are increasing in all future periods.

As shown in figure 38 below, period 2020 RH% values are almost the same as present file values in the first line graph from January to July except some few days where period 2020 recorded slightly less, and the values fluctuates from August to December. The second and third line graphs show that the RH% values of periods 2050 and 2080 are fluctuating all the time. Also, it is noted that periods 2050 and 2080 RH% values are significantly higher than the present values which indicates that there is an expected increase in relative humidity in the future.

Table (19): Highest and lowest average daily RH% of present and future Meteonorm tool weather files based on figure 38.				
Percentile	Present	2020	2050	2080
Highest global horizontal	313	317	301	310
Lowest global horizontal	74	74	64	74

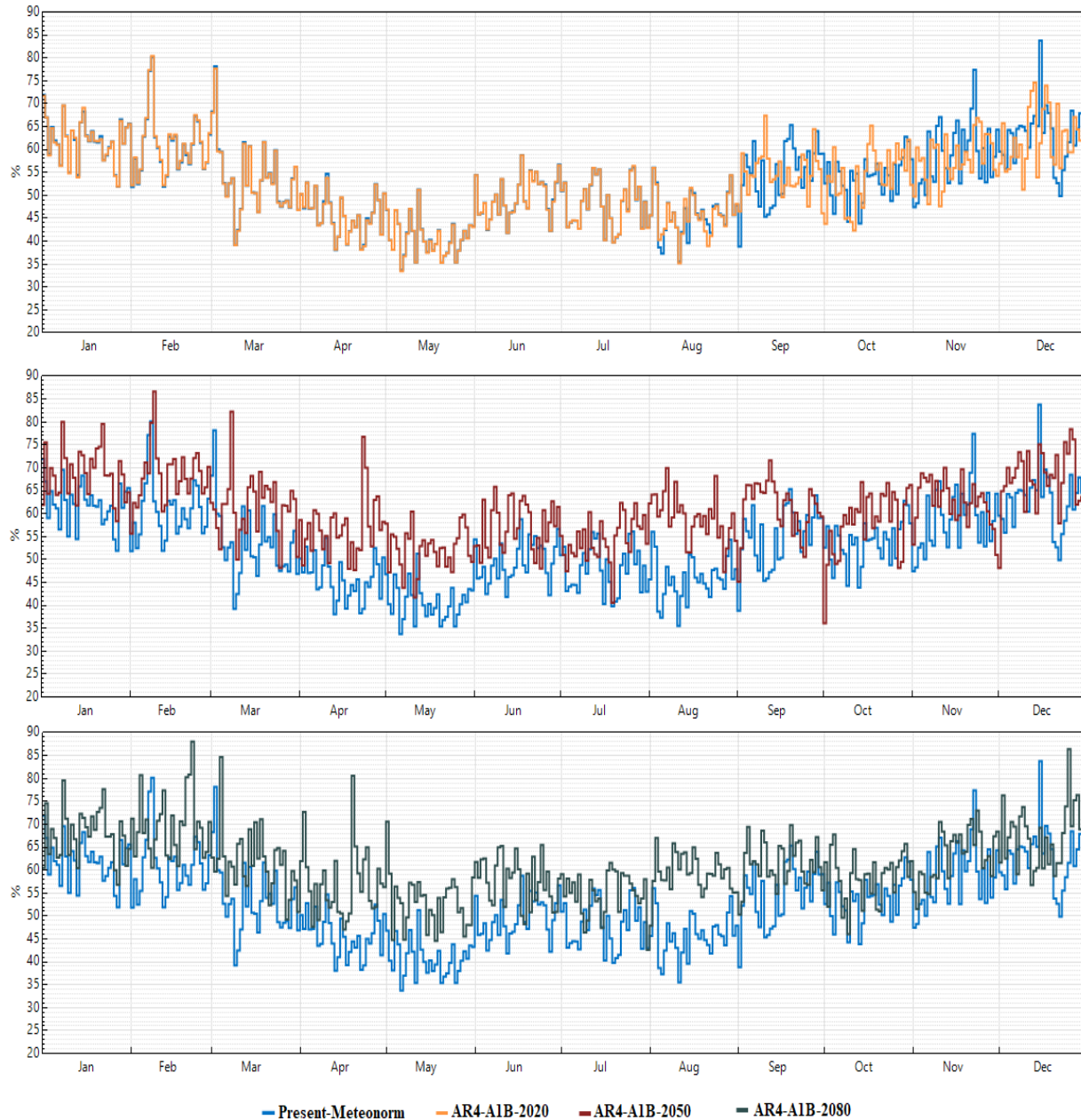


Figure 38: Comparison between the RH% between Meteonorm tool present and future predicted weather files (Dataviewer n.d.).

Figure 39 below provides a comparison between the global horizontal solar radiation of Meteonorm tool present and future predicted weather files. It shows that period 2020 has recorded the same values of present file in January, February, March, July, and the first 21 days of April, while results fluctuates on other days. Moreover, periods 2050 and 2080 values fluctuates

in all months and didn't record similar values with the present file unlike the WeatherShift™ and CCWorldWeatherGen tools future weather files.

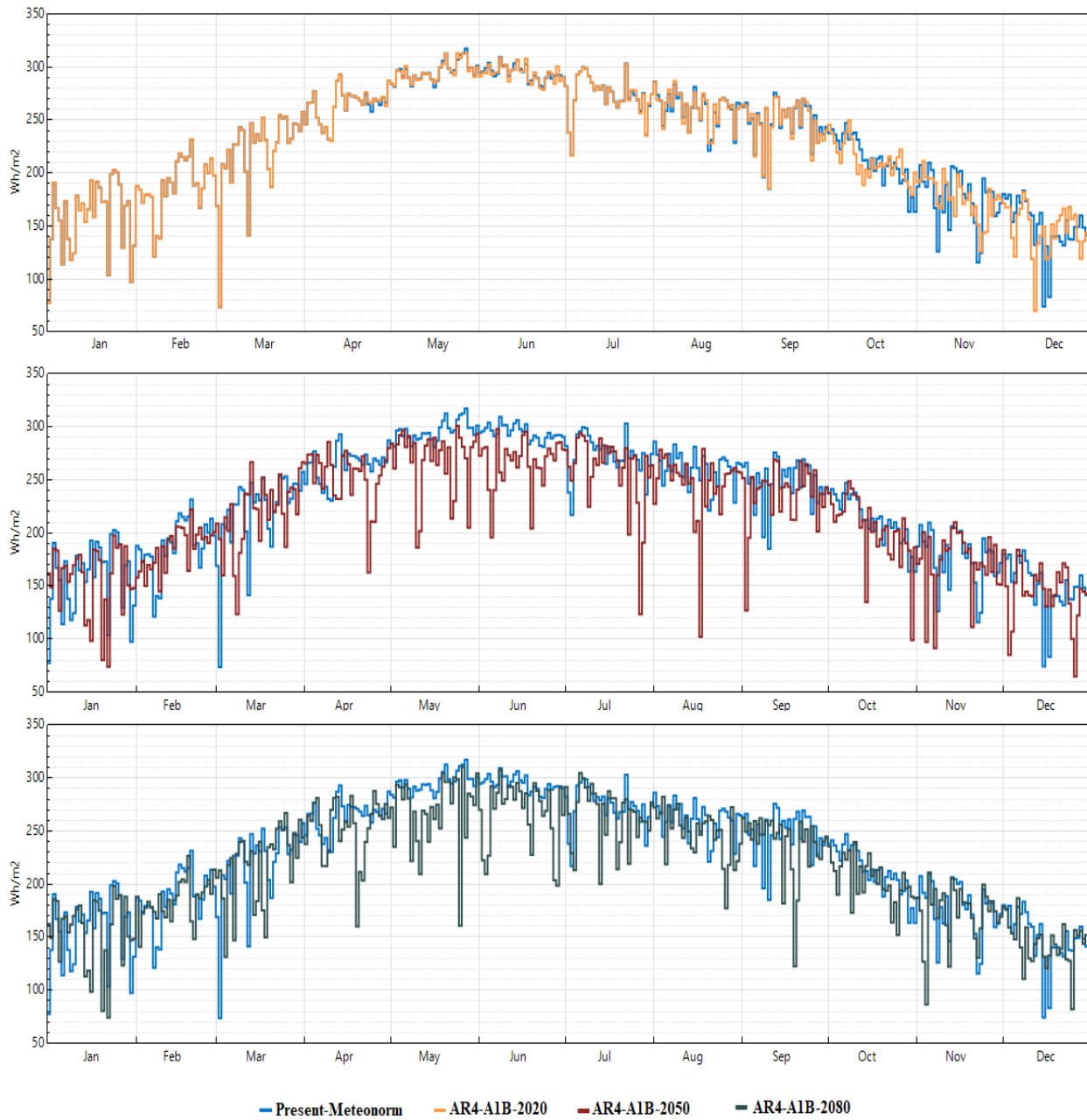


Figure 39: Comparison between the average daily global horizontal solar radiation between Meteornorm tool present and future predicted weather files (Dataviewer n.d.).

The highest and lowest daily global horizontal solar radiation recorded values of the four weather files are represented in table (20).

Table (20): Highest and lowest average daily global horizontal solar radiation in Wh/m² of the present and future Meteonorm tool files based on figure 39.				
Global horizontal radiation	Present	2020	2050	2080
Highest	313	317	301	310
Lowest	74	74	64	74

3.3- Energy saving solutions/technologies

Several energy saving technologies can be applied to buildings to reduce their energy consumption and cooling loads. As mentioned before, this study will test three types of solutions to investigate their present and future impact on total system and cooling energy consumption. Each technology has multiple configuration options that are applied to the base case model to find the most appropriate solution. Then, a comparison between the three types of options will be provided, and some suggestions will be offered based on the simulation results.

3.3.1- Increasing thermal insulation of the building

The first option is to increase the thermal insulation of the base case model by the addition of insulation layers. Insulation layers are designed to reduce the heat transfer through the external walls between the indoor conditioned spaces and outdoor ambient air which is produced by the three heat transfer processes, radiation, convection and conduction. Each insulation material has different thermal properties such as thermal conductivity, thermal resistance, and U-value (Wilson 2019). Thermal conductivity is constant for each type of materials, the lower the thermal conductivity, the better insulation will be provided. Good insulation layers have low thermal

conductivity and it is measured by W/m.K. Also, insulation layer thermal resistance is affected by material thickness and thermal conductivity, so it is different for each type of application and material. Moreover, application of insulation materials leading to lower U-values reduces heat transfer (Wilson 2019).

The base case model U-values for external wall and roof were selected to comply with ALSa'fat evaluation system which requires a maximum of 0.3 W/m²K for roof and 0.42 W/m²K for external walls to achieve Golden and Platinum Sa'fa (Al Safat, Dubai Green Building Evaluation System 2016).

In this study, two insulation materials will be applied to the base case model to improve the thermal performance of external walls. The first type is the mineral fiber, which is already applied to the base case model but with smaller thickness (75 mm), it will be replaced with higher thickness (150 mm) layer. The second option is a different insulation material (EPS), that will be applied with higher thickness (200 mm) and it will reduce external walls U-value significantly (see table (21) below). Also, simulation with the selected weather files will be applied to check how it will affect the present and future energy consumption. Those materials be added to the external wall of the base case model separately, thermal properties of the selected insulation materials are available in table (21), and construction materials of the external wall including options A1, and A2 are shown in appendix A in figures (A-1) and (A-2).

Table (21): Insulation materials types and thermal properties.							
Material type	Thickness (mm)	Thermal Conductivity W/ (m.K)	Density Kg/m ³	Specific heat J/(kg.K)	Resistance m ² K/W	External wall U-value W/m ² K	Life time (years)
MINERAL fiber slab	150	0.035	30	1000	0.357	0.1896	25

Expanded Polystyrene insulation (EPS)	200	0.025	20	1030	0.500	0.1113	25
--	-----	-------	----	------	-------	--------	----

3.3.2- Applying different glazing types for the base case model

Improving the glazing thermal properties of buildings in countries with long day time and high solar gains like UAE will reduce the cooling loads significantly. There are many types of glazing used in construction industry, those types differ by glazing layers, amount, coatings, and the air-fill placed between glazing layers. Using glazing type with high thermal properties for new buildings and retrofitting old windows in existing buildings is popular nowadays because it tends to be an affordable energy efficient solution (Donev et al. 2018).

Selecting the appropriate window type is dependent on the country climate, building window to wall ratio (WWR), and building orientation. The least energy efficient type of windows is the single-glazed window, it has one layer of glazing and can be available with reflective coatings which will enhance its thermal properties. Thus, single-glazed windows are rarely used in new projects. Double-glazed windows are the most commonly used type because they have better thermal properties. As shown in figure 40, double-glazed window consists of two glazing layers with air gap in between, this air gap is usually filled with inert gas (Argon or Krypton) or air. This air gap is placed between glazing layers to improve thermal and sound insulation, which will result in less solar radiation and heat gain entering the space (Donev et al. 2018). Triple-glazed windows are more efficient than double-glazed but they are rarely used due to their high cost. Figure 40 explains the layers structure of triple glazing as well, they consist of three glazing layers and two air gaps in between.

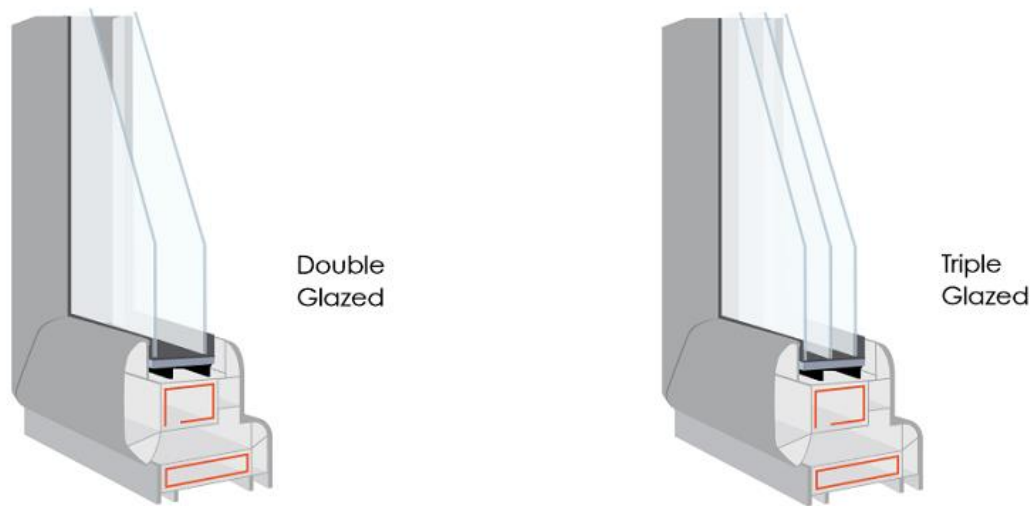


Figure 40: Structure of double and triple glazing windows (Pros & Cons of Double-Glazing Vs Triple-Glazing Windows 2020).

In this study, double and triple glazing windows with enhanced thermal properties will be applied to the base case model to check their impact on total system and cooling energy consumption. As shown in table (22), three types of windows are proposed in this study, each one of them has different thermal performance. Moreover, those types will be applied and simulated with the collected weather files that are mentioned in section (3.2) to find how each type will affect the present and future building energy consumption. This will give an insight for designers, and engineers about the most appropriate type of glazing that should be used for new and existing buildings in UAE.

The base case model windows are double-glazed with low U-value and high SHGC, they will be replaced with the three selected options and simulated in IES software. Type (a) is double-glazed window with reflective coating, and a cavity filled with Krypton gas, it has higher U-value and lower SHGC than the base case. The second option is type (b), it is double-glazed window as

well but with higher reflective coating, Krypton filled, and its U-value and SHGC are lower than the base case. The last proposed option is triple-glazed window and it has the most enhanced thermal properties. Although it has three glazing layer and two air gaps, its thermal properties are slightly better than type (b). The three options construction specifications are available in the appendix A in figures (A-3), (A-4), and (A-5).

Type	Glazing type	Material	Thickness	Gas	U-value (glass only)	SHGC	Emissivity		Reflectance	
							outside	inside	outside	inside
a	Double glazing	Outer pane	10 mm	-	2.6351	0.1143	0.837	0.837	0.19	0.19
		Cavity	12 mm	Krypton			-	-	-	-
		Inner pane	6 mm				0.837	0.837	0.072	0.072
b	Double glazing	Outer pane	6 mm	-	0.9860	0.1591	0.837	0.042	0.289	0.414
		Cavity	12 mm	Krypton			-	-	-	-
		Inner pane	6 mm				0.837	0.837	0.072	0.072
c	Triple glazing	Outer pane	6 mm	-	0.8100	0.1248	0.837	0.042	0.289	0.414
		Cavity	12 mm	Krypton			-	-	-	-
		Middle pane	6 mm				0.837	0.837	0.072	0.072
		Cavity	12 mm	Krypton			-	-	-	-
		Inner pane	6 mm				0.837	0.837	0.072	0.072

3.3.3- Adding heat exchanger and enthalpy recovery wheel (HRW) to the HVAC system

The last proposed solution is adding a heat exchanger/wheel to the HVAC system of the base case model. Three exchangers will be added to the three fresh air handling units (FAHUs) to

transfer the temperatures between exhaust air and incoming fresh air. This will reduce the temperature of the supplied fresh air which will result in cooling loads reduction. Energy recovery wheel and heat exchanger can be added to the HVAC system in IES software by applying air-to-air heat exchanger/enthalpy with temperature controller and selecting the required latent and sensible effectiveness. In this study, two options will be proposed, the first one is to add an energy recovery system with sensible heat exchange only and the second option is to apply a heat recovery wheel with both sensible and latent heat exchange.

In an HVAC system, the sensible heat exchange will result in changing the dry-bulb temperature of the incoming and outgoing air-streams. Therefore, the humidity ratio of the air will not change unless the warm air goes below its dew point temperature. While the latent heat exchange will affect the wet-bulb temperature and will result in increasing/decreasing the humidity ratio of the air-stream (Engineering ToolBox 2003).

In the first option, a cross flow air-to-air heat exchanger will be added to the HVAC system. As shown in figure 41, it consists of fixed plate heat exchanger that transfer the heat by allowing the supply and exhaust air to pass through the adjacent channels. The selected exchanger controls the sensible heat only and it is usually made of water-resistant material such as aluminum to prevent moisture exchange between air-streams. On the other hand, the second option will include an enthalpy heat recovery wheel. This rotating wheel is made of permeable material with large surface area to increase the heat exchange between air-streams and it rotates in 180° (see figure 42 below) to maximize the sensible and latent heat exchange between the two air-streams (Rafati Nasr et al. 2014).

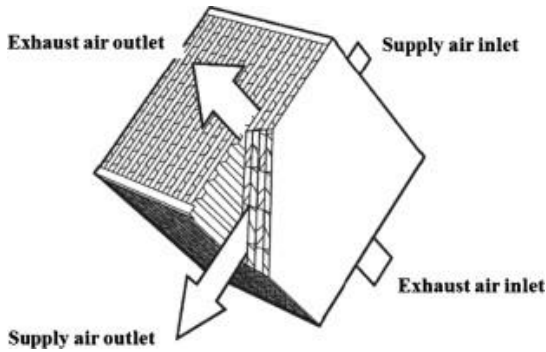


Figure 41: Cross flow air-to-air heat exchanger (ASHRAE 2008)

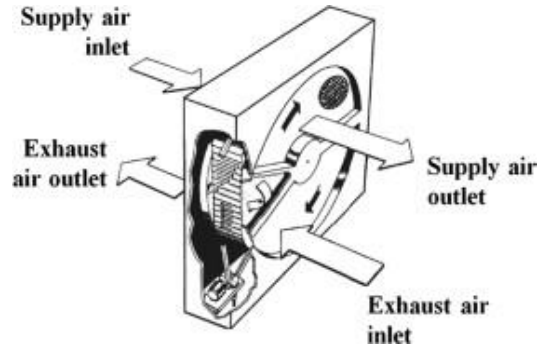


Figure 42: Enthalpy heat recovery wheel (ASHRAE 2008)

The performance of the selected options can be indicated by their effectiveness. The heat exchanger/wheel effectiveness is defined as the percentage of energy transferred by the recovery device to the supply and exhaust air-streams (Air Systems - Energy Series, *Energy Recovery Wheels* n.d.). According to ASHRAE standard 84 (1991), exchanger/wheel effectiveness can be calculated by the equation below:

$$\epsilon = [V_s \cdot (x_1 - x_2)] / [V_{\min} \cdot (x_1 - x_3)]$$

Where:

- | | | | |
|------------|--|------------|---|
| ϵ | = Sensible, or total effectiveness | x_2 | = SA temp (°Fdb) or enthalpy (btu/lb.) |
| x_1 | = OA temp (°Fdb) or enthalpy (btu/lb.) | x_3 | = RA temp. (°Fdb) or enthalpy (btu/lb.) |
| V_s | = Supply (or outside) air volume (cfm) | V_{\min} | = The lower of the exhaust or supply air volume (cfm) |

Moreover, the total energy transferred between supply and exhaust air is affected by exchanger effectiveness, volume of airflow, and the energy level variance between the two airflows.

In the first option, the sensible effectiveness will be added to the system assuming that there is no moisture exchange between incoming and exhaust air. According to Al Safat evaluation system,

the minimum sensible load efficiency for energy recovery systems are 70%, 75%, 80% for bronze and silver, gold, and platinum standards respectively (Al Safat, Dubai Green Building Evaluation System 2016). Therefore, the first option will be applied by simulating air-to-air heat exchanger with three different sensible energy effectiveness percentages (70%, 75%, and 80%) to check the amount of cooling energy reduction they will provide for the base case model. Then, the three options will be simulated with present and future weather files, this will clarify how air-to-air heat exchanger with different sensible efficiency will affect the cooling energy for UAE high-rise buildings with the predicted future climate change.

The second option is to add air-to-air heat exchanger/enthalpy to the system to represent HRW with sensible and latent effectiveness. The sensible energy effectiveness percentages will be the same as option one. The latent energy effectiveness percentages will be assumed as (2%-3%) less than the sensible energy effectiveness percentages similar to the desiccant based and synthetic fiber heat recovery wheels (Energy Recovery – Applied to IAQ 2011). Consequently, three selections with different sensible and latent effectiveness percentages will be applied and simulated to the base case HVAC system, the first one will have 70% sensible effectiveness and 68% latent effectiveness, the second will have 75% sensible effectiveness and 73% latent effectiveness, and the third will have 80% sensible effectiveness and 78% latent effectiveness. In addition, all proposed selections will be simulated with present and future weather files as well.

3.4 Summary of energy efficiency technologies tested

Table (23) below illustrates all proposed solutions/technologies options that will be tested in this study. Those options will be applied and simulated to the base case model separately to estimate the amount of total system and cooling energy reduction they will provide. Also, they will be tested with the proposed future weather files that are mentioned in section (3.2).

Table (23): Tested energy efficiency technology options.

Option reference	Option description	Option details
A	Increasing thermal insulation of the external wall	
A1	Additional 150 mm of MINERAL fiber slab external wall insulation	U-value = 0.1896 W/m ² K
A2	Additional 200 mm of EPS external wall insulation	U-value = 0.1113 W/m ² K
B	Different glazing types	
B1	10mm glass-12mm Krypton filled airgap- 6mm glass (28 mm)	U-value = 2.6351W/m ² K SHGC = 0.1143
B2	6mm glass-12mm Krypton filled airgap- 6mm glass (24 mm)	U-value = 0.9860 W/m ² K SHGC = 0.1591
B3	Triple, 6mm glass-12mm Krypton filled airgap- 6mm glass- 12mm Krypton filled airgap- 6mm glass (42 mm)	U-value = 0.8100 W/m ² K SHGC = 0.1248
C	Energy/heat recovery unit	
C1	Cross-flow air-to-air heat recovery unit (sensible only)	Sensible efficiency = 0.70 Latent efficiency = 0.00
C2	Cross-flow air-to-air heat recovery unit (sensible only)	Sensible efficiency = 0.75 Latent efficiency = 0.00
C3	Cross-flow air-to-air heat recovery unit (sensible only)	Sensible efficiency = 0.80 Latent efficiency = 0.00
C4	Enthalpy energy recovery wheel (sensible & latent)	Sensible efficiency = 0.70 Latent efficiency = 0.68
C5	Enthalpy energy recovery wheel (sensible & latent)	Sensible efficiency = 0.75 Latent efficiency = 0.73
C6	Enthalpy energy recovery wheel (sensible & latent)	Sensible efficiency = 0.80 Latent efficiency = 0.78

Chapter 4: Results and Discussion

To begin with, a base case model was created using IES software, the building has (G+24) floors with 4 rooms and in each floor and a core area in the middle as mentioned in section 3.1. An insulation layer was added to the external walls, double glazing external windows were selected too, and building properties selections comply with AlSa'fat evaluation system. To control the temperature in the rooms, building was divided into three zones and three fresh air handling units (FAHU's) were applied to those zones. Also, 125 fan coil units (FCU's) supplying recirculated air were used, each one of them will supply one room/space in the building.

To ensure an energy efficient HVAC system, reduce energy, and prevent over-sizing, IES auto-sizing was applied to the HVAC system by using ASHRAE heat balance method, results are discussed in details in section 4.1. Then, the base case model was simulated to check the energy consumption and thermal performance control of the building during the occupied hours. This base case model was designed to represent a typical high-rise building in Dubai, UAE.

The next stage was applying the selected energy efficient technologies/solutions to reduce the cooling energy consumption of the building. The proposed solutions are defined in table (23), chapter 3, and they include two different insulation layers, three external glazing types, and six HVAC system heat recovery units. Those solutions were selected based on previous researches/studies, then they were applied to the base case model resulting in 11 additional models. To study the resilience of high-rise buildings in UAE to climate change and its effect on energy demand, simulation was done to all solutions with the future selected weather files that are mentioned in section 3.2, and the results of total annual energy system and annual cooling system for the building were collected. Each option was added to the base case model and simulated separately, resulting in 192 total simulations.

Then, the percentage savings from the base case by adding each option separately in the same representative year will be calculated to investigate which solution would have more savings in future.

To do this the percentage reduction in total system and cooling energy was calculated by using the following equation and values were presented in a table for each solution:

$$\frac{\text{Amount of energy saving by applying option X to basecase in representative year Y}}{\text{Energy consumption of the basecase in representative year Y}} \times 100$$

Where,

- Amount of energy saving by applying option X to base case in representative year Y = Energy consumption of the base case in representative year Y - Energy consumption of the base case with option X in representative year Y.
- X is the selected option, and Y is the representative year (present or future).

According to simulation results, the trend of percentage reduction does not necessarily show increasing in future for all selected option. For example, considering the application of option B3, the percentage reduction in annual system and cooling energy decreases by time. While in option C6, the percentage reduction will increase in future, which means that option C6 will make the building more “resilient” than option B3 toward climate change in future.

Later on, the three most efficient solutions from external wall insulation layers, glazing, and heat recovery unit options were added to the base case and simulated with present and future files resulting in one additional model and 16 additional simulations (see section 4.7). This was done to measure the highest amount of energy saving in total system and cooling energy that could be achieved from using the three best solutions in present and future periods. Therefore, a total of

208 simulations were conducted in this study using IES-VE software, and all simulation results are represented and analyzed in this chapter.

4.1- Base case model HVAC system auto-sizing and simulation

4.1.1- HVAC system auto-sizing

As mentioned earlier, IES software was used to auto-size the HVAC system (see section 3.1). Figure 43 represents a schematic diagram of the HVAC system that is applied to each zone of the building, and table (24) explains the system FAHU and FCU design components in details. Cooling coil capacity and design air flow for FCU's were sized for each room depending on its heating and cooling loads which is described in table (25). HVAC system coefficient of performance (COP) is 3.125 which complies with AlSa'fat evaluation system as they have a minimum requirement of 1.9 COP (Al Safat, Dubai Green Building Evaluation System 2016).

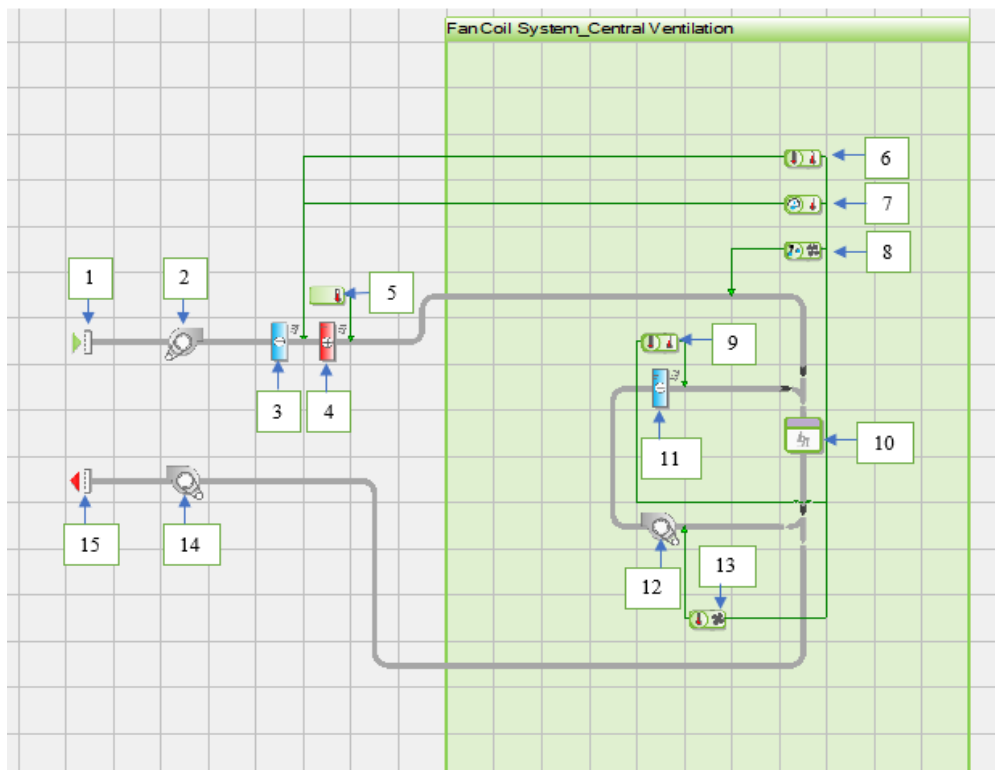


Figure 43: Schematic HVAC system for the base case model (IES Virtual Environment 2019).

Table (24): HVAC components details for Zone 1, Zone 2, and Zone 3 (IES Virtual Environment 2019).

Item #	description	Details
1	Air inlet	-
2	(FAHU) supply fan	Zone 1 and 2, design flowrate: 7680 l/s Zone 3, design flowrate: 8640 l/s
3	(FAHU) Cooling coil	Zone 1 and 2: Cooling capacity: 314 KW; oversizing factor: 1.15; contact factor: 0.94 Zone 3: Cooling capacity: 354 KW; oversizing factor: 1.15; contact factor: 0.94
4	(FAHU) Heating coil	Zone 1 and 2: heating capacity: 32.61 KW; oversizing factor: 1.25 Zone 3: heating capacity: 32.61 KW; oversizing factor: 1.25
5	(FAHU) heating coil temperature controller	Dry bulb temperature setpoint: 12.78° C (same for all zones)
6	(FAHU) Cooling coil independent controller with sensor- reset per zone demand (applied for each zone and room)	Dry bulb temperature setpoint: 23° C; setback: 25°C (same for all zones/rooms)
7	Independent humidity controller with sensor (applied for each zone and room)	Midband sensed relative humidity: 55% (same for all zones/rooms)
8	CO2 sensor with airflow controller* (applied for each zone and room)	Midband sensed CO ₂ concentration: 600 ppm (same for all zones/rooms)
9	Cooling Coil independent temperature controller with sensor (applied for each room)	On/off and proportional control with set point 22.5° C, setback 25.5° C (same for all rooms)
10	Conditioned rooms	All rooms + core

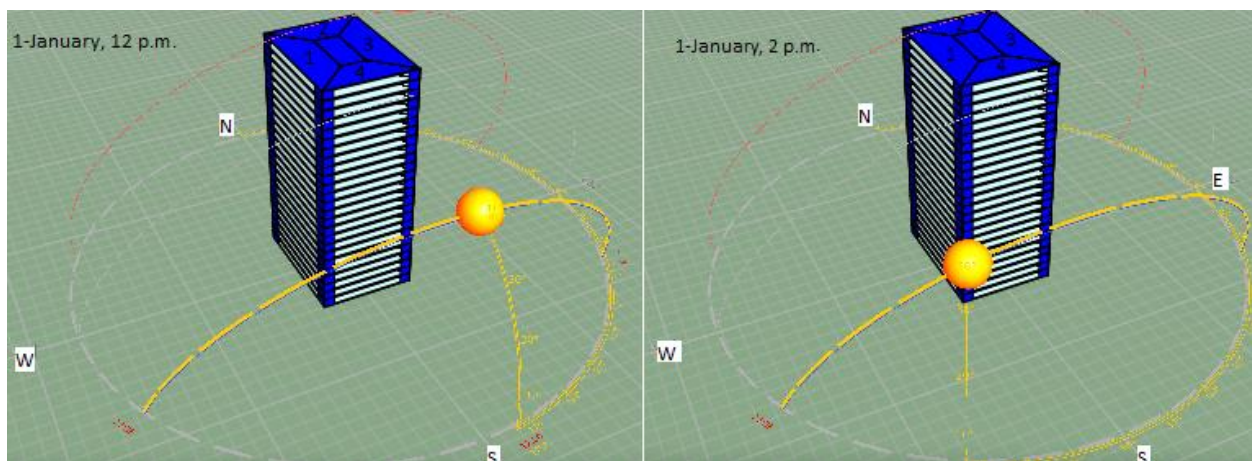
11	(FCU) Cooling coil	Design airflow and cooling capacity are mentioned in table (25) for each room
12	(FCU) fan	Design airflow is mentioned in table (25) for each room
13	Independent air flow controller with sensor	On/off and proportional control with set point 22.5° C, setback 25.5° C and dead band: 1.11° C (temperature control is same for all rooms, airflow is dependent on FCU fan see table (25))
13	(FAHU) exhaust fan	Zone 1 and 2, design flowrate: 7680 l/s Zone 3, design flowrate: 8640 l/s
14	(FAHU) Air outlet	Zone 1 and 2, exhaust flowrate: 7680 l/s Zone 3, exhaust flowrate: 8640 l/s
* CO2 sensor with airflow controller is an independent controller with sensor, sensor measures the CO2 level in each room from FCU returned air, and it gives a signal to the controller to supply fresh air when it drops lower than 600 ppm.		

Table (25): Fan coil unit design air-flow and cooling coil capacity for each room/space in the building, see layout in figure 20, chp.3 (IES Virtual Environment 2019).

Zone	Floor	Room 1			Room 2			Room 3			Room 4			core		
		Design airflow (l/s)		Cooling coil capacity (kw)	Design airflow (l/s)		Cooling coil capacity (kw)	Design airflow (l/s)		Cooling coil capacity (kw)	Design airflow (l/s)		Cooling coil capacity (kw)	Design airflow (l/s)		Cooling capacity (kw)
		Off coil	Off fan		Off coil	Off fan		Off coil	Off fan		Off coil	Off fan		Off coil	Off fan	
Zone 1	G	1977	1995	31.85	1043	1043	16.76	1909	1909	30.71	1368	1368	21.06	518	528	9.98
	1	1904	1931	30.62	998	998	16.08	1846	1846	29.79	1326	1326	20.08	489	490	9.6
	2	1900	1904	30.57	986	986	15.98	1843	1843	29.74	1324	1324	20.79	488	489	9.58
	3	1910	1910	30.65	986	986	15.98	1843	1843	29.74	1324	1324	20.79	488	489	9.58
	4	1900	1903	30.56	986	986	15.98	1843	1843	29.74	1324	1324	20.79	488	489	9.58
	5	1900	1903	30.57	986	986	15.98	1843	1843	29.74	1324	1324	20.79	488	489	9.58
	6	1896	1903	30.64	986	986	15.98	1843	1843	29.74	1324	1324	20.79	488	489	9.58
Zone 2	7	1896	1903	30.64	986	986	15.98	1843	1843	29.74	1324	1324	20.79	488	489	9.58
	8	1912	1912	30.67	983	983	15.87	1840	1840	29.71	1324	1324	20.80	488	489	9.58
	9	1912	1912	30.67	977	977	15.81	1840	1840	29.70	1324	1324	20.79	488	489	9.58
	10	1902	1930	30.59	966	976	15.83	1840	1840	29.70	1324	1324	20.79	488	489	9.58
	11	1902	1930	30.59	987	987	16.00	1840	1840	29.70	1324	1324	20.80	488	489	9.58
	12	1902	1930	30.59	987	987	16.00	1840	1840	29.70	1324	1324	20.78	488	489	9.58
	13	1902	1930	30.59	987	987	16.00	1840	1840	29.70	1324	1324	20.80	488	489	9.58
Zone 3	14	1902	1930	30.59	987	987	16.00	1840	1840	29.70	1324	1324	20.80	488	489	9.58
	15	1902	1909	30.59	988	987	16.00	1840	1840	29.70	1324	1324	20.80	488	489	9.58
	16	1899	1915	30.55	973	987	16.00	1833	1833	29.66	1324	1324	20.78	488	489	9.58
	17	1908	1908	30.62	981	981	15.85	1833	1833	29.66	1324	1324	20.78	500	501	9.72
	18	1899	1903	30.54	987	987	15.98	1832	1832	29.65	1324	1324	20.78	488	489	9.58

19	1895	1915	30.62	987	987	15.98	1832	1832	29.65	1324	1324	20.78	488	489	9.58
20	1899	1903	30.54	972	982	16.00	1833	1833	29.66	1324	1324	20.78	488	489	9.58
21	1899	1903	30.55	973	987	16.00	1833	1833	29.66	1324	1324	20.78	488	489	9.58
22	1899	1925	30.55	987	987	15.99	1832	1832	29.66	1324	1324	20.78	488	489	9.58
23	1899	1928	30.68	997	997	16.08	1816	1833	29.34	1326	1326	20.79	489	490	9.60
24	1965	1981	31.68	1018	1035	16.67	1909	1909	30.33	1352	1357	20.89	518	533	9.99

Table (25) above shows that the design air-flow and coil cooling capacity of the ground floor rooms is higher than the other rooms, this extra cooling load is due to the extra heat gain from the ground exposure. Also, the 24th floor would have an additional heat gain due to the roof solar exposure; however, this additional heat gain is considered to be small because of the high insulation level of the roof. As mentioned before, rooms 1 and 3 have the same area of 319m² and rooms 2 and 4 have the same area of 209m², but table (25) shows that room 1 requires more cooling than room 3 and room 4 requires more cooling than room 2. This extra heat gain is from external solar radiation because the building HVAC system is operated in occupied hours from 8 a.m. to 5 p.m. Which means there are a few hours after sunrise where solar gains don't affect cooling demand whereas room 1 and 4 facing west are exposed to sun in more hours (i.e. 12 p.m. to 5 p.m.) afternoon and this is increasing their cooling demand (see figure 44 below).



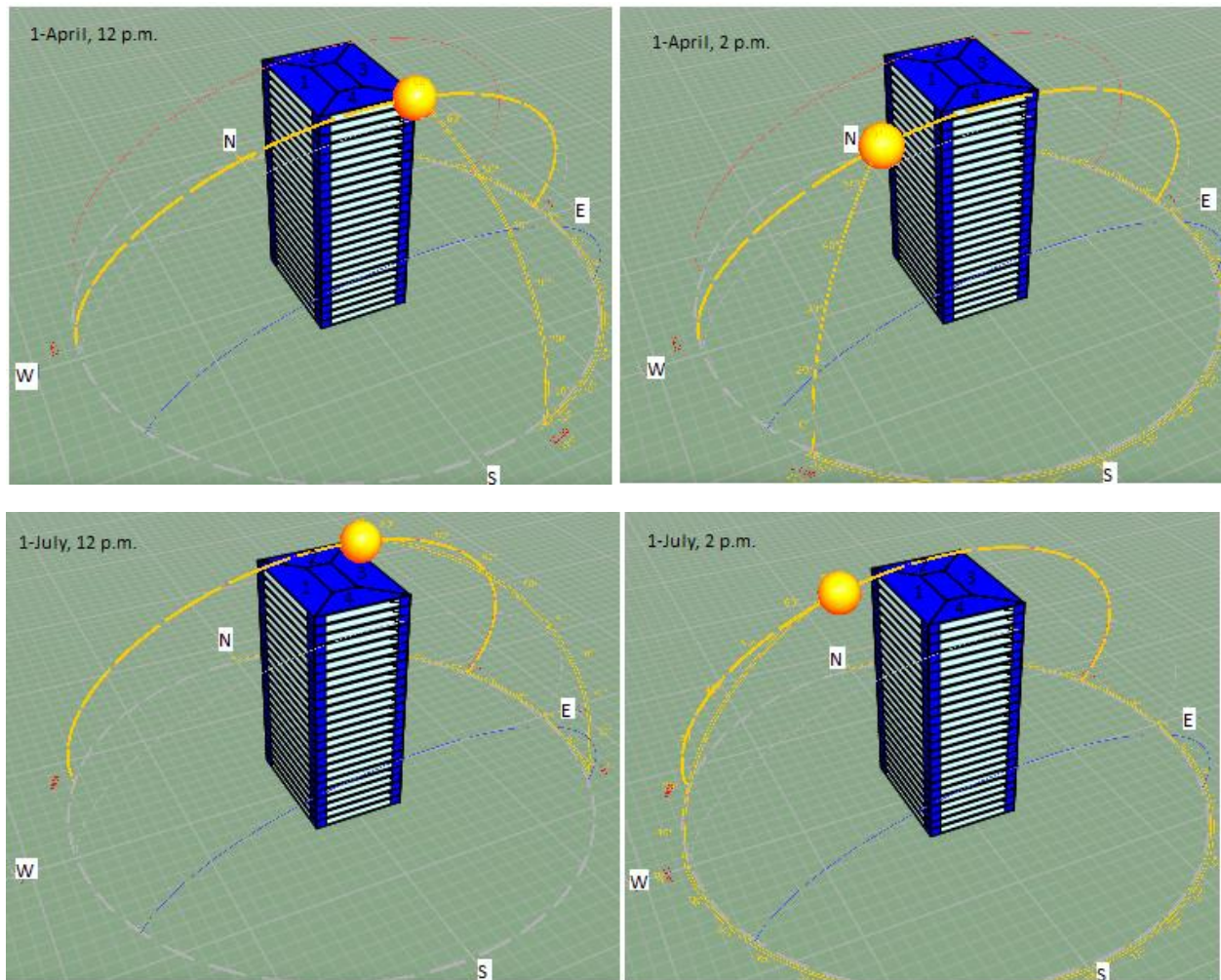


Figure 44: 3-D Sun cast view of the base case model in January, April, and July at 12p.m and 2p.m (IES Virtual Environment 2019).

4.1.2- Base case model simulation with present and future weather files

After auto-sizing the HVAC system, base case model was simulated with the present weather file that is provided by WeatherShift™ tool. This file will be used to represent the present weather conditions and will be compared with CCWorldWeatherGen, WeatherShift™, and Meteonorm future files to ensure comparison consistency.

Base case simulation with IWEC present file has resulted in 4983 MWh total system energy consumption by the building which is equivalent to 167.1 kwh/m².yr and 4130 MWh cooling energy consumption which is equivalent to 137.7 kwh/m².yr. This means that the building consumes around 83% of its energy for cooling. In this study, the total system energy represents the electric power consumed by building systems, small power systems, and lighting. While the total cooling energy represents the total amount of energy consumed by HVAC system to cool the spaces of the building (VistaPro Variables 2018).

According to Estidama pearl rating system, a typical office building in Abu Dhabi city consumes around 333 kwh/m².yr (The Pearl Rating System for Estidama Community Rating System (PCRS) Design & Construction 2010). On the other hand, the United Nations Environment Programme has reported that most of existing building in UAE consumes between 220-360 kwh/m².yr. While the retrofitted existing buildings annual energy consumption is between 160-260 kwh/m².yr, and the best practice energy efficient buildings consume around 110-160 kwh/m².yr (Clarke 2016). This means that the base case model energy consumption is considered acceptable but should be reduced to become a best practice energy efficient building.

The next step is to identify the effect of climate change on energy consumption for the base case model in future. Therefore, base case model was simulated with all selected weather files that are mentioned in section 3.2. The results of the simulation are shown in figures 45 and 46 below.

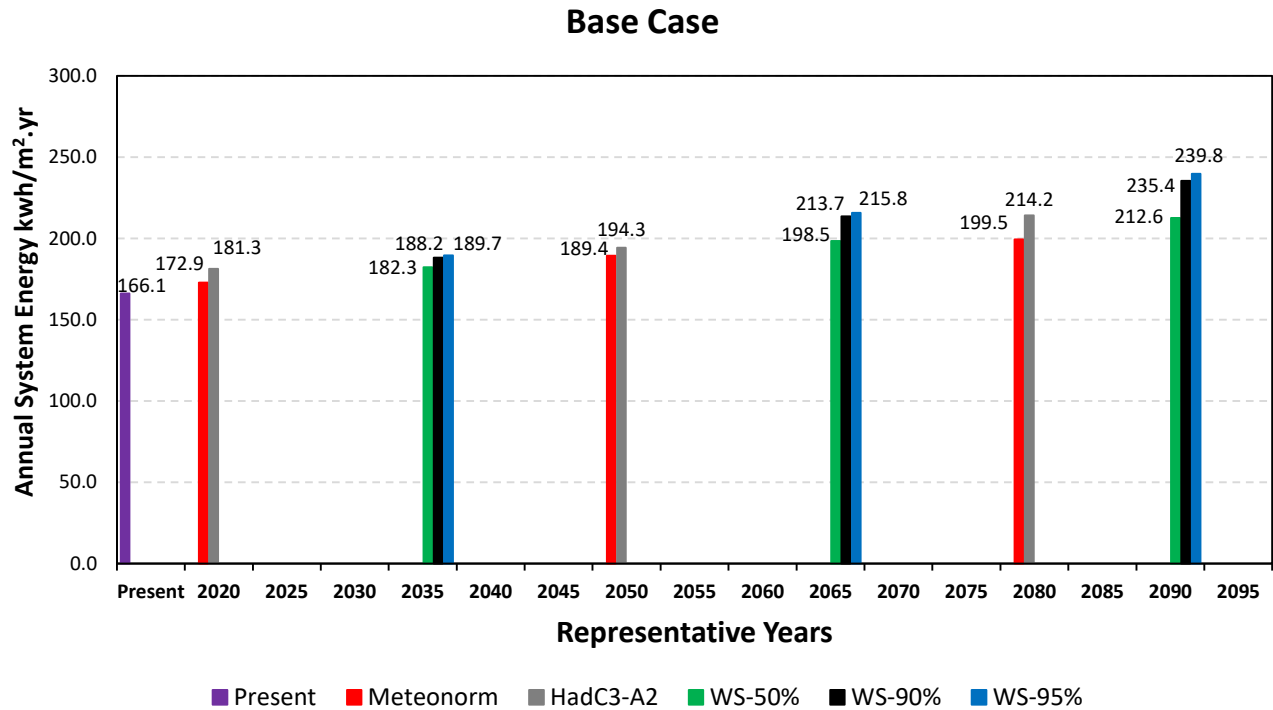


Figure 45: Total system energy of the base case model simulated with present and future weather files.

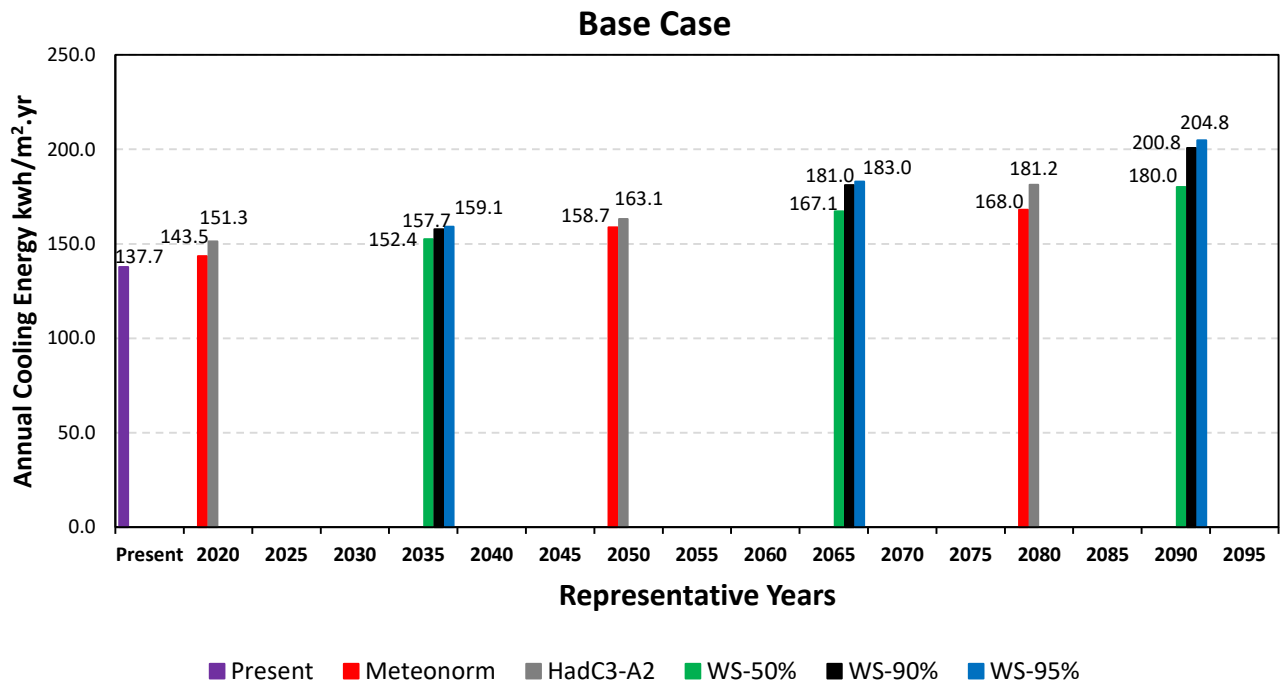


Figure 46: Total cooling energy of the base case model simulated with present and future weather files.

Based on the simulation outcomes, the following findings were concluded:

- The highest future values were recorded as 239.8 kwh/m².yr for total system energy and 204.8 kwh/m².yr for total cooling energy simulated with WeatherShift™ files that represents RCP8.5 emission scenario in period 2090 with 95% percentile followed by 235.4 kwh/m².yr for total system energy and 200.8 kwh/m².yr for total cooling energy in the same period with 90% percentile, see percentiles description in table (15). The third highest result was recorded in period 2080 as 214.2 kwh/m².yr for total system energy and 181.2 kwh/m².yr for total cooling energy simulated with CCWorldWeatherGen tool file that represents HadC3-A2 emission scenario.
- The lowest future values were recorded from stabilization emission scenario (AR4-A1B) Meteoronorm weather files with 172.9 kwh/m².yr for total system energy and 143.5 kwh/m².yr for total cooling energy in period 2020. The second lowest values are recorded for Hadc3-A2 emission scenario in period 2020 with 181.3 kwh/m².yr for total system energy and 151.3 kwh/m².yr for total cooling energy. The third lowest values are 182.3 kwh/m².yr for total system energy and 152.4 kwh/m².yr for total cooling energy recorded in RCP 8.5 emission scenario in period 2035 with 50% percentile.

As can be seen from the figures above, simulation with future weather files in all emission scenarios has increased the energy consumption of the building significantly. As mentioned before, the amount of energy increase in percentage for the base case simulated with all future weather files are compared with the present weather conditions by using WeatherShift™ IWEC present weather file. Percentage increase from the present consumption in total system energy is mentioned below in figure 47.

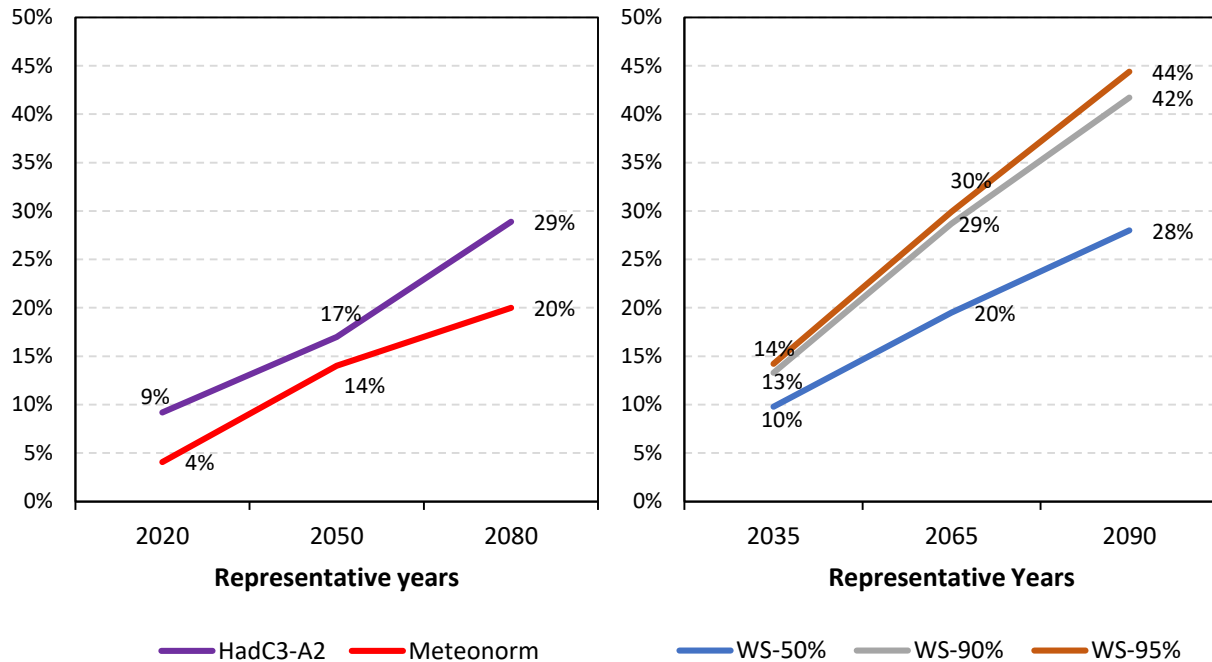


Figure 47: Percentage increase of the total system energy consumption of the base case in the future selected periods.

The base case simulation with Meteonorm files has the lowest percentage among other files in all future years, this is because those files are based on stabilization emission scenario (AR4-A1B).

The weather files from the other two tools are based on high emission scenarios, but the time slice of each period is different which is causing the difference in results (see section 3.2).

4.2- Increasing the thermal insulation of external walls

Results have shown that the energy consumption of the base case model is significantly increasing throughout the years in all emission scenarios. Therefore, energy efficient technologies/solutions are needed to improve building resilience to climate change and reduce energy consumption. Base case simulation concluded that 83% of energy consumption is coming from HVAC system, which is similar to most existing buildings in UAE where the HVAC system consumes around (80%~85%) of building total energy consumption (Kaul 2017). For that

reason, proposed solutions are selected to reduce building cooling loads which will reduce the building energy demand significantly.

To find the best solution that can resist global warming, several options were suggested and each one of them was simulated. The first proposed solution to reduce the cooling load of the building is by increasing the thermal insulation of external walls which would decrease their U-value. Simulation was conducted to check the effectiveness of this solution on building energy consumption. As mentioned earlier in table (21), two insulation materials with different thickness were tested and the results are shown in sections 4.2.1 and 4.2.2 below.

4.2.1- The effect of adding 150 mm of mineral fiber slab insulation for external wall.

Increasing the external wall insulation will reduce the amount of heat transfer from/to the building. The first option (A1) is to add 150 mm of mineral fiber slab insulation material to the external wall of the base case model which would reduce the U-value from 0.3194 W/m²K to 0.1896 W/m²K. Base case was simulated with option A1 and the results are shown below in figures 48 and 49.

Results have shown that decreasing the U-value by around 40% have reduced the total system energy consumption by 0.16% and the total cooling energy by 0.19% with the present weather conditions which is considered low. However, to investigate how this solution would affect the building resilience in future, all future results that are mentioned in figures 48 and 49 were compared with base case results and percentage reduction in energy consumption from base case for present and future periods are shown in table (26).

Option-A1

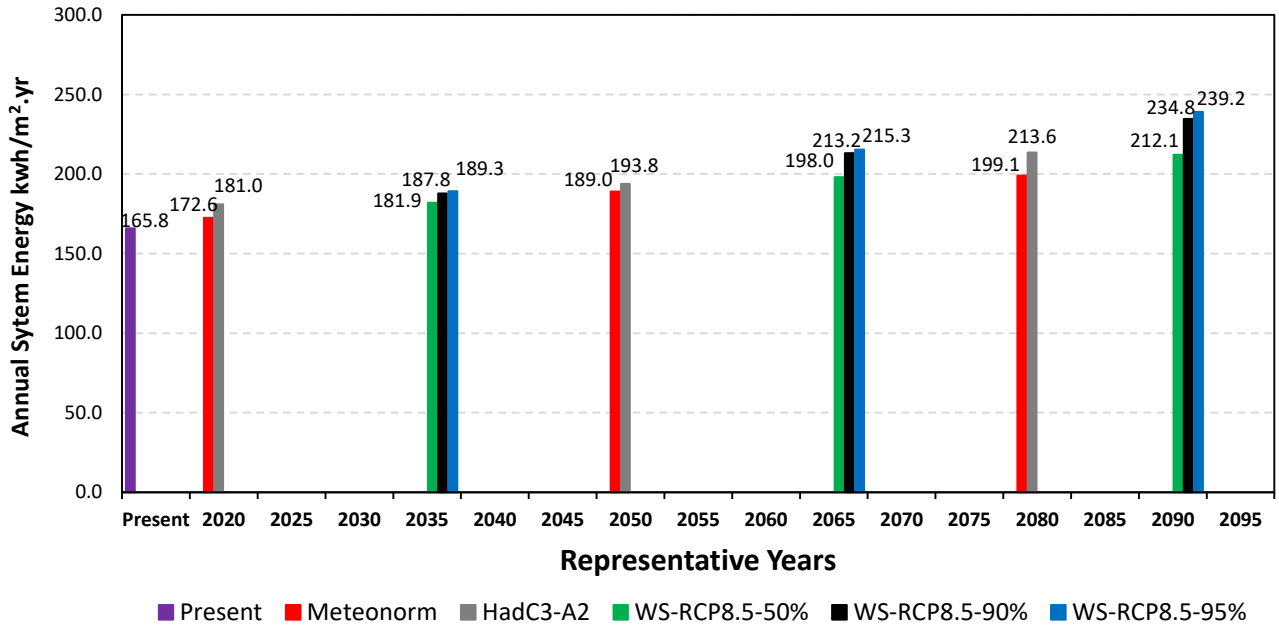


Figure 48: Total system energy of the base case model with option A1 simulated with present and future weather files.

Option- A1

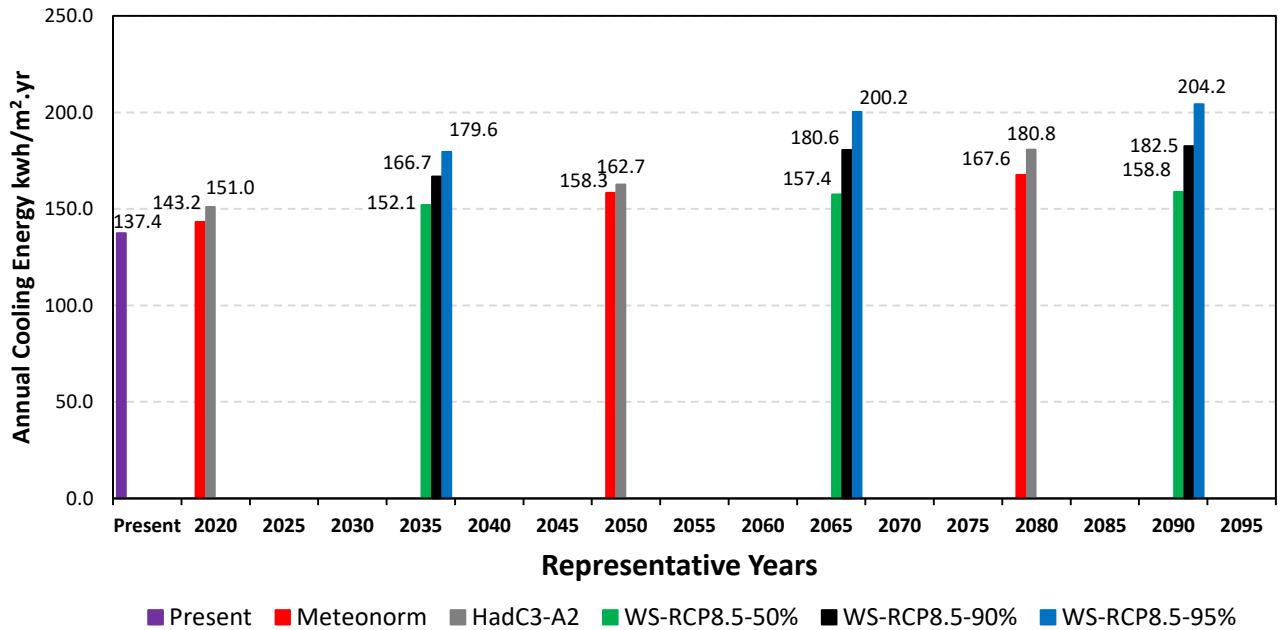


Figure 49: Total cooling energy of the base case model with option A1 simulated with present and future weather files.

Table (26): Percentage reduction in total system energy and total cooling energy from the base case model for present and future periods by applying option (A1)											
HadCM3-A2: CCWorldWeatherGen tool											
Period		HadCM3-A2-2020			HadCM3-A2-2050			HadCM3-A2-2080			
Total system energy		0.18%			0.22%			0.25%			
Total cooling energy		0.20%			0.25%			0.26%			
AR4-A1B: Meteonorm tool											
Period		2020			2050			2080			
Total system energy		0.19%			0.21%			0.20%			
Total cooling energy		0.21%			0.21%			0.24%			
RCP8.5: (WS) WeatherShift™ tool											
Period	Present	50% percentile			90% percentile			95% percentile			
		2035	2065	2090	2035	2065	2090	2035	2065	2090	
Total system energy		0.16%	0.22%	0.25%	0.24%	0.21%	0.23%	0.28%	0.21%	0.25%	0.28%
Total cooling energy		0.19%	0.24%	0.26%	0.24%	0.21%	0.26%	0.28%	0.21%	0.26%	0.31%

Table (26) illustrates that increasing the insulation level would slightly improve the building resilience in future. Although the percentage reduction is still low, but is increasing with time and this improvement is applicable for both total system and cooling energy for all emission scenarios. Moreover, low percentage reduction in results can be related to the margin of error which make the results not confidently applicable to confirm if there is an energy benefit or not. However, results show that high emission scenarios are expecting more reduction and this is due to the global warming where higher air temperatures are expected, so lowering the thermal transmittance is needed. For example, the total cooling energy for RCP 8.5 emission scenario in period 2090 with 95% percentile would have 0.31% less energy than the base case. While in the

same period the cooling energy reduction from base case for 90% and 50% percentiles are 0.28% and 0.24% respectively. Therefore, the results of applying option A1 to the base case model conclude that this solution will improve building resilience and reduce the energy consumption in future inconsiderably. Figure 50 illustrates the percentage increase in total system energy from present consumption when applying option A1 to the base case. Which means that applying option A1 would consume 165.8 kwh/m².yr in the present period and this is expected to increase by 44% in period 2090 with 95% percentile.

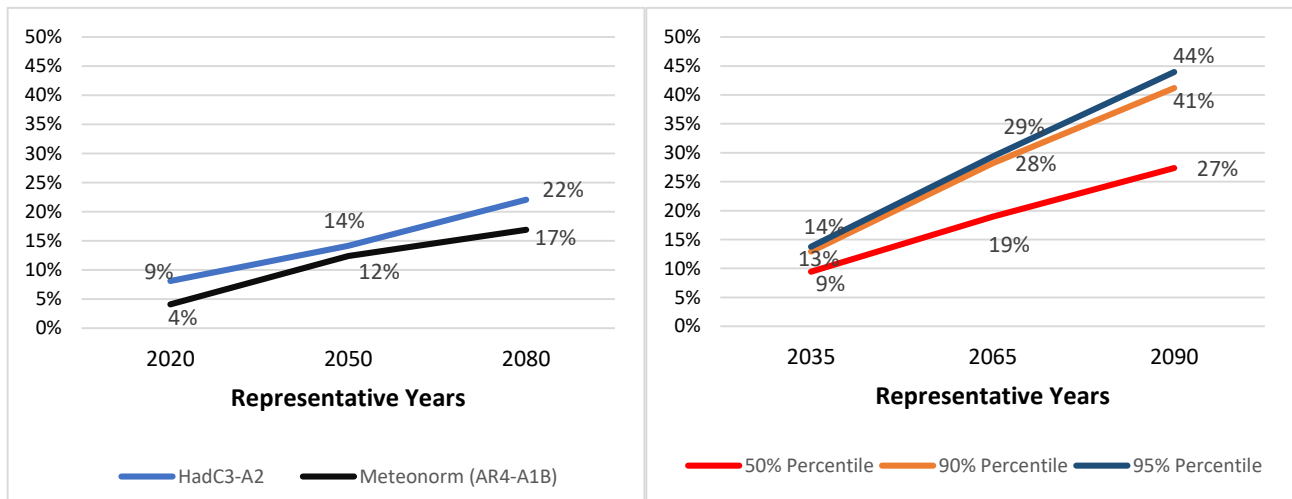


Figure 50: Percentage increase from present consumption in the total system energy of the base case with option A1 in the future selected periods.

4.2.2: The effect of adding 200 mm of (EPS) insulation material for external wall

The second proposed solution (A2) is to add 200 mm of Expanded Polystyrene (EPS) insulation material to the external wall of the base case model which would reduce its U-value to 0.1113 W/m²K. This solution was selected to discover the effect of external wall insulation and the amount of energy reduction that it can produce. Also, how it would affect the energy consumption in the future with the global warming and climate change. Therefore, U-value was

reduced by 65% and the model was simulated. Results of total system energy and total cooling energy of the base case model with option (A2) are represented in figures 51 and 52.

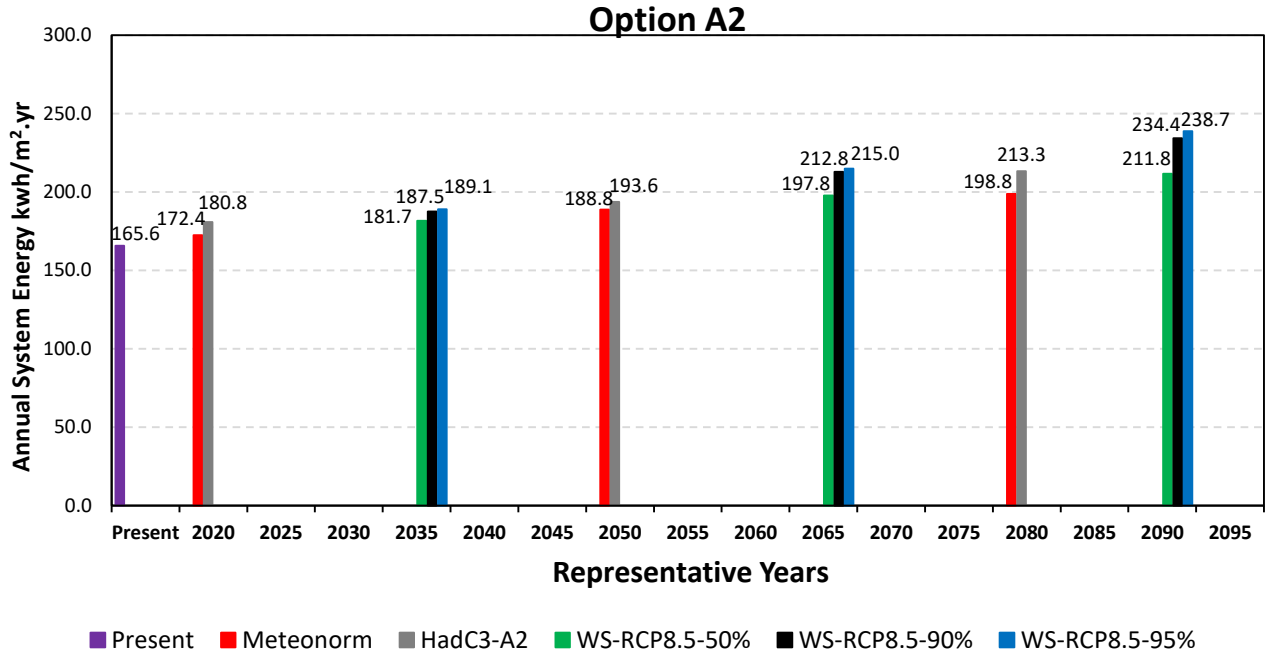


Figure 51: Total system energy of the base case model with option A2 simulated with present and future weather files.

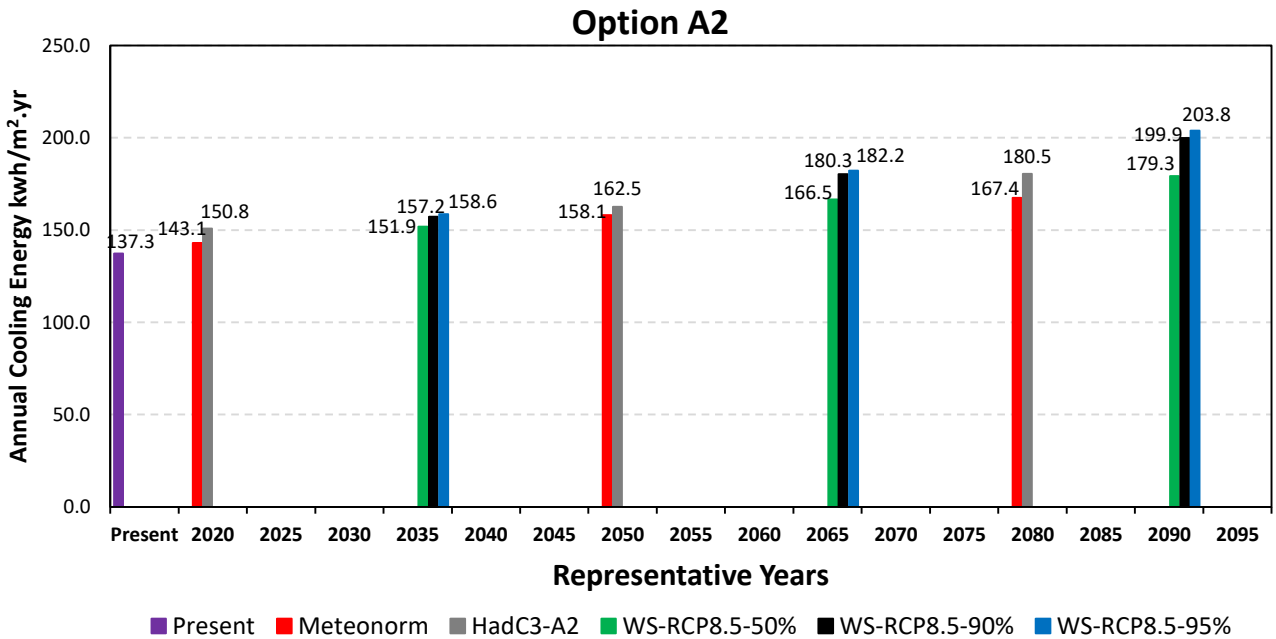


Figure 52: Total cooling energy of the base case model with option A2 simulated with present and future weather files.

Simulation results show that increasing the insulation of external walls will slightly reduce the energy consumption in present weather conditions. Also, reduction in energy for both total system energy and total cooling energy compared with option A1 is minimal. Table (27) represents the percentage reduction of energy from the base case model for present and future periods.

Table (27): Percentage reduction in total system energy and total cooling energy from the base case model for present and future periods by applying option (A2)											
HadCM3-A2: CCWorldWeatherGen tool											
Period		HadCM3-A2-2020			HadCM3-A2-2050			HadCM3-A2-2050			
Total system energy		0.31%			0.34%			0.39%			
Total cooling energy		0.33%			0.37%			0.42%			
AR4-A1B: Meteororm tool											
Period		2020			2050			2080			
Total system energy		0.31%			0.32%			0.35%			
Total cooling energy		0.33%			0.34%			0.38%			
RCP8.5: (WS) WeatherShift™ tool											
Period	Present	50% percentile			90% percentile			95% percentile			
		2035	2065	2090	2035	2065	2090	2035	2065	2090	
Total system energy		0.28%	0.33%	0.39%	0.39%	0.34%	0.41%	0.45%	0.33%	0.40%	0.46%
Total cooling energy		0.29%	0.37%	0.38%	0.41%	0.34%	0.42%	0.46%	0.36%	0.42%	0.49%

Results in table (27) reveal that increasing the insulation of the base case model will slightly improve the building resilience in future. Percentage reduction of energy from the base case could reach 0.49% for cooling energy and 0.46% for system energy in period 2090 with 95% percentile. While the present reduction is only 0.29% for cooling energy and 0.28% for system

energy of the building. As mentioned in section 4.2.1, this low reduction in energy saving would fall under margin of error in modelling. Moreover, this model shows that the heat gain from external walls is very small compared with windows heat gain, see peak cooling load of rooms 1, 2, 3, and 4 of the 12th floor in appendix B, table (B-1).

Figure 53 below demonstrates that the percentage increase in total system energy from present consumption when applying option A2 to the base case. For example, total system energy consumption of base case with option A2 would increase by 41% in period 2090 with 90% percentile from present consumption of base case with option A2.

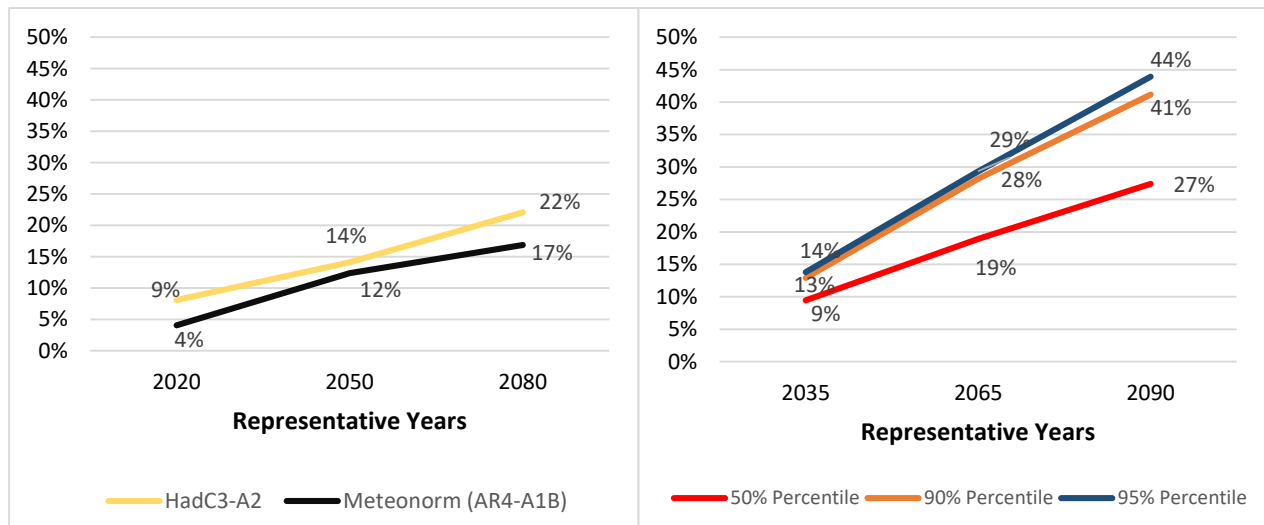


Figure 53: Percentage increase from present consumption in the total system energy of the base case with option A2 in the future selected periods.

4.3- Improving the glazing properties of the external windows.

The second proposed solution is to improve the glazing properties of the windows. In hot countries like UAE, the heat gain from windows is high due to the long day hours and high outdoor air temperatures. Therefore, three improved glazing options were tested, two of them are double glazed and one is triple glazed. Each option has different U-value and SHGC to

understand which thermal property would affect the energy consumption and improve the building resilience toward climate change in future.

4.3.1- Applying Krypton filled double glazing with lower SHGC and higher U-value

In this option (B1), Krypton filled double glazing with 10mm glass-12mm Krypton filled airgap-6mm glass (28 mm) thickness was applied to the base case model. This option will reduce the SHGC from 0.3955 to 0.1143 and will increase the U-value from 1.6753 W/m²K to 2.6351W/m²K. Simulating this option with present and future weather files will show if increasing thermal transmittance and reducing SHGC will affect future energy consumption as ambient air temperature is expected to increase whilst solar radiation remains relatively unchanged. The results obtained from simulation are shown in figures 54 and 55. Moreover, table (28) illustrates the percentage reduction of energy from the base case model by applying option B1

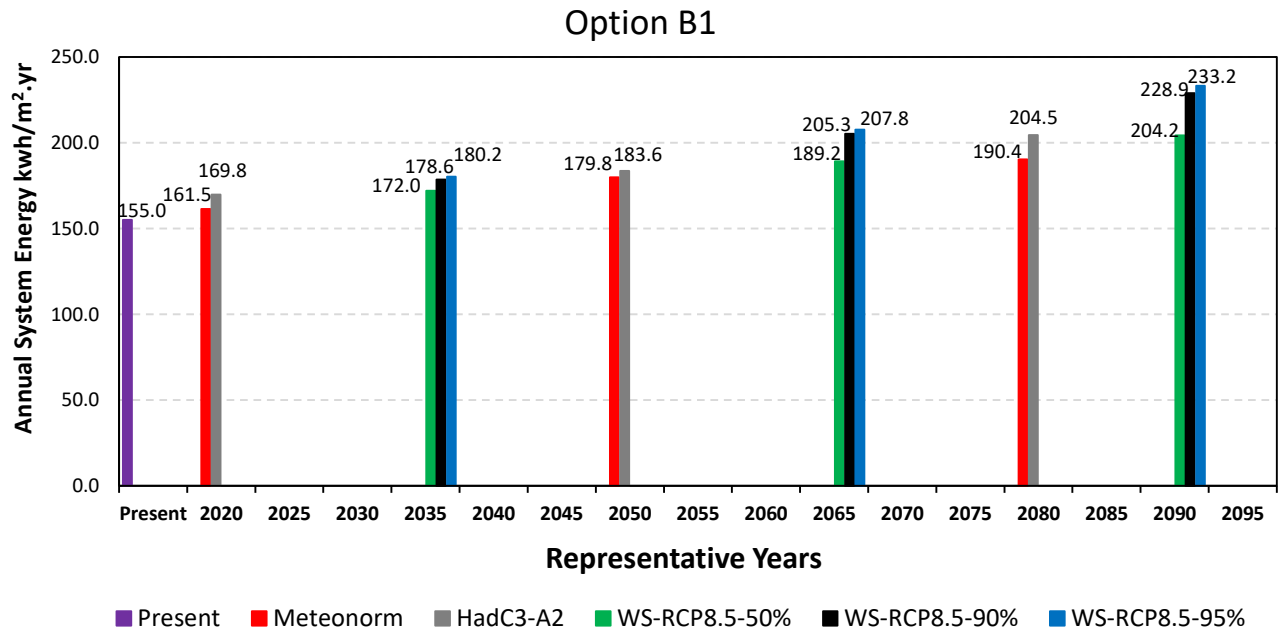


Figure 54: Total system energy of the base case model with option B1 simulated with present and future weather files.

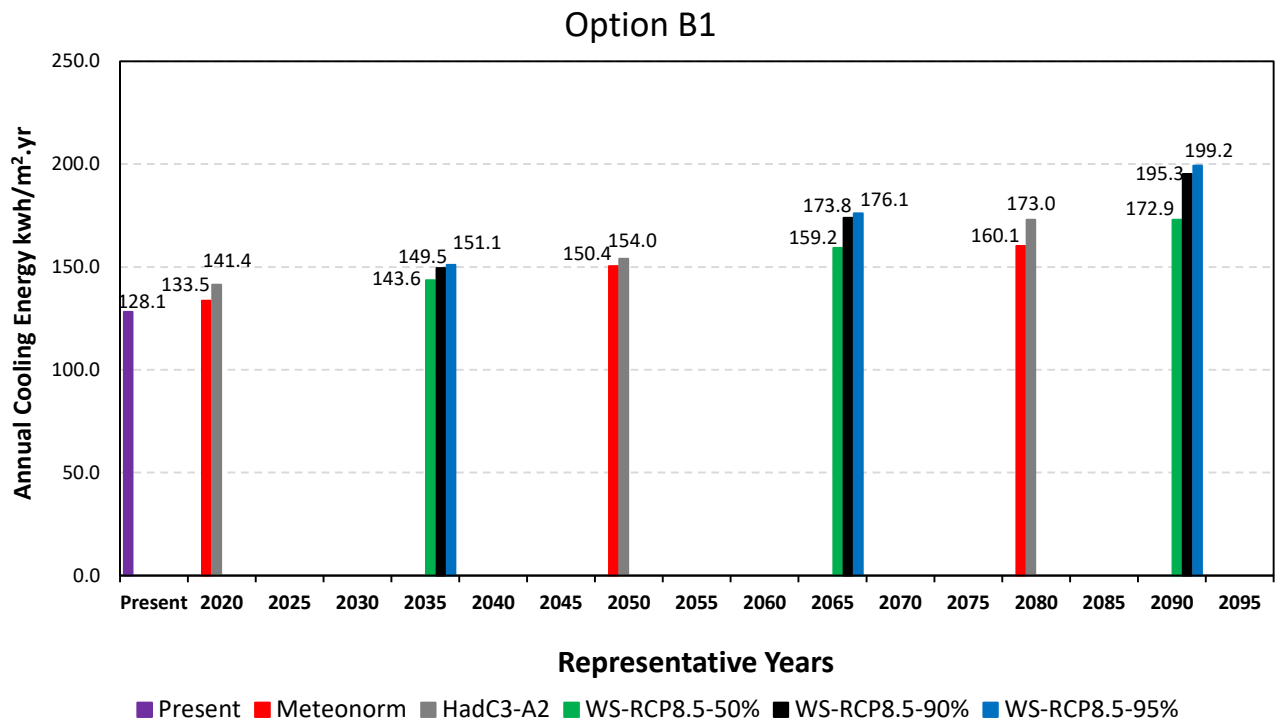


Figure 55: Total cooling energy of the base case model with option B1 simulated with present and future weather files.

The reduction in energy under the present weather conditions were 6.7% for total system energy and 6.9% for total cooling energy. Also, building energy consumption is gradually increasing in simulations with Meteonorm tool which represents (AR4-A1B) stabilization emission scenario. However, in high emission scenarios like RCP8.5 and HadCM3-A2, energy consumption is significantly increasing throughout the years. For example, as shown in figure 56 below, for the 95th percentile, additional 16% from present value for total system energy is expected to increase in period 2035, this means that the consumption of 155 kwh/m².yr will rise by 16% in that period to reach 180.2 kwh/m².yr. While in period 2065 with 95% percentile, the percentage increase from present consumption of base case with option B1 would rise to 34% for total system energy. Also, the total system energy has recorded 233.2 kwh/m².yr in period 2090 with 95% percentile which means that an increase of 50% from present value is expected to happen.

Base case with option B1

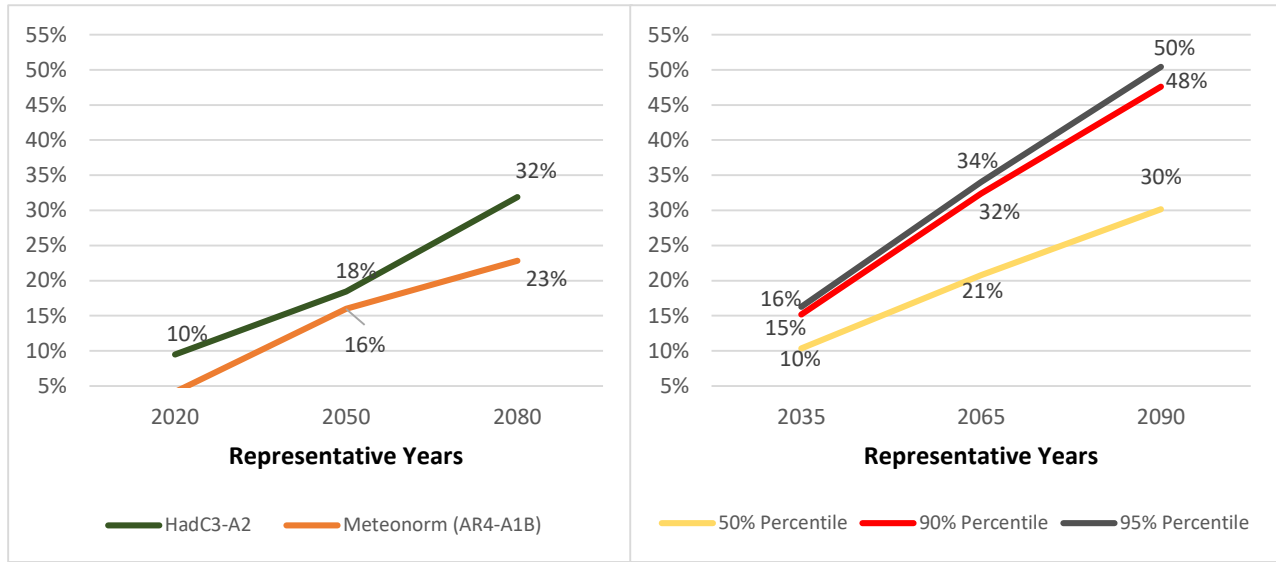


Figure 56: Percentage increase from present consumption in the total system energy of the base case with option B1 in the future selected periods.

Table (28): Percentage reduction in total system energy and total cooling energy from the base case model for present and future periods by applying option (B1).

HadCM3-A2: CCWorldWeatherGen tool											
Period		HadCM3-A2-2020	HadCM3-A2-2050	HadCM3-A2-2080							
Total system energy		6.4%	5.5%	4.5%							
Total cooling energy		6.5%	5.6%	4.6%							
AR4-A1B: Meteonorm tool											
Period		2020	2050	2080							
Total system energy		6.6%	5.1%	4.6%							
Total cooling energy		7.0%	5.2%	4.7%							
RCP8.5: (WS) WeatherShift™ tool											
Period	Present	50% percentile			90% percentile			95% percentile			
		2035	2065	2090	2035	2065	2090	2035	2065	2090	
Total system energy		6.7%	5.6%	4.7%	3.9%	5.1%	3.9%	2.8%	5.0%	3.7%	2.8%
Total cooling energy		6.9%	5.8%	4.7%	4.0%	5.2%	4.0%	2.8%	5.1%	3.8%	2.7%

Table (28) concludes that option B1 would reduce the energy consumption significantly by reducing the cooling loads of the building in the present weather conditions. Thus, this reduction depreciates throughout the years in all emission scenarios which will not increase the building resilience to climate change. Also, high emission scenarios would expect lower percentage reductions, this means that the higher the temperatures rise in the future the lower the savings that option B1 will provide due to its increased thermal transmittance counteracting reductions in solar heat gains provided by increased reflection/reduced SHGC. Therefore, reducing the SHGC and without minimizing the U-value, to the extent represented by option B1, will not improve the building resilience in the future.

4.3.2- Applying Krypton filled double glazing with lower SHGC and lower U-value

This option (B2) comprises of 6mm glass-12mm Krypton filled airgap- 6mm glass double-glazed window, its SHGC is 0.1591 and U-value is 0.9860 W/m²K (see type **b** in table (22)), and its total thickness is (24 mm). The reason of choosing this option is to test the effect of reducing both SHGC and U-value of the glazing in present and future weather conditions. Hence, it was applied to the base case model and simulated with all selected weather files. Results of simulation are represented in figures 57 and 58.

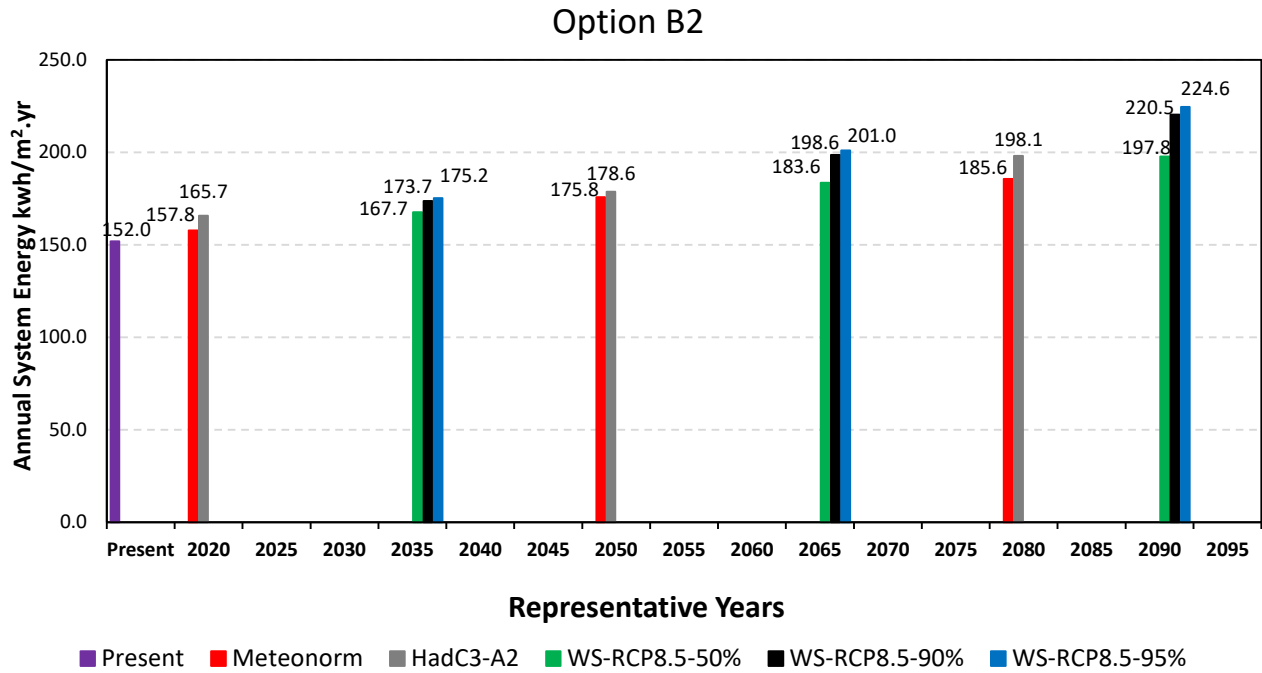


Figure 57: Total system energy of the base case model with option B2 simulated with present and future weather files.

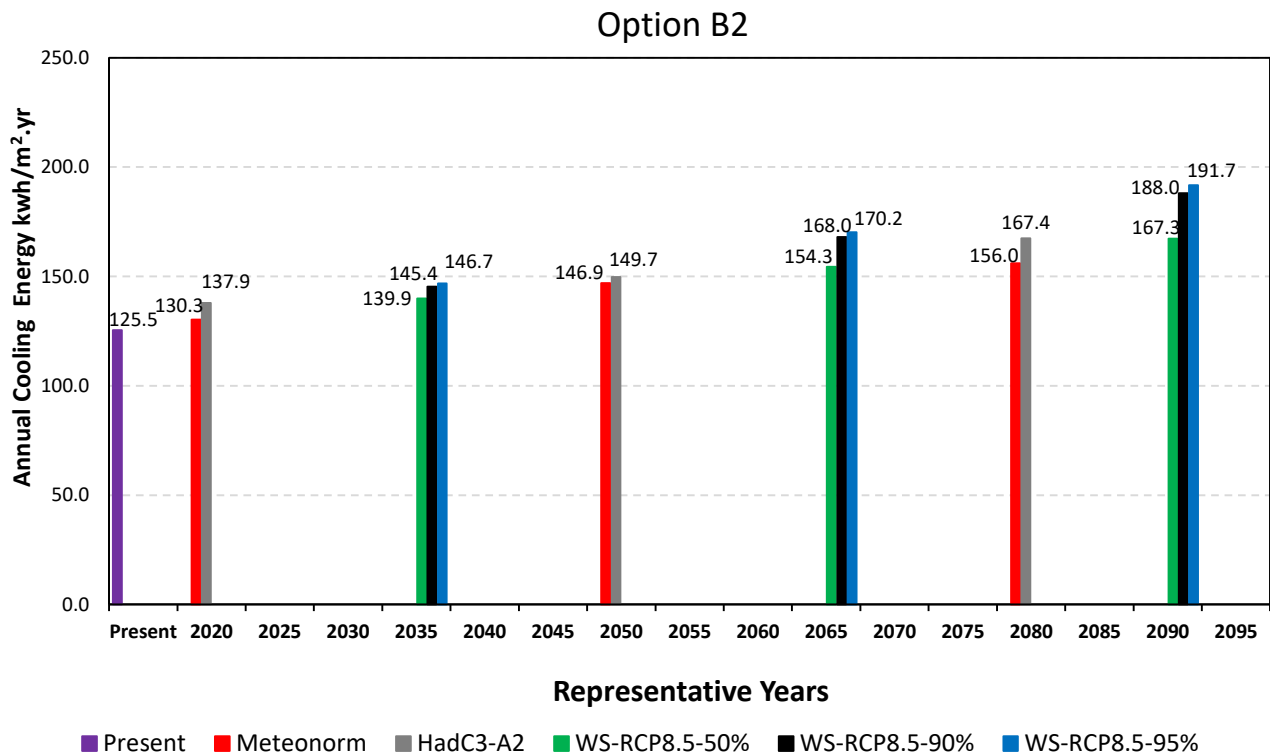


Figure 58: Total cooling energy of the base case model with option B2 simulated with present and future weather files.

As shown in figures 57 and 58, simulation with option B2 has recorded an energy consumption of 151 kwh/m².yr for total system energy and 125 kwh/m².yr for total cooling energy in present weather conditions. All results are increasing throughout the years in all emission scenarios. But the rise for the high emission scenarios are significantly higher than stabilization scenarios. For instance, a total energy system for simulation with (WS-RCP8.5) in period 2090 with 95% percentile weather file is 224.63 kwh/m².yr which is 21% more than Meteonorm-2080 weather file. Percentages increase in total system energy results from present consumption throughout the selected periods and emission scenarios are shown in figure 59 below.

Base case with options B2

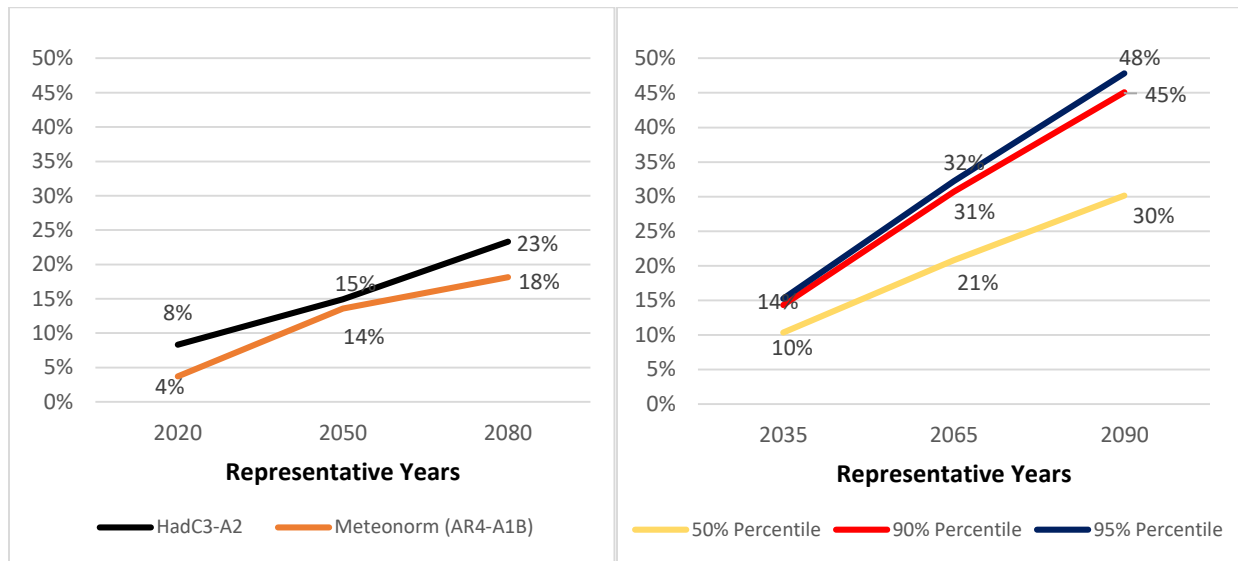


Figure 59: Percentage increase from present consumption in total system energy of the base case with option B2 in the future selected periods.

Additionally, the percentage reductions in energy from the base case for all selected future periods and emission scenarios are mentioned in table (29) below.

Table (29): Percentage reduction in total system energy and total cooling energy from the base case model for present and future periods by applying option (B2).										
HadCM3-A2: CCWorldWeatherGen tool										
Period	HadCM3-A2-2020			HadCM3-A2-2050			HadCM3-A2-2080			
Total system energy	8.6%			8.0%			7.5%			
Total cooling energy	8.8%			8.2%			7.6%			
AR4-A1B: Meteonorm tool										
Period	2020			2050			2080			
Total system energy	8.7%			7.2%			7.0%			
Total cooling energy	9.2%			7.4%			7.1%			
RCP 8.5: (WS) WeatherShift™ tool										
Period	Present	50% percentile			90% percentile			95% percentile		
		2035	2065	2090	2035	2065	2090	2035	2065	2090
Total system energy	8.5%	8.0%	7.5%	7.0%	7.7%	7.1%	6.3%	7.7%	6.9%	6.3%
Total cooling energy	8.8%	8.2%	7.7%	7.1%	7.8%	7.2%	6.4%	7.8%	7.0%	6.4%

The results in table (29) above show that this solution is able to reduce the total system energy by 8.5% and the total cooling energy by 8.8% for present weather data which is higher than option B1. Also, it is noted that the percentage reduction of total system energy is increasing for period 2020 with HadCM3-A2 and AR4-A1B emission scenarios, compared to the base case, but the total cooling energy percentage reduction for period 2020 with HadCM3-A2 remains the same as present. By comparing those percentages reduction with option B1 percentages reduction in table (28), it is noted that saving in both options will decrease in long term periods but option B2 will give the same saving or slightly higher due in period 2020 for HadCM3-A2 and AR4-A1B

emission scenarios due to the reduction of U-value. Furthermore, the smaller savings percentages under the WS 2035 weather years compared to those for the HadC3-A2 and Meteonorm 2020 weather years reflect the higher ambient temperatures projected in the WS future weather data, see table (16). This is due to a combination of differing emissions scenarios and timeframes across the three sources of future weather conditions. As mentioned in section (3.2), period 2020 are different for each tool where in HadCM3-A2 it is referred to 2011-2040, in Meteonorm tool files it is referred to 2020-2030, while period 2035 in (WS) tool is referred to 2026 to 2045 which means that the warming is higher. Therefore, this solution will improve the resilience of this type of buildings for the next 10~30 years and will depreciate after this period to achieve the lowest percentage reduction of 6.3% for its total system energy and 6.4% for total cooling energy in period 2090.

4.3.3- Applying Krypton filled triple glazing with lower SHGC and lower U-value

The third glazing option applied to the base case is B3, which comprises of triple glazed windows with 6mm glass-12mm Krypton filled airgap- 6mm glass-12mm Krypton filled airgap- 6mm glass. The U-value of this option is 0.8100 W/m²K and the SHGC is 0.1248, it has a thickness of (42 mm) producing the simulation results shown in Figures 60 and 61 below.

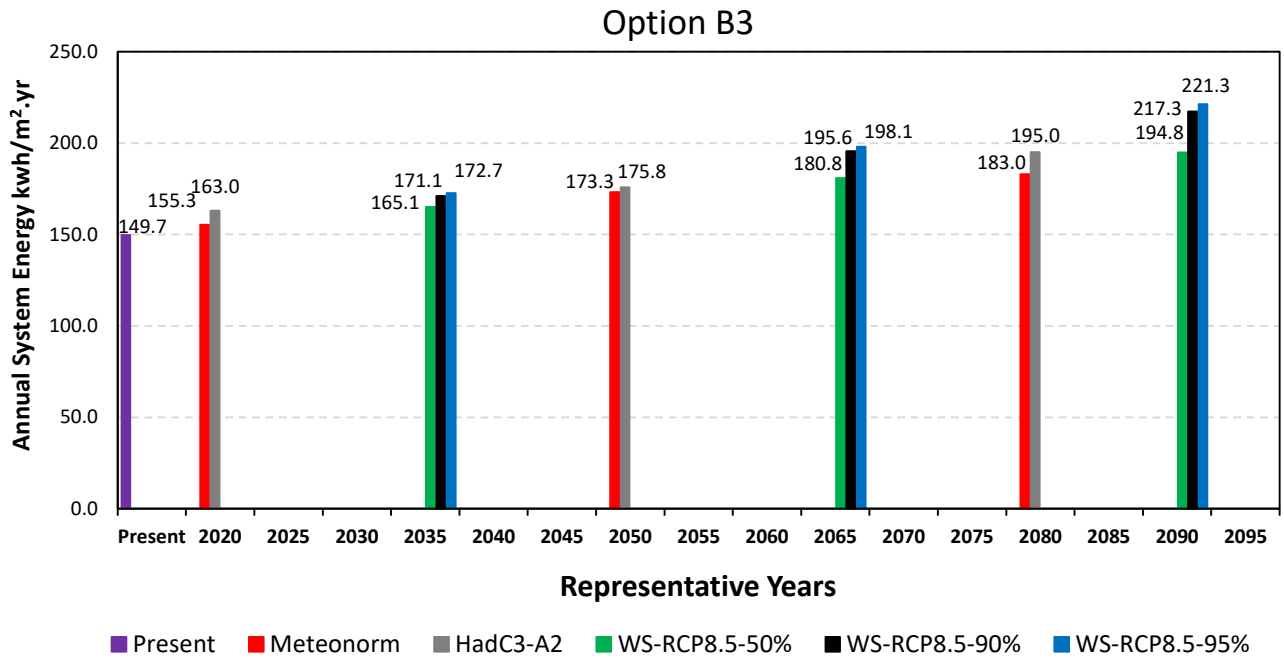


Figure 60: Total system energy of the base case model with option B3 simulated with present and future weather files.

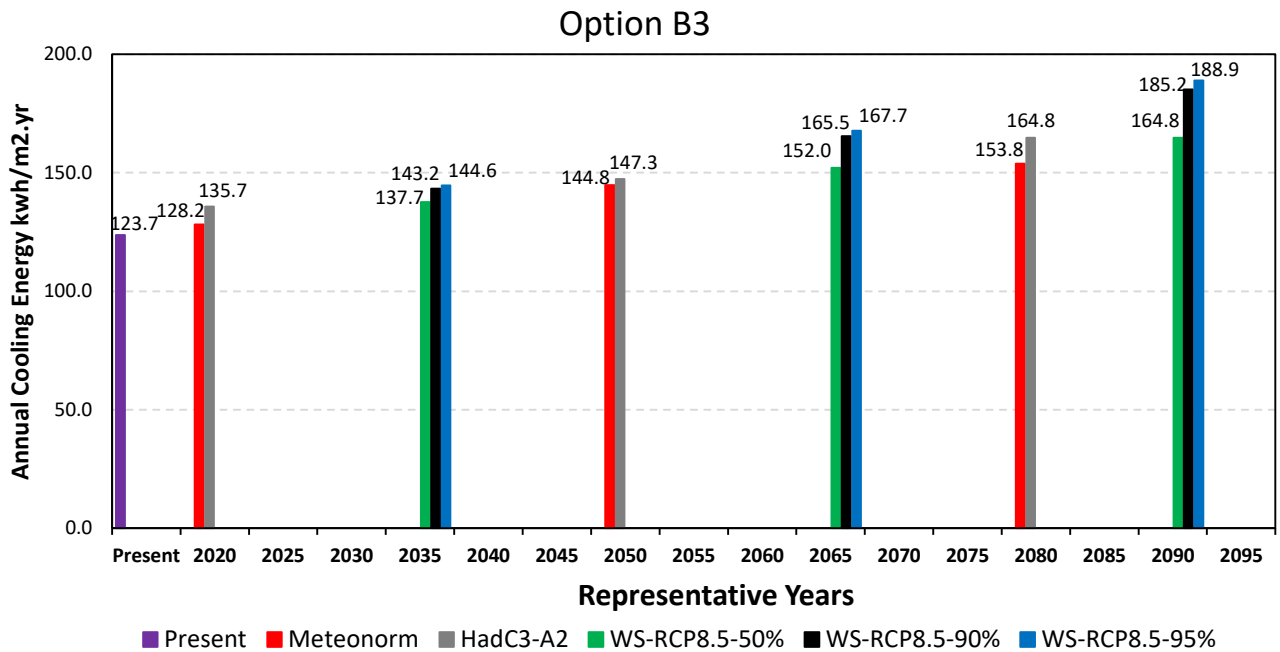


Figure 61: Total cooling energy of the base case model with option B3 simulated with present and future weather files.

The results in figures 60 and 61 illustrate that option B3 has recorded lower values than option B2. Reduction in energy consumption between the two options ranges between 2.2~3.3 kwh/m².yr for total system energy and between 1.8~2.9 kwh/m².yr for total cooling energy in present and future climate conditions. As mentioned before, the glazing area of the base case model is high. Figure 62 below provides an overview of the percentage increase in total system energy consumption compared with present result 149.7 kwh/m².yr in the selected future periods. The lowest future value was recorded as 155.3 kwh/m².yr for Meteoronorm AR4-A1B which is more than the present value by 4%, and the highest future value was recorded as 221.3 kwh/m².yr for WS period 2090 with 95% percentile which is higher than the present value by 48%. Moreover, percentage reduction from base case when applying option B3 is shown in table (30) below.

Base case with options B3

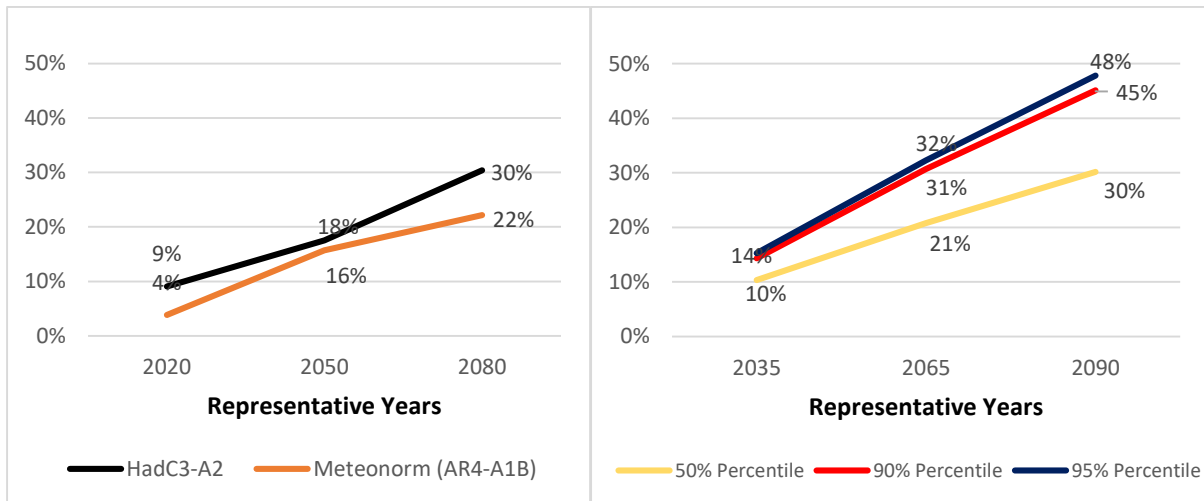


Figure 62: Percentage increase from present consumption in total system energy of the base case with option B3 in the future selected periods.

Table (30): Percentage reduction in total system energy and total cooling energy from the base case model for present and future periods by applying option (B3).											
HadCM3-A2: CCWorldWeatherGen tool											
Period		HadCM3-A2-2020			HadCM3-A2-2050			HadCM3-A2-2080			
Total system energy		10.1%			9.5%			8.9%			
Total cooling energy		10.3%			9.7%			9.1%			
AR4-A1B: Meteonorm tool											
Period		2020			2050			2080			
Total system energy		10.2%			8.5%			8.3%			
Total cooling energy		10.7%			8.8%			8.5%			
RCP8.5: (WS) WeatherShift™ tool											
Period	Present	50% percentile			90% percentile			95% percentile			
		2035	2065	2090	2035	2065	2090	2035	2065	2090	
Total system energy		9.9%	9.5%	8.9%	8.4%	9.1%	8.5%	7.7%	9.0%	8.2%	7.7%
Total cooling energy		10.2%	9.7%	9.0%	8.5%	9.2%	8.6%	7.8%	9.1%	8.3%	7.8%

Regarding the building resilience toward climate change in future, option B3 performed similar to option B2. Where some improvements are noticed in period 2020 simulated with AR4-A1B and HadCM3-A2 emission scenarios, but the percentages energy reduction from base case drops with time when simulating the building with future files that represents RCP8.5 emission scenario. Therefore, this option will save a little more energy in the coming 30 years than its efficiency will start to depreciate to reach its minimum of saving with 7.7% reduction in total system energy and 7.8% reduction in total cooling energy from the base case in period 2090 for 90th and 95th percentiles. Options B3 recorded higher savings in period 2020 simulated with HadC3-A2 and Meteonorm AR4-A1B which is quite similar to option B2 and this is due to lower U-value and the slight increase of SHGC.

The following observations were concluded by improving the glazing characteristics of the base case model in this study:

- In present weather conditions, improving the glazing properties of high-rise buildings will reduce the energy consumption significantly, especially in countries with long day hours and high ambient air temperature like UAE.
- Reducing the SHGC without reducing the U-value will have a positive impact on reducing present energy consumption but it will not improve the building resilience to climate change in the same way throughout the time, and it will not reduce the same amount of energy in future.
- Reducing the SHGC and U-value will reduce the energy consumption in the present conditions and the energy saving will increase for 30 years where it could achieve 10.2% less energy for total system energy and 10.7% less energy for total cooling energy. After this period, the efficiency of this solution will start to decrease and energy saving will be reduced by 0.5% to 2.2% for total system energy and by 0.2% to 2.4% for total cooling energy depending on the period and emission scenario.
- Double glazed window with good thermal properties would perform similarly to triple glazed window in regards to energy reduction and reducing cooling loads.

4.4- Adding a heat recovery unit to the building HVAC system

In this option, six heat recovery units were tested to observe the amount of energy saving that they would bring to the building. Three of them are cross flow air-to-air heat exchangers represented in IES software are a heat exchanger with zero latent effectiveness. The other three options are heat recovery wheels represented in IES software as heat wheels with different sensible and latent effectiveness. All six options were applied to the base case

model separately and tested with all selected weather file to study how they would affect the building total system and cooling energy consumption in present weather conditions and if they will make the building more resilient to future global warming.

4.4.1- Adding cross-flow air-to-air heat exchanger to the HVAC system with 70% sensible efficiency

The first option C1 is to apply three cross-flow air-to-air heat exchangers to the HVAC system, each one of them is added to one fresh air handling unit (FAHU). This option will offer sensible heat exchange only between the incoming and exhaust air-streams. Applying this solution will reduce the amount of energy required to cool the outside air before passing to the building. Applying option C1 to the base case was simulated with present and future weather files. The results of total system energy and total cooling energy of the building are presented in figures 63 and 64.

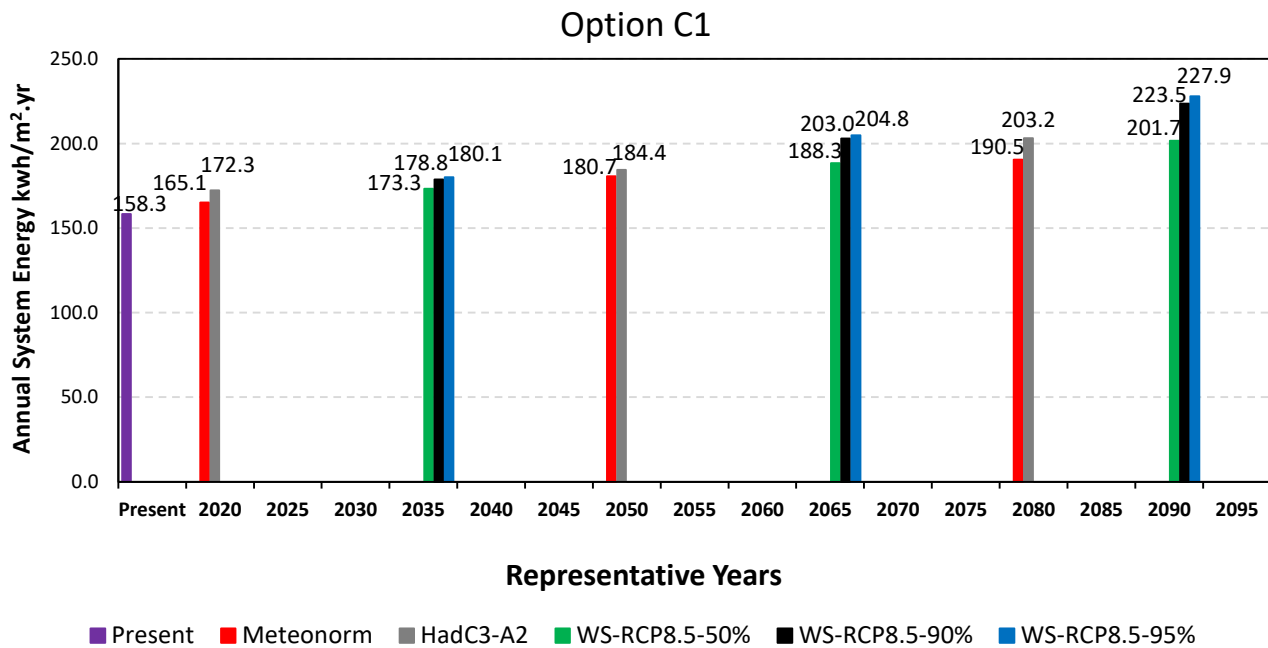


Figure 63: Total system energy of the base case model with option C1 simulated with present and future weather files.

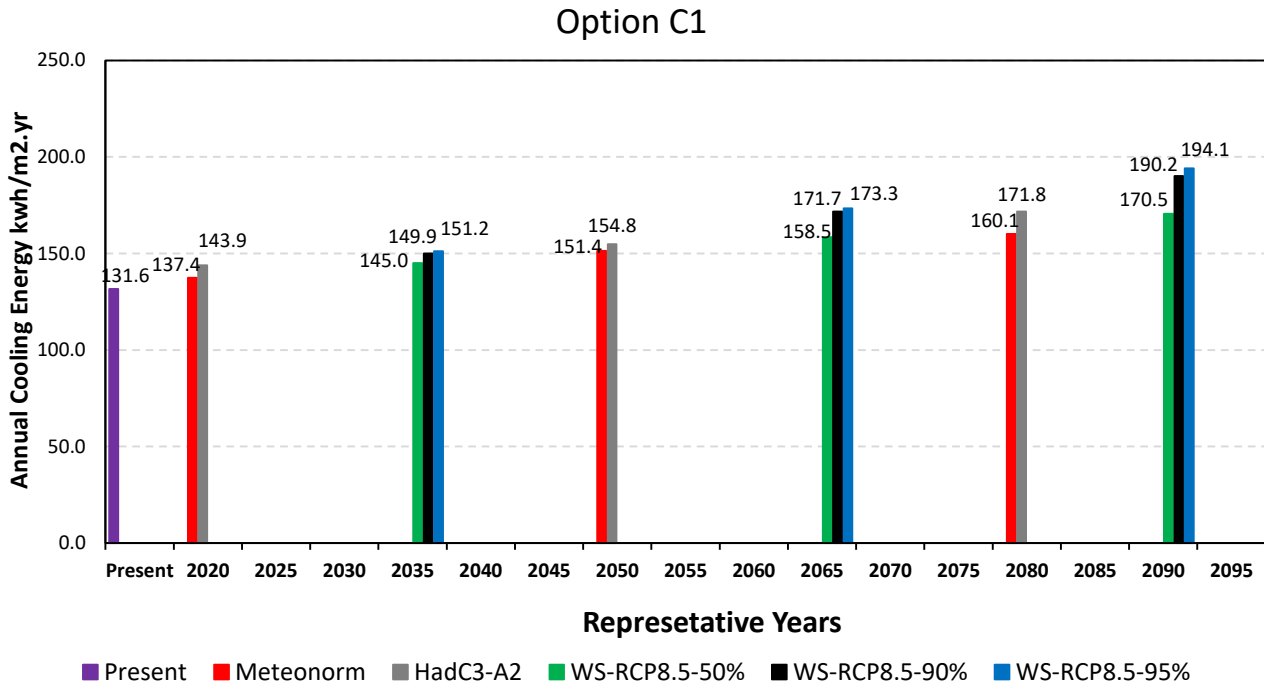


Figure 64: Total cooling energy of the base case model with option C1 simulated with present and future weather files.

Applying option C1 will reduce the total system energy from 166.1 kwh/m².yr to 158.3 kwh/m².yr and the total cooling energy from 137.8 kwh/m².yr to 131.6 kwh/m².yr in present weather conditions. This amount of energy reduction in the present time will make the building listed as best practice energy efficient building. Moreover, in all the future periods, for both stabilization and high emission scenarios, the energy consumption of both total system energy and cooling energy is increasing considerably. For example, as shown in figure 65 below, the total system energy is expected to increase to from 158.3 kwh/m².yr to 227.9 kwh/m².yr in period 2090 for 95th percentile which is 44% more than the present consumption. Also, the figure below shows that the building will consume more by 4% to 44% depending on the future period and emission scenario.

Base case with option C1

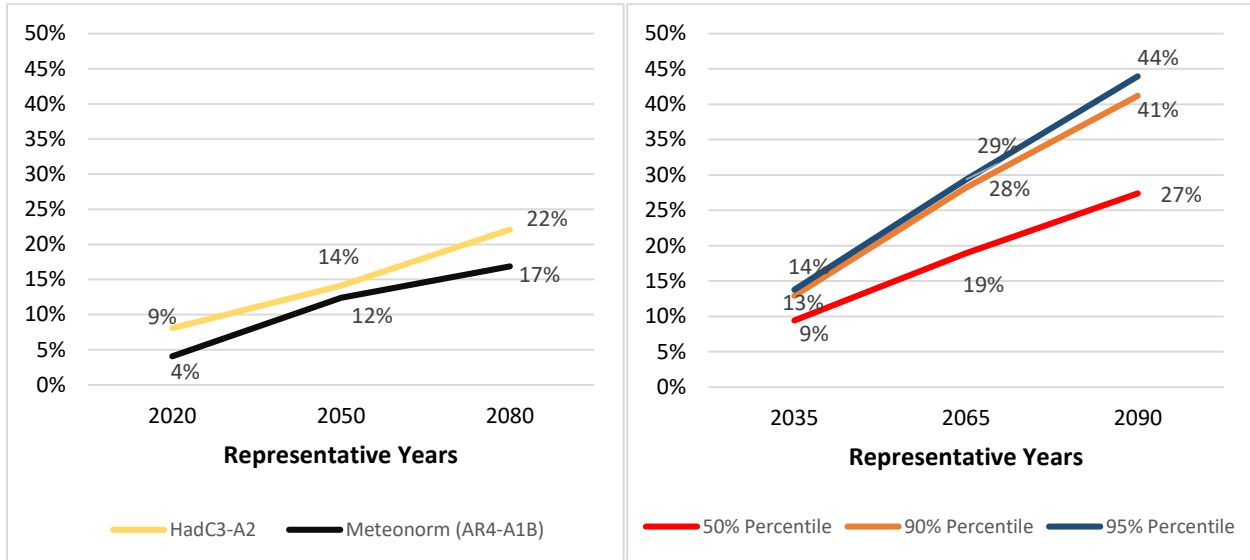


Figure 65: Percentage increase from present consumption of the total system energy of the base case with option C1 in the future selected periods.

Table (31): Percentage reduction in total system energy and total cooling energy from the base case model for present and future periods by applying option (C1).

HadCM3-A2: CCWorldWeatherGen tool											
Period		HadCM3-A2-2020	HadCM3-A2-2050	HadCM3-A2-2080							
Total system energy		5.0%	5.1%	5.1%							
Total cooling energy		4.8%	5.1%	5.2%							
AR4-A1B: Meteonorm tool											
Period		2020	2050	2080							
Total system energy		4.5%	4.6%	4.7%							
Total cooling energy		4.2%	4.6%	4.7%							
RCP 8.5: (WS) WeatherShift™ tool											
Period	Present	50% percentile			90% percentile			95% percentile			
		2035	2065	2090	2035	2065	2090	2035	2065	2090	
Total system energy		4.7%	5.0%	5.2%	5.1%	5.0%	5.0%	5.1%	5.0%	5.1%	5.0%
Total cooling energy		4.4%	4.9%	5.2%	5.3%	4.9%	5.2%	5.3%	5.0%	5.3%	5.2%

Table (31) demonstrates that option C1 is marginally beneficial in increasing building resilience toward climate change in future periods. The percentages reduction in energy from base case in present conditions are 4.7% for total system energy and 4.4% for total cooling energy. For both total system energy and total cooling energy, future percentage reduction has increased in high emission scenarios (RCP 8.5 and HadCM3-A2), decreased for period 2020 in (AR4-A1B) scenario and then it increased in the later periods of the same scenario. The reason of percentage reduction decreasing in period 2020 in (AR4-A1B) scenario is due to the different statistical method that is used to derive Meteoronorm files which leads to slight differences in results from RCP 8.5 and HadCM3-A2 weather files, see section 3.2.

4.4.2- Adding cross-flow air-to-air heat exchanger to the HVAC system with 75% sensible efficiency

In this option C2, the sensible effectiveness was increased to 75% for the three cross-flow air-to-air heat exchangers. This option will examine the amount of energy reduction that could be reached by improving the heat exchanger efficiency. Also, it will test how this will affect the building resilience to future climate change and its effect on energy demand.

Therefore, similar to the previous solutions, this option was applied to base case and simulated with all selected weather files. Results of simulation for total system energy and total cooling energy are shown in figures 66 and 67.

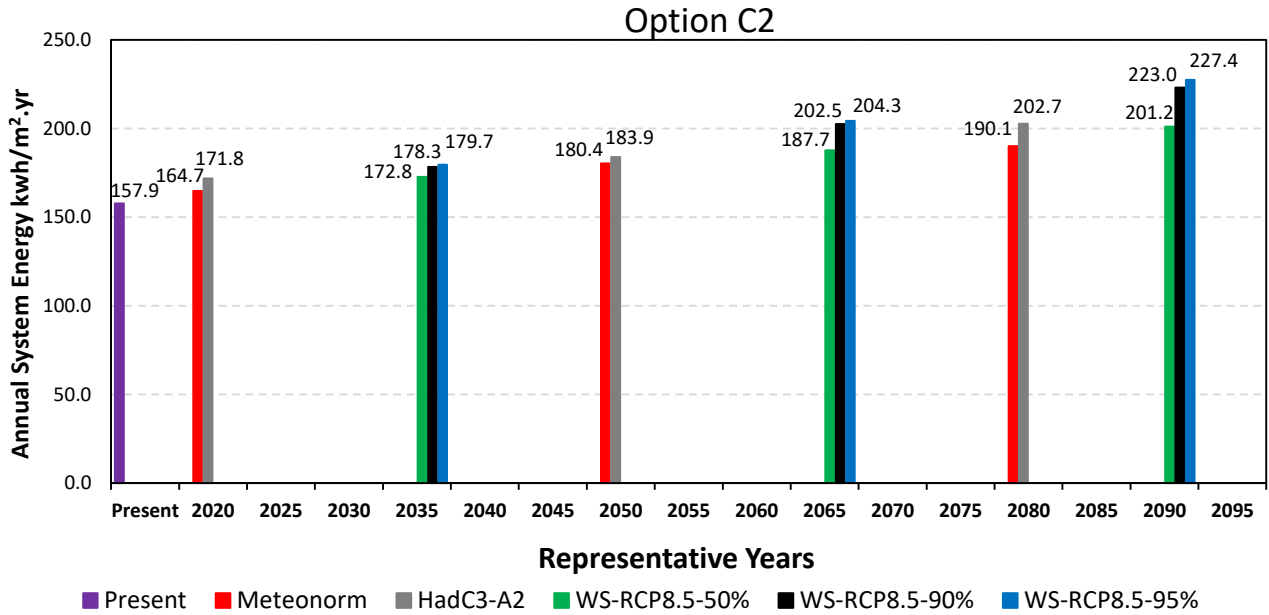


Figure 66: Total system energy of the base case model with option C2 simulated with present and future weather files.

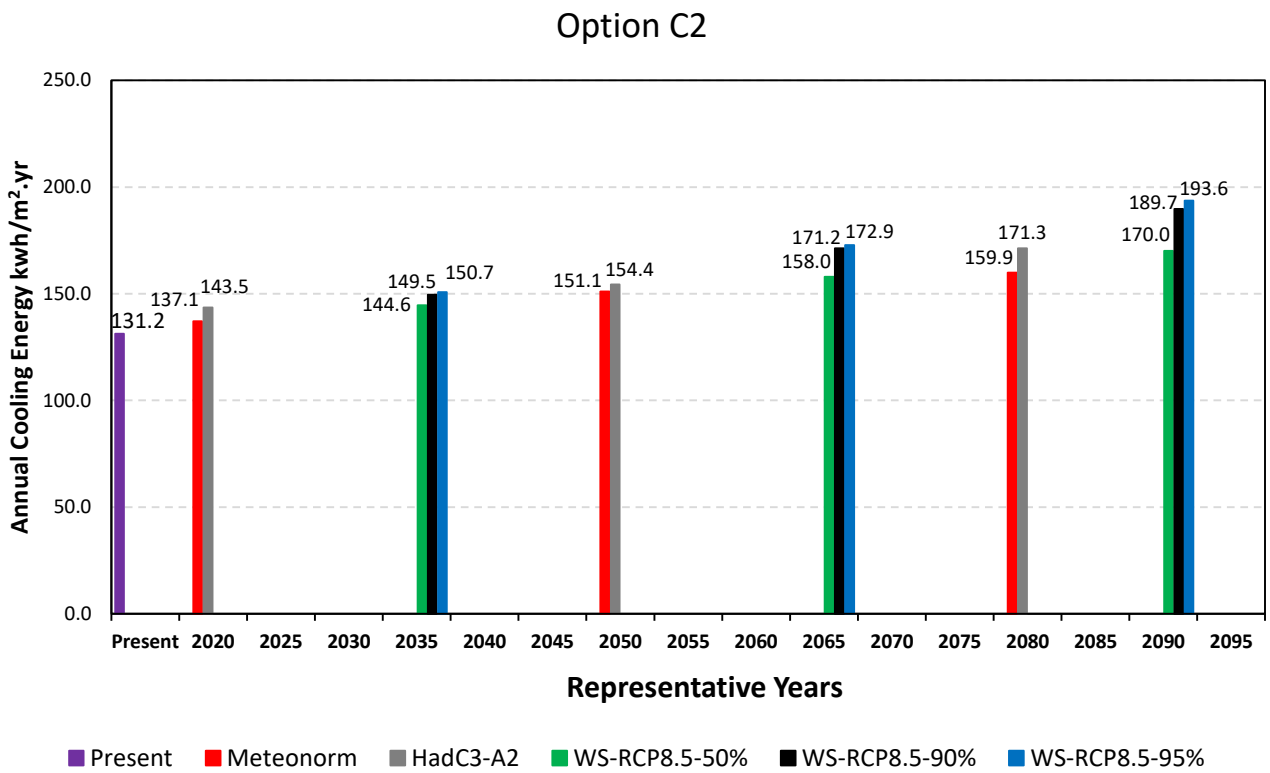


Figure 67: Total cooling energy of the base case model with option C2 simulated with present and future weather files.

The present energy consumption values were recorded as 157.9 kwh/m².yr for total system energy and 131.2 kwh/m².yr which is 0.3% less than option C1 results. Also, the differences between the two options are less in future years, taking an example of period 2080 base case results simulated with HadC3-A2 weather file has recorded a 0.25% improvement in energy consumption from option C1. While the simulation with future stabilization emission scenario (AR4-A1B), option C2 results are less than option C1 results by only 0.17% for period 2080. Therefore, improving the efficiency of cross-flow air-to-air exchanger from 70% to 75% has slightly improvements in energy consumption reduction. The percentage increase from present value is shown in figure 68 below which indicates that the base case with option C2 would consume up to 44% more in future.

Base case with option C2

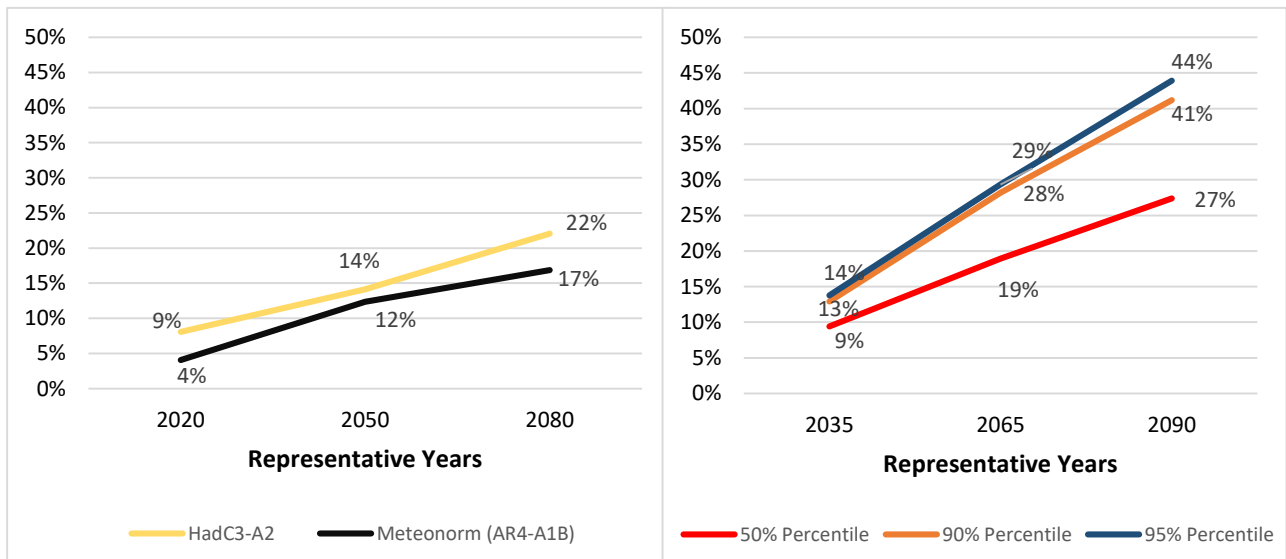


Figure 68: Percentage increase from present consumption of the total system energy of the base case with option C2 in the future selected periods.

Table (32): Percentage reduction in total system energy and total cooling energy from the base case model for present and future periods by applying option (C2).										
HadCM3-A2: CCWorldWeatherGen tool										
Period		HadCM3-A2-2020			HadCM3-A2-2050			HadCM3-A2-2080		
Total system energy		5.3%			5.3%			5.4%		
Total cooling energy		5.1%			5.3%			5.5%		
AR4-A1B: Meteonorm tool										
Period		2020			2050			2080		
Total system energy		4.7%			4.8%			4.7%		
Total cooling energy		4.5%			4.8%			4.8%		
RCP 8.5: (WS) WeatherShift™ tool										
Period	Present	50% percentile			90% percentile			95% percentile		
		2035	2065	2090	2035	2065	2090	2035	2065	2090
Total system energy	5.0%	5.2%	5.5%	5.4%	5.3%	5.3%	5.3%	5.3%	5.3%	5.2%
Total cooling energy	4.7%	5.1%	5.5%	5.6%	5.2%	5.4%	5.5%	5.3%	5.5%	5.5%

It is apparent from table (32) results that there are improvements in cooling energy consumptions in the future years for high emission scenarios weather files. While the stabilization emission scenario AR4 -A1B, the percentage reduction from base case was less for period 2020 but it rises up in periods 2050 and 2080. As mentioned before in section 4.4.1, the statistical method in deriving Meteonorm weather files is the stochastic method which is different than the morphing method that is used for WS present file and this would lead to small unexpected differences in results comparison. The total system energy percentage reduction from base case is increasing all over the years for high emission scenarios, however; in AR4 -A1B scenario percentage reduction decreases by 0.3% for 2020, 0.2% for 2050, and 0.2% for 2080. This means that option C2 is

efficient for high temperatures rise and would increase the building resilience in high emission scenarios.

4.4.3- Adding cross-flow air-to-air heat exchanger to the HVAC system with 80% sensible efficiency

The third proposed option is C3, in this option the cross-flow air-to-air heat exchanger sensible effectiveness will increase to 80%. Three of them will be added to the three FAHU's in the HVAC system. This option will test the enhancement in energy consumption of the building when adding a higher efficiency heat exchanger. Also, it will test the effectiveness of this option in the future years where higher temperature are expected. For that reason, after applying this option to the base case model, the building was simulated with all selected weather files and the results are shown in figures 69 and 70.

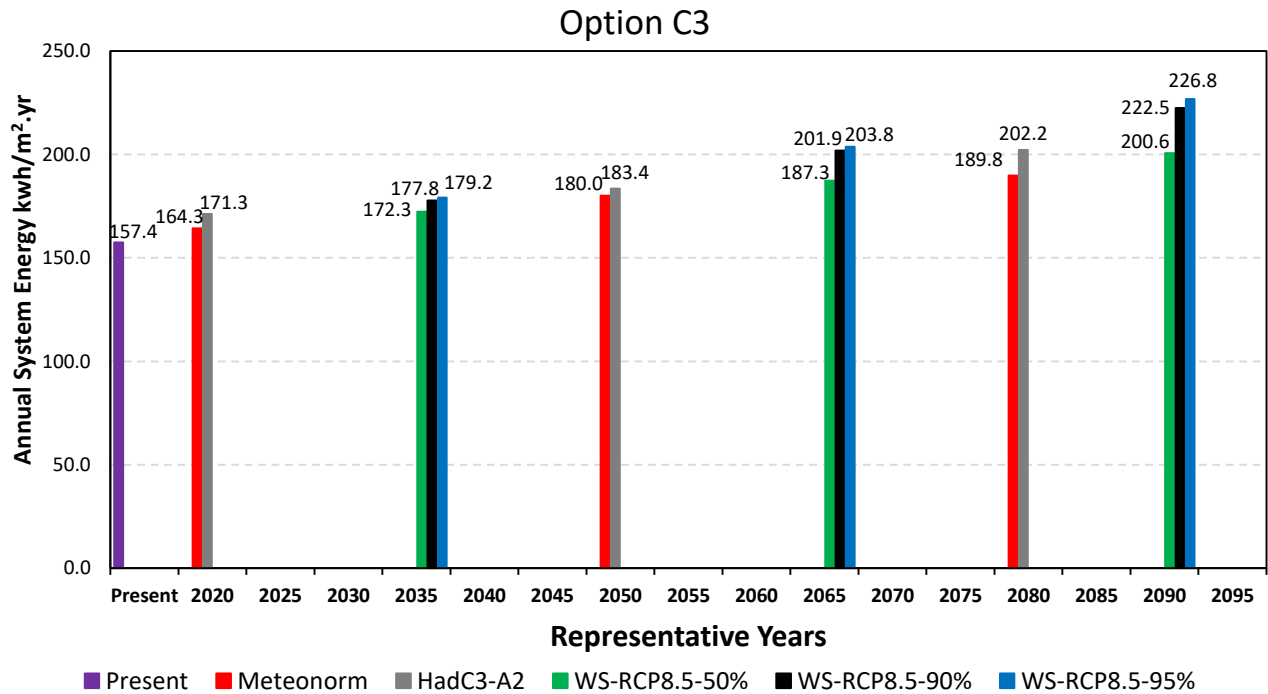


Figure 69: Total system energy of the base case model with option C3 simulated with present and future weather files.

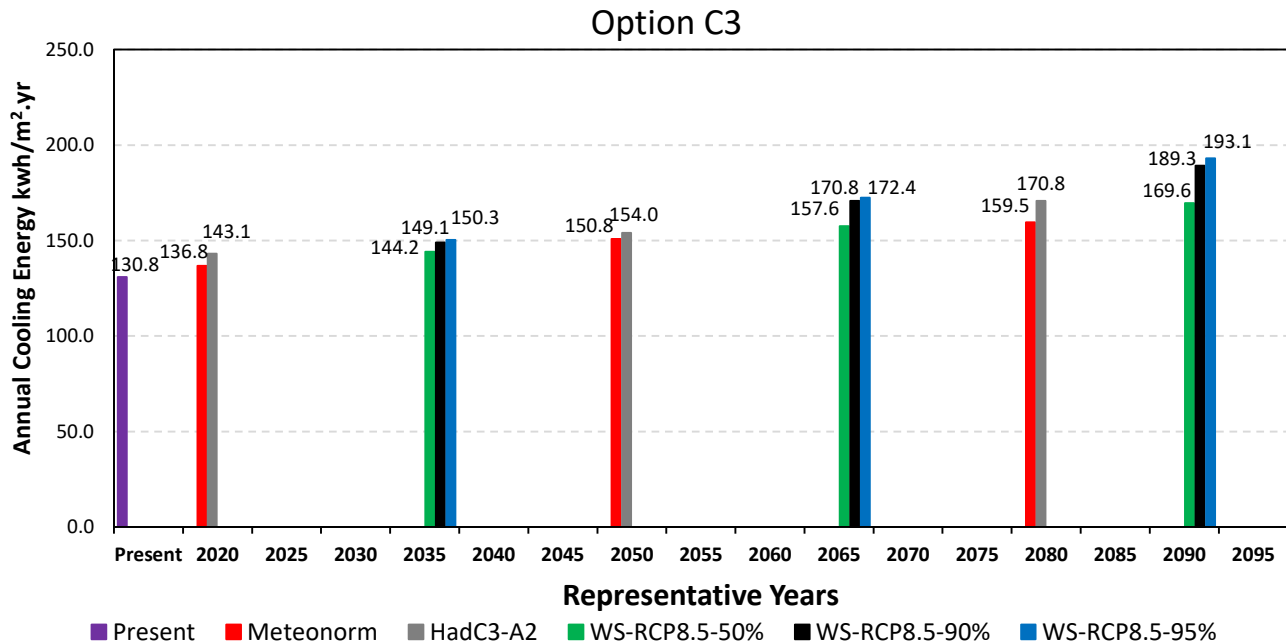


Figure 70: Total cooling energy of the base case model with option C2 simulated with present and future weather files.

According to simulation results, the total system energy in the present conditions was recorded as 157.43 kwh/m².yr and the total cooling energy was recorded as 130.83 kwh/m².yr which is less than option C1 by 0.6% and less than option C2 by 0.3% for the two results. Consequently, this study has discovered that the increasing the effectiveness of the two options (C2, and C3) would have a minimal improvement regarding energy consumption in both present and future weather conditions. Also, as shown in figure 71 below, the total system energy consumption is significantly increasing throughout the future years for all selected emission scenarios. The highest result was 226.63 kwh/m².yr for total system energy in period 2090 with 95th percentile which represents RCP 8.5 emission scenario, this result is 44% more than the present result. Alternatively, the lowest result for future periods has reached 164.33 kwh/m².yr for total system energy, 4% more than present result, simulated with Meteonorm tool weather file representing AR4-A1B emission scenario for period 2020.

Base case with option C3

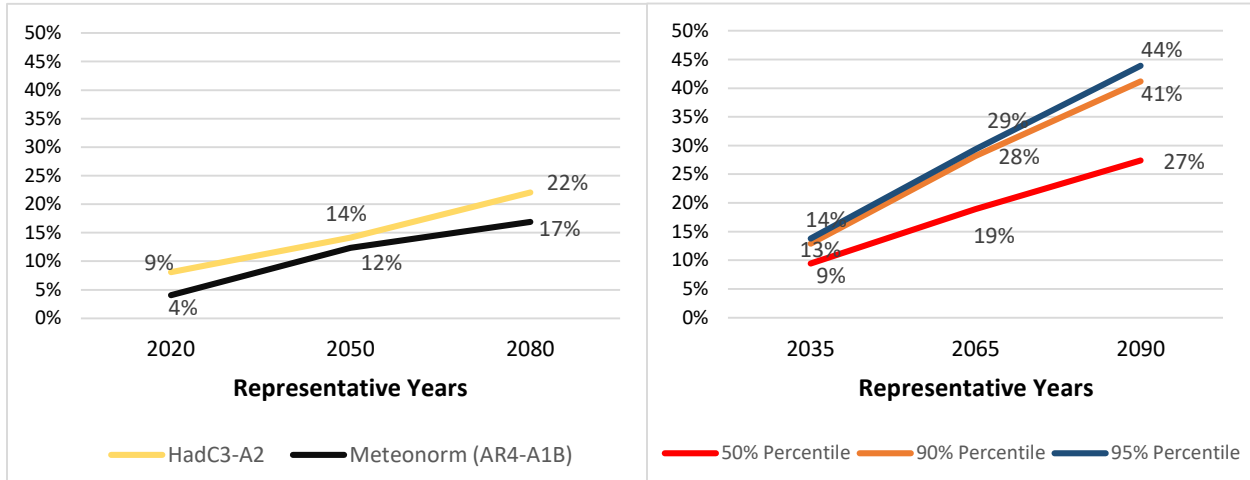


Figure 71: Percentage increase from present consumption of the total system energy of the base case with option C3 in the future selected periods.

Table (33): Percentage reduction in total system energy and total cooling energy from the base case model for present and future periods by applying option (C3).

HadCM3-A2: CCWorldWeatherGen tool											
Period		HadCM3-A2-2020			HadCM3-A2-2050			HadCM3-A2-2080			
Total system energy		5.5%			5.6%			5.6%			
Total cooling energy		5.4%			5.6%			5.7%			
AR4-A1B: Meteonorm tool											
Period		2020			2050			2080			
Total system energy		5.0%			4.9%			4.9%			
Total cooling energy		4.7%			5.0%			5.0%			
RCP 8.5: (WS) WeatherShift™ tool											
Period	Present	50% percentile			90% percentile			95% percentile			
		2035	2065	2090	2035	2065	2090	2035	2065	2090	
Total system energy		5.2%	5.5%	5.7%	5.6%	5.5%	5.5%	5.5%	5.6%	5.6%	5.4%
Total cooling energy		5.0%	5.4%	5.7%	5.8%	5.5%	5.7%	5.7%	5.5%	5.8%	5.7%

Results in table (33) show that this option would improve the building resilience toward climate change in high emission scenarios. In addition, in stabilization emission scenario (AR4-A1B), this option efficiency will slightly depreciate throughout the future years.

As a result of the expected air temperature increase in those scenarios, a solution is needed to reduce the energy consumed by HVAC unit to cool the outside air before supplying it to the building. This would make this solution beneficial, but the three previous options discussed in this study would only treat the sensible heat of the air. However, a recovery unit that treat latent and sensible energy would be beneficial especially in countries with high humidity ratios like UAE. Therefore, additional three recovery units that would reduce both sensible and latent energy of the air will be tested in this study to evaluate their effect on energy consumption in the future years.

4.4.4- Adding an enthalpy HRW to the HVAC system with 70% sensible efficiency and 68% latent efficiency

In this research, option C4 was proposed to study its effect on the present energy consumption and how it would affect building resilience in future with the expected global warming. This option will reduce the sensible and latent heat of the fresh air supplied to the building which will reduce the cooling loads and energy consumption. Therefore, this solution was implemented using IES software, three enthalpy heat wheels were added to the HVAC system with 70% sensible effectiveness and 68% latent effectiveness. After applying this solution, base case was simulated with all selected weather files and the results of simulation are represented in figures 72 and 73.

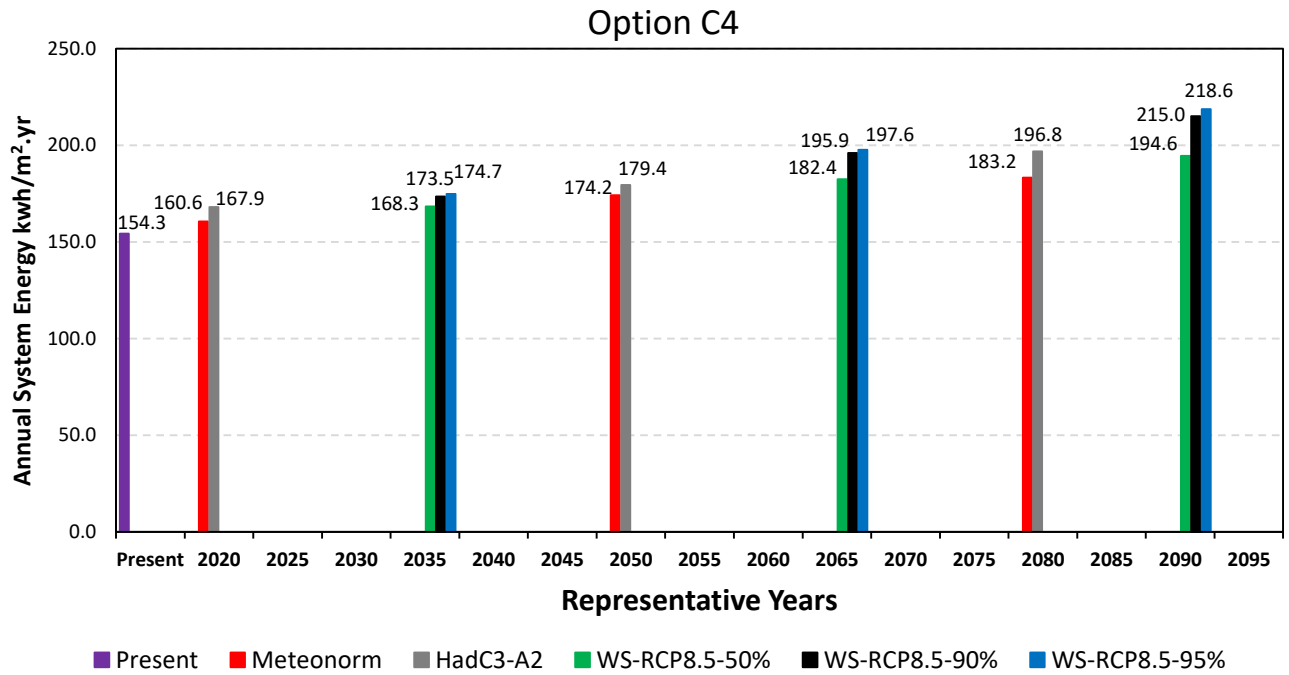


Figure 72: Total system energy of the base case model with option C4 simulated with present and future weather files.

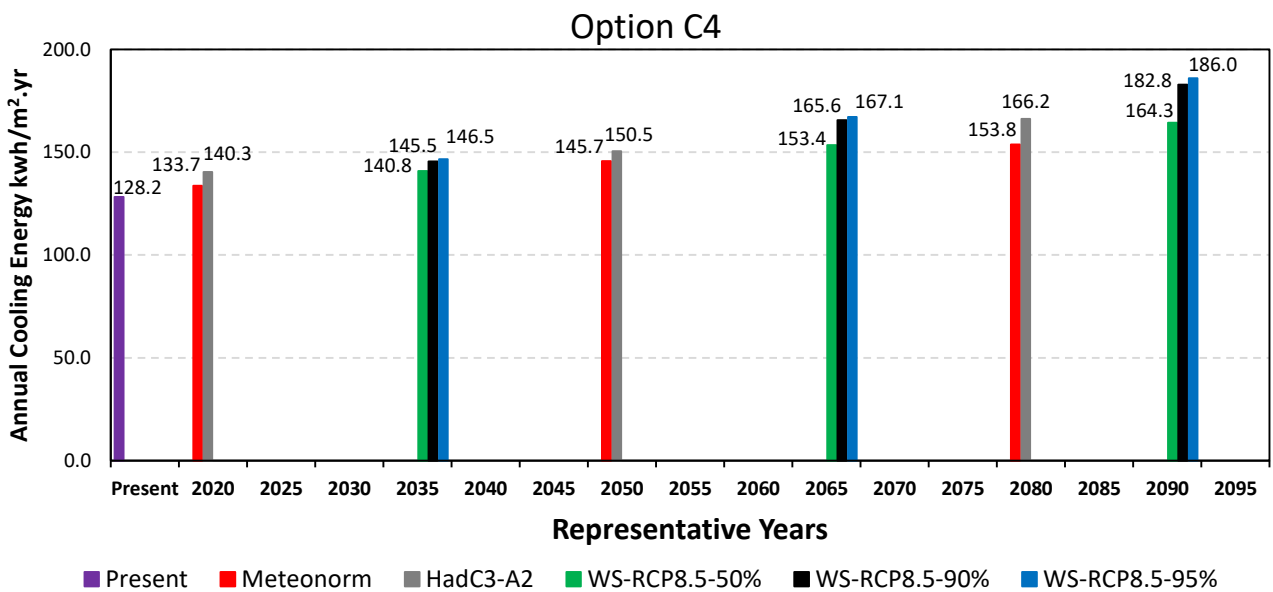


Figure 73: Total system energy of the base case model with option C4 simulated with present and future weather files.

Applying this option has reduced the total system energy to 154.27 kwh/m².yr and the total cooling energy to 128.2 kwh/m².yr. The highest recorded value is 218.6 kwh/m².yr for total system energy and 186 kwh/m².yr for total cooling energy in period 2090 with 95th percentile which is considered as worst-case scenario. This solution has significantly reduced the future energy consumption compared with the previous three options (C1, C2, and C3). Option C4 has recorded lower results in energy consumption than option C3 for both present and future periods, although this option has a sensible effectiveness less than option C3 by 10%. This means that applying a recovery unit with both sensible and latent heat exchange is more useful regarding energy consumption in hot countries like UAE. In the stabilization scenario (AR4-A1B), the highest value was recorded as 183.17 kwh/m².yr for total system energy and 153.77 kwh/m².yr for total cooling energy in period 2080. Correspondingly, the study has revealed that even by adding option C4, the total cooling energy would still consume between 83-85% of the total system energy for all selected periods. Moreover, by comparing this option percentages reduction in the table (34) below with option C1 percentages reduction which has the same sensible effectiveness of this option. It is clear that this option is more efficient where it could save up to 9.2% in future while the highest saving for option C1 was 5.2% only.

Base case with option C4

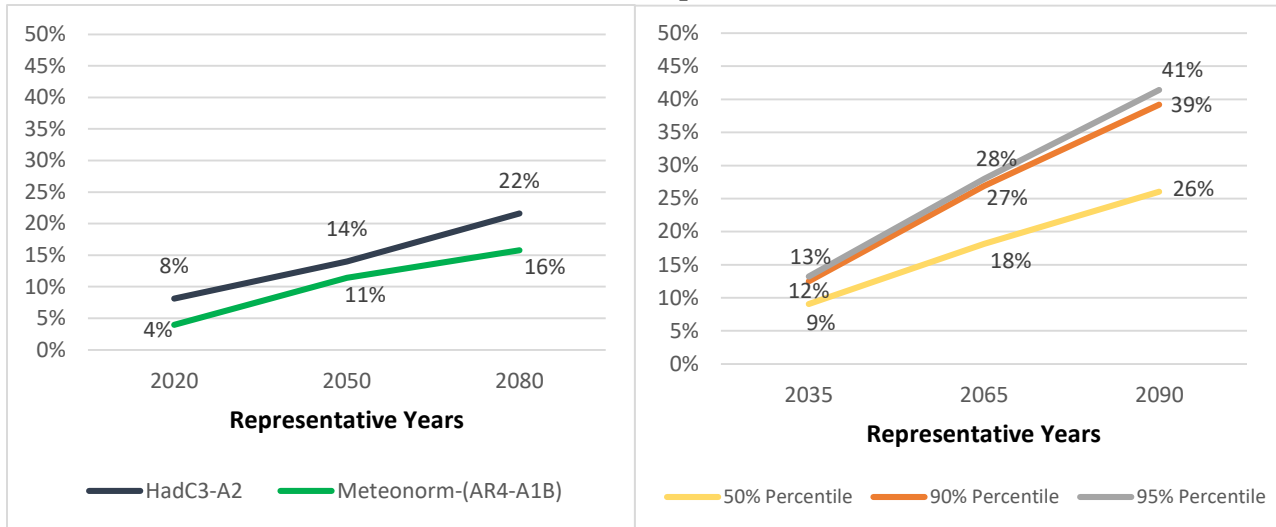


Figure 74: Percentage increase from present consumption of the total system energy of the base case with option C4 in the future selected periods.

According to table (34) below, applying this solution to the HVAC system will reduce the amount of energy consumption by 7.1% and 6.9% from the base case model. Moreover, the table shows that this reduction from base case is increasing in the future periods. This is due to the high humidity levels in UAE. As shown before in section (3.2), the relative humidity ratio of the selected weather files with high emission scenarios doesn't increase in all periods, however; it is still considered high. For that reason, this study has discovered that adding an enthalpy HRW to the HVAC system will make the building more resilient and would reduce the energy demand in future. In the two high emission scenarios (HadC3-A2 and RCP8.5), the reduction in energy is increasing throughout the future years and it is expected to reach 8.9% for total system energy and 9.2% for total cooling energy in period 2090 with 95th percentile. On the other hand, in the stabilization scenario (AR4-A1B), the percentage reduction in energy from base case will be the same for period 2020 but it will increase for the other two future periods where it would reach 8.2% for total system energy and 8.5% for total cooling energy in period 2080.

Table (34): Percentage reduction in total system energy and total cooling energy from the base case model for present and future periods by applying option (C4).											
HadCM3-A2: CCWorldWeatherGen tool											
Period		HadCM3-A2-2020			HadCM3-A2-2050			HadCM3-A2-2080			
Total system energy		7.4%			7.7%			8.1%			
Total cooling energy		7.2%			7.7%			8.3%			
AR4-A1B: Meteonorm tool											
Period		2020			2050			2080			
Total system energy		7.1%			8.0%			8.2%			
Total cooling energy		6.9%			8.2%			8.5%			
RCP 8.5: (WS) WeatherShift™ tool											
Period	Present	50% percentile			90% percentile			95% percentile			
		2035	2065	2090	2035	2065	2090	2035	2065	2090	
Total system energy		7.1%	7.7%	8.1%	8.5%	7.8%	8.3%	8.7%	7.9%	8.4%	8.9%
Total cooling energy		6.9%	7.7%	8.2%	8.7%	7.8%	8.5%	9.0%	7.9%	8.7%	9.2%

4.4.5- Adding an enthalpy HRW to the HVAC system with 75% sensible efficiency and 73% latent efficiency

The fifth option in this section is C5, in this option the sensible effectiveness of the enthalpy heat recovery wheels that are added to each FAHU's will be increased to 75% and the latent effectiveness will be increased to 73%. This option will examine how a higher efficiency enthalpy HRW will affect the total system and cooling energy consumption of the building. Also, option C4 has a noticeable improvement in making the building more resilient in the future. Therefore, this option will test if upgrading the efficiency will have better results. After applying

this option, simulation with all selected weather files was done and results are shown in figures 75 and 76.

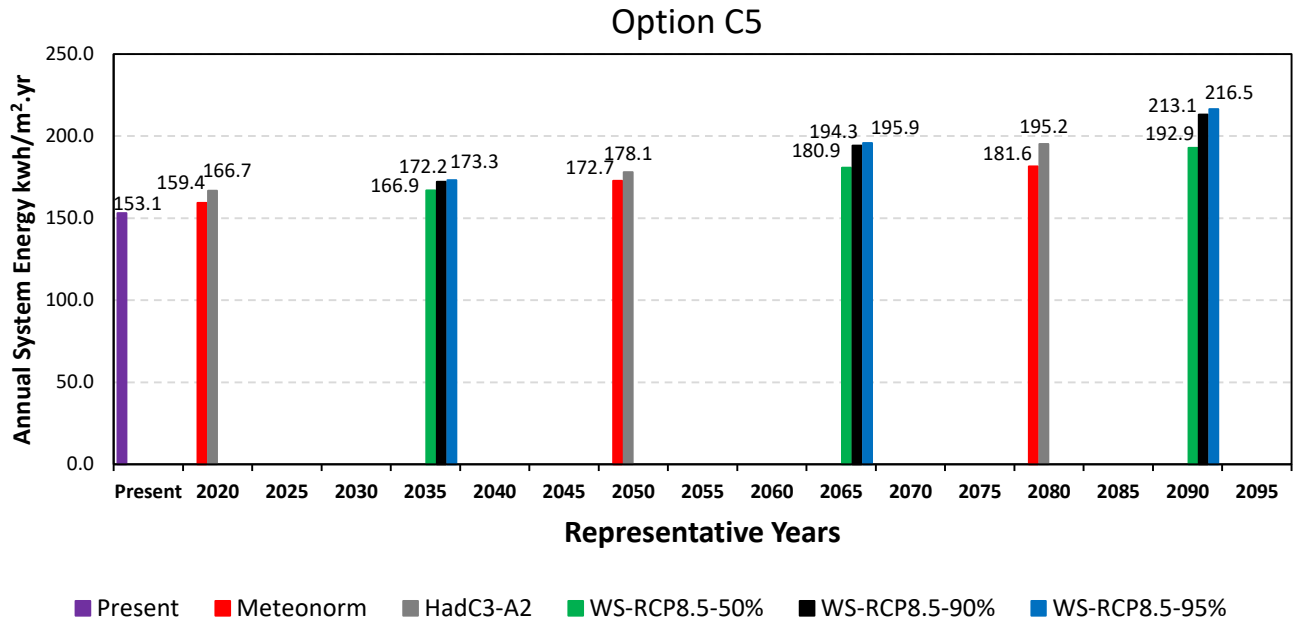


Figure 75: Total system energy of the base case model with option C5 simulated with present and future weather files.

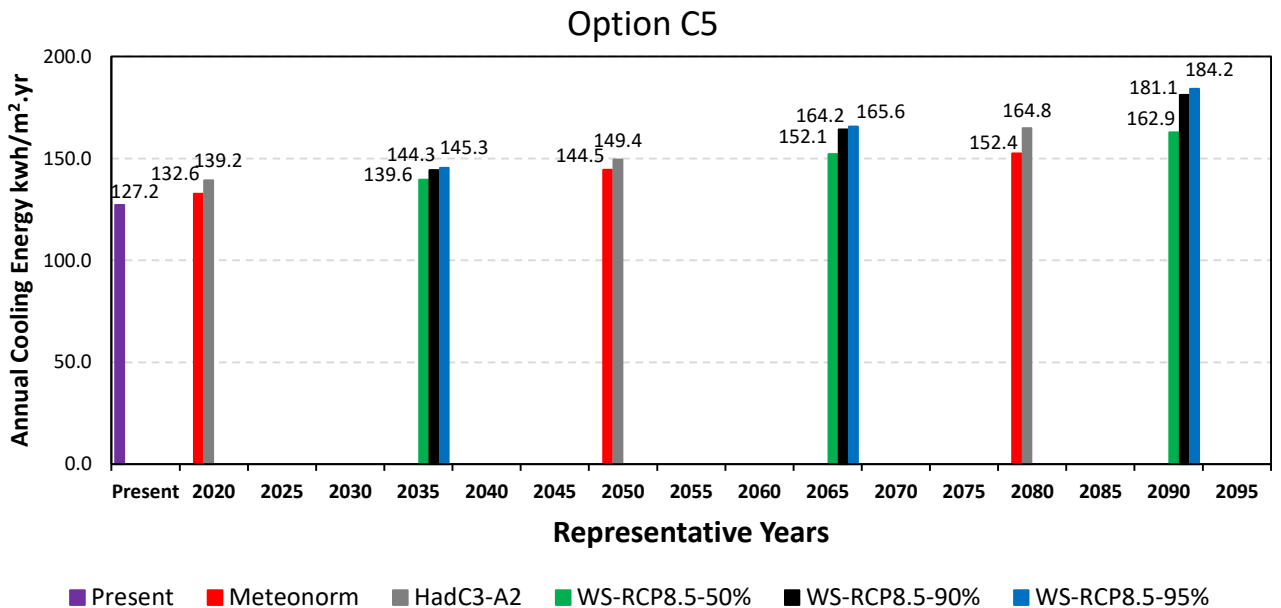


Figure 76: Total cooling energy of the base case model with option C5 simulated with present and future weather files.

The present results have recorded an annual total system energy of 153.07 kwh/m².yr and total cooling energy of 127.17 kwh/m².yr which is less than option C4 by 0.8%. The highest value was recorded as 216.47 kwh/m².yr for total system energy and 184.17 kwh/m².yr for total cooling energy in period 2090 with 95th percentile, those results are less than option C4 by 1%. Moreover, simulation with Meteonorm weather files (the stabilization emission scenario) has recorded 181.6 kwh/m².yr for total system energy and 152.43 kwh/m².yr for total cooling energy in period 2080, which is 0.9% less than option C4. The cooling energy of the base case with option C5 will consume around 83% from the total system energy in the present weather conditions and it would go up to 85% in future periods like 2090. The percentage increase from present consumption in total system energy of base case with option C5 is shown in figure 77 below. It is clear that the highest total system energy consumption of 216.5 kwh/m².yr in period 2090 with 95th percentile is 41% more from the present value.

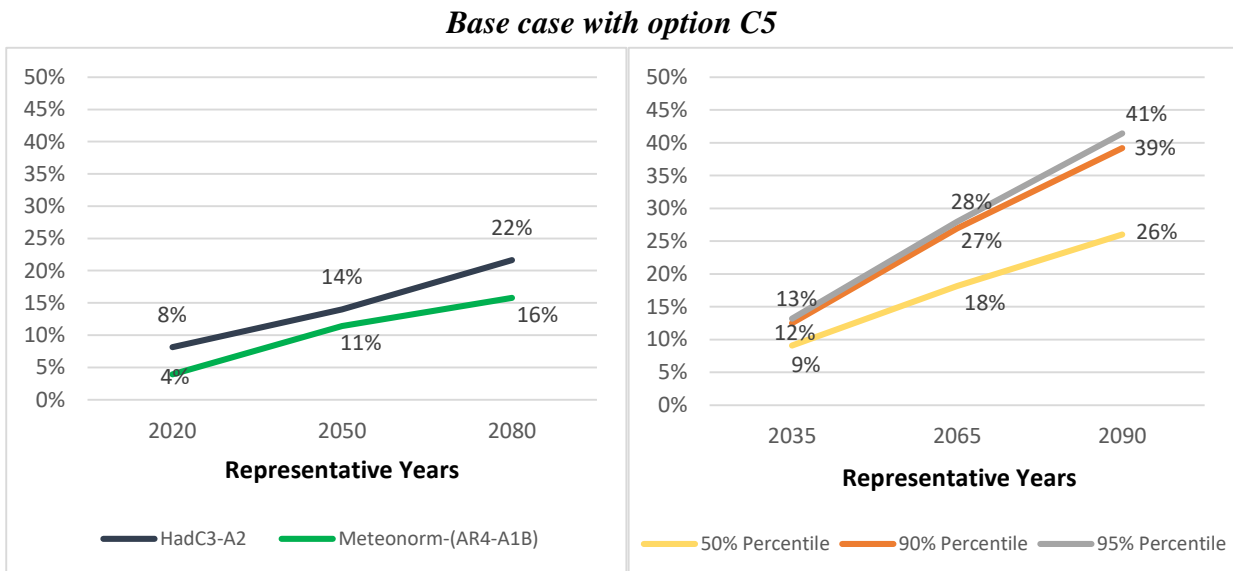


Figure 77: Percentage increase from present consumption of the total system energy of the base case with option C5 in the future selected periods.

Table (35) below represents the amount of energy reduction that would occur by applying option C5 to the base case model. In present weather conditions, this solution will reduce the energy by 7.8% for total system energy and 7.6% for total cooling energy. On the long-term, this percentage would increase with all emission scenarios. The highest percentage was recorded as 10.1% for period 2090 with 95th percentile, which means that this option will make the building more resistant to future climate change regarding energy demand. Consequently, this study confirms that applying enthalpy heat recovery units to HVAC system in high-rise buildings in UAE is an essential solution to make improve building resilience with the expected global warming in the future periods.

Table (35): Percentage reduction in total system energy and total cooling energy from the base case model for present and future periods by applying option (C5).										
HadCM3-A2: CCWorldWeatherGen tool										
Period		HadCM3-A2-2020			HadCM3-A2-2050			HadCM3-A2-2080		
Total system energy		8.1%			8.3%			8.8%		
Total cooling energy		8.0%			8.4%			9.0%		
AR4-A1B: Meteonorm tool										
Period		2020			2050			2080		
Total system energy		7.8%			8.8%			9.0%		
Total cooling energy		7.6%			8.9%			9.3%		
RCP 8.5: (WS) WeatherShift™ tool										
Period	Present	50% percentile			90% percentile			95% percentile		
		2035	2065	2090	2035	2065	2090	2035	2065	2090
Total system energy	7.8%	8.4%	8.9%	9.3%	8.5%	9.1%	9.5%	8.7%	9.3%	9.7%
Total cooling energy	7.6%	8.4%	9.0%	9.5%	8.5%	9.3%	9.8%	8.7%	9.5%	10.1%

4.4.6- Adding an enthalpy HRW to the HVAC system with 80% sensible efficiency and 78% latent efficiency

The last option C6 is to add three enthalpy HRW's having 80% sensible effectiveness and 78% latent effectiveness to the FAHU's of the base case HVAC system. For the purpose of the study, finding the best solution that would increase the building resilience toward climate change in future is required. In the previous section, Option C5 has shown significant results regarding energy consumption in future. Therefore, increasing the recovery unit efficiency is suggested in this option. Similar to the previous options, after applying this option to the base case model, simulation was done with all selected weather files and results are shown in figures 78 and 79.

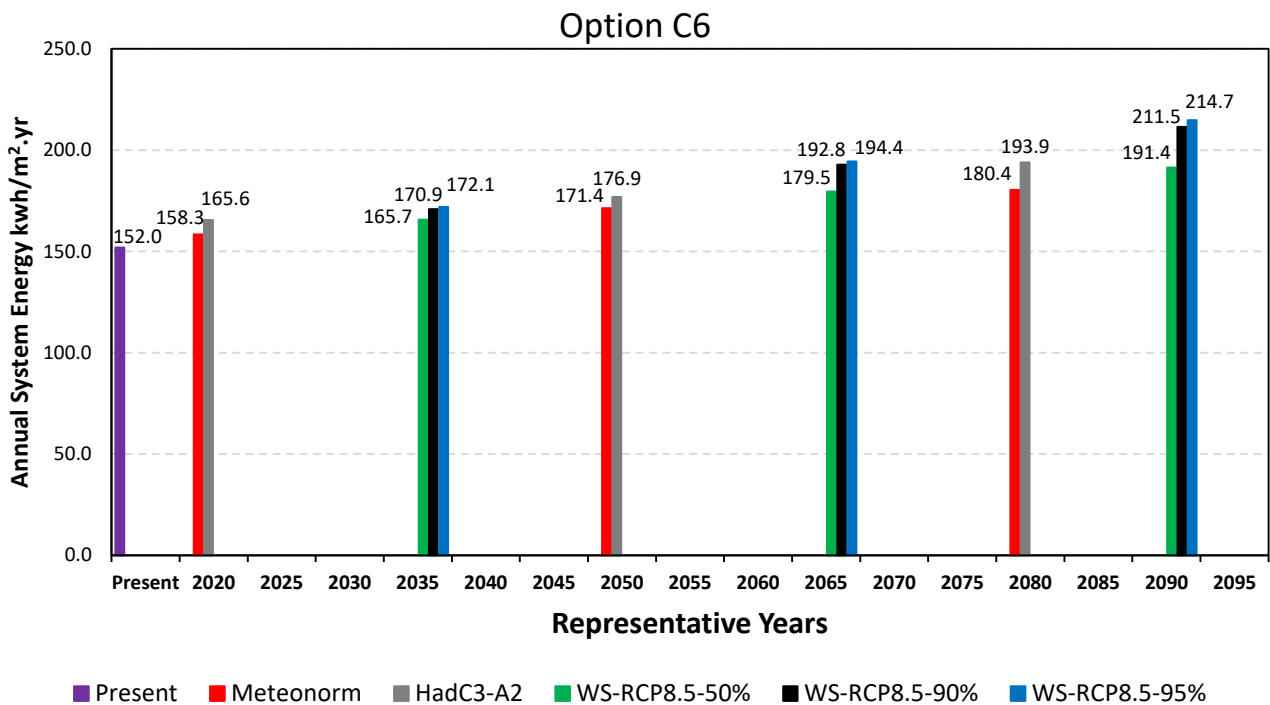


Figure 78: Total system energy of the base case model with option C2 simulated with present and future weather files.

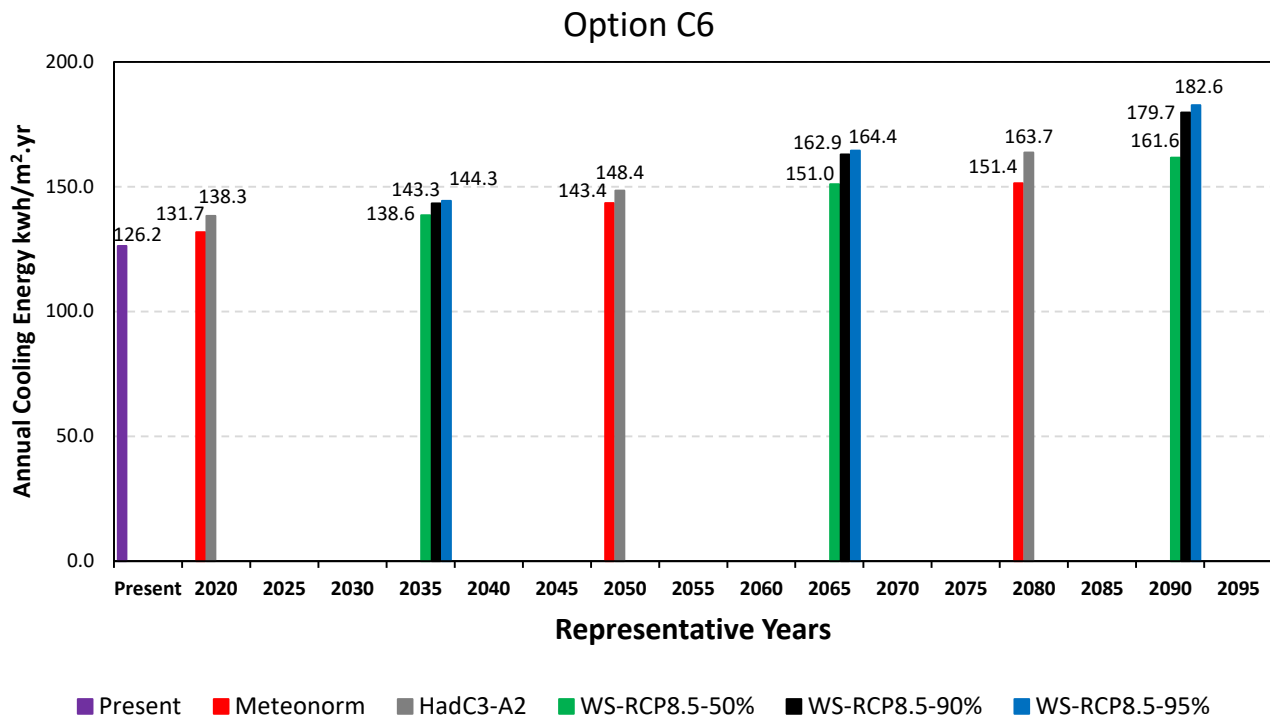


Figure 79: Total cooling energy of the base case model with option C2 simulated with present and future weather files.

The results of simulation have recorded 151.97 kwh/m².yr total system energy consumption of the building and 126.2 kwh/m².yr of this energy is consumed for cooling. By comparing the results of option C6 with options B2 and B3, it is noted that option C6 has higher values in present weather conditions. However, considering building resilience toward climate change, applying this option will make the building consumes less energy than options B2 and B3 in future. Also, there was no significant differences between options C5 and C6, only 0.7~0.8% reduction was observed by increasing the effectiveness of the enthalpy HRW. Similar to the previous options, the highest recorded values were obtained at period 2090 at 95th percentile, with 214.73 kwh/m².yr for total system energy and 182.63 kwh/m².yr for total cooling energy. It is apparent from the figures above that results of stabilization scenario are significantly less than

the high emission scenario where 180.4 kwh/m².yr for total system energy and 151.4 kwh/m².yr for total cooling energy were recorded in period 2080.

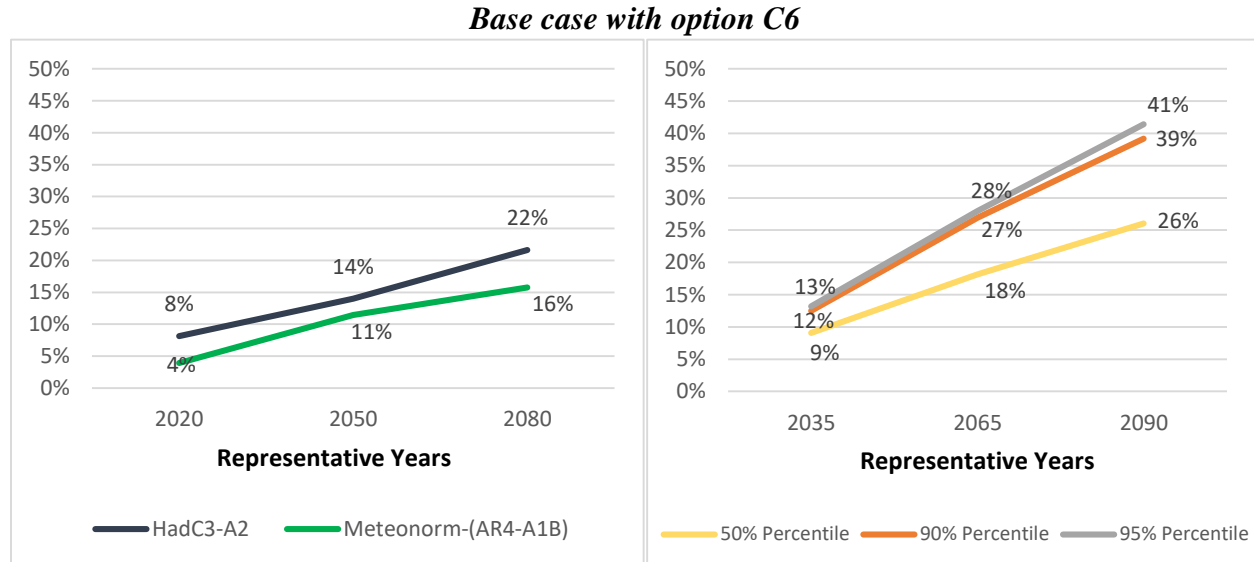


Figure 80: Percentage increase from present consumption of the total system energy of the base case with option C6 in the future selected periods.

Table (36): Percentage reduction in total system energy and total cooling energy from the base case model for present and future periods by applying option (C6).										
HadCM3-A2: CCWorldWeatherGen tool										
Period		HadCM3-A2-2020			HadCM3-A2-2050			HadCM3-A2-2080		
Total system energy		8.7%			8.9%			9.5%		
Total cooling energy		8.6%			9.0%			9.7%		
AR4-A1B: Meteonorm tool										
Period		2020			2050			2080		
Total system energy		8.4%			9.5%			9.6%		
Total cooling energy		8.2%			9.6%			9.9%		
RCP 8.5: (WS) WeatherShift™ tool										
Period	Present	50% percentile			90% percentile			95% percentile		
		2035	2065	2090	2035	2065	2090	2035	2065	2090

Total system energy	8.5%	9.1%	9.6%	10.0%	9.2%	9.8%	10.2%	9.3%	9.9%	10.5%
Total cooling energy	8.3%	9.1%	9.7%	10.2%	9.2%	10.0%	10.5%	9.3%	10.2%	10.8%

It can be seen from figure 80 above that the increase of total system energy from present value of the base case with option C6 has recorded between 4% to 41% for the selected future periods and emission scenarios.

Moreover, table (36) is quiet revealing in several ways. Firstly, the present values of energy consumption by applying option C6 are less than the base case model values by 8.5% for total system energy and 8.3% for total cooling energy. Also, an obvious increase in percentages is observed for most of the future periods. For example, the total system energy of the base case model will consume 9.7% more in period 2080 (based on HadC3-A2 emission scenario) if option C6 was not applied. Secondly, this option C6 was the best solution in this study that made the building more resilient to climate change in the future regarding energy consumption. We can conclude from the results that adding an enthalpy HRW to reduce the cooling loads of high-rise buildings is beneficial in reducing the energy demand in both present and future periods.

4.5- Comparison of this study with previous studies/researches

This study has analyzed the effect of applying a range of solutions/technologies to a typical highrise building in UAE to study the impact of climate change on total system and cooling energy. In the literature review, some previous studies on energy efficient solutions and climate change were introduced and they will be used to compare the results of this study with them.

Starting with the findings of Tibi and Mokhtar (2014) study which are consistent with this study results. In their study, they tested different glazing properties on a high-rise residential building

(30 m x 30 m) with 50% WWR. They found out that reducing the U-value and SHGC could reduce up to 9.7% from annual cooling loads. These results align with the finding of this study where improving the glazing properties of the double-glazed windows would reduce the present cooling energy consumption from 6.9% to 8.8%. Moreover, both studies have revealed that reducing the windows SHGC will have a better effect on present energy consumption more than reducing the U-value of the glazing.

Additionally, Shanks (2018) has tested some retrofit solutions that are similar to this study to find their effect on future energy consumption. He used EPW weather files provided by CCWorldWeatherGen. tool for three future periods (2020, 2050, 2080), then he examined how improving the glazing properties and increasing external walls insulation will affect the future energy consumption. In his study, he changed the glazing U-value from 1.8 to 0.76 W/m²K and the g-Value from 28% to 27% which reduced the annual cooling demand by 1.5% to 3.1%. If we compare those results with this study results, its apparent that improving the glazing properties of the base case by applying option B2 has reduced the U-value from 1.67 to 0.98 W/m²K with and the g-value from 40% to 16% which reduced the cooling energy consumption by 7.6% to 8.8%. The percentage energy reduction in this study is higher than Shanks (2018) results for many reasons. First, the WWR of this study is 60% which is significantly higher than the building in Shanks (2018) study which has 38% WWR, therefore; improving the glazing properties for this study would have more effect on energy consumption. Also, it seems possible that these higher percentages are due to the g-value in option B2 which is significantly less than Shanks (2018) glazing retrofit solution, this caused more future percentage reduction in cooling energy in this study even though the changes in U-value were close in both studies. On the other hand, if we compare Shanks (2018) retrofit option by reducing the external wall U-value from 0.35 to 0.18

W/m²K with option A1 in our study, we can find that Shanks (2018) has recorded slightly higher percentages reduction in the future. Option A1 in this study has reduced the external wall U-value from 0.34 to 0.2 W/m²K which is quite similar to Shanks (2018) external wall retrofit solution. However, in this study the future reduction in cooling energy was between 0.2% to 0.26%, while Shanks (2018) study has recoded 0.5% to 1% reduction from annual future cooling. As mentioned before, the variances between results is due to the differences in external wall area and WWR between the two buildings.

Another study by AL HUSSAINI and Khan (2017) has analyzed the amount of energy reduction that can be achieved by applying an enthalpy HRW to 6 air-handling units that are supplying an auditorium building in Hyderabad, India. They found out that the enthalpy HRW would reduce around 40% of the total energy consumption which is much higher than the results in this study. This rather contradictory results may be due to the differences in the HVAC systems between the two studies. In this study the percentage of fresh air supplied by the FAHU is considered low compared with the recirculated air supplied by the FCU (see tables (24) and (25)). Therefore, applying an enthalpy HRW for this type of HVAC system will reduce the present total energy by 7.1% to 8.5% depending on the enthalpy HRW effectiveness. Nevertheless, according to SULLIVAN (2010), the enthalpy wheel is able to reduce up to 80% of HVAC system energy consumption, this study contradicts with SULLIVAN (2010) findings where this high savings by applying heat recovery unit are not realistic. The percentage reduction in energy would depend on many factors such as the differences in temperatures and humidity ratio between the supplied and extracted air, the amount of fresh air supplied by HVAC system, type of HVAC system, and efficiency of the enthalpy HRW.

4.6- Summary of the simulation results

The annual total system energy and total cooling energy for the base case model alone and with each proposed option are shown in tables (37) and (38).

Table (38): Summary of annual total system energy for the base case and all proposed options in kwh/m².yr.

Total System Energy	Weather-Shift RCP8.5	CCWorldGen. (HadC3-A2)			Meteonorm (AR4-A1B)			WeatherShift tool - RCP 8.5								
								50 th percentile			90 th percentile			95 th percentile		
Years	Present	2020	2050	2080	2020	2050	2080	2035	2065	2090	2035	2065	2090	2035	2065	2090
Base case	166.1	181.3	194.3	214.2	172.9	189.4	199.5	182.3	198.5	212.6	188.2	213.7	235.4	189.7	215.8	239.8
A.1	165.8	181.0	193.8	213.6	172.6	189.0	199.1	181.9	198.0	212.1	187.8	213.2	234.8	189.3	215.3	239.2
A.2	165.6	180.8	193.6	213.3	172.4	188.8	198.8	181.7	197.8	211.8	187.5	212.8	234.4	189.1	215.0	238.7
B.1	155.0	169.8	183.6	204.5	161.5	179.8	190.4	172.0	189.2	204.2	178.6	205.3	228.9	180.2	207.8	233.2
B.2	152.0	165.7	178.6	198.1	157.8	175.8	185.6	167.7	183.6	197.8	173.7	198.6	220.5	175.2	201.0	224.6
B.3	149.7	163.0	175.8	195.0	155.3	173.3	183.0	165.1	180.8	194.8	171.1	195.6	217.3	172.7	198.1	221.3
C.1	158.3	172.3	184.4	203.2	165.1	180.7	190.5	173.3	188.3	201.7	178.8	203.0	223.5	180.1	204.8	227.9
C.2	157.9	171.8	183.9	202.7	164.7	180.4	190.1	172.8	187.7	201.2	178.3	202.5	223.0	179.7	204.3	227.4
C.3	157.4	171.3	183.4	202.2	164.3	180.0	189.8	172.3	187.3	200.6	177.8	201.9	222.5	179.2	203.8	226.8
C.4	154.3	167.9	179.4	196.8	160.6	174.2	183.2	168.3	182.4	194.6	173.5	195.9	215.0	174.7	197.6	218.6
C.5	153.1	166.7	178.1	195.2	159.4	172.7	181.6	166.9	180.9	192.9	172.2	194.3	213.1	173.3	195.9	216.5
C.6	152.0	165.6	176.9	193.9	158.3	171.4	180.4	165.7	179.5	191.4	170.9	192.8	211.5	172.1	194.4	214.7

Table (37): Summary of annual total cooling energy for the base case and all proposed options in kwh/m².yr.

Total Cooling Energy	Weather-Shift RCP 8.5	CCWorldGen. (HadC3-A2)			Meteonorm (AR4-A1B)			WeatherShift tool - RCP 8.5								
								50 th percentile			90 th percentile			95 th percentile		
Years	Present	2020	2050	2080	2020	2050	2080	2035	2065	2090	2035	2065	2090	2035	2065	2090
Base case	137.7	151.3	163.1	181.2	143.5	158.7	168.0	152.4	167.1	180.0	157.7	181.0	200.8	159.1	183.0	204.8
A.1	137.4	151.0	162.7	180.8	143.2	158.3	167.6	152.1	166.7	179.6	157.4	180.6	200.2	158.8	182.5	204.2
A.2	137.3	150.8	162.5	180.5	143.1	158.1	167.4	151.9	166.5	179.3	157.2	180.3	199.9	158.6	182.2	203.8
B.1	128.1	141.4	154.0	173.0	133.5	150.4	160.1	143.6	159.2	172.9	149.5	173.8	195.3	151.1	176.1	199.2
B.2	125.5	137.9	149.7	167.4	130.3	146.9	156.0	139.9	154.3	167.3	145.4	168.0	188.0	146.7	170.2	191.7
B.3	123.7	135.7	147.3	164.8	128.2	144.8	153.8	137.7	152.0	164.8	143.2	165.5	185.2	144.6	167.7	188.9
C.1	131.6	143.9	154.8	171.8	137.4	151.4	160.1	145.0	158.5	170.5	149.9	171.7	190.2	151.2	173.3	194.1
C.2	131.2	143.5	154.4	171.3	137.1	151.1	159.9	144.6	158.0	170.0	149.5	171.2	189.7	150.7	172.9	193.6
C.3	130.8	143.1	154.0	170.8	136.8	150.8	159.5	144.2	157.6	169.6	149.1	170.8	189.3	150.3	172.4	193.1
C.4	128.2	140.3	150.5	166.2	133.7	145.7	153.8	140.8	153.4	164.3	145.5	165.6	182.8	146.5	167.1	186.0
C.5	127.2	139.2	149.4	164.8	132.6	144.5	152.4	139.6	152.1	162.9	144.3	164.2	181.1	145.3	165.6	184.2
C.6	126.2	138.3	148.4	163.7	131.7	143.4	151.4	138.6	151.0	161.6	143.3	162.9	179.7	144.3	164.4	182.6

According to results above, applying options B3 and C6 to the base case model have achieved the lowest energy consumptions in both total system and cooling energy amongst other options.

In the present weather conditions, applying option B3 would reduce the energy consumption more than option C6. However, this will change for different future periods and emission scenarios. In high emission scenario HadC3-A2, option B3 will perform better than option C6 for periods 2020 and 2050, but option C6 will reduce more energy than option B3 in 2080 where the global warming is expected to be high, see tables (39) and (40) below. For the stabilization scenario (AR4-A1B), option C6 performed better than option B3 in periods 2050 and 2080. While in the other high emission scenario (RCP 8.5), option B3 will reduce more energy than option C6 in period 2035 with 50th percentile, however; in all other future periods and percentiles of this emission scenario option C6 will perform better than option B3.

Table (39): Summary of percentage reduction from base case in total system energy for all proposed options.

Total Cooling Energy	Weather-Shift RCP 8.5	CCWorldGen. (HadC3-A2)			Meteonorm (AR4-A1B)			WeatherShift tool - RCP 8.5								
		2020	2050	2080	2020	2050	2080	50 th percentile			90 th percentile			95 th percentile		
Years	Present	2020	2050	2080	2020	2050	2080	2035	2065	2090	2035	2065	2090	2035	2065	2090
A.1	0.16%	0.18%	0.22%	0.25%	0.19%	0.21%	0.20%	0.22%	0.25%	0.24%	0.21%	0.23%	0.28%	0.21%	0.25%	0.28%
A.2	0.28%	0.31%	0.34%	0.39%	0.31%	0.32%	0.35%	0.33%	0.39%	0.39%	0.34%	0.41%	0.45%	0.33%	0.40%	0.46%
B.1	6.7%	6.4%	5.5%	4.5%	6.6%	5.1%	4.6%	5.6%	4.7%	3.9%	5.1%	3.9%	2.8%	5.0%	3.7%	2.8%
B.2	8.5%	8.6%	8.0%	7.5%	8.7%	7.2%	7.0%	8.0%	7.5%	7.0%	7.7%	7.1%	6.3%	7.7%	6.9%	6.3%
B.3	9.9%	10.1%	9.5%	8.9%	10.2%	8.5%	8.3%	9.5%	8.9%	8.4%	9.1%	8.5%	7.7%	9.0%	8.2%	7.7%
C.1	4.7%	5.0%	5.1%	5.1%	4.5%	4.6%	4.7%	5.0%	5.2%	5.1%	5.0%	5.0%	5.1%	5.0%	5.1%	5.0%
C.2	5.0%	5.3%	5.3%	5.4%	4.7%	4.8%	4.7%	5.2%	5.5%	5.4%	5.3%	5.3%	5.3%	5.3%	5.3%	5.2%
C.3	5.2%	5.5%	5.6%	5.6%	5.0%	4.9%	4.9%	5.5%	5.7%	5.6%	5.5%	5.5%	5.5%	5.6%	5.6%	5.4%
C.4	7.1%	7.4%	7.7%	8.1%	7.1%	8.0%	8.2%	7.7%	8.1%	8.5%	7.8%	8.3%	8.7%	7.9%	8.4%	8.9%
C.5	7.8%	8.1%	8.3%	8.8%	7.8%	8.8%	9.0%	8.4%	8.9%	9.3%	8.5%	9.1%	9.5%	8.7%	9.3%	9.7%
C.6	8.5%	8.7%	8.9%	9.5%	8.4%	9.5%	9.6%	9.1%	9.6%	10.0%	9.2%	9.8%	10.2%	9.3%	9.9%	10.5%

Table (40): Summary of percentage reduction from base case in total cooling energy for all proposed options.

Total Cooling Energy	Weather-Shift RCP 8.5	CCWorldGen. (HadC3-A2)			Meteonorm (AR4-A1B)			WeatherShift tool - RCP 8.5								
		2020	2050	2080	2020	2050	2080	50 th percentile			90 th percentile			95 th percentile		
Years	Present	2020	2050	2080	2020	2050	2080	2035	2065	2090	2035	2065	2090	2035	2065	2090
A.1	0.19%	0.20%	0.25%	0.26%	0.21%	0.21%	0.24%	0.24%	0.26%	0.24%	0.21%	0.26%	0.28%	0.21%	0.25%	0.28%
A.2	0.29%	0.33%	0.37%	0.42%	0.33%	0.34%	0.38%	0.37%	0.38%	0.41%	0.34%	0.42%	0.46%	0.36%	0.42%	0.49%
B.1	6.9%	6.5%	5.6%	4.6%	7.0%	5.2%	4.7%	5.8%	4.7%	4.0%	5.2%	4.0%	2.8%	5.1%	3.8%	2.7%
B.2	8.8%	8.8%	8.2%	7.6%	9.2%	7.4%	7.1%	8.2%	7.7%	7.1%	7.8%	7.2%	6.4%	7.8%	7.0%	6.4%
B.3	10.2%	10.3%	9.7%	9.1%	10.7%	8.8%	8.5%	9.7%	9.0%	8.5%	9.2%	8.6%	7.8%	9.1%	8.3%	7.8%
C.1	4.4%	4.8%	5.1%	5.2%	4.2%	4.6%	4.7%	4.9%	5.2%	5.3%	4.9%	5.2%	5.3%	5.0%	5.3%	5.2%
C.2	4.7%	5.3%	5.3%	5.5%	4.5%	4.8%	4.8%	5.1%	5.5%	5.6%	5.2%	5.4%	5.5%	5.3%	5.5%	5.5%
C.3	5.0%	5.4%	5.6%	5.7%	4.7%	5.0%	5.0%	5.4%	5.7%	5.8%	5.5%	5.7%	5.7%	5.5%	5.8%	5.7%
C.4	6.9%	7.2%	7.7%	8.3%	6.9%	8.2%	8.5%	7.7%	8.2%	8.7%	7.8%	8.5%	9.0%	7.9%	8.7%	9.2%
C.5	7.6%	8.0%	8.4%	9.0%	7.6%	8.9%	9.3%	8.4%	9.0%	9.5%	8.5%	9.3%	9.8%	8.7%	9.5%	10.1%
C.6	8.3%	8.6%	9.0%	9.7%	8.2%	9.6%	9.9%	9.1%	9.7%	10.2%	9.2%	10.0%	10.5%	9.3%	10.2%	10.8%

Furthermore, it can be seen from tables (39) and (40) above that the percentage reduction from base case for total system and cooling energy is increasing in future periods in options A1, A2, C1, C2, C3, C4, C5, and C6. Which means that they will make the building more resilient to future climate change. While in options B1, B2, and B3, the percentage reduction from base case is decreasing in future, however; it is still considered as an energy efficient solution even though it will make the building less resilient to climate change.

This study can provide designers and engineers in UAE an overview on the selection of the appropriate solution for high-rise buildings based on the required energy saving and the life-time of the building.

4.7- Applying options A2, B3, and C6

In this section, the three best options from the insulation layers, glazing, and recovery units were applied to the base case model and simulated with present and future selected files to find out how a combination of energy efficient technologies on UAE high-rise building would improve

the building resilience toward climate change and its effect on energy demand. After applying options A2, B3, and C6 to the base case model, the model was simulated and the results are shown in figures 81 and 82.

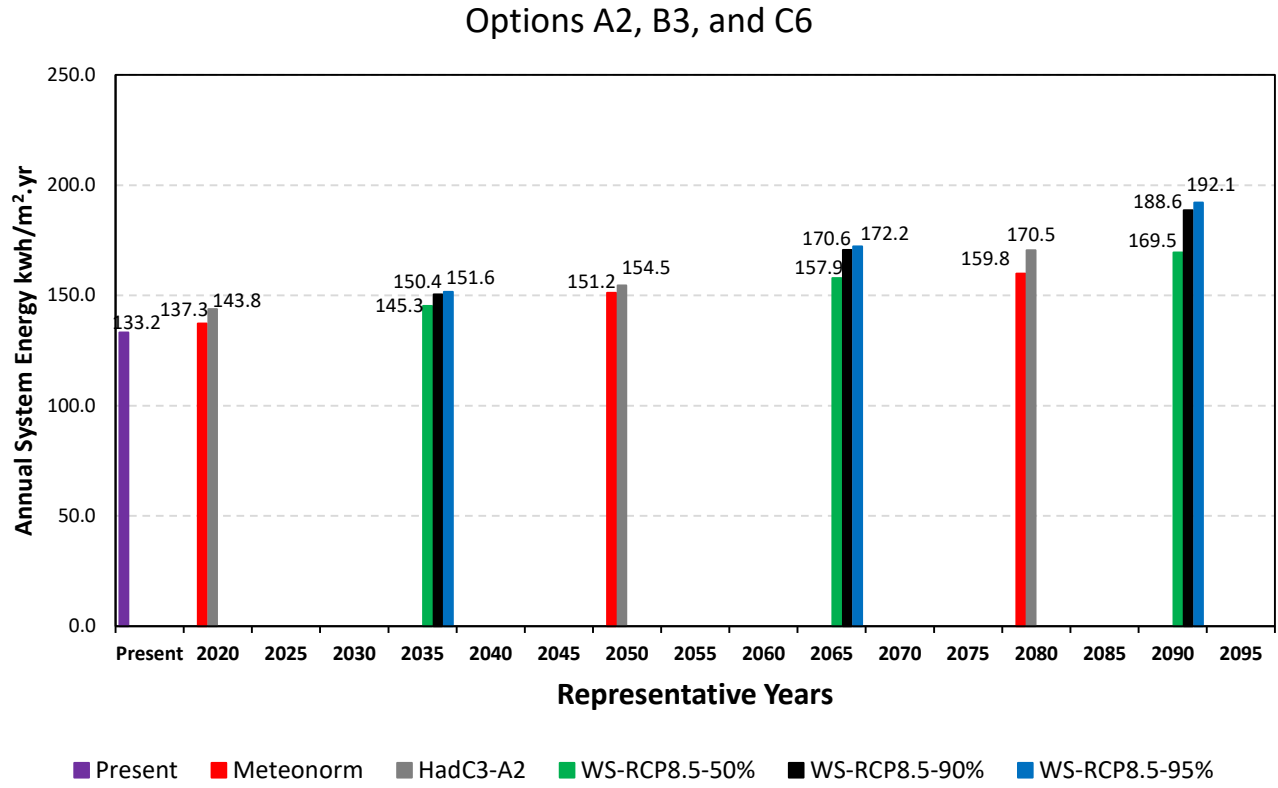


Figure 81: Total system energy of the base case model with options A2, B3, and C6 simulated with present and future weather files.

Options A2, B3, and C6

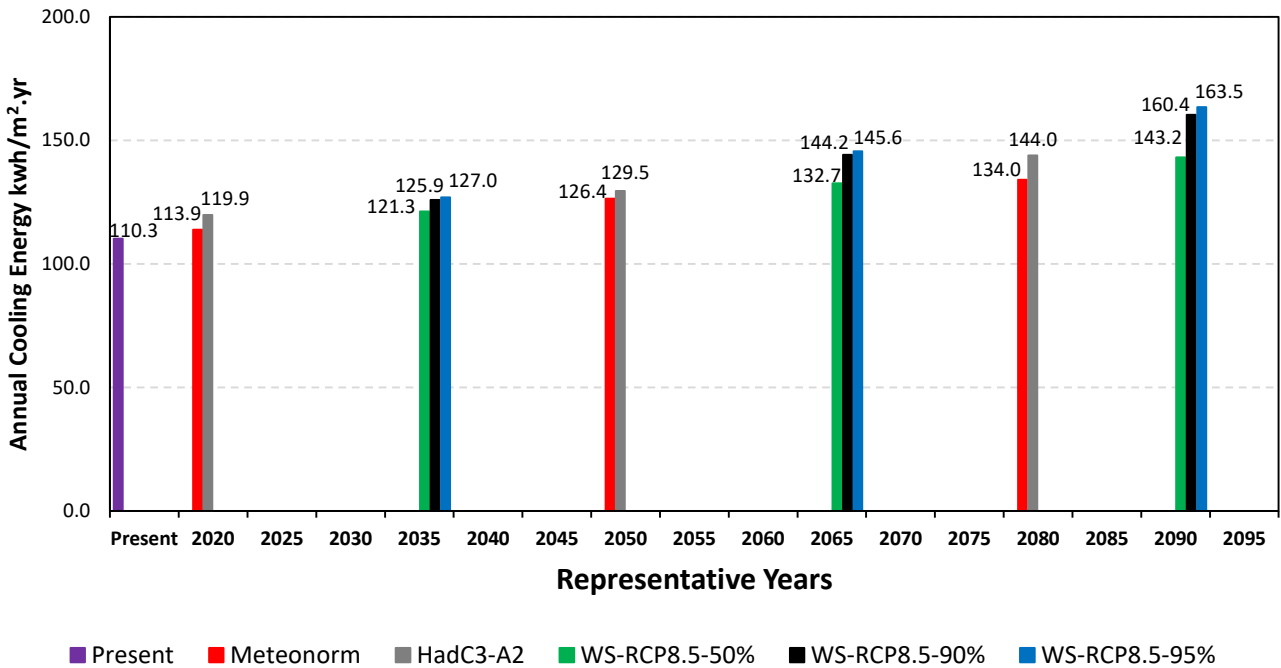


Figure 82: Total cooling energy of the base case model with options A2, B3, and C6 simulated with present and future weather files.

Applying the three best options has reduced the total system energy from 166.1 kwh/m².yr to 133.2 kwh/m².yr and the total cooling energy from 137.7 kwh/m².yr to 110.3 kwh/m².yr. As mentioned before in section 4.1.2, the best practice energy efficient buildings consume around 110-160 kwh/m².yr (Clarke 2016). Therefore, applying the three best options in this study will classify the building as best practice energy efficient building up to period 2050. Afterward, the total system energy consumption is more than 160 kwh/m².yr except for period 2065 with 50% percentile. The base case with options A2, B3, and C6 total system energy percentage increase from the present value is shown in figure 83 below. It is noticed that the future expected percentage increase is between 3% to 44% depending on the period and emission scenario.

Base case with options A2, B3 and C6

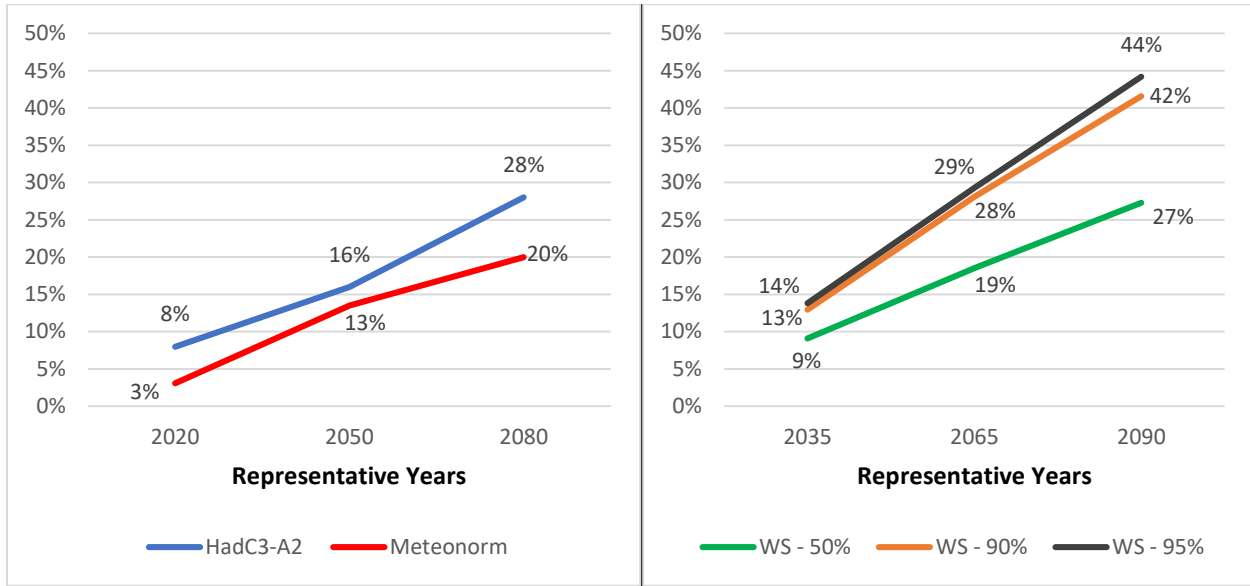


Figure 83: Percentage increase from present consumption of the total system energy of the base case with option C6 in the future selected periods.

Table (41): Percentage reduction in total system energy and total cooling energy from the base case model for present and future periods by applying options A2, B3, and C6.

HadCM3-A2: CCWorldWeatherGen tool										
Period		HadCM3-A2-2020			HadCM3-A2-2050			HadCM3-A2-2080		
Total system energy		21%			20%			20%		
Total cooling energy		21%			21%			21%		
AR4-A1B: Meteonorm tool										
Period		2020			2050			2080		
Total system energy		21%			20%			20%		
Total cooling energy		21%			20%			20%		
RCP 8.5: (WS) WeatherShift™ tool										
Period	Present	50% percentile			90% percentile			95% percentile		
		2035	2065	2090	2035	2065	2090	2035	2065	2090
Total system energy		20%	20%	20%	20%	20%	20%	20%	20%	20%
Total cooling energy		20%	20%	21%	20%	20%	20%	20%	20%	20%

As can be seen from the table above, the percentage reduction from the base case by applying the most three efficient solutions in this study will reduce the total system energy and the total cooling energy by 20% to 21% in present and future periods and in all emission scenarios, which will improve the building resilience toward climate change considerably.

Chapter 5: Conclusion and Recommendations

5.1- Conclusion

The main goal of this study was to determine the effect of climate change on the cooling energy demand of UAE high-rise buildings and to find the most energy efficiency solutions that would make those buildings more resilient to climate change and global warming. To achieve this goal, a base case model that represents a typical UAE high-rise building following Dubai regulations and international standards was prepared. Afterward, a range of present and future weather files representing stabilization and high emission scenarios derived from different international industry accepted data sources were collected and analyzed.

Then, several energy efficiency solutions were selected based on previous studies and researches. Those solutions included two external wall insulation layers, three glazing types with different thermal characteristics, and six HVAC heat recovery units. Moreover, a total of 208 simulations with the collected present and future weather files were conducted to discover the most energy efficient solution that would improve the building performance in present and future periods.

This research extends our knowledge on the different types of future weather files and the methods that are used to derive them. Generating future weather files can be done by using two different approaches, dynamical downscaling and statistical downscaling. In this study, future weather files derived by statistical downscaling were used. CCWorldWeatherGen tool files representing high emission scenario (HadC3-A2) and WeatherShift™ tool files representing high emission scenario (RCP 8.5) were generated by using morphing method, after analyzing those files several findings were concluded. First, by comparing the RCP 8.5 weather files with HadC3-A2 weather files, this study found out that RCP8.5 weather files have higher temperatures than HadC3-A2 files for Abu Dhabi city, UAE. Also, the air temperature is rising in future periods in both tools. However, the global horizontal solar radiation and the relative

humidity ratio were decreasing in future periods for both tools which contradicts with Glavan (2015) report where she confirmed the increase of those two weather parameters in UAE in the future by using dynamical downscaling. The third statistical tool that was used in this study is the Metoetorm tool which uses stochastic method to derive the weather files. This tool confirms that the air temperatures and RH% will increase in future while the global horizontal solar radiation values fluctuates throughout the years.

The present study confirms that applying glazing with low U-value and SHGC is important to reduce the cooling loads and energy consumption in the present and future periods in UAE high-rise buildings. Also, an important limitation in this study is the low energy savings from improving the external wall insulation layers which would be related to a margin of error in modelling.

After testing six HVAC heat recovery units, this study verifies that using sensible and latent recovery unit would have a better impact from using sensible only recovery units in UAE. The present energy saving from using 80% sensible and 78% latent recovery unit has reached 8.5% for total system energy and 8.3% for total cooling energy. Those savings would rise in future up to 10.5% and 10.8% for total system energy and total cooling energy respectively. Furthermore, taking into consideration the lower RH% in the RCP8.5 and HadC3-A2 future files, this study confirms that future savings would be higher than the founded.

This study highly recommends using glazing with good thermal properties with sensible and latent HVAC heat recovery unit in UAE high-rise buildings. Those two solutions are considered to be efficient to reduce the present energy consumption and improve the building resilience toward climate change in future.

Finally, the present study makes several noteworthy contributions to the effect of climate change and global warming on UAE high-rise buildings and how they will increase the future energy demand significantly. The total system energy consumption of UAE high-rise buildings would increase from present consumption by 3% to 50% in future depending on the period and emission scenario. Also, it has been discovered that applying the three best options to the base case model in this study will have a positive impact on energy consumption and will reduce the total system energy and the total cooling energy by 20% to 21% in present and future periods.

5.2- Research limitations and recommendations

There were several limitations to this study that need to be acknowledged. Starting with the present and future weather files that were used, the present file that was available for simulation is a default weather file derived from previous years, having a more recent weather file in a readable format by building simulation tools would be more useful in comparing with future periods which is not available for UAE. Furthermore, dynamically downscaled future weather files would produce more precise results than the statistically downscaled future weather files but they were not used in this study due to the difficulty of extracting those files and the restrictions by the Environmental Agency of Abu Dhabi (EAD).

This study has only examined high-rise buildings in UAE, covering more than one type was not possible in this study. Therefore, testing the effect of climate change of different types of buildings could be done in future researches. Also, only one HVAC system was used in this study, so measuring the effect of climate change on different types of HVAC systems can be done in future as well.

According to this study, it is recommended that further research be undertaken in the following areas:

- Further studies could investigate the most appropriate energy efficient solutions/techniques for different types of building such as mid-rise and low-rise buildings in UAE. Then they can investigate the efficiency of those solutions in future and how can they improve the building resilience toward climate change.
- A dynamically scaled future weather datasets for UAE can be generated in the cooperation with the Environmental Agency of Abu Dhabi (EAD). Those datasets will be useful for designers, engineers, and buildings regulation entities.
- It would be useful to assess the impact of climate change on UAE high-rise buildings in different simulation tools to compare them with the results of this study.
- Other researches could test the effectiveness of heat recovery units of different HVAC systems using present and future weather datasets.
- With the dynamically downscaled UAE weather datasets being currently unavailable, the statistically downscaled weather datasets become the only useful source to evaluate the resilience of UAE buildings to climate change.

References

Abdullah, E. (2001). "Experts discuss life span of buildings". *Gulfnews.com* [online]. [Accessed 4 April 2020]. Available at: <https://gulfnews.com/uae/experts-discuss-life-span-of-buildings-1.429893>

Air Systems - Energy Series, Energy Recovery Wheels. (n.d.). Pennsylvania, USA: YORK INTERNATIONAL. Viewed 7 May 2020. https://www.johnsoncontrols.com/-/media/jci/be/united-states/airside-systems/air-handling-units/files/be_appguide_energyrecoverywheel_ahu.pdf?la=en&hash=01540950F3E2B779DA8C7F625DFF96CB6EA14776

AL HUSSAINI, S. & Khan, I. (2017). Designing HVAC system with and without Heat Recovery Wheel using ECO-FRESH Enthalpy wheel. *International Journal of Scientific & Engineering Research*, vol. 8 (11), pp. 854-857. [Accessed 23 March 2020].

"Al Safat, Dubai Green Building Evaluation System". (2016). [Accessed 22 March 2020]. Available at: <https://www.dm.gov.ae/en/Business/DubaiCentralLaboratory/ProductCertificationServices/Documents/Green%20Building%20Certification/AL-SA%27FAT.pdf>

ASHRAE. (2008). *HVAC systems and equipment handbook*. Atlanta, USA:ASHRAE, Inc.

ASHRAE Fundamentals. (2017). Viewed 9 June 2020. <http://ashrae.org>

"ASHRAE International Weather Files for Energy Calculations 2.0 (IWEC2)". (2019). [Accessed 18 June 2020]. Available at: <https://www.ashrae.org/technical-resources/bookstore/ashrae-international-weather-files-for-energy-calculations-2-0-iwec2>

CIBSE guide A. (2015). Viewed 23 June 2020. <https://www.cibse.org/>

Clarke, K. (2016). "80% energy consumed by buildings". *Khaleej Times* [online]. [Accessed 2 May 2020]. Available at: <https://www.khaleejtimes.com/nation/abu-dhabi/80-energy-consumed-by-buildings>

"Climate Change World Weather File Generator for World-Wide Weather Data – CCWorldWeatherGen | Sustainable Energy Research Group". (n.d.). [Accessed 3 April 2020]. Available at: <http://www.energy.soton.ac.uk/ccworldweathergen/>

"Climate Data Download Center". (2013). [Accessed 11 April 2020]. Available at: http://www.equaonline.com/ice4user/new_index.html

"Climate Data Download Center". (2013). [Accessed 11 June 2020]. Available at: http://www.equaonline.com/ice4user/new_index.html#:~:text=The%20International%20Weather%20for%20Energy,the%20National%20Climatic%20Data%20Center.&text=The%20files%20are%20derived%20from,the%20National%20Climatic%20Data%20Center.

"Climatology - Paducah, KY - February Temperature Percentiles". (n.d.). [Accessed 13 April 2020]. Available at: <https://www.weather.gov/pah/PaducahFebruaryTemperaturePercentiles>

Cox, R., Drews, M., Rode, C. & Nielsen, S. (2015). Simple future weather files for estimating heating and cooling demand. *Building and Environment*, vol. 83, pp. 104-114. [Accessed 26 October 2019].

Dataviewer. (n.d.). Alliance for Sustainable Energy, LLC.

Donev, J., Halim, A., Jenden, J., Stenhouse, K. & Afework, B. (2018). "Glazing - Energy Education". *Energyeducation.ca* [online]. [Accessed 6 April 2020]. Available at: <https://energyeducation.ca/encyclopedia/Glazing>

"Dubai climate: average weather, temperature, precipitation, best time". (2020). [Accessed 29 February 2020]. Available at: <https://www.climatestotravel.com/climate/united-arab-emirates/dubai>

"Dubai Demand Side Management Strategy 2030 | innogy International Middle East". (2020). [Accessed 29 February 2020]. Available at: http://www.innogy.ae/case_studies/demand-side-management-program/

"Dubai Electricity & Water Authority (DEWA) | Annual Statistics". (2018). [Accessed 29 February 2020]. Available at: <https://www.dewa.gov.ae/en/about-us/media-publications/annual-statistics>

"Dubai Electricity & Water Authority (DEWA) | Sustainability Reports". (2018). [Accessed 29 February 2020]. Available at: <https://www.dewa.gov.ae/en/consumer/Sustainability/sustainability-reports>

"Energy Recovery – Applied to IAQ". (2011). [Accessed 7 April 2020]. Available at: http://ashraeqatar.com/images/ASHRAE_QATAR_Final_MM_12-02-2011_Compatibility_Mode_.pdf

"Energy Recovery Wheels". (2020). [Accessed 23 March 2020]. Available at: <http://www.dac-hvac.com/energy-recovery-wheels-what-is-an-enthalpy-wheel/>

"EnergyPlus Weather File (EPW) Data Dictionary: Auxiliary Programs — EnergyPlus 8.3". (2011). [Accessed 16 April 2020]. Available at: <https://bigladdersoftware.com/epx/docs/8-3/auxiliary-programs/energyplus-weather-file-epw-data-dictionary.html>

"Engineering ToolBox". (2003). [Accessed 7 May 2020]. Available at: https://www.engineeringtoolbox.com/latent-sensible-cooling-load-d_245.html

Farah, S., Whaley, D., Saman, W. & Boland, J. (2019). Integrating climate change into meteorological weather data for building energy simulation. *Energy and Buildings*, vol. 183, pp. 749-760.

Glavan, J. (2015). Technical Report: Regional Downscaled Climate Change Atmospheric Modeling Results. [Accessed 2 March 2020].

Global Alliance for Buildings and Construction. (2018). [online]. United Nations Environment Programme, 2018. [Accessed 13 June 2020]. Available at: <https://www.worldgbc.org/sites/default/files/2018%20GlobalABC%20Global%20Status%20Report.pdf>

Global CO2 emission by sector. (2019). image [online]. [Accessed 9 November 2019]. Available at: <https://globalabc.org/>

GlobalChange.gov. (2014). *Climate Change Impacts in the United States: The Third National Climate Assessment* [online]. [Accessed 14 April 2020]. Available at: <http://nca2014.globalchange.gov>.

"Greenhouse effect". (n.d.). [Accessed 17 June 2020]. Available at: <https://www.environment.gov.au/climate-change/climate-science-data/climate-science/greenhouse-effect>

Guan, L. (2009). Preparation of future weather data to study the impact of climate change on buildings. *Building and Environment*, vol. 44 (4), pp. 793-800. [Accessed 28 October 2019].

GUIDELINES FOR SPECIFYING WEATHERSHIFT™ FUTURE WEATHER FILES ARGOS ANALYTICS, LLC. (2017). Viewed 4 April 2020. <https://www.iesve.com/support/weather-files/user-guidelines.pdf>

Haggag, M. (2007). Building skin and energy efficiency in a hot climate with particular reference to Dubai, UAE. *Energy and Sustainability*,. [Accessed 16 March 2020].

"Heat Recovery Wheel (HW)". (2020). [Accessed 23 March 2020]. Available at: <http://www.maxellqatar.com/heat-recovery-wheel-hw/>

"How Do Double-Skin Façades Work?". (2020). [Accessed 26 February 2020]. Available at: https://www.archdaily.com/922897/how-do-double-skin-facades-work?ad_medium=gallery

IES Virtual Environment. (2019). Environmental Solutions Ltd. <https://www.iesve.com>.

"IPCC: Summary for Policymakers". (2013). [Accessed 30 October 2019]. Available at: https://www.ipcc.ch/pdf/assessment-report/ar5/wg1/wg1ar5_spm_final.pdf

Jentsch, M., James, P., Bourikas, L. & Bahaj, A. (2013). Transforming existing weather data for worldwide locations to enable energy and building performance simulation under future climates. *Renewable Energy*, vol. 55, pp. 514-524. [Accessed 4 April 2020].

Johnson, A. (2020). "Shaikh Zayed Road: Oasis of architecture". *Gulfnews.com* [online]. [Accessed 26 February 2020]. Available at: <https://gulfnews.com/uae/shaikh-zayed-road-oasis-of-architecture-1.670569>

Johny, A. & Shanks, K. (2018). Optimization of Double-Skin Facades for High-Rise Buildings in Hot Arid Climates. *International Journal of Environment and Sustainability*, vol. 7 (2).

Kaul, N. (2017). "The bad boys of energy consumption". *Gulfnews.com* [online]. [Accessed 12 May 2020]. Available at: <https://gulfnews.com/business/property/the-bad-boys-of-energy-consumption-1.2120451>

Košir, M. (2019). *Climate Adaptability of Buildings, Bioclimatic Design in the Light of Climate Change*.

Meteonorm 7. (2019).

Moazami, A., Nik, V., Carlucci, S. & Geving, S. (2019). Impacts of future weather data typology on building energy performance – Investigating long-term patterns of climate change and extreme weather conditions. *Applied Energy*, vol. 238, pp. 696-720. [Accessed 8 January 2020].

"NDC & INDC Factsheets | Climate and Energy College". (2020). [Accessed 8 January 2020]. Available at: http://climatecollege.unimelb.edu.au/ndc-indc-factsheets?order=field_fs_pc_reduction_2010_2030&sort=asc

"Pros & Cons of Double Glazing Vs Triple Glazing Windows". (2020). [Accessed 6 April 2020]. Available at: <https://www.thermoglaz.co.nz/blog/pros-cons-of-double-glazing-vs-triple-glazing-windows/>

Radhi, H., Sharples, S. & Fikiry, F. (2013). Will multi-facade systems reduce cooling energy in fully glazed buildings? A scoping study of UAE buildings. *Energy and Buildings*, vol. 56, pp. 179-188. [Accessed 19 March 2020].

Rafati Nasr, M., Fauchoux, M., Besant, R. & Simonson, C. (2014). A review of frosting in air-to-air energy exchangers. *Renewable and Sustainable Energy Reviews*, vol. 30, pp. 538-554. [Accessed 7 May 2020].

Shanks, K. (2018). Energy Performance Resilience of UAE Buildings to Climate Change. *International Journal of Environment and Sustainability*, vol. 7 (1).

Straube, J. & Straaten, R. (2001). The Technical Merit of Double Facades for Office buildings in Cool Humid Climates. [online]. [Accessed 26 February 2020]. Available at: <http://seedengr.com/The%20Technical%20Merit%20of%20Double%20Facades%20for%20Office%20Buildings%20in%20Cool%20Humid%20Climates.pdf>

SULLIVAN, C. (2010). "Heat Recovery Wheels for Energy Savings". *Buildings.com* [online]. [Accessed 23 March 2020]. Available at: <https://www.buildings.com/article-details/articleid/10812/title/heat-recovery-wheels-for-energy-savings>

The Pearl Rating System for Estidama Community Rating System (PCRS) Design & Construction. (2010). 1st edn. Viewed 9 May 2020.

Tibi, G. & Mokhtar, A. (2014). Glass Selection for High-rise Residential Buildings in the United Arab Emirates Based on Life Cycle Cost Analysis. *Energy Procedia*, vol. 62, pp. 270-279.

Tobias, L. & Vavaroutsos, G. (2012). *Retrofitting buildings to be green and energy-efficient*. Chicago:Urban Land Institute.

Tosh, M. (2017). "ASHRAE Heat Balance Method & Radiant Time Series – what's the difference? | Discoveries | IES". *Iesve.com* [online]. [Accessed 2 May 2020]. Available at: <https://www.iesve.com/discoveries/article/6560/ashrae-heat-balance-method-radiant-time-series-whats-the-difference>

Ueno, K. & Lstiburek, J. (2015). BA-1506: Field Testing of Compartmentalization Methods for Multifamily Construction. [online]. [Accessed 12 April 2020]. Available at: <https://www.buildingscience.com/documents/bareports/ba-1506-field-testing-compartmentalization-methods-multifamily/view>

"Understanding Energy Recovery Wheels - Uponor Blog". (2020). [Accessed 23 March 2020]. Available at: <https://web.uponor.hk/radiant-cooling-blog/understanding-energy-recovery-wheels/>

VistaPro Variables. (2018). [Accessed 1 July 2020]. Available at: https://help.iesve.com/ve2018/vistapro_variables.htm

"Weather Data Sources | EnergyPlus". (n.d.). [Accessed 16 June 2020]. Available at: <https://energyplus.net/weather/sources#IWEC>

"WeatherShift". (n.d.). [Accessed 4 April 2020]. Available at: <http://www.weather-shift.com/>

"Where is Dubai, the Emirate of Dubai, the United Arab Emirates on Map Lat Long Coordinates". (2020). [Accessed 29 February 2020]. Available at: <https://www.latlong.net/place/dubai-the-emirate-of-dubai-the-united-arab-emirates-2250.html>

"Why The Building Sector? – Architecture 2030". (2019). [Accessed 9 November 2019]. Available at: https://architecture2030.org/buildings_problem_why/

Wilson, M. (2019). "Thermal insulation for buildings". *Designingbuildings.co.uk* [online]. [Accessed 5 April 2020]. Available at: https://www.designingbuildings.co.uk/wiki/Thermal_insulation_for_buildings

Zhai, Z. & Helman, J. (2019). Implications of climate changes to building energy and design. *Sustainable Cities and Society*, vol. 44, pp. 511-519.

Appendices

Appendix A

Project Construction (Opaque: External Wall)

2013 External Wall

Performance: ASHRAE

U-value: 0.1896 W/m²·K

Thickness: 515.000 mm

Thermal mass Cm: 103.0000 kJ/(m²·K)

Total R-value: 5.1241 m²·K/W

Mass: 416.1000 kg/m²

Lightweight

Surfaces: Functional Settings Regulations RadianceIES

Outside

Emissivity: 0.900

Resistance (m²·K/W): 0.0299

Resistance (m²·K/W): 0.1198

Solar Absorbance: 0.700

Solar Absorbance: 0.550

Inside

Construction Layers (Outside To Inside)

Material	Thickness mm	Conductivity W/(m·K)	Density kg/m ³	Specific Heat Capacity J/(kg·K)	Resistance m ² ·K/W	Vapour Resistivity GN·s/(kg·m)	Category
[STD_SM1] Rainscreen	3.0	50.0000	7800.0	450.0	0.0001	-	Metals
Cavity	50.0	-	-	-	0.1300	-	-
[MFSL] MINERAL FIBRE SLAB	150.0	0.0350	30.0	1000.0	4.2857	6.000	Insulating Materials
[STD_USP] Cement bonded particle board	12.0	0.2300	1100.0	1000.0	0.0522	0.000	Boards, Sheets & Decking
Cavity	50.0	-	-	-	0.1800	-	-
[BRO] BRICKWORK (OUTER LEAF)	200.0	0.8400	1700.0	800.0	0.2381	58.000	Brick & Blockwork
[STD_US1] Plasterboard	50.0	0.2100	700.0	1000.0	0.2381	0.000	Plaster

System Materials... Project Materials...

Condensation Analysis... Derived Parameters...

Copy Paste Cavity Insert Add Delete Flip

OK Cancel

Figure A- 1: Base case external wall construction materials including option A1 (IES Virtual Environment 2019).

Project Construction (Opaque: External Wall)

Description: ID: External Internal

Performance: ASHRAE

U-value: W/m²·K
 Total R-value: m²K/W

Thickness: mm
 Mass: kg/m²

Thermal mass Cm: kJ/(m²·K)
 Lightweight

Surfaces: Functional Settings Regulations RadianceIES

Outside

Emissivity: Resistance (m²K/W): Default
 Solar Absorptance: Resistance (m²K/W): Default

Inside

Emissivity: Resistance (m²K/W): Default
 Solar Absorptance: Resistance (m²K/W): Default

Construction Layers (Outside To Inside)

Material	Thickness mm	Conductivity W/(m·K)	Density kg/m³	Specific Heat Capacity J/(kg·K)	Resistance m²K/W	Vapour Resistivity GN·s/(kg·m)	Category
[STD_SM1] Rainscreen Cavity	3.0	50.0000	7800.0	450.0	0.0001	-	Metals
[STD_EPS] Insulation	50.0	-	-	-	0.1300	-	-
[STD_USP] Cement bonded particle board Cavity	200.0	0.0250	20.0	1030.0	8.0000	-	Insulating Materials
[BRO] BRICKWORK (OUTER LEAF)	12.0	0.2300	1100.0	1000.0	0.0522	0.000	Boards, Sheets & Decking
[STD_US1] Plasterboard	50.0	-	-	-	0.1800	-	-
	200.0	0.8400	1700.0	800.0	0.2381	58.000	Brick & Blockwork
	50.0	0.2100	700.0	1000.0	0.2381	0.000	Plaster

System Materials... Project Materials...

Copy Paste Cavity Insert Add Delete Flip
 Condensation Analysis... Derived Parameters... OK Cancel

Figure A- 2: Base case external wall construction materials including option A2 (IES Virtual Environment 2019).

Project Construction (Glazed: External Window)

Description: 2013 External Window ID: STD_EXTW External Internal

Performance: ASHRAE

Net U-value (including frame): 2.8965 W/m²·K U-value (glass only): 2.6351 W/m²·K Total shading coefficient: 0.1314 SHGC (center-pane): 0.1143

Net R-value: 0.3795 m²·K/W g-value (EN 410): 0.1370 Visible light normal transmittance: 0.71

Surfaces Frame Shading Device Regulations UK Dwellings RadiancesIES

Outside

Emissivity: 0.837 Resistance (m²·K/W): 0.0299 Default

Inside

Emissivity: 0.837 Resistance (m²·K/W): 0.1198 Default

Construction Layers (Outside to Inside):

Material	Thickness mm	Conductivity W/(m·K)	Angular Dependence	Gas	Convection Coefficient W/m ² ·K	Resistance m ² ·K/W	Transmittance	Outside Reflectance	Inside Reflectance	Refractive Index	Outside Emissivity	Inside Emissivity	Visible Light Specified
[SC108] SUNCOOL™ PLAQUEE THERM-ACTIVE	10.0	1.0600	Fresnel	-	-	0.0094	0.050	0.190	0.190	1.526	0.837	0.837	No
Cavity	12.0	-	-	Krypton	0.9580	0.2147	-	-	-	-	-	-	-
[STD_INW2] Inner Pane	6.0	1.0600	Fresnel	-	-	0.0057	0.783	0.072	0.072	1.526	0.837	0.837	No

System Materials... Project Materials...

Copy Paste Insert Add Delete Flip Electrochromic

Condensation Analysis... Derived Parameters... More Data...

OK Cancel

Figure A- 3: Base case external window construction materials including option B1 (IES Virtual Environment 2019).

Project Construction (Glazed: External Window)

Description: 2013 External Window ID: STD_EXTW External Internal

Performance: ASHRAE

Net U-value (including frame): 1.4124 W/m²·K U-value (glass only): 0.9860 W/m²·K Total shading coefficient: 0.1746 SHGC (center-pane): 0.1519

Net R-value: 1.0142 m²·K/W g-value (EN 410): 0.1588 Visible light normal transmittance: 0.71

Surfaces Frame Shading Device Regulations UK Dwellings RadianceIES

Outside Emissivity: 0.837 Resistance (m²·K/W): 0.0299 Default

Inside Emissivity: 0.837 Resistance (m²·K/W): 0.1198 Default

Construction Layers (Outside to Inside):

Material	Thickness mm	Conductivity W/(m·K)	Angular Dependence	Gas	Convection Coefficient W/(m ² ·K)	Resistance m ² ·K/W	Transmittance	Outside Reflectance	Inside Reflectance	Refractive Index	Outside Emissivity	Inside Emissivity	Visible Light Specified
[STD_EXW] Outer Pane	6.0	1.0600	Fresnel	-	-	0.0057	0.150	0.289	0.414	1.526	0.837	0.042	No
Cavity	12.0	-	-	Krypton	0.9580	0.8531	-	-	-	-	-	-	-
[STD_INW2] Inner Pane	6.0	1.0600	Fresnel	-	-	0.0057	0.401	0.072	0.072	1.526	0.837	0.837	No

System Materials... Project Materials...

Copy Paste Insert Add Delete Filp Electrochromic Condensation Analysis... Derived Parameters... More Data... OK Cancel

Figure A- 4: Base case external window construction materials including option B2 (IES Virtual Environment 2019).

Project Construction (Glazed: External Window)

Description: 2013 External Window ID: STD_EXTW Internal

Performance: ASHRAE

Net U-value (including frame): 1.2540 W/m²·K U-value (glass only): 0.8100 W/m²·K Total shading coefficient: 0.1503 SHGC (center-pane): 0.1307

Net R-value: 1.2345 m²·K/W g-value (EN 410): 0.1366 Visible light normal transmittance: 0.71

Surfaces Frame Shading Device Regulations UK Dwellings RadianceIES

Outside

Emissivity: 0.837 Resistance (m²·K/W): 0.0299 Default

Resistance (m²·K/W): 0.837 Default

Construction Layers (Outside to Inside):

Material	Thickness mm	Conductivity W/(m·K)	Angular Dependence	Gas	Convection Coefficient W/m ² ·K	Resistance m ² ·K/W	Transmittance	Outside Reflectance	Inside Reflectance	Refractive Index	Outside Emissivity	Inside Emissivity	Visible Light Specified
[STD_EXW] Outer Pane	6.0	1.0600	Fresnel	-	-	0.0057	0.150	0.289	0.414	1.526	0.837	0.042	No
Cavity	12.0	-	-	Krypton	0.9580	0.8531	-	-	-	-	-	-	-
[STD_INW] Inner Pane	6.0	1.0600	Fresnel	-	-	0.0057	0.401	0.072	0.072	1.526	0.837	0.837	No
Cavity	12.0	-	-	Krypton	0.9580	0.2147	-	-	-	-	-	-	-
[STD_INW] Inner Pane	6.0	1.0600	Fresnel	-	-	0.0057	0.401	0.072	0.072	1.526	0.837	0.837	No

System Materials... Project Materials...

More Data...

Copy Paste Insert Add Delete Flip Electrochromic

Condensation Analysis... Derived Parameters...

OK Cancel

Figure A- 5: Base case external window construction materials including option B3 (IES Virtual Environment 2019).

Appendix B

Table (B- 1): Peak cooling load of rooms 1, 2, 3, and 4 of the 12th floor (IES Virtual Environment 2019).

Room 1

COOLING ZONE PEAK					
Time of Peak (Mo/Hr:Mn)					5 / 16:30
Outside Air (DB/WB/RH)					41.1 °C / 20.7 °C / 13.5 %
	Zone Sensible	Zone Latent	Net Value	Per Floor Area	Percent of Total
Envelope Gains/Losses	W	W	W	W/m ²	%
External Walls	137	-	137	0.4	0.5
Roofs	0	-	0	0.0	0.0
Ground/Exposed Floors	0	-	0	0.0	0.0
External Doors	0	-	0	0.0	0.0
Windows Conduction	2,834	-	2,834	8.9	10.0
Skylights Conduction	0	-	0	0.0	0.0
Solar	13,850	-	13,850	43.4	49.0
Infiltration	1,542	-735	807	2.5	2.9
Nat/Aux Vent	0	0	0	0.0	0.0
Internal Building Gains/Losses					
Internal Walls/Openings	-529	-	-529	-1.7	-1.9
Internal Floors	-1,380	-	-1,380	-4.3	-4.9
Internal Air & Furniture	0	-	0	0.0	0.0
Ceilings	-220	-	-220	-0.7	-0.8
Sub Total	16,232	-735	15,498	48.6	
Internal Gains					
Lights	3,190	-	3,190	10.0	11.3
People	2,871	1,914	4,785	15.0	16.9
Misc, Computers, Equip	4,785	0	4,785	15.0	16.9
Sub Total	10,846	1,914	12,760	40.0	
TOTAL	27,078	1,179	28,258	88.6	100

Room 2

COOLING ZONE PEAK					
Time of Peak (Mo/Hr:Mn)					7 / 8:30
Outside Air (DB/WB/RH)					38.4 °C / 21.5 °C / 21.0 %
	Zone Sensible	Zone Latent	Net Value	Per Floor Area	Percent of Total
Envelope Gains/Losses	W	W	W	W/m ²	%
External Walls	308	-	308	1.5	1.9
Roofs	0	-	0	0.0	0.0
Ground/Exposed Floors	0	-	0	0.0	0.0
External Doors	0	-	0	0.0	0.0
Windows Conduction	1,494	-	1,494	7.1	9.4
Skylights Conduction	0	-	0	0.0	0.0
Solar	2,356	-	2,356	11.3	14.8
Infiltration	775	-250	525	2.5	3.3
Nat/Aux Vent	0	0	0	0.0	0.0
Internal Building Gains/Losses					
Internal Walls/Openings	507	-	507	2.4	3.2
Internal Floors	616	-	616	2.9	3.9
Internal Air & Furniture	1,220	-	1,220	5.8	7.7
Ceilings	546	-	546	2.6	3.4
Sub Total	7,822	-250	7,572	36.2	
Internal Gains					
Lights	2,090	-	2,090	10.0	13.1
People	1,881	1,254	3,135	15.0	19.7
Misc, Computers, Equip	3,135	0	3,135	15.0	19.7
Sub Total	7,106	1,254	8,360	40.0	
TOTAL	14,928	1,004	15,932	76.2	100

Room 3

COOLING ROOM PEAK					
Time of Peak (Mo/Hr:Mn)					5 / 8:30
Outside Air (DB/WB/RH)					34.2 °C / 18.4 °C / 19.6 %
	Room Sensible	Room Latent	Net Value	Per Floor Area	Percent of Total
Envelope Gains/Losses	W	W	W	W/m ²	%
External Walls	168	-	168	0.5	0.6
Roofs	0	-	0	0.0	0.0
Ground/Exposed Floors	0	-	0	0.0	0.0
External Doors	0	-	0	0.0	0.0
Windows Conduction	1,692	-	1,692	5.3	5.7
Skylights Conduction	0	-	0	0.0	0.0
Solar	14,586	-	14,586	45.7	49.5
Infiltration	836	-832	4	0.0	0.0
Nat/Aux Vent	0	0	0	0.0	0.0
Internal Building Gains/Losses					
Internal Walls/Openings	16	-	16	0.1	0.1
Internal Floors	-1,388	-	-1,388	-4.4	-4.7
Internal Air & Furniture	1,863	-	1,863	5.8	6.3
Ceilings	-244	-	-244	-0.8	-0.8
Sub Total	17,530	-832	16,698	52.3	
Internal Gains					
Lights	3,190	-	3,190	10.0	10.8
People	2,871	1,914	4,785	15.0	16.2
Misc, Computers, Equip	4,785	0	4,785	15.0	16.2
Sub Total	10,846	1,914	12,760	40.0	
TOTAL	28,376	1,082	29,458	92.3	100

Room 4

COOLING ZONE PEAK					
Time of Peak (Mo/Hr:Mn)					9 / 12:30
Outside Air (DB/WB/RH)					41.0 °C / 22.3 °C / 18.3 %
	Zone Sensible	Zone Latent	Net Value	Per Floor Area	Percent of Total
Envelope Gains/Losses	W	W	W	W/m ²	%
External Walls	153	-	153	0.7	0.8
Roofs	0	-	0	0.0	0.0
Ground/Exposed Floors	0	-	0	0.0	0.0
External Doors	0	-	0	0.0	0.0
Windows Conduction	2,236	-	2,236	10.7	12.3
Skylights Conduction	0	-	0	0.0	0.0
Solar	7,505	-	7,505	35.9	41.1
Infiltration	957	-182	775	3.7	4.2
Nat/Aux Vent	0	0	0	0.0	0.0
Internal Building Gains/Losses					
Internal Walls/Openings	-298	-	-298	-1.4	-1.6
Internal Floors	-567	-	-567	-2.7	-3.1
Internal Air & Furniture	0	-	0	0.0	0.0
Ceilings	78	-	78	0.4	0.4
Sub Total	10,063	-182	9,881	47.3	
Internal Gains					
Lights	2,090	-	2,090	10.0	11.5
People	1,881	1,254	3,135	15.0	17.2
Misc, Computers, Equip	3,135	0	3,135	15.0	17.2
Sub Total	7,106	1,254	8,360	40.0	
TOTAL	17,169	1,072	18,241	87.3	100